Functional Analysis of *CNGA3* Missense Variants Associated with Achromatopsia Using an Aequorin-Based Bioassay

Dissertation

der Mathematisch-Naturwissenschaftlichen Fakultät

der Eberhard Karls Universität Tübingen

zur Erlangung des Grades eines

Doktors der Naturwissenschaften

(Dr. rer. nat.)

vorgelegt von

Maria Solaki

aus Nürtingen

Tübingen

2025

Gedruckt mit Genehmigung der Mathematisch-Naturwissenschaftlichen Fakultät der Eberhard Karls Universität Tübingen.

Tag der mündlichen Qualifikation:	20.05.2026
Dekan:	Prof. Dr. Thilo Stehle
1. Berichterstatter:	Prof. Dr. Bernd Wissinger
2. Berichterstatter:	Prof. Dr. Jennifer Ewald

Erklärung

Ich erkläre hiermit, dass ich die zur Promotion eingereichte Arbeit mit dem Titel:

Functional Analysis of CNGA3 Missense Variants Associated with Achromatopsia Using an Aequorin-Based Bioassay

selbständig verfasst, nur die angegebenen Quellen und Hilfsmittel benutzt und Stellen, die wörtlich oder inhaltlich nach den Werken anderer Autoren entnommen sind, als solche gekennzeichnet habe. Eine detaillierte Abgrenzung meiner eigenen Leistungen habe ich im Abschnitt „*Personal contribution*“ vorgenommen. Ich erkläre, dass die Richtlinien zur Sicherung guter wissenschaftlicher Praxis der Universität Tübingen (Beschluss des Senats vom 25.5.2000) beachtet wurden. Ich versichere an Eides statt, dass diese Angaben wahr sind und dass ich nichts verschwiegen habe. Mir ist bekannt, dass die falsche Abgabe einer Versicherung an Eides statt mit Freiheitsstrafe bis zu drei Jahren oder mit Geldstrafe bestraft wird.

Tübingen, den 23.10.2026

Maria Solaki

Table of contents

1. Abbreviations I
2. Summary II
3. Zusammenfassung IV
4. List of publications VI
5. Personal contribution VII
6. Introduction 1
6.1. The retina and the phototransduction cascade 1
6.1.1. Structure of the retina 1
6.1.2. Photoreceptors 3
6.1.3. Phototransduction cascade 4
6.2. Cyclic nucleotide-gated (CNG) channels 6
6.2.1. The family of mammalian cyclic nucleotide-gated (CNG) channels 6
6.2.2. Cyclic nucleotide-gated (CNG) channels in cones 7
6.3. Achromatopsia 10
6.3.1. Symptoms and genetic background of achromatopsia 10
6.3.2. *CNGA3* variant spectrum 11
6.4. Interpretation of sequence variants 12
6.5. Implementation of functional *in vitro* studies in the classification of sequence variants 14
7. Aim of this study 16
8. Results and discussion 17
8.1. *Publication I*: Comprehensive variant spectrum of the *CNGA3* gene in patients affected by achromatopsia. 17
8.1.1. Variant spectrum of the *CNGA3* gene in the Tübingen ACHM study cohort 17
8.1.2. Comprehensive *CNGA3* variant database: ACMG/AMP-based variant classification 19
8.1.3. Comprehensive *CNGA3* variant database: manual and expert-based variant categorization 20
8.1.4. Comprehensive *CNGA3* variant database: variant types and localization 20
8.1.5. Functional studies on *CNGA3* missense variants and their contribution to the ACMG/AMP-based classification 23
8.2. *Publication II*: Functional evaluation allows ACMG/AMP-based re-classification of *CNGA3* variants associated with achromatopsia 24
8.2.1. Further development and validation of the aequorin-based bioassay 24
8.2.2. Functional analysis of 150 *CNGA3* missense variants using the aequorin-based bioassay 27

8.2.3. ACMG/AMP-based re-classification of 150 *CNGA3* missense variants based on functional data 29
8.2.4. Further functional *in vitro* studies and their influence on VUS re-classification in a variety of genes 31
8.2.5. Limitations of the aequorin-based bioassay..... 32
8.3. *Publication III*: Paternal uniparental isodisomy of chromosome 2 in a patient with *CNGA3*-associated autosomal recessive achromatopsia. 33
8.3.1. Ophthalmological and genetic examination of the respective ACHM patient . 33
8.3.2. Functional evaluation of the identified *CNGA3* missense variant..... 34
8.3.3. Segregation analysis and confirmation of UPD of chromosome 2 35
8.3.4. Further cases of UPD of chromosome 2 in the scientific literature 35
8.4. Conclusion and outlook 36
9. References 38
10. Acknowledgement 50
11. Appendix 51

1. Abbreviations

8-Br-cGMP	8-Bromoguanosine 3', 5'-cyclic monophosphate
ACGS	Association for Clinical Genomic Science
ACHM	achromatopsia
ACMG	American College of Medical Genetics and Genomics
AMP	Association for Molecular Pathology
AUC	area under the curve
cAMP	cyclic adenosine monophosphate
cGMP	cyclic guanosine monophosphate
CLZ	carboxyterminal (C-terminal) leucine zipper
CNBD	cyclic nucleotide-binding domain
CNG channel	cyclic nucleotide-gated ion channel
CNV	copy number variation
ERG	electroretinography
GAP complex	GTPase-activating protein complex
GCAP	guanylyl cyclase-activating protein
GCL	ganglion cell layer
GDP	guanosine diphosphate
gnomAD	Genome Aggregation Database
GRK	G-protein coupled receptor kinase
GTP	guanosine triphosphate
HEK293	human embryonic kidney 293 cells
HEK293^{aequo}	human embryonic kidney 293 cells that stably express apo-aequorin
HEK293T	human embryonic kidney 293 cells that contain the SV40 T-antigen
HGMD®	Human Gene Mutation Database®
INL	inner nuclear layer
IPL	inner plexiform layer
IRD	inherited retinal diseases
LOVD	Leiden Open Variation Database
MAF	minor allele frequency
MMP	matrix metalloprotease
NCKX	Na^+/Ca^{2+}, K^+ exchanger
ONL	outer nuclear layer
OPL	outer plexiform layer
PCR	polymerase chain reaction
PDE	phosphodiesterase
retGC	retinal guanylyl cyclase
ROC	receiver operating characteristic
RP	retinitis pigmentosa
RPE	retinal pigment epithelium
STGD1	Stargardt disease 1
Td	transducin
TM	transmembrane helices
UPD	uniparental isodisomy
VUS	variant of uncertain significance

2. Summary

Detection of disease-associated sequence variants in patients with inherited retinal diseases has significantly improved with the introduction of high-throughput sequencing technologies allowing the simultaneous analysis of a large number of genes. Nevertheless, the primary challenge in the field of molecular genetic diagnosis remains the ability to discern which observed variant or genotype is causative for the disease phenotype in the respective patient.

The *CNGA3* gene codes for the main subunit of the cyclic nucleotide-gated ion channels in cone photoreceptors and is one of the major diseases-causative genes for achromatopsia (ACHM) – a rare autosomal recessive retinal disorder characterized by congenital cone photoreceptor dysfunction. So far, the majority of variants observed in the *CNGA3* gene are missense variants, a significant proportion of which remain functionally uncharacterized. Due to their rarity in the general population and the resulting lack of comprehensive genetic data, these sequence alterations are typically classified as variants of uncertain significance (VUS) in accordance with the current ACMG/AMP guidelines for variant interpretation and classification presenting a significant challenge for molecular genetic diagnosis. This highlights the need to develop suitable assays and readouts for functional *in vitro* studies to ensure an objective assessment of variant pathogenicity.

The aim of the present doctoral thesis was to provide an expert-based assessment of sequence alterations in the *CNGA3* gene by i. establishing a comprehensive *CNGA3* variant database by scientific literature, in-house, and public variant database research, ii. developing a medium-throughput bioassay to subsequently test the functionality of CNGA3 channels carrying functionally yet uncharacterized missense variants, and iii. incorporating the obtained functional data into the existing ACMG/AMP-based classification to unequivocally assess their pathogenic impact.

By compiling all *CNGA3* sequence alterations detected in our laboratory-intern ACHM study cohort, and complemented through a literature and public database research, the *CNGA3* variant spectrum was substantially expanded to a total of 316 sequence alterations. From these, 244 variants could be interpreted as “likely disease-causing” following extensive *in silico* variant assessment, ACMG/AMP-based classification, and manual/expert-based variant categorization. The predominant variant type among the “likely disease-causing” variants were missense substitutions displaying the highest

frequency of 66.8% whereas small indel (16.8%) and nonsense variants (12.3%) only played a subordinate role.

However, a considerable proportion of the identified *CNGA3* missense substitutions was functionally yet uncharacterized and their pathogenicity remained elusive. Therefore, a medium-throughput aequorin-based luminescence bioassay in transiently transfected human embryonic kidney (HEK293) cells was established and validated using a set of benign and pathogenic *CNGA3* sequence alterations in order to evaluate the pathogenicity of the tested variants via a luminescence-based quantification of the CNGA3 channel-mediated calcium influx. Using this approach, a total of 150 missense variants were functionally evaluated, of which 55 had initially been classified as VUS in the ACMG/AMP classification system. Of the 150 missense substitutions analysed, 25 exhibited channel function characteristics similar to those of the wild-type channels, and were considered “functionally normal”. In contrast, the remaining 125 missense substitutions displayed (severely) impaired or absent channel function, thus classifying them as “functionally abnormal”. The application of the obtained functional data to the preceding classification allowed substantial ACMG/AMP-based variant re-classification. Of the 55 VUS, 52 could be re-classified as either (likely) benign or likely pathogenic, leading to a VUS re-classification rate of 94.5%.

In summary, the expansion of the *CNGA3* variant spectrum, functional evaluation, and subsequent ACMG/AMP-based variant re-classification presented in this doctoral thesis will greatly facilitate the clinical variant interpretation with respect to the analysed *CNGA3* missense variants ensuring a molecular genetic diagnosis for *CNGA3*-associated achromatopsia patients, hereby identifying patients eligible for future gene therapeutic trials and treatments.

3. Zusammenfassung

Die Einführung von Hochdurchsatz-Sequenzierungstechnologien ermöglicht den Nachweis von krankheitsassoziierten Sequenzvarianten bei Patienten mit erblichen Netzhauterkrankungen in einer großen Anzahl von Genen. Eine große Herausforderung im Bereich der molekulargenetischen Diagnostik bleibt jedoch zu erkennen, welche der identifizierten Varianten oder welcher Genotyp für den Krankheitsphänotyp bei dem jeweiligen Patienten ursächlich ist.

Das *CNGA3*-Gen kodiert für die Hauptuntereinheit des zyklisch Nukleotid-gesteuerten Ionenkanals in Zapfen-Fotorezeptoren und ist eines der wichtigsten krankheitsassoziierten Gene für die Achromatopsie – einer seltenen autosomal rezessiven Netzhauterkrankung, die durch eine kongenitale Dysfunktion der Zapfen-Fotorezeptoren gekennzeichnet ist. *Missense*-Substitutionen stellen die häufigste im *CNGA3*-Gen beobachtete Variantenklasse dar und ein erheblicher Anteil davon war bislang funktionell nicht charakterisiert. Solche Sequenzveränderungen werden gemäß den aktuellen ACMG/AMP-Richtlinien für die Interpretation und Klassifizierung von Varianten in der Regel als Varianten unklarer Signifikanz (VUS) eingestuft, was eine erhebliche Herausforderung für die molekulargenetische Diagnostik darstellt. Dies unterstreicht die Notwendigkeit, geeignete Assays und *Readouts* für funktionelle *In-vitro*-Studien zu entwickeln, um eine objektive Bewertung der Pathogenität dieser Varianten zu gewährleisten.

Ziel der vorliegenden Doktorarbeit war es, eine Experten-basierte Bewertung von Sequenzveränderungen im *CNGA3*-Gen vorzunehmen. Dazu wurde zunächst eine umfassende *CNGA3*-Variantendatenbank erstellt, welche auf einer Recherche der wissenschaftlichen Literatur sowie der Auswertung unserer *in-house* Datenbank und zweier öffentlicher Variantendatenbanken basiert. Im nächsten Schritt wurde ein *Medium-Throughput* Bioassay entwickelt, um die Funktionalität von CNGA3-Kanälen zu testen, die funktionell noch nicht charakterisierte *Missense*-Varianten tragen. Die erhaltenen funktionellen Daten wurden anschließend in die bestehende ACMG/AMP-basierte Klassifizierung integriert, um die Pathogenität der getesteten Varianten eindeutig zu bewerten.

Durch die Zusammenstellung aller *CNGA3*-Sequenzveränderungen, die in unserer laborinternen ACHM-Studienkohorte entdeckt und durch eine Literatur- und Datenbankrecherche komplementiert wurden, konnte das *CNGA3*-Variantenspektrum

auf insgesamt 316 Sequenzveränderungen erheblich erweitert werden. Alle Sequenzveränderungen wurden einer umfassenden *in silico*-Variantenbewertung, einer ACMG/AMP-basierten Klassifizierung und einer manuellen Experten-basierten Variantenkategorisierung unterzogen. Von 316 bewerteten *CNGA3*-Varianten wurden somit 244 als „wahrscheinlich krankheitsverursachend“ klassifiziert, wobei *Missense*-Substitutionen mit 66,8% hierbei den häufigsten Variantentyp darstellten, gefolgt von *Small Indel*- (16,8%) und *Nonsense*-Varianten (12,3%).

Ein beträchtlicher Anteil der identifizierten *CNGA3*-*Missense*-Substitutionen war jedoch funktionell noch nicht charakterisiert, und ihre Pathogenität blieb folglich unbestimmt. Daher wurde ein *Medium-Throughput* Aequorin-basierter Lumineszenz-Bioassay in transient transfizierten humanen embryonalen Nierenzellen (HEK293) etabliert. Dieser wurde mit einer Reihe von benignen und pathogenen Varianten validiert, um final die Pathogenität der getesteten *CNGA3*-Sequenzveränderungen über eine Lumineszenz-basierte Quantifizierung des CNGA3-Kanal-vermittelten Kalziumeinstroms zu bewerten. Mit diesem Ansatz wurden insgesamt 150 *Missense*-Varianten funktionell analysiert, von denen 55 zunächst nach dem ACMG/AMP-Klassifizierungssystem als VUS eingestuft worden waren. Von den 150 analysierten *Missense*-Substitutionen wiesen 25 Wildtyp-ähnliche Lumineszenzsignale auf und wurden folglich als „funktionell normal“ kategorisiert. Im Gegensatz dazu wiesen die übrigen 125 Varianten eine z.T. stark beeinträchtigte oder fehlende Kanalfunktion auf, so dass sie als „funktionell abnormal“ eingestuft wurden. Der Einschluss der erhaltenen funktionellen Daten in die vorangegangene Klassifizierung beeinflusste die ACMG/AMP-basierte Reklassifizierung der Varianten deutlich. Von den 55 VUS konnten 52 entweder als (wahrscheinlich) benigne oder als wahrscheinlich pathogen eingestuft werden, was zu einer VUS-Reklassifizierungsrate von 94,5% führte.

Zusammenfassend konnte gezeigt werden, dass die Erweiterung des *CNGA3*-Variantenspektrums, die funktionelle Bewertung und die abschließende ACMG/AMP-basierte Klassifizierung der Varianten, die in dieser Doktorarbeit vorgestellt wurden, die klinische Varianteninterpretation der analysierten *CNGA3*-*Missense*-Varianten erheblich verbessert. Die erzielten Ergebnisse werden außerdem helfen geeignete *CNGA3*-assoziierte Achromatopsie-Patienten für zukünftige gentherapeutische Studien und Behandlungen auszuwählen.

4. List of publications

A) Accepted publications (in order of appearance in the present doctoral thesis)

I) **Solaki, M.**, Baumann, B., Reuter, P., Andreasson, S., Audo, I., Ayuso, C., Balousha, G., Benedicenti, F., Birch, D., Bitoun, P., Blain, D., Bocquet, B., Branham, K., Català-Mora, J., De Baere, E., Dollfus, H., Falana, M., Giorda, R., Golovleva, I., Gottlob, I., Heckenlively, J. R., Jacobson, S. G., Jones, K., Jägle, H., Janecke, A. R., Kellner, U., Liskova, P., Lorenz, B., Martorell-Sampol, L., Messias, A., Meunier, I., Porto, F. B. O., Papageorgiou, E., Plomp, A. S., de Ravel, T. J. L., Reiff, C. M., Renner, A. B., Rosenberg, T., Rudolph, G., Salati, R., Sener, E. C., Sieving, P. A., Stanzial, F., Traboulsi, E. I., Tsang, S. H., Varsanyi, B., Weleber, R. G., Zobor, D., Stingl, K., Wissinger, B., and Kohl, S. (2022). Comprehensive variant spectrum of the *CNGA3* gene in patients affected by achromatopsia. *Hum Mutat* 43(7)**,** 832-858. doi: 10.1002/humu.24371.

II) **Solaki, M.**, Wissinger, B., Kohl, S., and Reuter, P. (2023). Functional evaluation allows ACMG/AMP-based re-classification of *CNGA3* variants associated with achromatopsia. *Genet Med* 25(12)**,** 100979. doi: 10.1016/j.gim.2023.100979.

III) Kohl, S., Baumann, B., Dassie, F., Mayer, A.K., **Solaki, M.**, Reuter, P., Kühlewein, L., Wissinger, B., and Maffei, P. (2021). Paternal Uniparental Isodisomy of Chromosome 2 in a Patient with *CNGA3*-Associated Autosomal Recessive Achromatopsia. *Int J Mol Sci* 22(15). doi: 10.3390/ijms22157842.

5. Personal contribution

Publication I: Comprehensive variant spectrum of the *CNGA3* gene in patients affected by achromatopsia.

Overview: B.W., S.K., and P.R. conceived and designed the project. S.A., I.A., C.A., G.B., F.B., D.Bi., P.B., D.Bl., B.Bo., K.B., J.C.-M., E.D.B., H.D., M.F., R.G., I.Gol., I.Got., J.R.H., S.G.J., K.J., H.J., A.R.J., U.K., P.L., B.L., L.M.-S., A.M., I.M., F.B.O.P., E.P., A.S.P., T.J.L.D.R., C.M.R., A.B.R., T.R., G.R., R.S., E.C.S., P.A.S., F.S., E.I.T, S.H.T., B.V., R.G.W., D.Z., and K.S. provided blood, saliva or DNA samples from patients and available family members. B.Ba. performed molecular genetic screening of patients and segregation analyses in available family members. **M.S.** compiled and analysed all data. S.K. prepared the database records (ClinVar). **M.S.** wrote the main parts of the manuscript and prepared the majority of the figures and tables. K.S. wrote the section “Clinical and diagnostic aspects of ACHM” in the manuscript. P.R. and K.S. prepared Figure 3 and 4, respectively. All authors (including **M.S.**) read and revised the manuscript.

In detail: For the establishment of the comprehensive *CNGA3* variant spectrum, **M.S.** compiled all *CNGA3* variants identified in the in-house ACHM study cohort of 889 independent families and performed a scientific literature and public database research. **M.S.** established and revised the criteria for the manual/expert-based variant categorization. **M.S.** assessed the potential pathogenicity of all identified variants by performing the *in silico* variant assessment, variant classification according to the ACMG/AMP guidelines, and manual/expert-based variant categorization. **M.S.** wrote the manuscript (except the section “Clinical and diagnostic aspects of ACHM”) and prepared the tables and figures (except Figure 3 and 4).

Publication II: Functional evaluation allows ACMG/AMP-based re-classification of *CNGA3* variants associated with achromatopsia.

Overview: B.W., S.K., P.R., and **M.S.** conceived and designed the experiments. **M.S.** performed all experiments, except for: P.R. performed the Western Blot analysis of the p.(Glu590Lys) and p.(Pro592Leu) mutant whole cell lysates using the custom-made rabbit anti-human CNGA3 antibody SA3899. **M.S.** analysed the data and performed the receiver operating characteristic (ROC) analysis. **M.S.** wrote the manuscript. All authors (including **M.S.**) read and revised the manuscript.

In detail: **M.S.** performed the site-directed mutagenesis for the generation of 161 out of 174 mutant *CNGA3* expression constructs and generated the stable HEK293^{aequo} cells for the aequorin-based bioassay. **M.S.** established and validated the aequorin-based bioassay using a set of benign and pathogenic *CNGA3* sequence alterations. **M.S.** performed the ROC analysis based on the assay validation data set for the determination of thresholds for both the normalized overall luminescence signal and the normalized peak latency. **M.S.** evaluated the overall assay quality by calculating the Z' factor. **M.S.** conducted the functional characterization of all 150 selected *CNGA3* missense variants using the aequorin-based bioassay. **M.S.** performed dot blot analysis and/or Western blot analysis of whole cell lysates in one biological replicate of all samples analysed in the aequorin-based bioassay and from the assay validation data set using a commercial rabbit anti-human CNGA3 antibody. **M.S.** analysed all data obtained from the functional characterization of all 150 studied *CNGA3* missense variants using the aequorin-based bioassay and performed the variant re-classification according to the ACMG/AMP guidelines. **M.S.** wrote the manuscript and prepared the tables and figures.

Publication III: Paternal uniparental isodisomy of chromosome 2 in a patient with *CNGA3*-associated autosomal recessive achromatopsia.

Overview: S.K., P.R., and B.W. conceived and designed the project. S.K., F.D., B.B., A.K.M., **M.S.**, L.K., and P.M. performed the experiments and analysed the data. S.K. wrote the manuscript. B.B., **M.S.**, and S.K. prepared the figures for the manuscript. All authors (including **M.S.**) read and revised the manuscript.

In detail: **M.S.** classified the identified *CNGA3* missense variant c.778G>C; p.(Asp260His) according to the ACMG/AMP guidelines. **M.S.** performed the site-directed mutagenesis for the generation of the mutant *CNGA3* expression construct CNGA3$_{D260H}$ used in the aequorin-based bioassay. **M.S.** conducted the functional characterization of the identified *CNGA3* missense variant using the aequorin-based bioassay and verified CNGA3 protein expression in the transfected HEK293 cells using immunocytochemistry. **M.S.** prepared Figure 2 for the manuscript and read/revised the manuscript.

6. Introduction

6.1. The retina and the phototransduction cascade

6.1.1. Structure of the retina

The retina is a 0.2 mm thin, light-sensitive central nervous tissue located at the rear of the eye thereby representing the initial input station of the visual system. It both acts as a light detector and is responsible for image processing by amplifying, extracting, and compressing the detected signals before transmitting the retinal information via the midbrain and the thalamus to the primary visual cortex. The retina encompasses five major neuronal cell types which were generated from a common progenitor pool including photoreceptors, bipolar cells, horizontal cells, amacrine cells, and retinal ganglion cells. Furthermore, it contains the three glial cell types including microglia, astrocytes and Müller glia – the latter being the predominant type (Figure 1) (Joselevitch, 2008; Molday and Zhang, 2010; Sung and Chuang, 2010; Hussey et al., 2022).

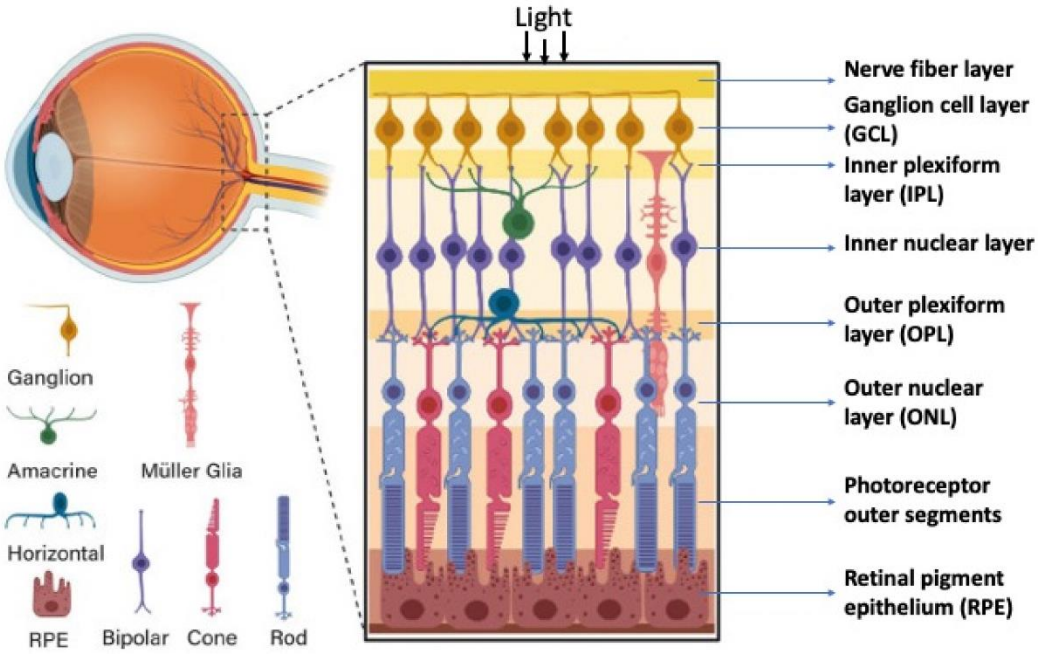


Figure 1: Schematic structure of the vertebrate retina (Grigoryan, 2022). The vertebrate retina contains five neuronal and three glial cell types organized in three layers of cell bodies and two plexiform layers displaying an inverted organization relative to the path of the light. Licensed by: Creative Commons Attribution (CC BY 4.0) (https://creativecommons.org/licenses/by/4.0/).

The cells in the vertebrate retina are organized in an orderly laminated structure thereby forming three layers of cell bodies and two plexiform layers. The nuclei of the photoreceptors form the outer nuclear layer (ONL) whereas the nuclei of the bipolar,

horizontal, and amacrine interneurons as well as the nuclei of the Müller glia cells form the inner nuclear layer (INL). The nuclei of the retinal ganglion cells are organized in the ganglion cell layer (GCL). Furthermore, the outer plexiform layer (OPL) contains the processes and synaptic terminals of the photoreceptors, horizontal, and bipolar cells whereas the inner plexiform layer (IPL) is formed by the processes and synaptic terminals of the bipolar, amacrine and retinal ganglion cells (Figure 1) (Sung and Chuang, 2010; Hussey et al., 2022).

One central property of the vertebrate retina is the inverted organization of the retinal layers relative to the path of the light. Before the light can be captured by the photoreceptors in the ONL, it needs to pass through four transparent inner retinal layers. Following photon absorption by the photoreceptors, the generated electrical signal is transmitted towards the inner retinal layers by the bipolar and horizontal cells in the INL thus conveying the signal to the retinal ganglion cells in the GCL. Finally, the neural signal is transmitted to the midbrain and the thalamus through the axons of the retinal ganglion cells which form the optical nerve (Hussey et al., 2022).

In contrast to the retinal neuronal cell types which are responsible for light detection and signal processing, Müller glia are, among other, important for removing excess neurotransmitter within the retina, functioning as sinks for metabolic waste products, and recycling the vitamin A-based chromophore required for light detection from *all-trans*-retinal into 11-*cis*-retinal exclusively for the cone photoreceptors (Newman, 1994; Tsacopoulos and Magistretti, 1996; Mata et al., 2002; Kolesnikov et al., 2021; Hussey et al., 2022). Furthermore, they function as living optical fibres by directly guiding the green-red part of the visible light spectrum onto cone photoreceptors improving cone-mediated day vision (Franze et al., 2007; Labin et al., 2014).

Finally, a melanin-rich epithelial cell layer called the retinal pigment epithelium (RPE) is located between the photoreceptors and the choroid and is involved in retinal homeostasis (Joselevitch, 2008; Hussey et al., 2022). The main functions of the RPE thereby include the absorption of stray photons, regeneration of the vitamin A-based chromophore 11-*cis*-retinal and its return to the photoreceptor cells ensuring photoreceptor health and function as well as phagocytosis of photoreceptor outer segments following their shedding (Gal et al., 2000; Baehr et al., 2003; Finnemann, 2003; Joselevitch, 2008; Hussey et al., 2022).

6.1.2. Photoreceptors

Photoreceptors are highly specialised sensory neurons representing the first neurons in the visual pathway thereby acting as adaptive light detectors. Two distinct types of photoreceptors can be distinguished in the vertebrate retina – cone and rod photoreceptors. Rod photoreceptors are capable of single photon detection mediating vision in dim light and motion detection whereas cone photoreceptors are much less sensitive light detectors being responsible for mediating vision in bright light and colour vision (Beavo et al., 2007; Sung and Chuang, 2010; Hussey et al., 2022).

Both rods and cones consist of three structurally and functionally distinct compartments. The detection of light and the conversion into an electrical signal takes place in the outer segment – a light-sensitive highly modified cilium containing high levels of visual pigment for optimized photon capture and other phototransduction proteins. The outer segment displays a distinct morphology in rods and cones. While rod outer segments consist of stacks of disc membranes surrounded by the plasma membrane, cone outer segments are formed by continuous invaginations of the plasma membrane displaying a tightly stacked lamellae structure. The inner segment acts as the metabolic compartment containing the nucleus, mitochondria, and other cellular organelles important for protein biosynthesis. Both the outer and the inner segment are connected through the connecting cilium – a non-motile cilium regulating the transport of protein and metabolites to the outer segment. Finally, transmission of the generated electrical signals to the secondary neurons of the retina takes place at the synaptic terminus which is formed by a ribbon synapse (Kawamura and Tachibanaki, 2008; Molday and Zhang, 2010; Lamb, 2022).

Rod and three distinct types of cone photoreceptors can be distinguished by their spectral sensitivity which is determined by the expression of distinct opsin photopigments. While rods exclusively use rhodopsin (λ=498 nm) as their visual pigment, three cone subtypes can be defined based on the expression of opsin proteins displaying an optimal sensitivity to different wavelengths of light in the primate retina: S- (short-wavelength/blue; λ=420 nm), M- (medium-wavelength/green; λ=534 nm), and L- (long-wavelength/red; λ=564 nm) cones (Bowmaker et al., 1980; Hussey et al., 2022). The human retina approximately contains 92 million rods and 4.6 million cones displaying an inhomogeneous distribution (Curcio et al., 1990). While the rod density peaks in the midperiphery, cones are present at a high density in the

fovea – a cone-rich region within the macula responsible for high visual acuity due to the displacement of the inner retinal layers limiting light scattering and the connection of one foveal cone to only one bipolar and one retinal ganglion cell (Molday and Zhang, 2010; Sung and Chuang, 2010; Hussey et al., 2022).

6.1.3. Phototransduction cascade

Phototransduction describes the transduction of light into a neuronal signal taking place in the outer segment of retinal rod and cone photoreceptors. Rods and cones thereby utilize distinct homologous proteins in the phototransduction cascade encoded by a distinct set of genes (Lamb and Pugh, 2006; Lamb, 2022). All proteins involved in the cone phototransduction cascade are located in or are associated to the plasma membrane which displays continuous invaginations. In contrast, the majority of proteins involved in the rod phototransduction cascade localize in or are associated to the disc membranes except the cyclic nucleotide-gated ion channels and the Na^+/Ca^{2+}, K^+ exchanger (NCKX) which are restricted in the plasma membrane (Lamb, 2022).

Under dark conditions, a small proportion of cGMP-gated channels is held open due to a cytoplasmic concentration of free cGMP of several µM. This creates an inward current into the outer segment composed of 85-90% Na^+ ions and 10-15% Ca^{2+} ions (Nakatani and Yau, 1988; Pugh Jr and Lamb, 2000). In contrast, a balancing outward current flows primarily through K^+ channels located in the plasma membrane of the inner segment. The inward current into the outer segment together with the balancing outward current from the inner segment forms a current loop known as dark current setting the normal resting potential of rods and cones at -35 to -45 mV sustaining synaptic glutamate release (Pugh Jr and Lamb, 2000; Yau and Hardie, 2009). Additionally, Na^+ ions are constantly pumped out via the Na^+-K^+ ATPase located at the inner segment while Ca^{2+} ions are expelled via the Na^+/Ca^{2+}, K^+ exchanger (NCKX) in the plasma membrane of the outer segment (Fu and Yau, 2007).

Upon light exposure, a single photopigment molecule – rhodopsin or its cone equivalent – absorbs a photon starting the phototransduction cascade. Opsin photopigments are light-sensitive G-protein-coupled receptors composed of the 7-transmembrane spanning apo-protein opsin which is covalently linked to a vitamin A-based chromophore called 11-*cis*-retinal (Palczewski et al., 2000; Yau and Hardie, 2009; Lamb, 2022). Photoisomerization of the chromophore to its

all-trans-retinal configuration following photon absorption leads to the activation of the photopigment. A single activated photopigment molecule subsequently activates multiple molecules of the G-protein transducin by binding to the GDP-bound form of the transducin αβγ-trimer triggering a GDP-GTP nucleotide exchange on the α-subunit (Arshavsky et al., 2002; Lamb, 2022). The GTP-bound α-subunit of transducin is released and binds to one of the inhibitory γ-subunits of the cGMP phosphodiesterase (PDE) resulting in its partly activation. Full PDE activation is only achieved by binding of an additional GTP-bound transducin α-subunit to the second inhibitory γ-subunit of PDE. Fully activating PDE enhances the rate of hydrolysis of the cytoplasmic messenger cGMP leading to a reduction in cGMP concentration. cGMP subsequently dissociates from the cyclic nucleotide-gated (CNG) ion channels causing channel closure and a reduction in the influx of cations (Figure 2). This consequently results in a membrane hyperpolarization decreasing the synaptic glutamate release (Arshavsky et al., 2002; Lamb and Pugh, 2006; Lamb, 2022).

Finally, deactivation of the phototransduction cascade is achieved by several mechanisms. Due to the closure of CNG channels blocking the Ca^{2+} influx and the continuous Ca^{2+} extrusion by the NCKX, the cytoplasmic Ca^{2+} concentration is profoundly reduced. This facilitates the activation of recoverin which promotes the phosphorylation of the activated opsin photopigment by a G-protein coupled receptor kinase (GRK) allowing the binding of arrestin. The catalytic site of the opsin photopigment is thereby blocked by arrestin preventing further activation of transducin (Yau and Hardie, 2009; Garafalo et al., 2021; Lamb, 2022). The reduction of cytoplasmic Ca^{2+} concentration also activates two guanylyl cyclase-activating proteins (GCAPs) which in turn stimulate the synthesis of cGMP at an elevated level by the retinal guanylyl cyclase (retGC) restoring the cytoplasmic cGMP concentration to its dark level thereby leading to the reopening of CNG channels (Arshavsky et al., 2002; Lamb, 2022).

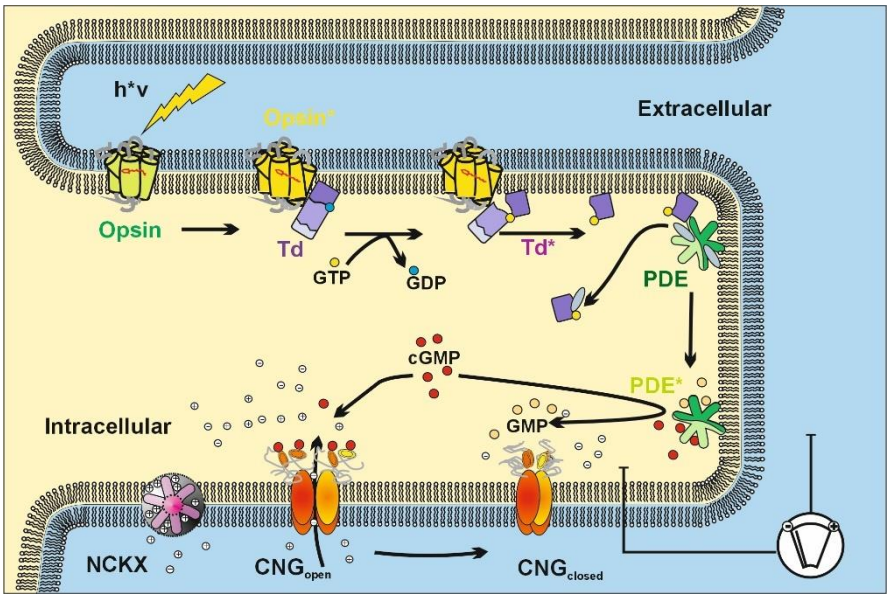


Figure 2: Schematic representation of the phototransduction cascade in the outer segment of cone photoreceptors (Wissinger and Kohl, 2005) (modified). Td, transducin; PDE, phosphodiesterase; CNG, cyclic nucleotide-gated ion channel; NCKX, Na^+/Ca^{2+}, K^+ exchanger.

Inactivation of transducin and PDE is achieved by the formation of a GTPase-activating protein (GAP) complex which enhances the intrinsic GTPase activity of the transducin α-subunit. Following GTP hydrolysis, the GDP-bound transducin α-subunit dissociates from the inhibitory PDE γ-subunit and reassociates with the transducin βγ-subunits allowing the inhibitory PDE γ-subunit to rebind and inhibit the active site of PDE. In rods, the GAP complex comprises, among others, the GTPase-activating enzyme RGS9, the RGS9-anchoring protein R9AP and the PDE γ-subunit (He et al., 1998; Makino et al., 1999; Hu and Wensel, 2002; Beavo et al., 2007; Yau and Hardie, 2009).

6.2. Cyclic nucleotide-gated (CNG) channels

6.2.1. The family of mammalian cyclic nucleotide-gated (CNG) channels

Cyclic nucleotide-gated (CNG) channels are ligand-activated, non-selective cation channels which belong to the superfamily of voltage-gated ion channels even if their activity displays very little voltage dependence. The opening of CNG channels is thereby mediated by direct binding of cyclic nucleotides including cGMP and cAMP. Furthermore, CNG channels are described as non-selective cation channels since they show a limited ability in discriminating between alkali ions and they are even permeable for divalent cations such as Ca^{2+} which is an important factor for excitation and adaptation of sensory cells (Kaupp and Seifert, 2002). CNG channels were not only identified in vertebrates but were also found in several invertebrates including *C. elegans* and *D. melanogaster* (Biel and Michalakis, 2009).

The family of mammalian CNG channels comprises six homologous members which are classified into two different subtypes according to sequence similarity: CNGA and CNGB. The first subtype includes four members – CNGA1, CNGA2, CNGA3, and CNGA4 – which are regarded as the main subunits conferring principal channel properties (Kaupp and Seifert, 2002; Matulef and Zagotta, 2003; Biel and Michalakis, 2009; Michalakis et al., 2018). Except for CNGA4, all CNGA subunits can form functional channels by themselves when expressed in heterologous expression systems (Cook et al., 1987; Bönigk et al., 1993; Barret et al., 2022a). The second subtype comprises two members – CNGB1 and CNGB3 – which are the modulatory subunits mediating proper channel localization to the outer segment and conferring specific biophysical properties (Kaupp and Seifert, 2002; Michalakis et al., 2018). Native CNG channels are heterotetramers showing specific subunit compositions and stoichiometries (Biel and Michalakis, 2009). CNG channels expressed in rod and cone photoreceptors display a 3:1 stoichiometry consisting of three CNGA1 and one CNGB1 subunit in rods and three CNGA3 and one CNGB3 subunit in cones, respectively (Weitz et al., 2002; Zheng et al., 2002; Zhong et al., 2002; Biel and Michalakis, 2009; Shuart et al., 2011; Barret et al., 2022b; Zheng et al., 2022). Additionally, CNG channels in olfactory neurons are composed of two CNGA2, one CNGA4 and one CNGB1b subunit – a splicing variant of CNGB1 (Zheng and Zagotta, 2004; Biel and Michalakis, 2009).

6.2.2. Cyclic nucleotide-gated (CNG) channels in cones

The structurally homologous channel subunits of the CNG channels in cone photoreceptors include three CNGA3 and one CNGB3 subunit which share some principal membrane topology (Biel and Michalakis, 2009). Both subunits are thereby composed of six transmembrane helices (TM1 to TM6) connected via several intracellular and extracellular loops and a pore-forming region including the pore helix which is located between the transmembrane helices TM5 and TM6. The cyclic nucleotide-binding domain (CNBD) is formed by three α-helices (αA to αC) and eight β-sheets (β1 to β8) whereas the C-linker consisting of six α-helices (αA’ to αF‘) connects and confers conformational changes occurring in the CNBD to TM6 (Gofman et al., 2014; Barret et al., 2022a). Finally, the subunit assembly is facilitated by the carboxyterminal leucine zipper (CLZ) which is only found within the CNGA3 subunit (Figure 3) (Zhong et al., 2002). The heterotetrameric cone CNG channels are thereby formed by three CNGA3 subunits and one CNGB3 subunit arranged around a centrally

located pore with the TM6 segments forming the ion-conducting pore (Zheng et al., 2022).

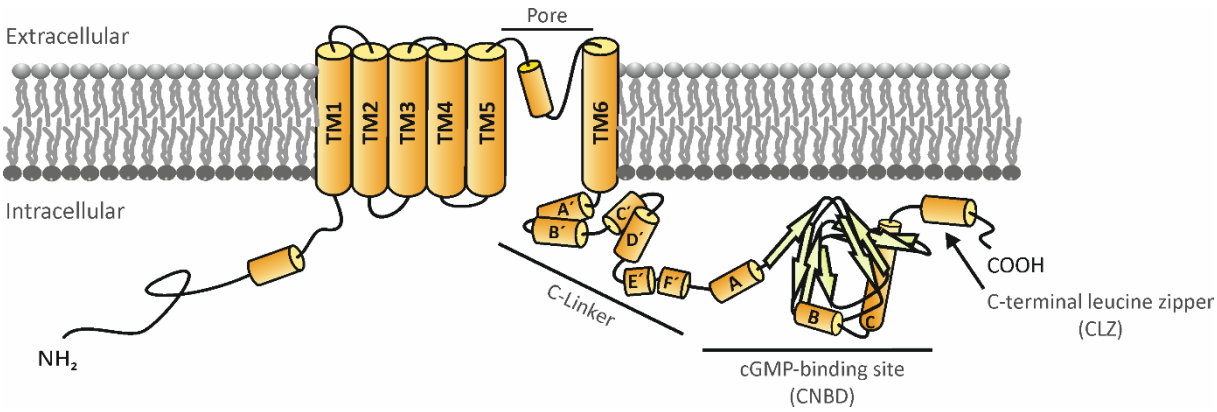


Figure 3: Topology model of the CNGA3 and CNGB3 subunit (Koeppen et al., 2008) (modified). Both the CNGA3 and the CNGB3 subunit consist of six transmembrane helices (TM), a pore helix between TM5 to TM6, a C-linker and a cGMP-binding site (CNBD). The carboxyterminal (C-terminal) leucine zipper (CLZ) is only present in the CNGA3 subunit. TM1-6, transmembrane helices 1-6.

Activation of the cone CNG channel is mediated by direct binding of cyclic nucleotides to the closed channel involving interactions between five amino acid residues located in the β-sheets β5 – β7 and the αC helix of the CNBD and the ribofuranose moiety of the cyclic nucleotide (Altenhofen et al., 1991; Tibbs et al., 1998; Scott et al., 2000; Kaupp and Seifert, 2002). This elicits an allosteric conformational change which is coupled to the ligand binding finally leading to the opening of the channel pore (Biel and Michalakis, 2009). Cone CNG channels thereby display a high degree of ligand specificity for the cyclic nucleotide cGMP over cAMP which is mediated by at least two amino acid residues in the CNBD corresponding to the residues Thr565 and Asp609 in the CNGA3 subunit (Altenhofen et al., 1991; Varnum et al., 1995; Matulef and Zagotta, 2003).

Following ligand binding, the αC helix of the CNBD moves upwards towards the membrane, resulting in an overall compaction of the CNBD. The αE’ and αF’ helices of the C-linker also move upward causing a counterclockwise rotation and an upward motion of the C-linker helices αA’ and αB’. Subsequently, the TM6 domains dislocate from the pore axis and rotate around a conserved glycine residue leading to an overall pore dilation. Finally, the hydrophobic amino acid residues forming the central channel gate rotate away from the ion-conducting pore permitting ion permeation (Barret et al., 2022a). Opening of the heterotetrameric CNG channel is mediated by the binding of maximally four ligand molecules in a cooperative manner (Kaupp and Seifert, 2002). However, full activation of the channel is accomplished by the binding of only two ligand

molecules (Biskup et al., 2007; Biel and Michalakis, 2009). Additionally, its opening probability increases with the increasing number of ligand molecules bound (Ruiz and Karpen, 1997; Liu et al., 1998; Matulef and Zagotta, 2003).

Modulation of cone CNG channels can be achieved by several mechanisms. The apparent ligand sensitivity for cGMP and the efficacy of cAMP was shown to be enhanced by the enzymatic activity of the matrix metalloproteases (MMPs) -2 and -9 via the proteolytic modification of the main CNGA3 subunits as it was demonstrated for both heterologously expressed and native CNG channels. Glycosylation of the CNGA3 subunits at a specific extracellular core glycosylation site was found to act in a protective manner since the abolishment of the CNGA3 glycosylation by mutating the amino acid residue Asn339 resulted in an enhanced susceptibility of the CNG channels to MMP-dependent proteolytic processing. Furthermore, prolonged MMP exposure was associated with the loss of conductive channels (Meighan et al., 2013).

Cone CNG channels can also be regulated by calcium-dependent factors. The human CNGB3 subunit has two calmodulin binding sites, one located in the aminoterminal cytoplasmic domain and one in the carboxyterminal cytoplasmic domain. Binding of calcium-calmodulin to one or both binding sites leads to a reduction in cGMP-sensitivity in recombinant heteromeric cone CNG channels (Peng et al., 2003). However, whether calcium-calmodulin is responsible for the modulation of native CNG channels in human cone photoreceptors is unclear. As demonstrated in cones of striped bass (*Morone saxatilis*), the ligand sensitivity of cone CNG channels can also be modulated by a soluble modulator protein called CNG-modulin in a calcium-dependent manner. CNG-modulin is thereby expressed in the cone outer segments and binds specifically to the amino terminus of the modulatory subunit of cone CNG channels modulating their apparent cGMP-sensitivity (Rebrik et al., 2012). However, the orthologous protein in humans still remains unknown. Furthermore, a decrease in the ligand sensitivity was observed upon phosphorylation of the amino acid residues Ser577 and Ser579 in the CNBD of heterologously expressed homomeric bovine CNGA3 channels by the protein kinase C (Müller et al., 2001; Matulef and Zagotta, 2003). Finally, a phosphoinositide (PIP)-mediated regulation of the heteromeric cone CNG channel was demonstrated to result in a decrease in its apparent cGMP-sensitivity in a heterologous expression system (Dai et al., 2013).

6.3. Achromatopsia

6.3.1. Symptoms and genetic background of achromatopsia

Achromatopsia (ACHM; rod monochromatism) is a rare autosomal recessively inherited retinal disease characterized by congenital cone photoreceptor dysfunction thereby displaying an overall prevalence of 1:30,000-50,000 (François, 1961). The disorder is associated with colour blindness, severely decreased visual acuity, marked photosensitivity and nystagmus clinically manifesting in early infancy (Michalakis et al., 2017; Hirji et al., 2018; Michalakis et al., 2022). ACHM patients display absent or severely reduced cone-mediated responses on electroretinography (ERG) whereas rod responses appear to be essentially normal, although mildly reduced rod responses and defects in post-receptor responses have occasionally been reported (Andreasson and Tornqvist, 1991; Khan et al., 2007; Aboshiha et al., 2014; Hirji et al., 2018; Maguire et al., 2018).

Depending on the degree of cone photoreceptor dysfunction, two forms of ACHM can be distinguished: complete and incomplete ACHM. Whereas patients affected by complete ACHM display no cone photoreceptor function, total colour blindness and severely reduced visual acuity, patients suffering from the incomplete form present with a milder phenotype showing retained residual colour discrimination, better visual acuity and/or residual photopic ERG responses (Hirji et al., 2018; Sun and Zhang, 2019). Originally, ACHM was considered to be a stationary disease since the symptoms, such as the decreased visual acuity, are stable in the patients. Yet, recent reports demonstrate a progressive loss of cone cells and degenerative changes in the retinal morphology in a portion of ACHM patients using non-invasive imaging technologies (Thiadens et al., 2010; Thomas et al., 2012; Georgiou et al., 2020; Triantafylla et al., 2022).

To date, pathogenic sequence variants in a total of six genes have been shown to be causative for autosomal recessive ACHM including *CNGA3* (Kohl et al., 1998), *CNGB3* (Kohl et al., 2000; Sundin et al., 2000), *GNAT2* (Aligianis et al., 2002; Kohl et al., 2002), *PDE6C* (Chang et al., 2009; Thiadens et al., 2009a), *PDE6H* (Kohl et al., 2012), and *ATF6* (Ansar et al., 2015; Kohl et al., 2015; Xu et al., 2015). Except for *ATF6* which codes for a transmembrane transcription factor in the endoplasmic reticulum involved in the unfolded protein response, all five remaining disease-associated genes code for essential cone phototransduction components (Michalakis et al., 2022). Molecular

genetic analyses in ACHM patients unveiled *CNGA3* as the most afflicted gene in Israeli/Palestinian (84%) and Chinese ACHM patients (80%) (Liang et al., 2015; Zelinger et al., 2015; Sun et al., 2020). In contrast, the prevalence of biallelic *CNGA3* variants in ACHM patients of European origin ranges between 5-44% rendering *CNGA3* the second most common disease-gene in this ethnic population following *CNGB3* (Wissinger et al., 2001; Johnson et al., 2004; Varsányi et al., 2005; Thiadens et al., 2009b).

6.3.2. CNGA3 variant spectrum

By compiling in-house cohort data with extensive literature research, a recent systematic review of the variant spectrum of the six ACHM-associated genes identified a total of 383 potentially pathogenic variants in 1,328 families. Biallelic causative variants in *CNGA3* were thereby detected in 30.8% (n=409) of the families included in this study underlining its important role in the ACHM variant spectrum. From the 169 potentially pathogenic variants identified in the *CNGA3* gene, 69.8% (118/169) were missense substitutions resulting in a single amino acid substitution in the CNGA3 polypeptide representing the most frequently observed variant type in *CNGA3* (Sun et al., 2020). The majority of the *CNGA3* missense alterations were shown to affect conserved amino acid residues in important functional domains of the CNGA3 protein. The residues Arg277, Arg283, Val529 and Phe547 located in the TM4 and the CNBD, respectively, were thereby found to be the most frequently mutated ones among Asian and Caucasian patients (Sun et al., 2020; Solaki et al., 2022).

Functional studies on *CNGA3* variants in heterologous expression systems assessing their pathogenic or benign impact have previously been conducted for a total of 54 missense alterations and two nonsense variants (Tränkner et al., 2004; Liu and Varnum, 2005; Patel et al., 2005; Muraki-Oda et al., 2007; Koeppen et al., 2008; Reuter et al., 2008; Koeppen et al., 2010; Matveev et al., 2010; Dai and Varnum, 2013; Meighan et al., 2015; Shaikh et al., 2015; Kuniyoshi et al., 2016; Burkard et al., 2018; Täger et al., 2018). One variant was thereby confirmed as a benign variant not impacting function of homomeric CNGA3 channels (Tränkner et al., 2004; Meighan et al., 2015). Twenty-seven out of 54 *CNGA3* missense substitutions displayed a complete abolishment of the channel functionality of the heterologously expressed mutant channels (Tränkner et al., 2004; Liu and Varnum, 2005; Patel et al., 2005;

Muraki-Oda et al., 2007; Koeppen et al., 2008; Koeppen et al., 2010; Matveev et al., 2010; Shaikh et al., 2015; Solaki et al., 2022).

Additionally, the formation of functional mutant channels presenting with impaired protein folding and/or channel trafficking or altered biophysical properties such as compromised apparent cGMP-sensitivity or ion selectivity was observed for 17 missense variants (Tränkner et al., 2004; Liu and Varnum, 2005; Patel et al., 2005; Muraki-Oda et al., 2007; Koeppen et al., 2008; Reuter et al., 2008; Dai and Varnum, 2013; Meighan et al., 2015; Burkard et al., 2018; Solaki et al., 2022). In addition, 21 canonical/non-canonical splice site variants in *CNGA3* were assessed using a minigene splice assay approach in HEK293T cells and/or murine cone photoreceptor-like 661W cells and an impact on splicing was confirmed for 11 of these variants (Burkard et al., 2018; Reuter et al., 2023). Five of the 21 variants represented missense substitutions and were included in the study of Reuter and colleagues since the causative nucleotide exchange was located at the exon-intron borders in the *CNGA3* gene. Only one of these nucleotide exchanges showed to impair splicing to a low extent whereas the remaining four missense variants showed no damaging impact on transcript splicing (Reuter et al., 2023). Functional data to assess if these missense variants impair CNG channel function were lacking for four out of the five analysed missense alterations and have been generated as part of this project.

6.4. Interpretation of sequence variants

The emergence of high-throughput sequencing technologies has contributed to the enlargement of the scale at which genetic testing can now be performed facilitating the detection of disease-causing variants in patients with inherited diseases. The Genome Aggregation Database (gnomAD) currently contains 17.2 million variants identified in 125,748 whole exome sequencing datasets and 261.9 million variants detected in 15,708 whole genome sequencing datasets which were both generated from unrelated individuals sequenced as part of various disease-specific and population genetic studies (Ellard et al., 2020; Karczewski et al., 2020). However, sequence variant interpretation and classification still remain the main hurdle in genetic diagnosis since each human genome contains three to four million variants compared to the reference human genome sequence from which only a minority are causative for monogenic diseases. Deciphering which variant or genotype is disease-related or not is crucial to

provide optimal care and targeted treatment for patients with inherited diseases (Ellard et al., 2020).

Therefore, the American College of Medical Genetics and Genomics (ACMG) and the Association for Molecular Pathology (AMP) revisited and published standards and guidelines for the interpretation of sequence variants in order to introduce the use of standard terminology in the scientific field of variant interpretation to describe sequence alterations detected in genes which are linked to Mendelian disorders. The proposed five-tier classification system thereby assigns five variant classes ranging from benign, likely benign, variant of uncertain significance (VUS), likely pathogenic, to pathogenic according to various criteria based on different types of variant evidence (Richards et al., 2015; Ellard et al., 2020).

The ACMG/AMP variant interpretation guidelines define two sets of criteria including 16 pathogenic and 12 benign criteria. They include, among others, criteria on variant frequency in the general population (gnomAD, https://gnomad.broadinstitute.org/) compared to the patient group, deleterious effects of the variant predicted by computational *in silico* tools and functional data obtained by functional *in vivo* or *in vitro* studies. In addition, the localization of variants in functionally important domains, availability of co-segregation data of the variant with the disease within a given family are also taken into consideration. The criteria are also based on *de novo* and allelic data, data on the pathogenicity classification of a variant from a reputable source such as the clinical-genetic database ClinVar (https://www.ncbi.nlm.nih.gov/clinvar/), and comprehensive knowledge of the patient's phenotype. Each pathogenic (P) and benign (B) criterion is weighted differently based on the level of evidence ranging from stand-alone (BA1), very strong (PVS1), strong (PS1-4 and BS1-4), moderate (PM1-6), to supporting (PP1-5 and BP1-6). Furthermore, the weight ((very) strong, moderate, and supporting) of certain criteria can be adjusted following professional judgement of the evidence collected for a given variant (Richards et al., 2015). For the final variant classification, the criteria are selected based on the evidence collected for the sequence alteration being evaluated. The selected criteria are then combined according to specific scoring rules to determine the assignment of the evaluated sequence variant to one of the five variant classes. In case a variant does not fulfil any of the benign or pathogenic criteria, or the evidence obtained is conflicting, the evaluated variant is classified as VUS (Richards et al., 2015).

Further development of the ACMG/AMP-based classification system is being undertaken in order to refine the currently applied guidelines. Tavtigian and colleagues suggested a point-based classification system assigning positive points to all pathogenic ACMG/AMP criteria and negative points to all benign criteria (Tavtigian et al., 2020). Depending on the evidence strength, different point values are assigned ranging from 1/−1 for the evidence strength “supporting” to 8/−8 for the level of evidence determined as “very strong”. All points are additive with the total defining the final variant class. The thresholds for classifying a variant as “pathogenic” or “likely pathogenic” are 10 points and 6 points, respectively, whereas the thresholds for a classification as “likely benign” or “benign” are −1 and −7 points, respectively. Sequence variants reaching a point range between 0 and 5 are classified as VUS (Tavtigian et al., 2020). In order to improve the classification of VUS, the Association for Clinical Genomic Science (ACGS) suggested a temperature gradient sub-classification for VUS based on a points scale derived from a Bayesian approach to convey the different levels of uncertainty within this variant class (Ellard et al., 2020).

Obtaining a clear variant classification as pathogenic or benign is challenging since extensive genetic information is required, ideally from independent patients originating from different families carrying the same variant. However, the majority of *CNGA3* variants are rare missense substitutions which are absent or only detected with a very low allele frequency in the general population (gnomAD) and most *CNGA3*-ACHM patients are carrying at least one missense variant in a (presumable) compound heterozygous state (Sun et al., 2020; Solaki et al., 2022). Based on current classification guidelines these variants are therefore typically categorized as VUS not providing clear information on whether a variant or genotype is relevant to the disease or not. This underlines the necessity for functional analyses of such variants to improve the classification of missense variants in the *CNGA3* gene.

6.5. Implementation of functional *in vitro* studies in the classification of sequence variants

Medium-/high-throughput *in vitro* assays have been developed and validated for a variety of genes to functionally analyse a large number of variants at a time providing a high amount of functional data which can be implemented in the classification of sequence variants identified in these genes. In 2019, Wan and colleagues established a higher-throughput flow cytometry-based assay to functionally characterize potentially

pathogenic rhodopsin (*RHO*) variants based on their surface expression deciphering their role in causing retinitis pigmentosa (RP) (Wan et al., 2019). Therefore, a library of 210 *RHO* variants including 175 known pathogenic variants, 14 VUS or potential benign polymorphisms, 11 synonymous control variants, and 10 novel VUS identified through in-house genetic diagnostic testing was constructed. Characterizing the surface expression of every *RHO* library variant using the developed functional genomics approach led to the re-classification of 37 variants. This ultimately solved three RP pedigrees carrying three different *RHO* variants with pathogenic surface expression levels which were previously classified as VUS (Wan et al., 2019).

In another study, Richardson and colleagues used a homology-directed DNA repair (HDR) assay to functionally analyse 186 missense variants in the *BRCA2* gene which had been observed in hereditary cancer testing (Richardson et al., 2021). Approximately 83% of these missense alterations (154/186) were classified as VUS in the ACMG/AMP-based classification system prior to functional analysis. However, the incorporation of the protein functional data obtained by the HDR assay led to the re-classification of 132 out of 154 *BRCA2* VUS as either (likely) pathogenic (39/132) or (likely) benign (93/132) reaching a VUS re-classification rate of 86% and substantially impacting the clinical management of individuals carrying these *BRCA2* variants (Richardson et al., 2021).

A functional *in vitro* assay based on the calcium-sensitive photoprotein aequorin was developed for CNGA3 allowing the evaluation of CNGA3 channel functionality via the detection of the CNGA3 channel-meditated calcium influx (Täger et al., 2021). This bioassay was subsequently used to perform a compound screening for chemical and pharmacological chaperones improving protein folding and/or surface localization of mutant, trafficking-deficient CNGA3 channels (Täger et al., 2021). As part of the present project, this previously established assay was further developed generating a medium-throughput platform to provide a suitable assay and functional read-out for the evaluation of disease-associated variants related to *CNGA3*-associated ACHM.

7. Aim of this study

Modern sequencing technologies have enabled the identification of disease-causing variants in patients with inherited retinal diseases (IRD) by allowing parallel analysis of many genes. Disease-associated variants in *CNGA3* are a known cause of autosomal recessive achromatopsia (ACHM). However, determining which variants are truly disease-associated remains a challenge. The predominant variant type in the *CNGA3* gene is missense variants, many of which are functionally uncharacterized and often classified as variants of uncertain significance (VUS), complicating diagnosis. To support genetic diagnosis, robust classification systems incorporating functional data are essential, underscoring the need for suitable assays for objective pathogenicity assessment.

The aim of this study was to: i. establish a *CNGA3* variant database and to provide an expert-based assessment of sequence variants in the *CNGA3* gene, ii. develop a medium-throughput bioassay to test the functionality of CNGA3 channels carrying functionally yet uncharacterized missense and in-frame variants versus wild-type channels; and iii. to incorporate the obtained functional data into the existing ACMG/AMP classification enabling revision or confirmation of the classification.

This ACMG/AMP-based variant re-classification of the yet uncharacterized *CNGA3* missense variants will aid to assure molecular diagnosis to patients affected by *CNGA3*-associated ACHM thereby identifying patients which would be eligible for future gene therapeutic trials and treatment.

8. Results and discussion

The data presented and discussed in this Results and Discussion Section have been published in:

I) **Solaki, M.**, Baumann, B., Reuter, P., Andreasson, S., Audo, I., Ayuso, C., et al. (2022). Comprehensive variant spectrum of the *CNGA3* gene in patients affected by achromatopsia. *Hum Mutat* 43(7)**,** 832-858. doi: 10.1002/humu.24371.

II) **Solaki, M.**, Wissinger, B., Kohl, S., and Reuter, P. (2023). Functional evaluation allows ACMG/AMP-based re-classification of *CNGA3* variants associated with achromatopsia. *Genet Med* 25(12)**,** 100979. doi: 10.1016/j.gim.2023.100979.

III) Kohl, S., Baumann, B., Dassie, F., Mayer, A.K., **Solaki, M.**, Reuter, P., et al. (2021). Paternal Uniparental Isodisomy of Chromosome 2 in a Patient with *CNGA3*-Associated Autosomal Recessive Achromatopsia. *Int J Mol Sci* 22(15). doi: 10.3390/ijms22157842.

8.1. Publication I: Comprehensive variant spectrum of the *CNGA3* gene in patients affected by achromatopsia.

8.1.1. Variant spectrum of the CNGA3 gene in the Tübingen ACHM study cohort

The present study aimed to establish a comprehensive summary of the variant spectrum of the *CNGA3* gene in patients affected by ACHM by compiling genetic data from an ACHM study cohort genetically characterized in Tübingen, the literature and three different mutation databases and to finally provide a standardised classification of all identified *CNGA3* variants according to the ACMG/AMP guidelines. The complete Tübingen ACHM study cohort was compiled through in-house genetic analyses and database research, comprising 1,060 affected individuals from 889 independent families carrying biallelic causative variants in the six known ACHM-associated genes. Within this laboratory-intern cohort, 385 index patients from 304 independent families were shown to carry likely disease-causing variants in *CNGA3*, emphasizing its role as the second major ACHM gene in a cohort mainly including patients of Western European and Northern American descent (36.3% patients/34.2% families; Supplementary Figure 1, Publication I, Appendix). Similar observations were reported in previously conducted studies, where the

prevalence of *CNGA3* sequence alterations in cohorts of Dutch, British, Danish and Brazilian patients ranged from 5% to 41% (Johnson et al., 2004; Thiadens et al., 2009b; Amaral et al., 2023; Andersen et al., 2023). A total of 238 *CNGA3*-ACHM patients in our cohort carry two heterozygous sequence alterations in a (presumable) compound heterozygous state whereas 147 cases were identified to harbour likely disease-associated *CNGA3* variants in an (apparent) homozygous state. However, the presence and independent inheritance of two mutant biallelic *CNGA3* alleles could only be confirmed for 269 affected individuals, where segregation analysis was conducted in either both parents, in a single parent and/or in other family members (Supplementary Table 2, Publication I, Appendix).

In a total of 140 distinct potentially disease-causing variants in the ACHM study cohort genetically characterized in Tübingen, the ten most common *CNGA3*-ACHM-associated alleles were predominantly missense substitutions. The variants c.1641C>A; p.(Phe547Leu) and c.847C>T; p.(Arg283Trp) thereby exhibited the highest allele frequency of 86 and 84 chromosomes, respectively, out of a total of 773 chromosomes (Table 1, Publication I, Appendix). Correlating allele frequency and patient origin revealed some descent-specific enrichment for some alleles: the two most commonly observed alleles c.1641C>A; p.(Phe547Leu) and c.847C>T; p.(Arg283Trp) were frequently detected in German and South Tyrolean ACHM patients, respectively (n=21 and n=14 affected individuals, respectively). In addition, the c.1641C>A; p.(Phe547Leu) substitution was also often observed in patients of Middle Eastern origin (n=15). The third most common *CNGA3*-ACHM-related allele in our cohort is the missense substitution c.829C>T; p.(Arg277Cys) which was predominantly detected in German and US patients (n=18 and n=6, respectively). In summary, five of the ten most commonly observed *CNGA3* alleles associated with ACHM in our study cohort affect the three amino acid residues Arg277, Arg283 and Phe547 in the CNGA3 protein (Table 1 and Figure 1, Publication I, Appendix). In a recent study, these three residues were also found to be the most frequently mutated ones among Caucasian patients (Sun et al., 2020). Two out of these three amino acid residues – the residues Arg277 and Arg283 – are located in the transmembrane domain TM4 of the CNGA3 polypeptide and are part of the voltage sensor motif. Similar to voltage-gated K^+-channels, this sequence motif contains four tandem repeats of the sequence –R/K-X-X–. As CNG channels do not show any voltage dependence, the functional relevance of this voltage sensor motif remains unclear. However, replacing

any or all charged residues in the TM4 motif with neutral ones results in impaired protein maturation and loss of channel function (Kaupp and Seifert, 2002; Faillace et al., 2004). The residue Phe547 is located in the CNBD and functional studies performed in heterologous expression systems suggested that the common disease-causing variant p.(Phe547Leu) leads to the complete abolishment of the channel functionality by interfering with protein folding/trafficking and negatively affecting the allosteric transition of the CNBD upon ligand binding (Muraki-Oda et al., 2007; Reuter et al., 2008; Matveev et al., 2010).

8.1.2. Comprehensive CNGA3 variant database: ACMG/AMP-based variant classification

The present study aimed to extend the variant spectrum of the *CNGA3* gene underlying ACHM through the establishment of a comprehensive *CNGA3* variant database. This was achieved by compiling all *CNGA3* sequence alterations detected in our laboratory-intern ACHM study cohort and identified through literature research on PubMed® and public database research on HGMD®, LOVD, and the clinical-genetic database ClinVar. A total of 316 *CNGA3* variants were compiled in the database and were subsequently subjected to an extensive *in silico* evaluation and classification according to the ACMG/AMP guidelines.

The ACMG/AMP classification system represents an unbiased classification system to classify sequence variants using different types of variant evidence, eventually grouping the identified alterations into the following five variant classes: benign, likely benign, VUS, likely pathogenic, and pathogenic (Richards et al., 2015; Ellard et al., 2020). Out of the 316 *CNGA3* sequence alterations in the comprehensive variant database, 67 and 152 variants were grouped in the pathogenic and likely pathogenic category, respectively, whereas 71 were classified as VUS. Only a minority of 12 and 10 sequence changes were categorized as likely benign and benign, respectively (Table 2 and Supplementary Table 3, Publication I, Appendix). However, four variants out of the 316 sequence alterations in our comprehensive *CNGA3* database remained unclassified since they are located in the alternatively spliced exon (exon 3b) and its flanking intronic sequences. As no functional relevance and disease association has ever been described for exon 3b in the scientific literature, these four *CNGA3* variants were deemed to be “likely benign”.

8.1.3. Comprehensive CNGA3 variant database: manual and expert-based variant categorization

To further refine the variant classification, all 316 sequence alterations listed in our comprehensive *CNGA3* database were subjected to a manual and expert-based revision and categorization into the following three categories: “likely benign”, “VUS”, and “likely disease-causing”. The in-house criteria established for this purpose were based, among others, on the preceding ACMG/AMP-based classification, the *in silico* evaluation according to nine different applied algorithms, previously published functional data, genotype data established from the scientific literature or public/in-house database data, the variants’ minor allele frequency (MAF) obtained from the gnomAD database, and the detected variant type/localization. A detailed description of all in-house criteria used for the categorization into the three categories “likely benign”, “VUS”, and “likely disease-causing” are listed in the section “Comprehensive *CNGA3* variant database” of the manuscript (Publication I, Appendix). In summary, 44 variants were expert-categorized as “likely benign”, 28 as “VUS” and 244 sequence alterations compiled in our *CNGA3* database were manually revised as “likely disease-causing” (Table 2 and Supplementary Table 3, Publication I, Appendix). The 244 sequence alterations expert categorized as “likely disease-causing” included i. variants designated as (likely) pathogenic in the ACMG/AMP classification system, ii. missense and non-canonical splice site variants classified as VUS according to the ACMG/AMP guidelines but predicted to display a deleterious effect by at least three *in silico* algorithms, iii. functionally analysed missense substitutions adversely affecting CNGA3 protein function, iv. sequence alterations probably resulting in null alleles, and v. in-frame deletions leading to the loss of (completely) conserved amino acid residues.

8.1.4. Comprehensive CNGA3 variant database: variant types and localization

Among these 244 “likely disease-causing” variants, missense substitutions resulting in an amino acid exchange displayed the highest frequency of 66.8% whereas small indel (16.8%) and nonsense variants (12.3%) only represented a minority in the variant spectrum of the *CNGA3* gene (Figure 2, Publication I, Appendix). A comparable frequency of missense substitutions was reported in previously conducted studies ranging from 61.5% to 80% thereby indicating a low tolerance of the CNGA3 polypeptide towards single amino acid substitutions (Wissinger et al., 2001; Li et al., 2014; Liang et al., 2015; Amaral et al., 2023). In contrast, the variant spectrum of *CNGB3* encoding the modulatory CNGB3 subunit of the cone channel showed a

totally different distribution with missense substitutions representing only the minority of the observed variants in patients affected by *CNGB3*-associated ACHM (Mayer et al., 2017; Amaral et al., 2023).

Copy number variations (CNVs) also belong to one of the underrepresented variant types in the *CNGA3* variant spectrum as only one CNV leading to the complete deletion of exon 8 of the *CNGA3* gene has been identified (Figure 2, Publication I, Appendix). This 5.19 kb deletion (NC_000002.12:g.98393909_98399093del (GRCh38/hg38)) was detected through deletion mapping via PCR and primer walking in an ACHM patient included in the Tübingen ACHM study cohort in compound heterozygous state with the common missense variant c.847C>T; p.(Arg283Trp) (Supplementary Table 2, Publication I, Appendix). On the other hand, CNVs play a greater role in the variant spectrum of other ACHM-related genes such as *CNGB3*, *GNAT2*, and *ATF6*. Ten disease-associated CNVs are part of the *CNGB3* variant spectrum detected in a large cohort of ACHM patients whereas a total of four CNVs were identified in the mutation spectrum of *GNAT2* and *ATF6*, respectively (Kohl et al., 2002; Mayer et al., 2017; Felden et al., 2019; Lee et al., 2020).

Of the 244 sequence alterations designated as “likely disease-causing” within the comprehensive *CNGA3* variant database, 236 variants are exonic with the majority being located in the final coding exon 8 of the *CNGA3* gene. This exon encodes most of the CNGA3 polypeptide including the following functional domains: TM3 to TM6, the pore helix, the C-linker, the CNBD, and the CLZ. These exonic variants encompass 140 missense variants, 46 nonsense and small indel alterations, and one CNV leading to the complete deletion of exon 8 (Table 2 and Figure 3, Publication I, Appendix). In contrast, only 49 variants are distributed across the coding exons 2 to 7 including 23 missense substitutions, 25 nonsense and small indel variants, and one start loss variant affecting the start codon of the *CNGA3* gene. The exons 6 and 7, which encode the transmembrane helices TM1 and TM2, harbour triple the amount of *CNGA3* variants (n=34) as the exons 2 to 5 (n=15), only coding for the aminoterminal region of the CNGA3 polypeptide (Table 2 and Figure 3, Publication I, Appendix). The notion that the majority of the disease-causing variants in *CNGA3* are located in the exonic sequences of the gene is further supported by the fact, that single heterozygous cases were rarely detected in patients with *CNGA3*-related ACHM. For example, only one out of 385 cases in the ACHM study cohort genetically characterized in Tübingen

carried a single heterozygous *CNGA3* variant (Supplementary Table 2, Publication I, Appendix). In contrast, a much higher amount of 44 out of 552 patients with *CNGB3*-related ACHM were detected to carry a single heterozygous disease-causing variant in *CNGB3* in a study using standard variant screening and CNV analysis for variant detection (Mayer et al., 2017).

Regarding the localization of the "likely disease-causing" *CNGA3* variants on protein level, two major groups can be observed – one that is distributed across the six transmembrane helices and their intracellular/extracellular connecting loops (n=82 variants) and the second clustering within the CNBD (n=57). Furthermore, both the C-linker and the pore-forming region contain a similar amount of "likely disease-causing" variants (n=36 and n=30, respectively) with the pore-forming region displaying the highest variant density within the functional domains of the CNGA3 protein since it only spans around 46 amino acids. A total of 22 sequence alterations are located in the aminoterminal region of the CNGA3 polypeptide from which the majority are nonsense variants and small indels in contrast to the variants within the CNGA3 protein which mainly comprise missense substitutions. Finally, the CLZ domain harbours the smallest number of "likely disease-causing" *CNGA3* variants (n=8) (Figure 3, Publication I, Appendix).

A total of eight out of 244 sequence alterations classified as "likely disease-causing" affect the intronic sequences of the *CNGA3* gene, thereby representing only a minority within the comprehensive *CNGA3* variant database (Figure 3, Publication I, Appendix). Six of these intronic single nucleotide substitutions are directly located at the canonical splice sites, which are defined as the first two and last two positions of an intron, either resulting in a nucleotide exchange at these positions (c.-37-1G>C, c.101+1G>A, c.395+1G>T, c.450-1G>A, and c.674-2A>C) or in the duplication of three nucleotides at the exon/intron border (c.396-2_398dup). Based on the five used *in silico* splicing algorithms, five out of these six variants were consistently predicted to result in a decrease of the splice site strength and subsequently in a loss of the respective canonical donor or acceptor site, whereas the c.396-2_398dup variant was predicted to exert a minor effect on transcript splicing only by the SpliceAI *in silico* algorithm. Furthermore, two intronic variants are located in the close proximity of a highly conserved splice acceptor site (c.450-15T>G and c.396-11C>G) and are predicted to not only reduce the strength of the respective canonical splice acceptor site but also

activate an intronic cryptic acceptor site, thereby possibly interfering with normal transcript splicing. All eight canonical/non-canonical splice site variants in *CNGA3* were assessed in further studies using a minigene splice assay approach in HEK293T cells and/or murine cone photoreceptor–like 661W cells. These studies revealed that the variants caused different missplicing events ranging from intronic nucleotide retention, exonic nucleotide deletion to exon skipping, thereby producing one to six different transcripts (Burkard et al., 2018; Reuter et al., 2023). These observations are in line with the predictions of the *in silico* splicing algorithms – even for the variant c.396-2_398dup, for which only SpliceAI had predicted a minor effect on transcript splicing (Supplementary Table 3, Publication I, Appendix). This underlines the necessity for performing *in vitro* assays in order to interpret the pathogenic effect of the identified *CNGA3* variants in a correct manner.

8.1.5. Functional studies on CNGA3 missense variants and their contribution to the ACMG/AMP-based classification

Of the total 316 sequence alterations listed in the comprehensive *CNGA3* variant database, 205 are missense substitutions, of which a large number of 54 variants are classified as VUS according to the current ACMG/AMP classification guidelines and manual and expert-based revision. Comprehensive genetic information on these missense variants to obtain a clear classification as pathogenic or benign is lacking as these rare missense substitutions are often private to single patients and are usually not detected in recurrent independent patients originating from different families. In addition, they are either absent or identified at very low allele frequencies in the general population (gnomAD) (Sun et al., 2020; Solaki et al., 2022). This leaves the affected patients, the clinician and the genetic counsellor without clear information as to the relevance of a variant or genotype for the disease. Therefore, functional (*in vitro*) assays to assess the functionality of mutant CNGA3 channels and to finally validate the potential pathogenic effect of the respective *CNGA3* missense variants are needed.

Common methods used in different studies analysing a total of 54 missense alterations include calcium imaging and patch-clamp recordings of mutant CNGA3 channels expressed in heterologous systems such as HEK293 cells or *Xenopus laevis* oocytes. These functional data contributed to the classification of 41 missense variants as pathogenic and 11 as likely pathogenic. The previous studies have shown that the

variants negatively affected ligand sensitivity, gating, ion selectivity and protein folding and/or trafficking of CNGA3 channels or even lead to complete channel (function) loss (Tränkner et al., 2004; Liu and Varnum, 2005; Patel et al., 2005; Muraki-Oda et al., 2007; Koeppen et al., 2008; Reuter et al., 2008; Koeppen et al., 2010; Matveev et al., 2010; Dai and Varnum, 2013; Meighan et al., 2015; Shaikh et al., 2015; Kuniyoshi et al., 2016; Burkard et al., 2018). One missense variant remained a VUS even after functional testing because of conflicting results from different studies, showing either increased apparent ligand sensitivity or wild-type like characteristics of the mutant channels (Liu and Varnum, 2005; Muraki-Oda et al., 2007). Finally, one missense substitution could be confirmed as benign since a wildtype-like function in homomeric CNGA3 channels was observed using different functional approaches (Tränkner et al., 2004; Meighan et al., 2015). However, 150 out 204 currently known *CNGA3* missense variants remain functionally uncharacterized, of which a large number of 53 variants is of uncertain pathogenicity, highlighting the need to perform functional analysis of such variants to improve the classification of missense variants in the *CNGA3* gene.

8.2. Publication II: Functional evaluation allows ACMG/AMP-based re-classification of *CNGA3* variants associated with achromatopsia.

8.2.1. Further development and validation of the aequorin-based bioassay

As mentioned above, functional studies are sometimes the only mean to unambiguously assess the pathogenicity of sequence variants in the *CNGA3* gene since comprehensive genetic information is often lacking due to the rarity of the identified variants. This represents the main hurdle in genetic diagnosis of ACHM patients since these sequence alterations typically remain classified as VUS. As several gene therapy trials for *CNGA3*-associated ACHM have been conducted (NCT02610582, NCT02935517, NCT03758404, NCT03278873) (Fischer et al., 2020; Reichel et al., 2022), functional assays are needed to unequivocally classify the identified *CNGA3* variants, hereby facilitating the selection of patients who would be eligible for such interventions.

In a previously conducted study by Täger and colleagues, an *in vitro* bioassay based on the calcium-sensitive photoprotein aequorin was developed for the *CNGA3* gene. The objective was to perform a compound screening for chemical and pharmacological chaperones in order to ameliorate the surface localization of mutant trafficking-deficient CNGA3 channels (Täger et al., 2021).

One of the main aims of the present project was to expand the field of application of this existing bioassay so it can be used as a medium-throughput platform for the functional characterization of disease-associated variants detected in patients with *CNGA3*-ACHM. In order to perform the assay with medium throughput in a 96-well format, apo-aequorin was stably expressed in HEK293 cells (HEK293^{aequo} cells) transiently transfected with wild-type or mutant CNGA3-encoding plasmids. Luminescence measurement was performed using an automated luminometer, thereby recording the luminescence signals 6 seconds before and 394 seconds after automatic application of the membrane-permeable ligand 8-Br-cGMP. This further development of the assay enabled the parallel analysis of up to 11 mutant CNGA3 channels in comparison to the wild-type channels on one 96-well plate. For the final variant evaluation both the overall luminescence signal (area under the curve [AUC]) and the luminescence peak latency were assessed in a specific time window after ligand addition and compared to the values of the wild-type channels. To finally distinguish functionally normal from abnormal variant channels, thresholds for both the normalized AUC and the normalized peak latency were defined. For verification of CNGA3 protein expression, dot blot analysis was established and conducted by using whole lysates of the transfected HEK293^{aequo} cells.

In summary, the established luminescence assay detects the CNGA3 channel-mediated calcium influx following activation of the CNGA3 channels by the membrane-permeable ligand 8-Br-cGMP by using the calcium-sensitive reporter photoprotein aequorin. The generated transient luminescence signal is proportional to the amount of calcium present. It therefore correlates with the functionality of the CNGA3 channels tested, as these are the only cGMP-inducible calcium source in the HEK293^{aequo} cells. Thus, the bioassay allows assessment of CNGA3 channel functionality as a result of calcium conductivity and is capable of detecting variant CNGA3 channel dysfunction relative to wild-type channels.

The aequorin-based bioassay was evaluated regarding its reliability of discriminating between functionally normal and abnormal homomeric CNGA3 channels regardless of the defect in the mutant channel being evaluated. A total of 24 control *CNGA3* sequence alterations composed of nine benign and 15 pathogenic variants were selected to perform the assay validation (Supplementary Table 3, Publication II, Appendix). The benign variant dataset included a total of four missense variants either

showing wild-type-like function in homomeric CNGA3 channels in previously conducted experiments (n=1) (Tränkner et al., 2004; Meighan et al., 2015) or being detected homozygously in at least four healthy individuals on the gnomAD database (n=3) and five synonymous variants found on the gnomAD database. Finally, the pathogenic variant dataset was composed of 15 previously functionally characterized missense alterations either proven to display aberrant channel function (n=8) due to a variety of functional defects including aberrant ligand sensitivity, gating, ion selectivity and protein folding and/or trafficking, or completely absent channel function (n=7) compared to the wild-type channel (Tränkner et al., 2004; Liu and Varnum, 2005; Muraki-Oda et al., 2007; Koeppen et al., 2008; Reuter et al., 2008; Koeppen et al., 2010; Matveev et al., 2010).

All nine benign variants in the validation dataset displayed comparable luminescence responses as the CNGA3 wild-type channels with regard to overall luminescence and luminescence peak latency. The functional data obtained by the aequorin-based bioassay for the 15 pathogenic variants differed in comparison to CNGA3 wild-type channels indicating altered/impaired channel functionality. This was in line with the observations from previous studies using calcium imaging or electrophysiological recordings (Figure 1A and 1B, Publication II, Appendix). All seven pathogenic missense alterations previously displaying completely absent channel function were also identified as non-functional in the aequorin-based bioassay (Muraki-Oda et al., 2007; Koeppen et al., 2008; Reuter et al., 2008; Koeppen et al., 2010; Matveev et al., 2010). Furthermore, the used bioassay showed a sufficient sensitivity, as all eight pathogenic variants with residual channel function were also observed to have residual but aberrant luminescence signals compared to the wild-type channels (Tränkner et al., 2004; Liu and Varnum, 2005; Muraki-Oda et al., 2007; Koeppen et al., 2008; Reuter et al., 2008).

In order to distinguish functionally normal from abnormal variants, a receiver operating characteristic (ROC) analysis was performed to define thresholds for both the normalized AUC and the normalized peak latency. Since the aequorin-based bioassay provided a sufficient dynamic range between the benign and pathogenic variants evaluated in the assay validation dataset, it was possible to establish a total of three precise pathogenicity thresholds. The threshold for the normalized AUC was calculated to be at 0.65, thereby reaching a sensitivity of 93.3% as only one out of the

15 pathogenic assay validation variants could not be identified as functionally abnormal applying only this threshold. However, the specificity was 100%, as all nine benign variants of the assay validation dataset were correctly identified as functionally normal with respect to the AUC (Figure 1C and 1D, Publication II, Appendix). Two separate pathogenicity thresholds were set for the normalized peak latency – one for increased peak latency at 1.10, and one for reduced peak latency at 0.74, based on the functional data of the eight pathogenic variants with residual channel function and the nine benign variants of the assay validation dataset, reaching both a sensitivity and specificity of 100% (Figure 1C and 1E, Publication II, Appendix). By combining all three pathogenicity thresholds, a clear separation and correct classification as functionally normal and abnormal could be achieved for all 24 control *CNGA3* sequence alterations in the assay validation dataset (Figure 1F, Publication II, Appendix). Additionally, expression verification in all tested samples of the 24 assay validation variants was performed by Western blot and dot blot analysis of whole-cell lysates confirming CNGA3 protein expression (Supplementary Figure 2 and 7, Publication II, Appendix). Finally, 15 individual assay plates containing both positive (HEK293^{aequo} cells transfected with the CNGA3 wild-type expression construct) and negative controls (untransfected HEK293^{aequo} cells) were used to calculate the Z' factor to assess the overall assay quality. As the mean Z' factor was shown to be 0.87±0.08 (median: 0.9), an excellent assay quality could be confirmed. To sum up, the aequorin-based bioassay could therefore be used as a strong line of evidence to evaluate mutant CNGA3 channel function and to re-classify ACHM-associated *CNGA3* variants in the ACMG/AMP classification system.

8.2.2. Functional analysis of 150 CNGA3 missense variants using the aequorin-based bioassay

Using the aequorin-based luminescence bioassay, the present study aimed to functionally assess and re-classify a total of 149 *CNGA3* missense variants lacking functional data, and one *CNGA3* missense alteration displaying conflicting results in previously conducted studies (Liu and Varnum, 2005; Muraki-Oda et al., 2007). All analysed variants were thereby retrieved from the comprehensive *CNGA3* variant database compiled by Solaki et al. (n=147 variants) (Solaki et al., 2022), the LOVD database (n=2) and an ACHM cohort study recently published by Brunetti-Pierri et al. (n=1) (Brunetti-Pierri et al., 2021).

Of the 150 functionally evaluated *CNGA3* missense alterations, a high number of 80 variants were shown to encode non-functional channels displaying no increase in the luminescence signal after application of the ligand 8-Br-cGMP for channel activation (Figure 2, Publication II, Appendix). This corresponds to 53.3% of all analysed variants which is consistent with the findings of previous functional studies, in which 50% of the 54 missense variants analysed thus far were found to significantly impair channel functionality (Tränkner et al., 2004; Liu and Varnum, 2005; Patel et al., 2005; Muraki-Oda et al., 2007; Koeppen et al., 2008; Koeppen et al., 2010; Matveev et al., 2010; Shaikh et al., 2015). Most of these variants designated as non-functional using the aequorin-based bioassay are located in functional or structural relevant domains of the CNGA3 protein. These include the transmembrane helices/pore helix (n=33 variants), the CNBD (n=23), and the C-linker (n=7), all of them showing a high level of conservation across the CNGA3 orthologs and its rod equivalent CNGA1. This suggests that the CNGA3 polypeptide is particularly susceptible to exhibit a functional defect due to an amino acid substitution in these domains.

Thirty-six CNGA3 variant channels displayed overall luminescence signals similar to the wild-type channel. However, five of these exhibited an increased and six variants – predominantly located in the CLZ domain – a reduced luminescence peak latency compared to the wild-type channel. This ultimately led to the classification of these variants as functionally abnormal emphasising the necessity to consider both measures for final variant evaluation.

In contrast, the remaining 25 missense alterations, of which 11 affected amino acid residues in the aminoterminal part of the CNGA3 polypeptide, additionally displayed wild-type-like luminescence peak latency values rendering them as functionally normal. Furthermore, 34 CNGA3 variant channels demonstrated diminished overall luminescence values in comparison to the wild-type channel. In addition, 27 of these missense variant channels displayed increased luminescence peak latency values, and three exhibited reduced values in comparison to wild-type channels. These findings led to the classification of these 34 variant channels as functionally abnormal (Figure 2 and 3, Publication II, Appendix). Finally, the successful expression of all analysed variant channels in the transiently transfected HEK293^{aequo} cells was confirmed by dot blot analysis and, in one instance, by Western blot analysis of whole cell lysates. This ruled out the possibility of e.g. cell transfection failure or defective

CNGA3 expression constructs being the cause of reduced or absent luminescence signals in the bioassay (Supplementary Figure 2 and 7, Publication II, Appendix).

8.2.3. ACMG/AMP-based re-classification of 150 CNGA3 missense variants based on functional data

The functional data obtained by the aequorin-based bioassay were subsequently used for the ACMG/AMP-based re-classification of the 150 analysed *CNGA3* missense substitutions. As the bioassay was deemed to constitute a strong line of evidence for the evaluation of mutant CNGA3 channels following the successful assay validation, the criterion PS3_strong was applied to 125 functionally abnormal missense substitutions whereas BS3_strong was assigned to 25 missense variants observed to give rise to functionally normal CNGA3 channels (Supplementary Table 4, Publication II, Appendix). Based on this approach, the initial ACMG/AMP classification of the two likely benign and 92 of the 93 (likely) pathogenic variants could be confirmed or even downgraded to benign or upgraded to pathogenic, respectively (Figure 4A, 4C, and 5, Publication II, Appendix).

However, one missense substitution – the p.(Arg436Gln) variant – initially classified as likely pathogenic was re-classified as VUS (Figure 4C and 5, Publication II, Appendix). In contrast to the known pathogenic alternative amino acid substitution p.(Arg436Trp) at the same codon, which displayed an impaired responsiveness to ligands and cytosolic aggregation resulting in a complete loss of channel functionality (Wissinger et al., 2001; Muraki-Oda et al., 2007; Matveev et al., 2010), the p.(Arg436Gln) variant was identified as functionally normal showing both wild-type-like overall luminescence signals and peak latency in the aequorin-based bioassay. Given its rarity in the general population (gnomAD), its deleterious *in silico* prediction, and its localization at a completely conserved amino acid residue in the C-linker region, where a known pathogenic alternative amino acid exchange has already been described in the scientific literature, even the application of the functional data as a strong line of evidence only resulted in a post-assay ACMG/AMP classification as VUS. Since the p.(Arg436Gln) variant was only observed once as part of a complex allele together with the pathogenic variant p.(Phe322Ser) (Li et al., 2014), its contribution to the disease phenotype in this ACHM patient remains elusive. Nevertheless, this case reinforces the need for functionally analysing novel missense variants, as demonstrated by the

differential impact that missense alterations can have on CNGA3 protein function, even when affecting the same amino acid residue.

One of the main aims of the present study was to provide an unambiguous classification based on functional evaluation for a total of 55 missense variants in the *CNGA3* gene, which have been previously designated as uncertain in terms of their pathogenicity, to finally assure molecular diagnosis to the ACHM patients carrying such variants. Using our medium-throughput functional approach, one of 55 VUS could be re-classified as benign, 18 of 55 as likely benign, and 33 of 55 as likely pathogenic, hereby considerably consolidating variant interpretation in a clinical context by reaching a VUS re-classification rate of 94.5% (Figure 4B and 5, Publication II, Appendix). One example for a VUS re-classified as likely pathogenic with the aid of the aequorin-based bioassay is the missense variant p.(Asn471Ser). This sequence alteration has so far only been observed as a single heterozygous variant in a patient affected by cone-rod dystrophy (Wissinger et al., 2001) and previous functional characterizations yielded conflicting results displaying either an increased apparent ligand sensitivity or no change compared to homomeric wild-type channels (Liu and Varnum, 2005; Muraki-Oda et al., 2007). The functional data obtained by the aequorin-based bioassay provided evidence to support the observation of altered variant channel function as postulated by Liu and Varnum (Liu and Varnum, 2005). This was demonstrated by the detection of a reduction in luminescence peak latency in the context of an unaltered overall luminescence signal, deeming the variant CNGA3 channel as functionally abnormal, ultimately resulting in a post-assay ACMG/AMP classification as likely pathogenic.

In contrast, ACMG/AMP-based variant re-classification from VUS to another pathogenicity class was unsuccessful for three missense substitutions located in the CNBD and CLZ domains despite characterizing these variants as functionally normal in the aequorin-based bioassay. Following the ACMG/AMP rules, application of the functional data as strong evidence (BS3_strong) was not sufficient to shift the classification of the variants p.(Lys595Arg), p.(Arg646His), and p.(Val669Leu) (Figure 4B and 5, Publication II, Appendix). However, it was still proposed that these sequence alterations may not result in a functional defect in the CNGA3 protein, given the unambiguous functional evidence provided by the luminescence bioassay and the currently available genotype data. The p.(Arg646His) variant has only been observed

in a single heterozygous state lacking a second disease-associated allele (Li et al., 2014), whereas for the p.(Lys595Arg) and p.(Val669Leu) variants no genotype could be established as this information was not provided in the respective ClinVar database entries (ClinVar Variation IDs: 896798 and 897276), a limitation of these variant databases.

8.2.4. Further functional in vitro studies and their influence on VUS re-classification in a variety of genes

In conclusion, incorporating the outcome of the functional data in the ACMG/AMP-based classification system resulted in a VUS re-classification rate of 94.5%, with 52 of the 55 analysed VUS in the *CNGA3* gene being re-classified as either (likely) benign or likely pathogenic. This result is comparable or even superior to other functional studies that have been used to improve the classification of a high number of VUS in genes such as *BRCA2* and *OTC* thereby reaching re-classification rates between 68.8% and 92.5% (Richardson et al., 2021; Hu et al., 2022; Lo et al., 2023). Two of these functional studies used a validated functional assay to assess the pathogenicity of missense variants in the *BRCA2* gene by measuring homologous recombination DNA-repair activity. The application of these protein functional data in the ACMG/AMP-based classification framework led to the re-classification of 132 of 154 tested *BRCA2* VUS (86%) in the first study (Richardson et al., 2021) and 62 of 67 VUS (92.5%) in the second approach, determining the clinical relevance of these variants (Hu et al., 2022). Moreover, a high-throughput complementation assay was used by Lo and colleagues to differentiate between benign and pathogenic variants, as well as neonatal and late-onset disease variants in the *OTC* gene based on their functional impact. Subsequent pilot ACMG/AMP-based re-classification of 34 missense variants with complete loss of activity, previously classified as VUS, changed the classification of 22 of these missense substitutions (68.8%) to clinically actionable, likely pathogenic variants (Lo et al., 2023).

Functional approaches for facilitation of variant interpretation have also been developed for other IRD-associated genes such as *RHO* and *ABCA4* (Wan et al., 2019; Curtis et al., 2020; Garces et al., 2020). Using a higher-throughput flow cytometry-based assay, three out of nine rare *RHO* VUS identified through genetic diagnostic testing could be linked to be causative for the RP phenotype in these pedigrees due to pathogenic surface expression levels detected in the assay (Wan et

al., 2019). Furthermore, Curtis and colleagues determined the effect of 22 disease-causing missense variants in the *ABCA4* gene on ABCA4 protein expression and ATPase activity. The researchers established three different variant classes, depending on the extend of the functional defect, which correlated with disease onset and severity in individuals affected by Stargardt disease 1 (STGD1) carrying these variants in a homozygous state. These results provide a better understanding of genotype-phenotype correlations in STGD1 patients (Curtis et al., 2020). In summary, the high VUS re-classification rates achieved in this work and the studies mentioned above show that functional assays are essential powerful tools for improving the classification of sequence variants and can significantly improve molecular diagnostics in patients.

8.2.5. Limitations of the aequorin-based bioassay

However, the aequorin-based bioassay shows some limitations which need to be taken into consideration when interpreting the obtained functional data. The native cone CNG channel is composed of CNGA3 and CNGB3 subunits. The assessed variant channels were heterologously expressed as homomeric CNGA3 channels in the absence of the modulatory CNGB3 subunit in the HEK293^{aequo} cells. In studies conducted previously, it has been shown that the presence of the wild-type CNGB3 subunit can improve functionality of heteromeric CNG channels with variants in the CNGA3 subunit. However, only a partial rescue effect was achieved for five of 54 missense variants by co-expressing the CNGB3 subunit in combination with lowering the cell cultivation temperature from the standard 37°C to 27°C to support protein folding and trafficking. Nevertheless, wild-type-like function could not be restored as these variant heteromeric channels still exhibited altered biophysical properties (Liu and Varnum, 2005; Muraki-Oda et al., 2007; Reuter et al., 2008; Koeppen et al., 2010). It can therefore be concluded that the assessment of CNGA3 variant effects in homomeric channels is a sufficient and effective method for the evaluation of pathogenicity. In the current assay set up, the assessed variant homomeric channels carried only a single missense alteration in the CNGA3 subunit, which reflects a homozygous genotype in ACHM patients. But two recent ACHM cohort studies have shown that most patients with *CNGA3*-associated ACHM – ranging from 61.8% to 79.4% – harbour two (likely compound) heterozygous variants (Sun et al., 2020; Solaki et al., 2022). It is feasible to co-express two mutant CNGA3 subunits carrying two distinct missense variants in the HEK293^{aequo} cells. As the final subunit composition of the resulting channels could

not be reconstructed, the informative value of how these mutant subunits would interact with each other and influence CNGA3 protein function would only be limited. Finally, interference with splicing was suspected by using *in silico* splicing algorithms for a total of three missense variants tested in the aequorin-based bioassay including p.(Arg189Lys), p.(Thr224Ala), and p.(Thr224Ile). The suspected splicing effect for these variants located at the exon-intron borders could not be evaluated in the context of the bioassay since a *CNGA3* cDNA expression construct was used. This limitation was overcome by performing minigene splice assays in a complementary study, showing that only the p.(Arg189Lys) variant interfered with splicing resulting in the use of an exonic cryptic donor site in a minor fraction of transcripts (Reuter et al., 2023). In contrast, an impairment of CNGA3 channel function could be observed for all three tested variants in the aequorin-based bioassay demonstrating that these alterations exert a pathogenic effect by acting as missense variants rather than as splicing variants. However, these results underline the importance to combine both the aequorin-based bioassay and a minigene splice assay to conclusively evaluate the pathogenicity of *CNGA3* variants located at the exon-intron borders of the gene.

In conclusion, despite the limitations listed above, the medium-throughput aequorin-based bioassay still exhibited important implications for clinical variant interpretation by re-classifying 94.5% of the tested *CNGA3* VUS and substantially improving genetic diagnosis for patients with *CNGA3*-associated ACHM carrying such missense substitutions, thereby enabling their selection for future gene therapeutic interventions.

8.3. Publication III: Paternal uniparental isodisomy of chromosome 2 in a patient with *CNGA3*-associated autosomal recessive achromatopsia.

8.3.1. Ophthalmological and genetic examination of the respective ACHM patient

The present study reported the first case of ACHM which was caused by uniparental isodisomy (UPD) of chromosome 2. The female patient of Italian origin presented with photophobia since birth and received a clinical diagnosis of ACHM at the age of 10 years. Ophthalmological examinations of this patient revealed a visual acuity of 20/200 Snellen, severely reduced cone responses and abnormal rod responses as well as abnormal dark adaptation curves and colour vision typical for ACHM.

Furthermore, a fine pendular nystagmus was observed. Her family history regarding ACHM was reported to be negative.

The patient was subsequently referred to the Centre for Ophthalmology Tübingen to perform genetic testing in a research setting. Sanger sequencing of all coding exons of the *CNGA3* gene identified the missense variant c.778G>C; p.(Asp260His) located in the coding exon 8 in an apparent homozygous state. The detected variant had not been previously reported in the scientific literature or in various mutation databases including HGMD®, ClinVar, and LOVD. According to the ACMG/AMP guidelines, the missense substitution was initially classified as likely pathogenic based on its low MAF of <0.039% in the reference population database gnomAD, the localization of the variant in the transmembrane domain TM3 affecting a completely conserved amino acid residue (Figure 1C, Publication III, Appendix) at which an alternative amino acid substitution p.(Asp260Asn) had already been identified as pathogenic (Wissinger et al., 2001; Solaki et al., 2022), and the *in silico* prediction as disease-causing by various tools.

8.3.2. Functional evaluation of the identified CNGA3 missense variant

Functional characterization of the p.(Asp260His) variant using the bioluminescent aequorin-based bioassay in HEK293 cells transiently expressing apo-aequorin and CNGA3 revealed that this missense alteration results in a complete loss of channel function (Figure 2A, Publication III, Appendix) similar to the alternative amino acid substitution p.(Asp260Asn) which has also been shown to completely abolish channel function in a previous *in vitro* study (Muraki-Oda et al., 2007). Despite the undetectable calcium influx in the aequorin-based bioassay, the expression of the mutant CNGA3 channel carrying the p.(Asp260His) variant could be confirmed by immunocytochemistry in the transfected cells (Figure 2B, Publication III, Appendix). In conclusion, the pathogenicity of the analysed missense substitution could be confirmed thereby upgrading its ACMG/AMP-based classification to pathogenic (Solaki et al., 2023). The presented case was also included in the ACHM study cohort genetically characterized in Tübingen thereby expanding the spectrum of disease-associated *CNGA3* variants (Solaki et al., 2022).

8.3.3. Segregation analysis and confirmation of UPD of chromosome 2

To confirm the homozygosity of the missense variant c.778G>C; p.(Asp260His) in the patient, segregation analysis by PCR and Sanger sequencing was performed in both parents. Surprisingly, only the patient's father was identified to be a heterozygous carrier whereas the variant was absent in the patient's mother (Figure 1A, Publication III, Appendix). As a heterozygous deletion on the second allele was excluded in the mother by long-distance PCR and a SYBR Green-based quantitative real-time PCR copy number assay, a microsatellite marker analysis using a total of ten markers covering the entire chromosome 2 was executed in the three family members. This analysis revealed that the patient was homozygous for all ten markers for the paternal allele providing evidence that the homozygosity of the *CNGA3* variant identified in the patient resulted from a partial or complete paternal uniparental isodisomy (UPD) of chromosome 2 (Figure 1B, Publication III, Appendix).

8.3.4. Further cases of UPD of chromosome 2 in the scientific literature

So far, maternal or paternal UPD of chromosome 2 was described as the underlying cause of an autosomal recessive disorder in a total of 42 cases in the scientific literature. In these cases, the respective recessive variant manifested in the patient through inheritance of two copies of the recessive variant from a single parent due to the UPD (Kelkar et al., 2024). In the context of ocular disorders such as primary congenital glaucoma, retinal dystrophy, and syndromes with retinal involvement, including Alström syndrome and Jalili syndrome, five cases of UPD2 have been reported involving the genes *CYP1B1*, *MERTK*, *CNNM4*, and *ALMS1*, respectively (Thompson et al., 2002; Lopez-Garrido et al., 2009; Souzeau et al., 2019; Prasov et al., 2020; Lopour et al., 2023; Kelkar et al., 2024). However, phenotypically normal and generally healthy individuals with UPD2 have also been identified in several studies by genome-wide SNP scan or parentage testing (Bernasconi et al., 1996; Heide et al., 2000; Keller et al., 2009; Ou et al., 2013; Chen et al., 2019; Zhang et al., 2019; Doniec et al., 2021; Song et al., 2021; Kelkar et al., 2024). A total of six genes on chromosome 2 have either been predicted (i.e., *OTX1*, *VAX2*, *CYP1B1*) or experimentally confirmed to be imprinted (i.e., *LRRTM1*, *GPR1*, *ZDBF2*) based on the imprinted gene database Geneimprint (https://www.geneimprint.com/site/genes-by-species). Nevertheless, no association between these genes and imprinting diseases has been described thus far according to the OMIM® database (https://omim.org). These findings indicate that the disease phenotype in UPD2 cases rather results from manifesting classical point

variants than imprinting effects, which is also in-line with the observation made in the present study where the described UPD2 patient is of general good health only showing the isolated retinal phenotype of ACHM.

In summary, the present study reported the first case of ACHM which was caused by paternal UPD of chromosome 2. The UPD2 thereby uncovered the recessive missense variant c.778G>C; p.(Asp260His) in *CNGA3* in the patient's father, which ultimately is causative for ACHM in the index patient. The study presented herein underlines the necessity of performing segregation analysis in both parents especially in patients with recessive variants in an apparent homozygous state, as UPD has considerable implications for genetic counselling with a very low recurrence risk assessment in these families. Furthermore, the study demonstrated the importance of functionally analysing rare missense variants in *CNGA3* as the identified missense variant c.778G>C; p.(Asp260His) could be classified as pathogenic using the bioluminescent aequorin-based bioassay thereby confirming the molecular genetic diagnosis of the presented index patient.

8.4. Conclusion and outlook

In conclusion, the present doctoral thesis substantially expanded the *CNGA3* variant spectrum to a total of 316 sequence alterations by compiling genetic data from a large in-house ACHM cohort of 889 independent families with those reported in the scientific literature and public variant databases further underlining the importance of the *CNGA3* gene as one of the major disease-causing genes in ACHM. By providing extensive *in silico* variant assessment data, ACMG/AMP classification, and manual/expert-based variant categorization for the identified variants, a total of 244 sequence alterations could be interpreted as "likely disease-causing" (Solaki et al., 2022). As a high number of missense substitutions in the *CNGA3* gene was functionally uncharacterized and still of uncertain pathogenicity, a medium-throughput aequorin-based luminescence bioassay in transiently transfected HEK293^{aequo} cells was established and validated using a set of benign and pathogenic *CNGA3* sequence alterations. Using this bioassay, functional data were generated for a total of 150 missense variants, of which 55 were of uncertain pathogenicity (VUS), displaying 25 as functionally normal and 125 as functionally abnormal. The obtained functional data had a substantial impact on the ACMG/AMP-based re-classification of the analysed variants as 52 of 55 VUS could be re-classified as either (likely) benign or

likely pathogenic resulting in a VUS re-classification rate of 94.5% (Solaki et al., 2023). Furthermore, the missense variant c.778G>C; p.(Asp260His) identified in a homozygous state as a result of paternal UPD2 in a patient of the in-house ACHM study cohort was proven to completely abolish CNGA3 channel function using the aequorin-based bioassay thereby re-classifying the variant from likely pathogenic to pathogenic (Kohl et al., 2021; Solaki et al., 2023).

To sum up, the functional data presented in this doctoral thesis substantially facilitated the clinical variant interpretation of the analysed *CNGA3* missense variants. Molecular genetic diagnosis could therefore be improved for ACHM patients carrying these *CNGA3* variants making them eligible for future gene therapeutic interventions. In future studies, the presented bioassay could be adapted to functionally characterize missense variants in other IRD-associated genes coding for subunits of CNG channels such as *CNGB3* in ACHM and *CNGA1*/*CNGB1* in autosomal recessive retinitis pigmentosa potentially facilitating variant interpretation in these genes.

9. References

Aboshiha, J., Luong, V., Cowing, J., Dubis, A. M., Bainbridge, J. W., Ali, R. R., et al. (2014). Dark-adaptation functions in molecularly confirmed achromatopsia and the implications for assessment in retinal therapy trials. *Invest Ophthalmol Vis Sci,* 55(10), 6340–6349. doi:10.1167/iovs.14-14910.

Aligianis, I. A., Forshew, T., Johnson, S., Michaelides, M., Johnson, C. A., Trembath, R. C., et al. (2002). Mapping of a novel locus for achromatopsia (ACHM4) to 1p and identification of a germline mutation in the alpha subunit of cone transducin (GNAT2). *J Med Genet,* 39(9), 656–660. doi:10.1136/jmg.39.9.656.

Altenhofen, W., Ludwig, J., Eismann, E., Kraus, W., Bonigk, W., and Kaupp, U. B. (1991). Control of ligand specificity in cyclic nucleotide-gated channels from rod photoreceptors and olfactory epithelium. *Proc Natl Acad Sci U S A,* 88(21), 9868–9872. doi:10.1073/pnas.88.21.9868.

Amaral, R. A. S., Motta, F. L., Zin, O. A., da Palma, M. M., Rodrigues, G. D., and Sallum, J. M. F. (2023). Molecular and Clinical Characterization of CNGA3 and CNGB3 Genes in Brazilian Patients Affected with Achromatopsia. *Genes (Basel),* 14(6). doi:10.3390/genes14061296.

Andersen, M. K. G., Bertelsen, M., Gronskov, K., Kohl, S., and Kessel, L. (2023). Genetic and Clinical Characterization of Danish Achromatopsia Patients. *Genes (Basel),* 14(3). doi:10.3390/genes14030690.

Andreasson, S., and Tornqvist, K. (1991). Electroretinograms in patients with achromatopsia. *Acta Ophthalmol (Copenh),* 69(6), 711–716. doi:10.1111/j.1755-3768.1991.tb02048.x.

Ansar, M., Santos-Cortez, R. L., Saqib, M. A., Zulfiqar, F., Lee, K., Ashraf, N. M., et al. (2015). Mutation of ATF6 causes autosomal recessive achromatopsia. *Hum Genet,* 134(9), 941–950. doi:10.1007/s00439-015-1571-4.

Arshavsky, V. Y., Lamb, T. D., and Pugh, E. N., Jr. (2002). G proteins and phototransduction. *Annu Rev Physiol,* 64, 153–187. doi:10.1146/annurev.physiol.64.082701.102229.

Baehr, W., Wu, S. M., Bird, A. C., and Palczewski, K. (2003). The retinoid cycle and retina disease. *Vision Res,* 43(28), 2957–2958. doi:10.1016/j.visres.2003.10.001.

Barret, D. C. A., Kaupp, U. B., and Marino, J. (2022a). The structure of cyclic nucleotide-gated channels in rod and cone photoreceptors. *Trends Neurosci,* 45(10), 763–776. doi:10.1016/j.tins.2022.07.001.

Barret, D. C. A., Schertler, G. F. X., Kaupp, U. B., and Marino, J. (2022b). The structure of the native CNGA1/CNGB1 CNG channel from bovine retinal rods. *Nat Struct Mol Biol,* 29(1), 32–39. doi:10.1038/s41594-021-00700-8.

Beavo, J., Francis, S. H., and Houslay, M. D. (2007). *Cyclic nucleotide phosphodiesterases in health and disease*. Boca Raton: CRC Press/Taylor & Francis.

Bernasconi, F., Karaguzel, A., Celep, F., Keser, I., Luleci, G., Dutly, F., et al. (1996). Normal phenotype with maternal isodisomy in a female with two isochromosomes: i(2p) and i(2q). *Am J Hum Genet,* 59(5), 1114–1118.

Biel, M., and Michalakis, S. (2009). Cyclic nucleotide-gated channels. *Handb Exp Pharmacol* (191), 111–136. doi:10.1007/978-3-540-68964-5_7.

Biskup, C., Kusch, J., Schulz, E., Nache, V., Schwede, F., Lehmann, F., et al. (2007). Relating ligand binding to activation gating in CNGA2 channels. *Nature,* 446(7134), 440–443. doi:10.1038/nature05596.

Bönigk, W., Altenhofen, W., Muller, F., Dose, A., Illing, M., Molday, R. S., et al. (1993). Rod and cone photoreceptor cells express distinct genes for cGMP-gated channels. *Neuron,* 10(5), 865–877. doi:10.1016/0896-6273(93)90202-3.

Bowmaker, J. K., Dartnall, H. J., and Mollon, J. D. (1980). Microspectrophotometric demonstration of four classes of photoreceptor in an old world primate, Macaca fascicularis. *J Physiol,* 298, 131–143. doi:10.1113/jphysiol.1980.sp013071.

Brunetti-Pierri, R., Karali, M., Melillo, P., Di Iorio, V., De Benedictis, A., Iaccarino, G., et al. (2021). Clinical and Molecular Characterization of Achromatopsia Patients: A Longitudinal Study. *Int J Mol Sci,* 22(4). doi:10.3390/ijms22041681.

Burkard, M., Kohl, S., Kratzig, T., Tanimoto, N., Brennenstuhl, C., Bausch, A. E., et al. (2018). Accessory heterozygous mutations in cone photoreceptor CNGA3 exacerbate CNG channel-associated retinopathy. *J Clin Invest,* 128(12), 5663–5675. doi:10.1172/JCI96098.

Chang, B., Grau, T., Dangel, S., Hurd, R., Jurklies, B., Sener, E. C., et al. (2009). A homologous genetic basis of the murine cpfl1 mutant and human achromatopsia linked to mutations in the PDE6C gene. *Proc Natl Acad Sci U S A,* 106(46), 19581–19586. doi:10.1073/pnas.0907720106.

Chen, M., Jiang, J., Li, C., Ren, H., Chen, W., Liu, Z., et al. (2019). Non-pathological complete paternal uniparental isodisomy of chromosome 2 revealed in a maternity testing case. *Int J Legal Med,* 133(4), 993–997. doi:10.1007/s00414-018-1857-x.

Cook, N. J., Hanke, W., and Kaupp, U. B. (1987). Identification, purification, and functional reconstitution of the cyclic GMP-dependent channel from rod photoreceptors. *Proc Natl Acad Sci U S A,* 84(2), 585–589. doi:10.1073/pnas.84.2.585.

Curcio, C. A., Sloan, K. R., Kalina, R. E., and Hendrickson, A. E. (1990). Human photoreceptor topography. *J Comp Neurol,* 292(4), 497–523. doi:10.1002/cne.902920402.

Curtis, S. B., Molday, L. L., Garces, F. A., and Molday, R. S. (2020). Functional analysis and classification of homozygous and hypomorphic ABCA4 variants associated with Stargardt macular degeneration. *Hum Mutat,* 41(11), 1944–1956. doi:10.1002/humu.24100.

Dai, G., Peng, C., Liu, C., and Varnum, M. D. (2013). Two structural components in CNGA3 support regulation of cone CNG channels by phosphoinositides. *J Gen Physiol,* 141(4), 413–430. doi:10.1085/jgp.201210944.

Dai, G., and Varnum, M. D. (2013). CNGA3 achromatopsia-associated mutation potentiates the phosphoinositide sensitivity of cone photoreceptor CNG channels by altering intersubunit interactions. *Am J Physiol Cell Physiol,* 305(2), C147–159. doi:10.1152/ajpcell.00037.2013.

Doniec, A., Luczak, W., Wrobel, M., Janula, M., Ossowski, A., Grzmil, P., et al. (2021). Confirmation of Paternity despite Three Genetic Incompatibilities at Chromosome 2. *Genes (Basel),* 12(1). doi:10.3390/genes12010062.

Ellard, S., Baple, E., Callaway, A., Berry, I., Forrester, N., Turnbull, C., et al. (2020). ACGS best practice guidelines for variant classification in rare disease 2020. *Retrieved from: https://www.acgs.uk.com/media/11631/uk-practice-guidelines-for-variant-classification-v4-01-2020.pdf*.

Faillace, M. P., Bernabeu, R. O., and Korenbrot, J. I. (2004). Cellular processing of cone photoreceptor cyclic GMP-gated ion channels: a role for the S4 structural motif. *J Biol Chem,* 279(21), 22643–22653. doi:10.1074/jbc.M400035200.

Felden, J., Baumann, B., Ali, M., Audo, I., Ayuso, C., Bocquet, B., et al. (2019). Mutation spectrum and clinical investigation of achromatopsia patients with mutations in the GNAT2 gene. *Hum Mutat,* 40(8), 1145–1155. doi:10.1002/humu.23768.

Finnemann, S. C. (2003). Focal adhesion kinase signaling promotes phagocytosis of integrin-bound photoreceptors. *EMBO J,* 22(16), 4143–4154. doi:10.1093/emboj/cdg416.

Fischer, M. D., Michalakis, S., Wilhelm, B., Zobor, D., Muehlfriedel, R., Kohl, S., et al. (2020). Safety and Vision Outcomes of Subretinal Gene Therapy Targeting Cone Photoreceptors in Achromatopsia: A Nonrandomized Controlled Trial. *JAMA Ophthalmol,* 138(6), 643–651. doi:10.1001/jamaophthalmol.2020.1032.

François, J. (1961). *Heredity in ophthalmology*. St. Louis: Mosby.

Franze, K., Grosche, J., Skatchkov, S. N., Schinkinger, S., Foja, C., Schild, D., et al. (2007). Muller cells are living optical fibers in the vertebrate retina. *Proc Natl Acad Sci U S A,* 104(20), 8287–8292. doi:10.1073/pnas.0611180104.

Fu, Y., and Yau, K. W. (2007). Phototransduction in mouse rods and cones. *Pflugers Arch,* 454(5), 805–819. doi:10.1007/s00424-006-0194-y.

Gal, A., Li, Y., Thompson, D. A., Weir, J., Orth, U., Jacobson, S. G., et al. (2000). Mutations in MERTK, the human orthologue of the RCS rat retinal dystrophy gene, cause retinitis pigmentosa. *Nat Genet,* 26(3), 270–271. doi:10.1038/81555.

Garafalo, A. V., Sheplock, R., Sumaroka, A., Roman, A. J., Cideciyan, A. V., and Jacobson, S. G. (2021). Childhood-onset genetic cone-rod photoreceptor diseases and underlying pathobiology. *EBioMedicine,* 63, 103200. doi:10.1016/j.ebiom.2020.103200.

Garces, F. A., Scortecci, J. F., and Molday, R. S. (2020). Functional Characterization of ABCA4 Missense Variants Linked to Stargardt Macular Degeneration. *Int J Mol Sci,* 22(1). doi:10.3390/ijms22010185.

Georgiou, M., Singh, N., Kane, T., Zaman, S., Hirji, N., Aboshiha, J., et al. (2020). Long-Term Investigation of Retinal Function in Patients with Achromatopsia. *Invest Ophthalmol Vis Sci,* 61(11), 38. doi:10.1167/iovs.61.11.38.

Gofman, Y., Scharfe, C., Marks, D. S., Haliloglu, T., and Ben-Tal, N. (2014). Structure, dynamics and implied gating mechanism of a human cyclic nucleotide-gated channel. *PLoS Comput Biol,* 10(12), e1003976. doi:10.1371/journal.pcbi.1003976.

Grigoryan, E. N. (2022). Self-Organization of the Retina during Eye Development, Retinal Regeneration In Vivo, and in Retinal 3D Organoids In Vitro. *Biomedicines,* 10(6). doi:10.3390/biomedicines10061458.

He, W., Cowan, C. W., and Wensel, T. G. (1998). RGS9, a GTPase accelerator for phototransduction. *Neuron,* 20(1), 95–102. doi:10.1016/s0896-6273(00)80437-7.

Heide, E., Heide, K. G., and Rodewald, A. (2000). Maternal uniparental disomy (UPD) for chromosome 2 discovered by exclusion of paternity. *Am J Med Genet,* 92(4), 260–263.

Hirji, N., Aboshiha, J., Georgiou, M., Bainbridge, J., and Michaelides, M. (2018). Achromatopsia: clinical features, molecular genetics, animal models and therapeutic options. *Ophthalmic Genet,* 39(2), 149–157. doi:10.1080/13816810.2017.1418389.

Hu, C., Susswein, L. R., Roberts, M. E., Yang, H., Marshall, M. L., Hiraki, S., et al. (2022). Classification of BRCA2 Variants of Uncertain Significance (VUS) Using an ACMG/AMP Model Incorporating a Homology-Directed Repair (HDR) Functional Assay. *Clin Cancer Res,* 28(17), 3742–3751. doi:10.1158/1078-0432.CCR-22-0203.

Hu, G., and Wensel, T. G. (2002). R9AP, a membrane anchor for the photoreceptor GTPase accelerating protein, RGS9-1. *Proc Natl Acad Sci U S A,* 99(15), 9755–9760. doi:10.1073/pnas.152094799.

Hussey, K. A., Hadyniak, S. E., and Johnston, R. J., Jr. (2022). Patterning and Development of Photoreceptors in the Human Retina. *Front Cell Dev Biol,* 10, 878350. doi:10.3389/fcell.2022.878350.

Johnson, S., Michaelides, M., Aligianis, I. A., Ainsworth, J. R., Mollon, J. D., Maher, E. R., et al. (2004). Achromatopsia caused by novel mutations in both CNGA3 and CNGB3. *J Med Genet,* 41(2), e20. doi:10.1136/jmg.2003.011437.

Joselevitch, C. (2008). Human retinal circuitry and physiology. *Psychology & Neuroscience,* 1(2), 141–165. doi:10.3922/j.psns.2008.2.008.

Karczewski, K. J., Francioli, L. C., Tiao, G., Cummings, B. B., Alfoldi, J., Wang, Q., et al. (2020). The mutational constraint spectrum quantified from variation in 141,456 humans. *Nature,* 581(7809), 434–443. doi:10.1038/s41586-020-2308-7.

Kaupp, U. B., and Seifert, R. (2002). Cyclic nucleotide-gated ion channels. *Physiol Rev,* 82(3), 769–824. doi:10.1152/physrev.00008.2002.

Kawamura, S., and Tachibanaki, S. (2008). Rod and cone photoreceptors: molecular basis of the difference in their physiology. *Comp Biochem Physiol A Mol Integr Physiol,* 150(4), 369–377. doi:10.1016/j.cbpa.2008.04.600.

Kelkar, J., DiMaio, M., Ma, D., and Zhang, H. (2024). Maternal Uniparental Isodisomy of Chromosome 2 Leading to Homozygous Variants in SPR and ZNF142 : A Case Report and Review of the UPD2 Literature. *Glob Med Genet,* 11(1), 100–112. doi:10.1055/s-0044-1785442.

Keller, M. C., McRae, A. F., McGaughran, J. M., Visscher, P. M., Martin, N. G., and Montgomery, G. W. (2009). Non-pathological paternal isodisomy of chromosome 2 detected from a genome-wide SNP scan. *Am J Med Genet A,* 149A(8), 1823–1826. doi:10.1002/ajmg.a.32973.

Khan, N. W., Wissinger, B., Kohl, S., and Sieving, P. A. (2007). CNGB3 achromatopsia with progressive loss of residual cone function and impaired rod-mediated function. *Invest Ophthalmol Vis Sci,* 48(8), 3864–3871. doi:10.1167/iovs.06-1521.

Koeppen, K., Reuter, P., Kohl, S., Baumann, B., Ladewig, T., and Wissinger, B. (2008). Functional analysis of human CNGA3 mutations associated with colour blindness suggests impaired surface expression of channel mutants A3(R427C) and A3(R563C). *Eur J Neurosci,* 27(9), 2391–2401. doi:10.1111/j.1460-9568.2008.06195.x.

Koeppen, K., Reuter, P., Ladewig, T., Kohl, S., Baumann, B., Jacobson, S. G., et al. (2010). Dissecting the pathogenic mechanisms of mutations in the pore region of the human cone photoreceptor cyclic nucleotide-gated channel. *Hum Mutat,* 31(7), 830–839. doi:10.1002/humu.21283.

Kohl, S., Baumann, B., Broghammer, M., Jagle, H., Sieving, P., Kellner, U., et al. (2000). Mutations in the CNGB3 gene encoding the beta-subunit of the cone photoreceptor cGMP-gated channel are responsible for achromatopsia (ACHM3) linked to chromosome 8q21. *Hum Mol Genet,* 9(14), 2107–2116. doi:10.1093/hmg/9.14.2107.

Kohl, S., Baumann, B., Dassie, F., Mayer, A. K., Solaki, M., Reuter, P., et al. (2021). Paternal Uniparental Isodisomy of Chromosome 2 in a Patient with CNGA3-Associated Autosomal Recessive Achromatopsia. *Int J Mol Sci,* 22(15). doi:10.3390/ijms22157842.

Kohl, S., Baumann, B., Rosenberg, T., Kellner, U., Lorenz, B., Vadala, M., et al. (2002). Mutations in the cone photoreceptor G-protein alpha-subunit gene GNAT2 in patients with achromatopsia. *Am J Hum Genet,* 71(2), 422–425. doi:10.1086/341835.

Kohl, S., Coppieters, F., Meire, F., Schaich, S., Roosing, S., Brennenstuhl, C., et al. (2012). A nonsense mutation in PDE6H causes autosomal-recessive incomplete achromatopsia. *Am J Hum Genet,* 91(3), 527–532. doi:10.1016/j.ajhg.2012.07.006.

Kohl, S., Marx, T., Giddings, I., Jagle, H., Jacobson, S. G., Apfelstedt-Sylla, E., et al. (1998). Total colourblindness is caused by mutations in the gene encoding the alpha-subunit of the cone photoreceptor cGMP-gated cation channel. *Nat Genet,* 19(3), 257–259. doi:10.1038/935.

Kohl, S., Zobor, D., Chiang, W. C., Weisschuh, N., Staller, J., Gonzalez Menendez, I., et al. (2015). Mutations in the unfolded protein response regulator ATF6 cause the cone dysfunction disorder achromatopsia. *Nat Genet,* 47(7), 757–765. doi:10.1038/ng.3319.

Kolesnikov, A. V., Kiser, P. D., Palczewski, K., and Kefalov, V. J. (2021). Function of mammalian M-cones depends on the level of CRALBP in Muller cells. *J Gen Physiol,* 153(1). doi:10.1085/jgp.202012675.

Kuniyoshi, K., Muraki-Oda, S., Ueyama, H., Toyoda, F., Sakuramoto, H., Ogita, H., et al. (2016). Novel mutations in the gene for alpha-subunit of retinal cone cyclic nucleotide-gated channels in a Japanese patient with congenital achromatopsia. *Jpn J Ophthalmol,* 60(3), 187–197. doi:10.1007/s10384-016-0424-6.

Labin, A. M., Safuri, S. K., Ribak, E. N., and Perlman, I. (2014). Müller cells separate between wavelengths to improve day vision with minimal effect upon night vision. *Nat Commun,* 5, 4319. doi:10.1038/ncomms5319.

Lamb, T. D. (2022). Photoreceptor physiology and evolution: cellular and molecular basis of rod and cone phototransduction. *J Physiol,* 600(21), 4585–4601. doi:10.1113/JP282058.

Lamb, T. D., and Pugh, E. N., Jr. (2006). Phototransduction, dark adaptation, and rhodopsin regeneration the proctor lecture. *Invest Ophthalmol Vis Sci,* 47(12), 5137–5152. doi:10.1167/iovs.06-0849.

Lee, E. J., Chiang, W. J., Kroeger, H., Bi, C. X., Chao, D. L., Skowronska-Krawczyk, D., et al. (2020). Multiexon deletion alleles of ATF6 linked to achromatopsia. *JCI Insight,* 5(7). doi:10.1172/jci.insight.136041.

Li, S., Huang, L., Xiao, X., Jia, X., Guo, X., and Zhang, Q. (2014). Identification of CNGA3 mutations in 46 families: common cause of achromatopsia and cone-rod dystrophies in Chinese patients. *JAMA Ophthalmol,* 132(9), 1076–1083. doi:10.1001/jamaophthalmol.2014.1032.

Liang, X., Dong, F., Li, H., Li, H., Yang, L., and Sui, R. (2015). Novel CNGA3 mutations in Chinese patients with achromatopsia. *Br J Ophthalmol,* 99(4), 571–576. doi:10.1136/bjophthalmol-2014-305432.

Liu, C., and Varnum, M. D. (2005). Functional consequences of progressive cone dystrophy-associated mutations in the human cone photoreceptor cyclic nucleotide-gated channel CNGA3 subunit. *Am J Physiol Cell Physiol,* 289(1), C187–198. doi:10.1152/ajpcell.00490.2004.

Liu, D. T., Tibbs, G. R., Paoletti, P., and Siegelbaum, S. A. (1998). Constraining ligand-binding site stoichiometry suggests that a cyclic nucleotide-gated channel is composed of two functional dimers. *Neuron,* 21(1), 235–248. doi:10.1016/s0896-6273(00)80530-9.

Lo, R. S., Cromie, G. A., Tang, M., Teng, K., Owens, K., Sirr, A., et al. (2023). The functional impact of 1,570 individual amino acid substitutions in human OTC. *Am J Hum Genet,* 110(5), 863–879. doi:10.1016/j.ajhg.2023.03.019.

Lopez-Garrido, M. P., Campos-Mollo, E., Harto, M. A., and Escribano, J. (2009). Primary congenital glaucoma caused by the homozygous F261L CYP1B1 mutation and paternal isodisomy of chromosome 2. *Clin Genet,* 76(6), 552–557. doi:10.1111/j.1399-0004.2009.01242.x.

Lopour, M. Q. R., Schimmenti, L. A., Boczek, N. J., Kearney, H. M., Drack, A. V., and Brodsky, M. C. (2023). Alström syndrome caused by maternal uniparental disomy. *Am J Ophthalmol Case Rep,* 29, 101745. doi:10.1016/j.ajoc.2022.101745.

Maguire, J., McKibbin, M., Khan, K., Kohl, S., Ali, M., and McKeefry, D. (2018). CNGB3 mutations cause severe rod dysfunction. *Ophthalmic Genet,* 39(1), 108–114. doi:10.1080/13816810.2017.1368087.

Makino, E. R., Handy, J. W., Li, T., and Arshavsky, V. Y. (1999). The GTPase activating factor for transducin in rod photoreceptors is the complex between RGS9 and type 5 G protein beta subunit. *Proc Natl Acad Sci U S A,* 96(5), 1947–1952. doi:10.1073/pnas.96.5.1947.

Mata, N. L., Radu, R. A., Clemmons, R. C., and Travis, G. H. (2002). Isomerization and oxidation of vitamin a in cone-dominant retinas: a novel pathway for visual-pigment regeneration in daylight. *Neuron,* 36(1), 69–80. doi:10.1016/s0896-6273(02)00912-1.

Matulef, K., and Zagotta, W. N. (2003). Cyclic nucleotide-gated ion channels. *Annu Rev Cell Dev Biol,* 19, 23–44. doi:10.1146/annurev.cellbio.19.110701.154854.

Matveev, A. V., Fitzgerald, J. B., Xu, J., Malykhina, A. P., Rodgers, K. K., and Ding, X. Q. (2010). The disease-causing mutations in the carboxyl terminus of the cone cyclic nucleotide-gated channel CNGA3 subunit alter the local secondary structure and interfere with the channel active conformational change. *Biochemistry,* 49(8), 1628–1639. doi:10.1021/bi901960u.

Mayer, A. K., Van Cauwenbergh, C., Rother, C., Baumann, B., Reuter, P., De Baere, E., et al. (2017). CNGB3 mutation spectrum including copy number variations in 552 achromatopsia patients. *Hum Mutat,* 38(11), 1579–1591. doi:10.1002/humu.23311.

Meighan, P. C., Peng, C., and Varnum, M. D. (2015). Inherited macular degeneration-associated mutations in CNGB3 increase the ligand sensitivity and spontaneous open probability of cone cyclic nucleotide-gated channels. *Front Physiol,* 6, 177. doi:10.3389/fphys.2015.00177.

Meighan, S. E., Meighan, P. C., Rich, E. D., Brown, R. L., and Varnum, M. D. (2013). Cyclic nucleotide-gated channel subunit glycosylation regulates matrix metalloproteinase-dependent changes in channel gating. *Biochemistry,* 52(46), 8352–8362. doi:10.1021/bi400824x.

Michalakis, S., Becirovic, E., and Biel, M. (2018). Retinal Cyclic Nucleotide-Gated Channels: From Pathophysiology to Therapy. *Int J Mol Sci,* 19(3). doi:10.3390/ijms19030749.

Michalakis, S., Gerhardt, M., Rudolph, G., Priglinger, S., and Priglinger, C. (2022). Achromatopsia: Genetics and Gene Therapy. *Mol Diagn Ther,* 26(1), 51–59. doi:10.1007/s40291-021-00565-z.

Michalakis, S., Schön, C., Becirovic, E., and Biel, M. (2017). Gene therapy for achromatopsia. *J Gene Med,* 19(3). doi:10.1002/jgm.2944.

Molday, R. S., and Zhang, K. (2010). Defective lipid transport and biosynthesis in recessive and dominant Stargardt macular degeneration. *Prog Lipid Res,* 49(4), 476–492. doi:10.1016/j.plipres.2010.07.002.

Müller, F., Vantler, M., Weitz, D., Eismann, E., Zoche, M., Koch, K. W., et al. (2001). Ligand sensitivity of the α2 subunit from the bovine cone cGMP-gated channel is modulated by protein kinase C but not by calmodulin. *J Physiol,* 532(Pt 2), 399–409. doi:10.1111/j.1469-7793.2001.0399f.x.

Muraki-Oda, S., Toyoda, F., Okada, A., Tanabe, S., Yamade, S., Ueyama, H., et al. (2007). Functional analysis of rod monochromacy-associated missense mutations in the CNGA3 subunit of the cone photoreceptor cGMP-gated channel. *Biochem Biophys Res Commun,* 362(1), 88–93. doi:10.1016/j.bbrc.2007.07.152.

Nakatani, K., and Yau, K. W. (1988). Calcium and magnesium fluxes across the plasma membrane of the toad rod outer segment. *J Physiol,* 395, 695–729. doi:10.1113/jphysiol.1988.sp016942.

Newman, E. A. (1994). A physiological measure of carbonic anhydrase in Müller cells. *Glia,* 11(4), 291–299. doi:10.1002/glia.440110402.

Ou, X., Liu, C., Chen, S., Yu, J., Zhang, Y., Liu, S., et al. (2013). Complete paternal uniparental isodisomy for Chromosome 2 revealed in a parentage testing case. *Transfusion,* 53(6), 1266–1269. doi:10.1111/j.1537-2995.2012.03863.x.

Palczewski, K., Kumasaka, T., Hori, T., Behnke, C. A., Motoshima, H., Fox, B. A., et al. (2000). Crystal structure of rhodopsin: A G protein-coupled receptor. *Science,* 289(5480), 739–745. doi:10.1126/science.289.5480.739.

Patel, K. A., Bartoli, K. M., Fandino, R. A., Ngatchou, A. N., Woch, G., Carey, J., et al. (2005). Transmembrane S1 mutations in CNGA3 from achromatopsia 2 patients cause loss of function and impaired cellular trafficking of the cone CNG channel. *Invest Ophthalmol Vis Sci,* 46(7), 2282–2290. doi:10.1167/iovs.05-0179.

Peng, C., Rich, E. D., Thor, C. A., and Varnum, M. D. (2003). Functionally important calmodulin-binding sites in both NH2- and COOH-terminal regions of the cone photoreceptor cyclic nucleotide-gated channel CNGB3 subunit. *J Biol Chem,* 278(27), 24617–24623. doi:10.1074/jbc.M301699200.

Prasov, L., Ullah, E., Turriff, A. E., Warner, B. M., Conley, J., Mark, P. R., et al. (2020). Expanding the genotypic spectrum of Jalili syndrome: Novel CNNM4 variants and uniparental isodisomy in a north American patient cohort. *Am J Med Genet A,* 182(3), 493–497. doi:10.1002/ajmg.a.61484.

Pugh Jr, E. N., and Lamb, T. D. (2000). Phototransduction in vertebrate rods and cones: molecular mechanisms of amplification, recovery and light adaptation. *Handbook of biological physics* (Vol. 3, pp. 183–255): Elsevier.

Rebrik, T. I., Botchkina, I., Arshavsky, V. Y., Craft, C. M., and Korenbrot, J. I. (2012). CNG-modulin: a novel Ca-dependent modulator of ligand sensitivity in cone photoreceptor cGMP-gated ion channels. *J Neurosci,* 32(9), 3142–3153. doi:10.1523/JNEUROSCI.5518-11.2012.

Reichel, F. F., Michalakis, S., Wilhelm, B., Zobor, D., Muehlfriedel, R., Kohl, S., et al. (2022). Three-year results of phase I retinal gene therapy trial for CNGA3-mutated achromatopsia: results of a non randomised controlled trial. *Br J Ophthalmol,* 106(11), 1567–1572. doi:10.1136/bjophthalmol-2021-319067.

Reuter, P., Koeppen, K., Ladewig, T., Kohl, S., Baumann, B., Wissinger, B., et al. (2008). Mutations in CNGA3 impair trafficking or function of cone cyclic nucleotide-gated channels, resulting in achromatopsia. *Hum Mutat,* 29(10), 1228–1236. doi:10.1002/humu.20790.

Reuter, P., Walter, M., Kohl, S., and Weisschuh, N. (2023). Systematic analysis of CNGA3 splice variants identifies different mechanisms of aberrant splicing. *Sci Rep,* 13(1), 2896. doi:10.1038/s41598-023-29452-9.

Richards, S., Aziz, N., Bale, S., Bick, D., Das, S., Gastier-Foster, J., et al. (2015). Standards and guidelines for the interpretation of sequence variants: a joint consensus recommendation of the American College of Medical Genetics and Genomics and the Association for Molecular Pathology. *Genet Med,* 17(5), 405–424. doi:10.1038/gim.2015.30.

Richardson, M. E., Hu, C., Lee, K. Y., LaDuca, H., Fulk, K., Durda, K. M., et al. (2021). Strong functional data for pathogenicity or neutrality classify BRCA2 DNA-binding-domain variants of uncertain significance. *Am J Hum Genet,* 108(3), 458–468. doi:10.1016/j.ajhg.2021.02.005.

Ruiz, M. L., and Karpen, J. W. (1997). Single cyclic nucleotide-gated channels locked in different ligand-bound states. *Nature,* 389(6649), 389–392. doi:10.1038/38744.

Scott, S. P., Cummings, J., Joe, J. C., and Tanaka, J. C. (2000). Mutating three residues in the bovine rod cyclic nucleotide-activated channel can switch a nucleotide from inactive to active. *Biophys J,* 78(5), 2321–2333. doi:10.1016/S0006-3495(00)76778-6.

Shaikh, R. S., Reuter, P., Sisk, R. A., Kausar, T., Shahzad, M., Maqsood, M. I., et al. (2015). Homozygous missense variant in the human CNGA3 channel causes cone-rod dystrophy. *Eur J Hum Genet,* 23(4), 473–480. doi:10.1038/ejhg.2014.136.

Shuart, N. G., Haitin, Y., Camp, S. S., Black, K. D., and Zagotta, W. N. (2011). Molecular mechanism for 3:1 subunit stoichiometry of rod cyclic nucleotide-gated ion channels. *Nat Commun,* 2, 457. doi:10.1038/ncomms1466.

Solaki, M., Baumann, B., Reuter, P., Andreasson, S., Audo, I., Ayuso, C., et al. (2022). Comprehensive variant spectrum of the CNGA3 gene in patients affected by achromatopsia. *Hum Mutat,* 43(7), 832–858. doi:10.1002/humu.24371.

Solaki, M., Wissinger, B., Kohl, S., and Reuter, P. (2023). Functional evaluation allows ACMG/AMP-based re-classification of CNGA3 variants associated with achromatopsia. *Genet Med,* 25(12), 100979. doi:10.1016/j.gim.2023.100979.

Song, J., Zhu, L., Zhang, C., Wu, Y., and Wang, B. (2021). A rare case of complete uniparental isodisomy of chromosome 2 with no phenotypic abnormalities. *Taiwan J Obstet Gynecol,* 60(2), 378–379. doi:10.1016/j.tjog.2021.01.024.

Souzeau, E., Dubowsky, A., Ruddle, J. B., and Craig, J. E. (2019). Primary congenital glaucoma due to paternal uniparental isodisomy of chromosome 2 and CYP1B1 deletion. *Mol Genet Genomic Med,* 7(8), e774. doi:10.1002/mgg3.774.

Sun, W., Li, S., Xiao, X., Wang, P., and Zhang, Q. (2020). Genotypes and phenotypes of genes associated with achromatopsia: A reference for clinical genetic testing. *Mol Vis,* 26, 588–602.

Sun, W., and Zhang, Q. (2019). Diseases associated with mutations in CNGA3: Genotype-phenotype correlation and diagnostic guideline. *Prog Mol Biol Transl Sci,* 161, 1–27. doi:10.1016/bs.pmbts.2018.10.002.

Sundin, O. H., Yang, J. M., Li, Y., Zhu, D., Hurd, J. N., Mitchell, T. N., et al. (2000). Genetic basis of total colourblindness among the Pingelapese islanders. *Nat Genet,* 25(3), 289–293. doi:10.1038/77162.

Sung, C. H., and Chuang, J. Z. (2010). The cell biology of vision. *J Cell Biol,* 190(6), 953–963. doi:10.1083/jcb.201006020.

Täger, J., Kohl, S., Birch, D. G., Wheaton, D. K. H., Wissinger, B., and Reuter, P. (2018). An early nonsense mutation facilitates the expression of a short isoform of CNGA3 by alternative translation initiation. *Exp Eye Res,* 171, 48–53. doi:10.1016/j.exer.2018.02.027.

Täger, J., Wissinger, B., Kohl, S., and Reuter, P. (2021). Identification of Chemical and Pharmacological Chaperones for Correction of Trafficking-Deficient Mutant Cyclic Nucleotide-Gated A3 Channels. *Mol Pharmacol,* 99(6), 460–468. doi:10.1124/molpharm.120.000180.

Tavtigian, S. V., Harrison, S. M., Boucher, K. M., and Biesecker, L. G. (2020). Fitting a naturally scaled point system to the ACMG/AMP variant classification guidelines. *Hum Mutat,* 41(10), 1734–1737. doi:10.1002/humu.24088.

Thiadens, A. A., den Hollander, A. I., Roosing, S., Nabuurs, S. B., Zekveld-Vroon, R. C., Collin, R. W., et al. (2009a). Homozygosity mapping reveals PDE6C mutations in patients with early-onset cone photoreceptor disorders. *Am J Hum Genet,* 85(2), 240–247. doi:10.1016/j.ajhg.2009.06.016.

Thiadens, A. A., Slingerland, N. W., Roosing, S., van Schooneveld, M. J., van Lith-Verhoeven, J. J., van Moll-Ramirez, N., et al. (2009b). Genetic etiology and clinical consequences of complete and incomplete achromatopsia. *Ophthalmology,* 116(10), 1984–1989 e1981. doi:10.1016/j.ophtha.2009.03.053.

Thiadens, A. A., Somervuo, V., van den Born, L. I., Roosing, S., van Schooneveld, M. J., Kuijpers, R. W., et al. (2010). Progressive loss of cones in achromatopsia: an imaging study using spectral-domain optical coherence tomography. *Invest Ophthalmol Vis Sci,* 51(11), 5952–5957. doi:10.1167/iovs.10-5680.

Thomas, M. G., McLean, R. J., Kohl, S., Sheth, V., and Gottlob, I. (2012). Early signs of longitudinal progressive cone photoreceptor degeneration in achromatopsia. *Br J Ophthalmol,* 96(9), 1232–1236. doi:10.1136/bjophthalmol-2012-301737.

Thompson, D. A., McHenry, C. L., Li, Y., Richards, J. E., Othman, M. I., Schwinger, E., et al. (2002). Retinal dystrophy due to paternal isodisomy for chromosome 1 or chromosome 2, with homoallelism for mutations in RPE65 or MERTK, respectively. *Am J Hum Genet,* 70(1), 224–229. doi:10.1086/338455.

Tibbs, G. R., Liu, D. T., Leypold, B. G., and Siegelbaum, S. A. (1998). A state-independent interaction between ligand and a conserved arginine residue in cyclic nucleotide-gated channels reveals a functional polarity of the cyclic nucleotide binding site. *J Biol Chem,* 273(8), 4497–4505. doi:10.1074/jbc.273.8.4497.

Tränkner, D., Jagle, H., Kohl, S., Apfelstedt-Sylla, E., Sharpe, L. T., Kaupp, U. B., et al. (2004). Molecular basis of an inherited form of incomplete achromatopsia. *J Neurosci,* 24(1), 138–147. doi:10.1523/JNEUROSCI.3883-03.2004.

Triantafylla, M., Papageorgiou, E., Thomas, M. G., McLean, R., Kohl, S., Sheth, V., et al. (2022). Longitudinal Evaluation of Changes in Retinal Architecture Using Optical Coherence Tomography in Achromatopsia. *Invest Ophthalmol Vis Sci,* 63(9), 6. doi:10.1167/iovs.63.9.6.

Tsacopoulos, M., and Magistretti, P. J. (1996). Metabolic coupling between glia and neurons. *J Neurosci,* 16(3), 877–885. doi:10.1523/JNEUROSCI.16-03-00877.1996.

Varnum, M. D., Black, K. D., and Zagotta, W. N. (1995). Molecular mechanism for ligand discrimination of cyclic nucleotide-gated channels. *Neuron,* 15(3), 619–625. doi:10.1016/0896-6273(95)90150-7.

Varsányi, B., Wissinger, B., Kohl, S., Koeppen, K., and Farkas, A. (2005). Clinical and genetic features of Hungarian achromatopsia patients. *Mol Vis,* 11, 996–1001.

Wan, A., Place, E., Pierce, E. A., and Comander, J. (2019). Characterizing variants of unknown significance in rhodopsin: A functional genomics approach. *Hum Mutat,* 40(8), 1127–1144. doi:10.1002/humu.23762.

Weitz, D., Ficek, N., Kremmer, E., Bauer, P. J., and Kaupp, U. B. (2002). Subunit stoichiometry of the CNG channel of rod photoreceptors. *Neuron,* 36(5), 881–889. doi:10.1016/s0896-6273(02)01098-x.

Wissinger, B., Gamer, D., Jagle, H., Giorda, R., Marx, T., Mayer, S., et al. (2001). CNGA3 mutations in hereditary cone photoreceptor disorders. *Am J Hum Genet,* 69(4), 722–737. doi:10.1086/323613.

Wissinger, B., and Kohl, S. (2005). Genetische Ursachen des Farbensehens (Vol. 11. Jahrgang Nr.1, pp. 29–33). BIOspektrum: Elsevier.

Xu, M., Gelowani, V., Eblimit, A., Wang, F., Young, M. P., Sawyer, B. L., et al. (2015). ATF6 Is Mutated in Early Onset Photoreceptor Degeneration With Macular Involvement. *Invest Ophthalmol Vis Sci,* 56(6), 3889–3895. doi:10.1167/iovs.15-16778.

Yau, K. W., and Hardie, R. C. (2009). Phototransduction motifs and variations. *Cell,* 139(2), 246–264. doi:10.1016/j.cell.2009.09.029.

Zelinger, L., Cideciyan, A. V., Kohl, S., Schwartz, S. B., Rosenmann, A., Eli, D., et al. (2015). Genetics and Disease Expression in the CNGA3 Form of Achromatopsia: Steps on the Path to Gene Therapy. *Ophthalmology,* 122(5), 997–1007. doi:10.1016/j.ophtha.2014.11.025.

Zhang, X., Ding, Z., He, R., Qi, J., Zhang, Z., and Cui, B. (2019). Complete Paternal Uniparental Disomy of Chromosome 2 in an Asian Female Identified by Short Tandem Repeats and Whole Genome Sequencing. *Cytogenet Genome Res,* 157(4), 197–202. doi:10.1159/000499893.

Zheng, J., Trudeau, M. C., and Zagotta, W. N. (2002). Rod cyclic nucleotide-gated channels have a stoichiometry of three CNGA1 subunits and one CNGB1 subunit. *Neuron,* 36(5), 891–896. doi:10.1016/s0896-6273(02)01099-1.

Zheng, J., and Zagotta, W. N. (2004). Stoichiometry and assembly of olfactory cyclic nucleotide-gated channels. *Neuron,* 42(3), 411–421. doi:10.1016/s0896-6273(04)00253-3.

Zheng, X., Hu, Z., Li, H., and Yang, J. (2022). Structure of the human cone photoreceptor cyclic nucleotide-gated channel. *Nat Struct Mol Biol,* 29(1), 40–46. doi:10.1038/s41594-021-00699-y.

Zhong, H., Molday, L. L., Molday, R. S., and Yau, K. W. (2002). The heteromeric cyclic nucleotide-gated channel adopts a 3A:1B stoichiometry. *Nature,* 420(6912), 193–198. doi:10.1038/nature01201.

10. Acknowledgement

Finally, I would like to shortly reflect on all people who have made it possible for me to complete my doctoral thesis with their contribution.

First, I would like to thank Prof. Dr. Bernd Wissinger for the opportunity to conduct and write my dissertation at the Molecular Genetics Laboratory at the Institute for Ophthalmic Research as well as for the excellent supervision and the review of this doctoral thesis.

I would also like to thank my co-supervisor Prof. Dr. Jennifer Ewald for reviewing my thesis and for all the helpful advice she gave me in our supervisory meetings.

A special thanks goes to Dr. Susanne Kohl and Dr. Peggy Reuter for their dedicated scientific supervision of the project, their guidance, and for the deep knowledge they have always shared with me to carry out the project successfully. Without your important contribution, this research would never have been so fruitful! Thank you very much for all the help you gave me in writing my thesis and for all your efforts and suggestions for improvement!

I would also like to take this opportunity to thank my fellow labmates at the Molecular Genetics Laboratory: Dr. Nicole Weisschuh, Sinja Kieninger, Ting Xiao, Pietro De Angeli, Britta Baumann, Jennifer Schröder, and Eva Weber. Thank you for the pleasant working atmosphere, the helpfulness, the inspiring discussions that have contributed to the success of this thesis, and for all the fun we have had together over the past few years!

Last but not least, I would like to thank my parents, my brother, and my friends for their moral and emotional support and for always encouraging me during my studies. Thank you for always standing by my side, especially during the difficult times, and for always believing in me. None of this would have been possible without your active support!

Thank you very much!

11. Appendix

Publication I

Comprehensive variant spectrum of the *CNGA3* gene in patients affected by achromatopsia.

Solaki, M., Baumann, B., Reuter, P., Andreasson, S., Audo, I., Ayuso, C., Balousha, G., Benedicenti, F., Birch, D., Bitoun, P., Blain, D., Bocquet, B., Branham, K., Català-Mora, J., De Baere, E., Dollfus, H., Falana, M., Giorda, R., Golovleva, I., Gottlob, I., Heckenlively, J. R., Jacobson, S. G., Jones, K., Jägle, H., Janecke, A. R., Kellner, U., Liskova, P., Lorenz, B., Martorell-Sampol, L., Messias, A., Meunier, I., Porto, F. B. O., Papageorgiou, E., Plomp, A. S., de Ravel, T. J. L., Reiff, C. M., Renner, A. B., Rosenberg, T., Rudolph, G., Salati, R., Sener, E. C., Sieving, P. A., Stanzial, F., Traboulsi, E. I., Tsang, S. H., Varsanyi, B., Weleber, R. G., Zobor, D., Stingl, K., Wissinger, B., and Kohl, S.

Human Mutation.

2022 Jul;43(7):832-858.

doi: 10.1002/humu.24371.

This article is distributed under the terms and conditions of the Creative Commons Attribution-NonCommercial License (CC BY-NC 4.0) (https://creativecommons.org/licenses/by-nc/4.0/).

Check for updates

Received: 13 August 2021 | Revised: 23 February 2022 | Accepted: 22 March 2022

DOI: 10.1002/humu.24371

MUTATION UPDATE

Human Mutation HGVS HUMAN GENOME VARIATION SOCIETY WILEY

Comprehensive variant spectrum of the *CNGA3* gene in patients affected by achromatopsia

Maria Solaki[1] | Britta Baumann[1] | Peggy Reuter[1] | Sten Andreasson[2] | Isabelle Audo[3,4] | Carmen Ayuso[5,6] | Ghassan Baloushа[7] | Francesco Benedicenti[8] | David Birch[9] | Pierre Bitoun[10] | Delphine Blain[11] | Beatrice Bocquet[12] | Kari Branham[13] | Jaume Català-Mora[14] | Elfride De Baere[15] | Helene Dollfus[16,17] | Mohammed Falana[7] | Roberto Giorda[18] | Irina Golovleva[19] | Irene Gottlob[20] | John R. Heckenlively[13] | Samuel G. Jacobson[21] | Kaylie Jones[9] | Herbert Jägle[22] | Andreas R. Janecke[23] | Ulrich Kellner[24,25] | Petra Liskova[26,27] | Birgit Lorenz[28,29] | Loreto Martorell-Sampol[30] | André Messias[31] | Isabelle Meunier[32,33] | Fernanda Belga Ottoni Porto[34] | Eleni Papageorgiou[35] | Astrid S. Plomp[36] | Thomy J. L. de Ravel[37] | Charlotte M. Reiff[38] | Agnes B. Renner[39] | Thomas Rosenberg[40] | Günther Rudolph[41] | Roberto Salati[42] | E. Cumhur Sener[43] | Paul A. Sieving[44] | Franco Stanzial[8] | Elias I. Traboulsi[45] | Stephen H. Tsang[46] | Balázs Varsanyi[47] | Richard G. Weleber[48] | Ditta Zobor[49,50] | Katarina Stingl[51,52] | Bernd Wissinger[1] | Susanne Kohl[1]

[1]Centre for Ophthalmology, Institute for Ophthalmic Research, University of Tübingen, Tübingen, Germany

[2]Department of Ophthalmology, University Hospital Lund, Lund, Sweden

[3]Sorbonne Université, INSERM, CNRS, Institut de la Vision, Paris, France

[4]CHNO des Quinze-Vingts, Centre de Référence Maladies Rares REFERET, and INSERM-DGOS CIC1423, Paris, France

[5]Department of Genetics & Genomics, Instituto de Investigación Sanitaria - Fundación Jiménez Díaz University Hospital - Universidad Autónoma de Madrid (IIS-FJD, UAM), Madrid, Spain

[6]Center for Biomedical Network Research on Rare Diseases (CIBERER), ISCIII, Madrid, Spain

[7]Department of Pathology and Histology, Faculty of Medicine, Al-Quds University, Eastern Jerusalem, Palestine

[8]Clinical Genetics Service and South Tyrol Coordination Center for Rare Diseases, Department of Pediatrics, Regional Hospital of Bolzano, Bolzano, Italy

[9]Retina Foundation of the Southwest, Dallas, Texas, USA

[10]Genetique Medicale, CHU Paris Nord, Hopital Jean Verdier, Bondy Cedex, France

[11]National Eye Institute/NEI, Bethesda, Maryland, USA

[12]National Reference Centre for Inherited Sensory Diseases, Institute for Neurosciences of Montpellier (INM), University of Montpellier, INSERM, Montpellier, France

[13]Department of Ophthalmology and Visual Sciences, Kellogg Eye Center, University of Michigan, Ann Arbor, Michigan, USA

[14]Unitat de Distròfies Hereditàries de Retina Hospital Sant Joan de Déu, Barcelona, Esplugues de Llobregat, Spain

[15]Department of Biomolecular Medicine, Center for Medical Genetics, Ghent University and Ghent University Hospital, Ghent, Belgium

This is an open access article under the terms of the Creative Commons Attribution-NonCommercial License, which permits use, distribution and reproduction in any medium, provided the original work is properly cited and is not used for commercial purposes.
© 2022 The Authors. *Human Mutation* published by Wiley Periodicals LLC.

[16]CARGO, Hôpitaux Universitaires de Strasbourg, Strasbourg, France

[17]U-1112, Inserm, Faculté de Médecine, Université de Strasbourg, Strasbourg, France

[18]Molecular Biology Laboratory, Scientific Institute IRCCS E. Medea, Bosisio Parini, Lecco, Italy

[19]Department of Medical Biosciences/Medical and Clinical Genetics, University of Umea, Umea, Sweden

[20]The University of Leicester Ulverscroft Eye Unit, Leicester Royal Infirmary, Leicester, UK

[21]Department of Ophthalmology, Perelman School of Medicine, Scheie Eye Institute, University of Pennsylvania, Philadelphia, Pennsylvania, USA

[22]Department of Ophthalmology, University of Regensburg, Regensburg, Germany

[23]Institute of Human Genetics, Medical University of Innsbruck, Innsbruck, Austria

[24]Zentrum für Seltene Netzhauterkrankungen, AugenZentrum Siegburg, MVZ Augenärztliches Diagnostik- und Therapiecentrum Siegburg GmbH, Siegburg, Germany

[25]RetinaScience, Bonn, 53192, Germany

[26]Department of Paediatrics and Inherited Metabolic Disorders, First Faculty of Medicine, Charles University and General University Hospital in Prague, Prague, Czech Republic

[27]Department of Ophthalmology, First Faculty of Medicine, Charles University and General University Hospital in Prague, Prague, Czech Republic

[28]Department of Ophthalmology, Justus-Liebig University Giessen, Giessen, Germany

[29]Department of Ophthalmology, Universitaetsklinikum Bonn, Bonn, Germany

[30]Genetica Molecular-Edifici Docent, Hospital Sant Joan de Deu, Esplugues-Barcelona, Spain

[31]Department of Ophthalmology, Otorhinolaryngology, and Head and Neck Surgery, School of Medicine of Ribeirão Preto, University of São Paulo, Ribeirão Preto, Brazil

[32]National Reference Centre for Inherited Sensory Diseases, Montpellier University Hospital, University of Montpellier, Montpellier, France

[33]Sensgene Care Network, France

[34]INRET Clínica e Centro de Pesquisa, IEP Santa Casa Belo Horizonte, Belo Horizonte, MG, Brazil

[35]Department of Ophthalmology, University Hospital of Larissa, Mezourlo, Larissa, Greece

[36]Department of Human Genetics, Amsterdam UMC, University of Amsterdam, Amsterdam, The Netherlands

[37]Centre for Medical Genetics, University Hospital Brussels, Brussels, Belgium

[38]Augenarztpraxis am Stadttheater, Freiburg, Germany

[39]Augenarztpraxis Regensburg, Regensburg, Germany

[40]Department of Ophthalmology, National Eye Clinic, Glostrup Hospital, Glostrup, Denmark

[41]University Eye Hospital, Ludwig Maximilians University, Munich, Germany

[42]Scientific Institute, IRCCS Eugenio Medea, Pediatric Ophthalmology Unit, Bosisio Parini, Lecco, Italy

[43]Strabismus and Pediatric Ophthalmology, Private Practice, Ankara, Turkey

[44]Center for Ocular Regenerative Therapy, School of Medicine, University of California Davis, Sacramento, USA

[45]Center for Genetic Eye Diseases, Cole Eye Institute, Cleveland Clinic Foundation, Cleveland, Ohio, USA

[46]Department of Ophthalmology, Pathology and Cell Biology, College of Physicians and Surgeons, Columbia Stem Cell Initiative, Columbia University, New York City, New York, USA

[47]Department of Ophthalmology, Medical School, University of Pécs and Ganglion Medical Center, Pécs, Pécs, Hungary

[48]Oregon Health & Science University, Ophthalmic Genetics Service of the Casey Eye Institute, 515 SW Campus Drive, 97239, Portland, Oregon, USA

[49]Centre for Ophthalmology, Institute for Ophthalmic Research, University Hospital Tübingen, Tübingen, Germany

[50]Department of Ophthalmology, Semmelweis University Budapest, Budapest, Hungary

[51]Center for Ophthalmology, University Eye Hospital, University of Tübingen, Tübingen, Germany

[52]Center for Rare Eye Diseases, University of Tübingen, Tübingen, Germany

Correspondence
Susanne Kohl, Molecular Genetics Laboratory, Institute for Ophthalmic Research, Centre for Ophthalmology, University Clinics Tübingen, Elfriede-Aulhorn-Strasse 5–7, 72076 Tübingen, Germany.
Email: susanne.kohl@med.uni-tuebingen.de

Abstract

Achromatopsia (ACHM) is a congenital cone photoreceptor disorder characterized by impaired color discrimination, low visual acuity, photosensitivity, and nystagmus. To date, six genes have been associated with ACHM (*CNGA3*, *CNGB3*, *GNAT2*, *PDE6C*, *PDE6H*, and *ATF6*), the majority of these being implicated in the cone phototransduction cascade. *CNGA3* encodes the CNGA3 subunit of the cyclic

10981004, 2022, 7, Downloaded from https://onlinelibrary.wiley.com/doi/10.1002/humu.24371, Wiley Online Library on [09/12/2024]. See the Terms and Conditions (https://onlinelibrary.wiley.com/terms-and-conditions) on Wiley Online Library for rules of use; OA articles are governed by the applicable Creative Commons License

Funding information
Deutsche Forschungsgemeinschaft, Grant/Award Numbers: KO 2176/3-1, 398539671, STI 727/1-1, 399487883; Foundation Fighting Blindness, Grant/Award Numbers: BR-GE-0120-0775-LUMC, BR-GE-0619-0761-INSERM; Instituto de Salud Carlos III (ISCIII) of the Spanish Ministry of Health, Grant/Award Number: FIS PI19/00321; Ministry of Health of the Czech Republic, Grant/Award Number: AZV NU20-07-00182

nucleotide-gated ion channel in cone photoreceptors and is one of the major disease-associated genes for ACHM. Herein, we provide a comprehensive overview of the *CNGA3* variant spectrum in a cohort of 1060 genetically confirmed ACHM patients, 385 (36.3%) of these carrying "likely disease-causing" variants in *CNGA3*. Compiling our own genetic data with those reported in the literature and in public databases, we further extend the *CNGA3* variant spectrum to a total of 316 variants, 244 of which we interpreted as "likely disease-causing" according to ACMG/AMP criteria. We report 48 novel "likely disease-causing" variants, 24 of which are missense substitutions underlining the predominant role of this mutation class in the *CNGA3* variant spectrum. In addition, we provide extensive *in silico* analyses and summarize reported functional data of previously analyzed missense, nonsense and splicing variants to further advance the pathogenicity assessment of the identified variants.

KEYWORDS
achromatopsia, *CNGA3*, cyclic nucleotide-gated ion channel, in silico analysis, variant classification, variant spectrum

1 | BACKGROUND

Achromatopsia (ACHM; rod monochromacy) is a rare autosomal recessively inherited retinal disorder characterized by impaired cone photoreceptor function. The disease is estimated to affect one in 30,000–50,000 live births worldwide (François, 1961). Signs and symptoms of the disorder manifest in early infancy and include marked photosensitivity, nystagmus, severely reduced visual acuity (<0.1), and the inability to discriminate colors (Hirji et al., 2018; Michalakis et al., 2017; Sun & Zhang, 2019).

ACHM is a phenotypically and genetically heterogeneous inherited retinal disorder. To date, pathogenic variants in six genes have been identified to cause ACHM. Five of these genes, namely *CNGA3* (MIM# 600053) (Kohl et al., 1998), *CNGB3* (MIM# 605080) (Kohl et al., 2000; Sundin et al., 2000), *GNAT2* (MIM# 139340) (Aligianis et al., 2002; Kohl et al., 2002), *PDE6C* (MIM# 600827) (Chang et al., 2009; Thiadens et al., 2009), and *PDE6H* (MIM# 601190) (Kohl et al., 2012), encode key components of the cone phototransduction cascade. Only *ATF6* (MIM# 605537) is not a part of this pathway, but codes for a transcription factor involved in the unfolded protein response (Ansar et al., 2015; Kohl et al., 2015; Xu et al., 2015).

Molecular genetic analyses in ACHM patients revealed that a large proportion of these cases carry causative variants in the *CNGA3* gene though its prevalence varies among different ethnic populations. While biallelic *CNGA3* mutations are the most common cause of ACHM among patients of Chinese (80%) or Israeli/Palestinian (84%) origin (Liang et al., 2015; Sun et al., 2020; Zelinger et al., 2015), its prevalence ranges between 5% and 44% in European and US ACHM patients of European origin, thus representing the second most commonly afflicted gene in the latter countries after *CNGB3* (Johnson et al., 2004; Thiadens et al., 2009; Varsányi et al., 2005; Wissinger et al., 2001).

CNGA3 encodes for the A3 subunit of the cyclic nucleotide-gated (CNG) channel in cone photoreceptors outer segments, a key component of the phototransduction cascade (Kaupp & Seifert, 2002). Cone CNG channels are ligand-activated, nonselective cation channels forming heterotetrameric complexes via assembly of three CNGA3 and one CNGB3 subunit (Barret et al., 2022; Biel & Michalakis, 2009; Shuart et al., 2011; Zheng et al., 2022; Zhong et al., 2002). Both subunits are structurally homologous proteins comprising six transmembrane helices (TM1–TM6) which are connected via intracellular and extracellular loops (also compare Figure 3b). The pore region including the pore helix is located between TM5 and TM6. The cyclic nucleotide-binding domain (CNBD) consists of three α-helices (αA–αC) and eight β-sheets (β1–β8), and is connected via the C-linker—formed by six α-helices (αA′–αF′)–to TM6 (Gofman et al., 2014). Furthermore, the CNGA3 subunit comprises a C-terminal leucine zipper (CLZ) domain important for subunit assembly (Dai et al., 2013; Zagotta & Siegelbaum, 1996).

Nonsense and frameshift variants likely result in the loss of the CNGA3 subunit, while some missense variants in the CNGA3 subunit have been shown to impair or even abolish CNG channel function and/or protein folding and trafficking leading to impaired phototransduction and impaired or lost cone function (Burkard et al., 2018; Dai & Varnum, 2013; Duricka et al., 2012; Koeppen et al., 2008, 2010; Kuniyoshi et al., 2016; Liu & Varnum, 2005; Matveev et al., 2010; Meighan et al., 2015; Michalakis et al., 2017; Muraki-Oda et al., 2007; Patel et al., 2005; Reuter et al., 2008; Shaikh et al., 2015; Täger et al., 2018; Tränkner et al., 2004).

ACHM caused by pathogenic variants in *CNGA3* is of strong current interest as a first gene supplementation therapy trial has been

10981004, 2022, 7, Downloaded from https://onlinelibrary.wiley.com/doi/10.1002/humu.24371, Wiley Online Library on [09/12/2024]. See the Terms and Conditions (https://onlinelibrary.wiley.com/terms-and-conditions) on Wiley Online Library for rules of use; OA articles are governed by the applicable Creative Commons License

completed for *CNGA3*-ACHM (CNGA3: NCT02610582; Fischer et al., 2020; Reichel et al., 2021), and a number of such therapy trials are ongoing at several sites all over the world for both *CNGA3*- and *CNGB3*-ACHM (NCT03758404, NCT02935517, and NCT02599922). Although the primary endpoint of such a trial is safety—which was confirmed, the functional benefits were limited but persistent for the adult treated patients for a period of 3 years (Fischer et al., 2020; Reichel et al., 2021). These included slight improvement in color contrast sensitivity, improvements in the ability to fixate, to recognize letters and numbers as well as in photoaversion. It has been discussed whether treatment of younger patients may result in greater functional benefit by avoiding amblyopia as a potential limiting factor (Reichel et al., 2021). The emergence of therapeutic studies highlights the necessity to classify the pathogenicity of disease-associated variants as unambiguously as possible to enable the right selection of patients for these trials.

In the present study, we aim to provide a complete and comprehensive spectrum overview of variants in the *CNGA3* gene. The *CNGA3* variant database combines the variants of our Tübingen in-house investigated ACHM cohort, variants from literature, and mutation databases and is complemented by extensive *in silico* analysis of the identified variants for assessing their pathogenic effect. In addition, we provide an overview of clinical and diagnostic aspects of ACHM and the animal models of *CNGA3*-associated ACHM.

2 | MATERIAL AND METHODS

2.1 | Patient cohort, clinical examination, and ethical considerations

Patients with a clinical diagnosis of ACHM were recruited over a period of 25 years (1996–2020) in various ophthalmic centers predominantly located in Europe (Austria, Belgium, Czech Republic, Denmark, France, Germany, Greece, Hungary, Italy, the Netherlands, Spain, Sweden, and United Kingdom), but also in Brazil, Israel, Palestine, Turkey, and in the USA. In total, our entire Tübingen ACHM cohort of genetically confirmed ACHM patients includes 1060 affected individuals diagnosed with ACHM originating from 889 independent families.

Clinical diagnosis was established by standard clinical ophthalmologic examination and depended on the local clinical protocol (i.e., color vision testing, best-corrected visual acuity, electroretinography [ERG], fundus photography, and optical coherence tomography).

The study was conducted in accordance with the principles of the Declaration of Helsinki. Blood, saliva, or DNA samples of the ACHM patients and family members were collected over a period of 25 years after informed consent approved by the respective local research and ethical boards and/or dependent on the local regulatory bodies and regulations. Specifically, the study was approved by the Ethics Board of the University of Tübingen under the study no. 349/2003V and 116/2015BO2.

2.2 | Variant screening

Peripheral blood, saliva or DNA samples from patients diagnosed with ACHM and family members were sent to the Institute for Ophthalmic Research, Tübingen (Germany) for genetic testing. Extraction of whole genomic DNA was performed according to standard procedures. Molecular genetic screening of the *CNGA3* gene was executed as previously described (Kohl et al., 1998; Wissinger et al., 2001). Primers used for PCR amplification and Sanger sequencing are provided in Table S1. If two potential disease-causing *CNGA3* alleles were identified in cases that were analyzed within a research setting, no further genetic analysis in other ACHM genes was performed. In case DNA samples from additional family members were available, segregation analysis was performed to validate the presence and the independent segregation of two mutant *CNGA3* alleles using either restriction fragment length polymorphism analysis or Sanger sequencing.

2.3 | Variant nomenclature and establishment of the *CNGA3* variant database

Variant nomenclature of the identified *CNGA3* sequence alterations was based on the NCBI reference sequence NM_001298.2 and the Ensembl transcript reference sequence ENST00000272602.7 (GRCh38/hg38 genome assembly) comprising seven coding exons. The first nucleotide of the translation initiation codon ATG is denoted as nucleotide 1. Moreover, all variants located in the alternatively spliced exon 3b (formerly named exon 2b; Wissinger et al., 2001; now renamed exon 3b) and its flanking intronic sequences were denoted based on NCBI reference sequence XM_011510554.2 (GRCh38/hg38). Validation of the variant nomenclature was performed using the web-based Mutalyzer name checker tool (https://mutalyzer.nl/name-checker).

To establish a comprehensive *CNGA3* variant database, a literature search was conducted on the free search engine PubMed® (https://pubmed.ncbi.nlm.nih.gov/) (last queried on January 11, 2021). In addition, web-based databases including the Human Gene Mutation Database (HGMD®) (http://www.hgmd.cf.ac.uk/ac/index.php) (Stenson et al., 2017), the Leiden Open Variation Database (LOVD) for *CNGA3* (https://www.lovd.nl/CNGA3), and the public archive of human genetic variants ClinVar (https://www.ncbi.nlm.nih.gov/clinvar/) (Landrum et al., 2014) were searched for entries regarding *CNGA3* disease-associated variants (searches conducted on January 11, 2021 and March 18, 2021). Variants retrieved from public databases (i.e., LOVD and ClinVar) that have not been associated with a retinal phenotype (i.e., ACHM or allied disease) were not included and not validated. Finally, all *CNGA3* variants identified in our ACHM cohort were entered into our in-house *CNGA3* variant database. Variants identified in the ACHM cohort genetically characterized in Tübingen that were not yet published in a journal listed on PubMed® are referred to as "novel." All novel variants were submitted to the ClinVar database with accession

10981004, 2022, 7, Downloaded from https://onlinelibrary.wiley.com/doi/10.1002/humu.24371, Wiley Online Library on [09/12/2024]. See the Terms and Conditions (https://onlinelibrary.wiley.com/terms-and-conditions) on Wiley Online Library for rules of use; OA articles are governed by the applicable Creative Commons License

numbers from SCV001571262 to SCV001571322. Additionally, these variants will be submitted to the Global Variome shared LOVD database and can be accessed using the following URL: databases.lovd.nl/shared.

2.4 | *In silico* variant assessment

Sequence alterations listed in the *CNGA3* variant database were subjected to *in silico* analysis to evaluate their pathogenic impact. The Combined Annotation Dependent Depletion (CADD) tool was used to score the deleteriousness of both coding and noncoding single-nucleotide variants in the *CNGA3* gene (https://cadd.gs.washington.edu/). CADD provides PHRED-scaled scores ranging from 1 to 99. A scaled CADD score of 10 thereby indicates a variant being amongst the top 10% of deleterious variants in the human genome whereas a score of 20 is used to describe variants that are amongst the top 1% of deleterious variants and so on (Kircher et al., 2014). To score the identified variants, we used the CADD model GRCh38-v1.6 and applied a PHRED-scaled score of 20 as a cutoff for deleteriousness as suggested by the authors (Rentzsch et al., 2021). Three *in silico* prediction algorithms for the evaluation of missense variants were used as embedded in Alamut Genova v.1.4/Alamut Visual v.2.14.0: SIFT (Sorting Intolerant From Tolerant, v4.0.3/v6.2.0) applies a score range of 0.0 for a deleterious effect to 1.0 for the substitution being tolerated (http://sift.bii.a-star.edu.sg/) (Kumar et al., 2009), whereas MutationTaster (v2013) classifies the variants either as "disease-causing" or as a "polymorphism" with the *p* value indicating the certainty of the prediction (http://www.mutationtaster.org/) (Schwarz et al., 2010). The third prediction algorithm, Align-GVGD (v2007), provides prediction classes defining a spectrum of classifications with C0 suggesting least likely to interfere with protein function to C65 being most likely to affect functionality of the protein (https://agvgd.iarc.fr/index.php) (Tavtigian et al., 2006). In addition, phyloP scores and the Grantham distance were computed as embedded in Alamut Genova v.1.4/Alamut Visual v.2.14.0 to further elucidate the possible pathogenic effect of missense variants. PhyloP determines the evolutionary conservation and acceleration of a given nucleotide. Positive scores are assigned to sites predicted to be conserved whereas negative scores indicate a fast-evolving site (Pollard et al., 2010). The Grantham distance scores missense substitutions regarding the physicochemical difference between the exchanged amino acids with scores ranging from 0 to 215 (Grantham, 1974).

To further assess the conservation of amino acid residues of missense substitutions, we, in addition, performed a protein sequence alignment of *Homo sapiens* CNGA3 against its orthologues from seven other species, the *Homo sapiens* CNGA1 protein and its orthologues from additional five species using Clustal Omega (https://www.ebi.ac.uk/Tools/msa/clustalo/) (Sievers et al., 2011) and the alignment visualization tool BoxShade version 3.21 (https://embnet.vital-it.ch/software/BOX_form.html) (Figure S2).

Minor allele frequencies were retrieved from the Genome Aggregation Database (gnomAD) (v2.0.2/v2.1) (https://gnomad.broadinstitute.org/).

In silico evaluation of variants affecting either canonical or noncanonical splice sites was conducted using the splicing algorithms SpliceSiteFinder-like [0-100] (Shapiro & Senapathy, 1987), MaxEntScan [donor sites: 0-12 & acceptor sites: 0-16] (Yeo & Burge, 2004), NNSplice [0-1] (Reese et al., 1997), GeneSplicer [0-15] (Pertea et al., 2001) as embedded in Alamut Genova v.1.4/Alamut Visual v.2.14.0, and SpliceAI [0-1] (Jaganathan et al., 2019) (https://spliceailookup.broadinstitute.org/). Furthermore, variants affecting noncanonical exonic splice site sequences (cutoff: first/last five nucleotides of an exon) were also evaluated using the above-mentioned splicing algorithms. All *in silico* tools were used following the guidelines for the use of prediction tools (Vihinen, 2013).

2.5 | Variant classification

The pathogenic impact of the *CNGA3* variants listed in this study was automatically and/or semi-automatically classified according to the standards and guidelines provided by the American College of Medical Genetics and Genomics (ACMG) and the Association for Molecular Pathology (AMP) (Richards et al., 2015) using the web-based variant interpretation tool Franklin (Genoox Ltd, https://franklin.genoox.com/). The criterion PP1 was thereby used for sequence alterations showing co-segregation of the variant(s) with disease in multiple affected family members, either performed in-house or documented in previously published studies. *CNGA3* variants which were functionally analyzed in previously published studies and proven to have a damaging effect on protein function were assigned the criterion PS3. The criterion PP3 was used for missense variants that were predicted to be deleterious by CADD and MutationTaster, and for canonical/noncanonical splice site variants unanimously predicted to affect splicing using the above-mentioned *in silico* tools. If the applied *in silico* tools did not suggest a pathogenic effect, the criterion BP4 was assigned. For *CNGA3* variants having a minor allele frequency of <0.1% on gnomAD, the criterion PM2 was applied. In contrast, variants with a minor allele frequency of >0.1% were assigned the criterion BS1.

3 | OVERVIEW OF *CNGA3* VARIANTS UNDERLYING ACHM

3.1 | Spectrum of *CNGA3* gene variants in our ACHM study cohort genetically characterized in Tübingen

Our total ACHM cohort genetically characterized in Tübingen comprises 1060 affected individuals from 889 independent families carrying "likely disease-causing" variants in the six genes associated with ACHM. Among these, 385 patients from 304 distinct families

10981004, 2022, 7, Downloaded from https://onlinelibrary.wiley.com/doi/10.1002/humu.24371, Wiley Online Library on [09/12/2024]. See the Terms and Conditions (https://onlinelibrary.wiley.com/terms-and-conditions) on Wiley Online Library for rules of use; OA articles are governed by the applicable Creative Commons License

carry likely biallelic ACHM-related variants in the *CNGA3* gene, hereby revealing that *CNGA3* is the second most commonly mutated gene in our study cohort (36.3% patients/34.2% families, Figure S1). Of note, 216 of these families have not been published previously.

In total, we detected 221 distinct genotypes of *CNGA3* sequence alterations in our patient cohort (Table S2). Segregation analysis was performed in both parents for 181 affected individuals and in a single parent and/or in other family members (i.e., siblings, cousins, or offspring) for 88 ACHM patients confirming the presence and independent inheritance of two mutant biallelic *CNGA3* alleles. In 116 cases no relatives were available for segregation analysis which corresponds to 116 families out of 304 families in the cohort missing segregation analysis (38.2%). One hundred and forty-seven affected individuals carry possibly disease-causing *CNGA3* variants in an (apparent) homozygous state whereas 238 solved cases harbor two (likely compound) heterozygous variants expected to explain the ACHM phenotype. Homozygosity for the c.1641C>A/p.(Phe547Leu) or the c.847C>T/p.(Arg283Trp) *CNGA3* variant were by far the most common genotypes in our cohort ($n = 23$ and $n = 22$ affected individuals, respectively; Table S2).

Moreover, we observed one family in our study cohort with pseudo-dominant inheritance involving two mutant *CNGA3* alleles. In this family, the affected mother was homozygous for the c.847C>T/p.(Arg283Trp) variant and the clinically unaffected spouse was a heterozygous carrier of the c.488C>T/p.(Pro163Leu) variant. Both affected children in this family were compound heterozygous for the two *CNGA3* variants inherited from the parents (Table S2).

One patient in our study cohort was shown to harbor two heterozygous missense variants (c.353A>G/p.(Gln118Arg) and c.1615G>A/p.(Val539Met); Table S2), of which the c.353A>G variant was classified as likely benign and the c.1615G>A alteration as a variant of uncertain significance (VUS) according to ACMG/AMP guidelines. Notably, this male patient was in the meantime shown to carry an alteration at the *OPN1LW/OPN1MW* gene cluster compatible with a genetic diagnosis of blue cone monochromacy, an X-linked incomplete form of ACHM. In one patient, only a single heterozygous *CNGA3* variant was identified. Of note, in this patient screening of all other ACHM-associated genes did not identify any other likely causative variants. Both above-mentioned cases were excluded from the group of genetically solved ACHM cases.

In the ACHM cohort genetically characterized in Tübingen, we identified 140 different potential disease-associated variants. The ten most common *CNGA3*-ACHM-related alleles detected in our patient cohort are presented in Table 1. All but one of these are missense sequence alterations. The two missense substitutions c.1641C>A/p.(Phe547Leu) and c.847C>T/p.(Arg283Trp) are the by far most commonly observed *CNGA3*-associated alleles for ACHM in our cohort, both with a similar allele frequency ($n = 86$ chromosomes for c.1641C>A/p.(Phe547Leu) and $n = 84$ chromosomes for c.847C>T/p.(Arg283Trp)). Both alleles are frequently seen in ACHM patients originating from Germany (c.1641C>A/p.(Phe547Leu): $n = 21$ affected individuals; c.847C>T/p.(Arg283Trp): $n = 22$) and in the case of the c.1641C>A/p.(Phe547Leu) variant also in the Middle East ($n = 15$). Further common *CNGA3* alleles associated with ACHM include the missense substitution c.829C>T/p.(Arg277Cys) ($n = 48$ chromosomes) which is mainly seen in German ($n = 18$) and US ACHM patients ($n = 6$). Similarly, we observed some descent-specific enrichment for c.1279C>T/p.(Arg427Cys) (total $n = 26$ chromosomes) in US patients ($n = 9$), as well as for the c.848G>A/p.(Arg283Gln) variant (total $n = 20$ chromosomes) observed in 5 out of 15 individuals who originated from Great Britain. Furthermore, the c.1495C>T/p.(Arg499Ter) variant (total $n = 19$ chromosomes) is the only nonsense variant detected in the spectrum of commonly observed *CNGA3*-ACHM-related alleles and was predominantly identified in French patients ($n = 6$) (Table 1 and Figure 1).

TABLE 1 Ten most common *CNGA3*-ACHM-associated alleles in the ACHM study cohort genetically characterized in Tübingen

Alteration nucleotide sequence[a]	Alteration polypeptide	Total number of chromosomes
c.1641C>A	p.(Phe547Leu)	86
c.847C>T	p.(Arg283Trp)	84
c.829C>T	p.(Arg277Cys)	48
c.1306C>T	p.(Arg436Trp)	32
c.1279C>T	p.(Arg427Cys)	26
c.1114C>T	p.(Pro372Ser)	25
c.667C>T	p.(Arg223Trp)	20
c.848G>A	p.(Arg283Gln)	20
c.830G>A	p.(Arg277His)	19
c.1495C>T	p.(Arg499Ter)	19

Abbreviation: ACHM, achromatopsia.

[a]Variant designation is based on NM_001298.2 (GRCh38/hg38).

3.2 | Comprehensive *CNGA3* variant database

To create a comprehensive *CNGA3* variant database, we combined all *CNGA3* variants identified in our ACHM cohort with all *CNGA3* sequence alterations obtained after an extensive literature search on PubMed®, and database search in HGMD®, LOVD and ClinVar. The so established *CNGA3* variant database currently comprises 316 variants (Tables 2 and S3). Of these, four variants are located in the alternate exon 3b and its flanking intronic sequences. As the functional relevance of this sequence remains unclear and no association with disease has ever been reported, these variants were not further analyzed and were classified as "likely benign."

Following the standards and guidelines of ACMG/AMP, 67 out of the remaining 312 variants were classified as pathogenic, 152 as likely pathogenic, and 71 were categorized as variants of uncertain

10981004, 2022, 7, Downloaded from https://onlinelibrary.wiley.com/doi/10.1002/humu.24371, Wiley Online Library on [09/12/2024]. See the Terms and Conditions (https://onlinelibrary.wiley.com/terms-and-conditions) on Wiley Online Library for rules of use; OA articles are governed by the applicable Creative Commons License

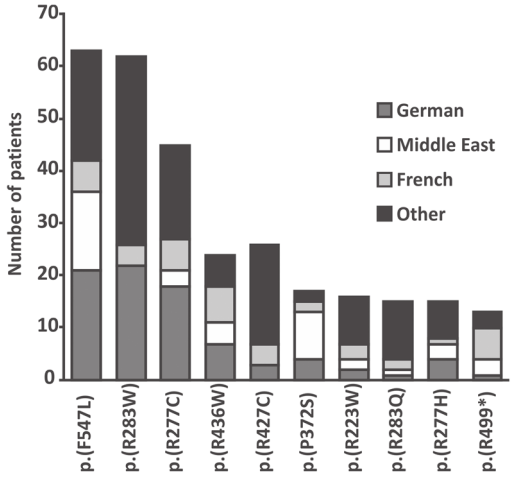


FIGURE 1 Geographic descent of patients carrying the ten most common *CNGA3*-ACHM-related alleles in the ACHM study cohort genetically characterized in Tübingen. The number of patients is determined by considering all affected individuals carrying the 10 most common *CNGA3*-ACHM-related alleles either in a homozygous or (compound) heterozygous state. The c.1641C>A/p.(Phe547Leu) variant (*n* = 63 patients) is the most common *CNGA3*-ACHM-associated variant in our cohort and was frequently observed in ACHM patients of German (*n* = 21) and Middle Eastern origin (*n* = 15). ACHM, achromatopsia.

significance (VUS). Furthermore, 12 out of 312 sequence alterations were classified as likely benign and 10 as benign (Tables 2 and S3).

The 316 *CNGA3* variants listed in our *CNGA3* variant database were revised manually and expert-categorized into "likely benign," "VUS," and "likely disease-causing" applying the following criteria. Variants categorized as "likely benign" (*n* = 44 variants; Tables 2 and S3) included: (1) variants classified as likely benign or benign according to ACMG/AMP guidelines, (2) synonymous variants that are not predicted to affect splicing, (3) missense variants with a minor allele frequency (MAF) higher than 0.1% and predicted to be tolerated by at least two *in silico* algorithms, (4) missense variants predicted to be tolerated by at least two *in silico* tools and only observed in a heterozygous state in the absence of a second "likely disease-causing" allele, (5) noncanonical splice variants not predicted to affect splicing and (6) variants located in the alternate exon 3b and its flanking intronic sequences.

Variants classified as "VUS" (*n* = 28; Tables 2 and S3) comprised missense variants that were classified as VUS following the ACMG/AMP guidelines and were predicted to be tolerated by at least two *in silico* tools. In addition, 15 variants were grouped in this category since no genotype could be established from the literature or database data. If the following criteria for a "VUS" were fulfilled, we considered patients carrying such variants with respect to the phenotype as solved cases: (1) observation of the variant in a heterozygous state with a (known) "likely disease-causing" variant and/or (2) segregation analysis demonstrated independent segregation of two variants and/or co-segregation of the variant with the disease.

All variants in the *CNGA3* variant database not meeting the above-mentioned criteria were categorized as "likely disease-causing" (*n* = 244; Tables 2 and S3). Thus, we included the following variants in this "likely disease-causing" category: (1) variants classified as pathogenic or likely pathogenic following the ACMG/AMP guidelines, (2) variants representing likely null alleles (nonsense, start loss, canonical splice site, and frameshift variants), (3) missense variants classified as VUS following ACMG/AMP guidelines, but predicted to be deleterious by at least three *in silico* tools, (4) missense variants for which functional analysis revealed a deleterious effect on protein function, (5) noncanonical splice site variants classified as VUS following ACMG/AMP guidelines, but predicted to have an effect on splicing by at least three *in silico* tools, and (6) in-frame deletions affecting (completely) conserved amino acid residues. Consequently, all patients carrying *CNGA3* variants categorized as "likely disease-causing" were designated as solved cases with respect to the ACHM phenotype.

Among 316 *CNGA3* variants listed in the *CNGA3* variant database, 251 variants were already published in the literature and in public databases. From these, we classified 196 variants as "likely disease-causing", 23 as "VUS" and 32 as "likely benign" following manual and expert-based revision (Table S3). Only a small number of previously published missense variants were categorized as "likely benign" including the variants p.(Thr20Ile), p.(Pro48Leu), p.(Thr153Met), and p.(Val540Ile) based on the following observations: (1) All but one of these are located in the N-terminal region affecting residues which are neither conserved within CNGA3 orthologues nor the rod homolog CNGA1—only the p.(Val540Ile) variant affects a conserved residue in the CNBD. (2) All above-mentioned missense variants have a MAF higher than 0.1% and were predicted to be tolerated by *in silico* tools underlining their presumably nonpathogenic impact.

Within our *CNGA3* variant database, we report 48 novel "likely disease-causing" variants detected in our ACHM cohort with six variants classified as pathogenic, 36 as likely pathogenic, and six as VUS following ACMG/AMP classification (Table S3). These previously unpublished variants comprise 24 missense substitutions, 14 small indel variants, and 6 nonsense substitutions creating a premature stop codon.

Overall, out of the 244 "likely disease-causing" variants in the *CNGA3* variant database, missense substitutions were the most frequently observed variant type (66.8%) followed by small indel variants (16.8%) and nonsense alterations (12.3%) creating a premature stop codon (Figure 2). An overview of the mutation types and the respective frequencies of these "likely disease-causing" *CNGA3* variants within our database is provided in Figure 2.

In addition, we observed one novel start loss variant affecting the first nucleotide of the translation initiation codon ATG (c.1A>T/p.(?)) and one copy number variation leading to the complete deletion of exon 8 (NC_000002.12:g.98393909_98399093del (GRCh38/hg38)). Actually, this deletion is the first large structural variation/copy number variation observed and reported for the *CNGA3* gene and

10981004, 2022, 7, Downloaded from https://onlinelibrary.wiley.com/doi/10.1002/humu.24371, Wiley Online Library on [09/12/2024]. See the Terms and Conditions (https://onlinelibrary.wiley.com/terms-and-conditions) on Wiley Online Library for rules of use; OA articles are governed by the applicable Creative Commons License

TABLE 2 Variants in the *CNGA3* gene reported in the literature, mutation databases and novel variants identified in the ACHM study cohort genetically characterized in Tübingen

Location *CNGA3*	Alteration nucleotide sequence[a]	Alteration polypeptide	Location protein domain[b]	References	ACMG/AMP classification
Likely disease-causing variants					
Intron 1	c.-37-1G>C	p.(?)	-	Burkard et al. (2018)	Pathogenic
Exon 2	c.1A>T	p.(?)	N-Term.	This study	VUS
Exon 2	c.40del	p.(Thr14ProfsTer5)	N-Term.	Liang et al. (2015)	Pathogenic
Exon 2	c.62C>G	p.(Ser21Ter)	N-Term.	Li et al. (2014)	Pathogenic
Exon 2	c.67C>T	p.(Arg23Ter)	N-Term.	Johnson et al. (2004)	Pathogenic
Intron 2	c.101+1G>A	p.(?)	-	Abdelkader et al. (2018)	Pathogenic
Exon 3	c.107_110del	p.(His36ArgfsTer136)	N-Term.	Thomas et al. (2012)	Pathogenic
Exon 3	c.128C>A	p.(Ser43Ter)	N-Term.	Sun et al. (2020)	Likely pathogenic
Exon 3	c.130_151dup	p.(Ala51ValfsTer16)	N-Term.	Zelinger et al. (2015)	Pathogenic
Exon 3	c.139C>T	p.(Gln47Ter)	N-Term.	Zobor et al. (2017)	Likely pathogenic
Exon 3	c.147dup	p.(Ile50AspfsTer10)	N-Term.	Wissinger et al. (2001)	Likely pathogenic
Exon 3	c.162_163insT	p.(Arg55Ter)	N-Term.	Ezquerra-Inchausti et al. (2018)	Pathogenic
Exon 4	c.248G>A	p.(Trp83Ter)	N-Term.	Ellingford et al. (2016)	Pathogenic
Exon 4	c.332_333delinsAA	p.(Ser111Ter)	N-Term.	This study	Pathogenic
Exon 4	c.340G>T	p.(Glu114Ter)	N-Term.	This study	Pathogenic
Exon 4	c.384_387del	p.(Asp128GlufsTer44)	N-Term.	This study	Likely pathogenic
Exon 4	c.387del	p.(Arg131GlufsTer42)	N-Term.	This study	Likely pathogenic
Intron 4	c.395+1G>T	p.(?)	-	Abdelkader et al. (2018)	Likely pathogenic
Intron 4	c.396-2_398dup	p.(?)	-	This study	Likely pathogenic
Intron 4	c.396-11C>G	p.(?)	-	Li et al. (2014)	VUS
Intron 5	c.450-1G>A	p.(?)	-	Georgiou et al. (2019)	Likely pathogenic
Intron 5	c.450-15T>G	p.(?)	-	This study	VUS
Exon 6	c.464del	p.(Lys155ArgfsTer18)	N-Term.	This study	Pathogenic
Exon 6	c.478G>A	p.(Val160Met)	N-Term.	ClinVar	VUS
Exon 6	c.479T>G	p.(Val160Gly)	N-Term.	This study	VUS
Exon 6	c.485A>T	p.(Asp162Val)	N-Term.	Wissinger et al. (2001)	Likely pathogenic
Exon 6	c.488C>T	p.(Pro163Leu)	N-Term.	Kohl et al. (1998)	Pathogenic
Exon 6	c.489_492del	p.(Ser164AlafsTer8)	N-Term.	LOVD	Pathogenic
Exon 6	c.499del	p.(Leu167CysfsTer6)	N-Term.	Weisschuh et al. (2020)	Pathogenic
Exon 6	c.512G>A	p.(Trp171Ter)	TM1	Li et al. (2014)	Pathogenic
Exon 6	c.513G>T	p.(Trp171Cys)	TM1	Li et al. (2014)	VUS
Exon 6	c.513G>A	p.(Trp171Ter)	TM1	This study	Pathogenic
Exon 6	c.536T>A	p.(Val179Asp)	TM1	Dubis et al. (2014)	VUS
Exon 6	c.542A>G	p.(Tyr181Cys)	TM1	Wissinger et al. (2001)	Pathogenic
Exon 6	c.544A>G	p.(Asn182Asp)	TM1	This study	Likely pathogenic
Exon 6	c.544A>T	p.(Asn182Tyr)	TM1	Wissinger et al. (2001)	Likely pathogenic

(Continues)

10981004, 2022, 7, Downloaded from https://onlinelibrary.wiley.com/doi/10.1002/humu.24371, Wiley Online Library on [09/12/2024]. See the Terms and Conditions (https://onlinelibrary.wiley.com/terms-and-conditions) on Wiley Online Library for rules of use; OA articles are governed by the applicable Creative Commons License

TABLE 2 (Continued)

Location *CNGA3*	Alteration nucleotide sequence[a]	Alteration polypeptide	Location protein domain[b]	References	ACMG/AMP classification
Exon 6	c.556C>T	p.(Leu186Phe)	TM1	Wissinger et al. (2001)	Likely pathogenic
Exon 6	c.560T>C	p.(Ile187Thr)	TM1 - TM2	Taylor et al. (2017)	Likely pathogenic
Exon 6	c.566G>A	p.(Arg189Lys)	TM1 - TM2	This study	VUS
Exon 7	c.572G>A	p.(Cys191Tyr)	TM1 - TM2	Wissinger et al. (2001)	Likely pathogenic
Exon 7	c.580G>A	p.(Glu194Lys)	TM1 - TM2	Wissinger et al. (2001)	Likely pathogenic
Exon 7	c.584T>C	p.(Leu195Pro)	TM1 - TM2	ClinVar	VUS
Exon 7	c.586C>T	p.(Gln196Ter)	TM1 - TM2	Johnson et al. (2004)	Likely pathogenic
Exon 7	c.589T>C	p.(Ser197Pro)	TM2	ClinVar	Likely pathogenic
Exon 7	c.591del	p.(Glu198SerfsTer3)	TM2	This study	Likely pathogenic
Exon 7	c.608G>A	p.(Trp203Ter)	TM2	Georgiou et al. (2019)	Likely pathogenic
Exon 7	c.609G>A	p.(Trp203Ter)	TM2	Sun et al. (2020)	Likely pathogenic
Exon 7	c.609G>T	p.(Trp203Cys)	TM2	This study	VUS
Exon 7	c.624C>G	p.(Tyr208Ter)	TM2	Hull et al. (2020)	Likely pathogenic
Exon 7	c.633T>A	p.(Asp211Glu)	TM2	Liang et al. (2015)	VUS
Exon 7	c.649G>C	p.(Asp217His)	TM2	ClinVar	VUS
Exon 7	c.661C>T	p.(Arg221Ter)	TM2	Johnson et al. (2004)	Pathogenic
Exon 7	c.667C>T	p.(Arg223Trp)	TM2	Wissinger et al. (2001)	Pathogenic
Exon 7	c.667C>G	p.(Arg223Gly)	TM2	Wiszniewski et al. (2007)	Likely pathogenic
Exon 7	c.668G>A	p.(Arg223Gln)	TM2	Li et al. (2014); Greenberg et al. (2014)	Pathogenic
Exon 7	c.671C>G	p.(Thr224Arg)	TM2 - TM3	Wissinger et al. (2001)	Likely pathogenic
Intron 7	c.674-2A>C	p.(?)	-	Li et al. (2014)	Likely pathogenic
Exon 8	c.674-1935_*1838del (Deletion Exon 8)	p.(?)	-	This study	Pathogenic
Exon 8	c.682G>A	p.(Glu228Lys)	TM2 - TM3	Reuter et al. (2008)	Pathogenic
Exon 8	c.704A>T	p.(Asp235Val)	TM2 - TM3	Weisschuh et al. (2020)	VUS
Exon 8	c.742C>T	p.(Gln248Ter)	TM3	This study	Likely pathogenic
Exon 8	c.746T>C	p.(Phe249Ser)	TM3	Nishiguchi et al. (2005)	VUS
Exon 8	c.754G>A	p.(Asp252Asn)	TM3	Koeppen et al. (2008)	Likely pathogenic
Exon 8	c.755A>C	p.(Asp252Ala)	TM3	Sun et al. (2020)	VUS
Exon 8	c.772C>G	p.(Pro258Ala)	TM3	This study	VUS
Exon 8	c.773C>G	p.(Pro258Arg)	TM3	Li et al. (2014)	VUS
Exon 8	c.778G>A	p.(Asp260Asn)	TM3	Wissinger et al. (2001)	Pathogenic
Exon 8	c.778G>C	p.(Asp260His)	TM3	This study	Likely pathogenic
Exon 8	c.778dup	p.(Asp260GlyfsTer27)	TM3	LOVD	Pathogenic
Exon 8	c.787T>G	p.(Tyr263Asp)	TM3	Nishiguchi et al. (2005)	Likely pathogenic
Exon 8	c.800G>A	p.(Gly267Asp)	TM3 - TM4	Wissinger et al. (2001)	Pathogenic
Exon 8	c.811C>G	p.(Pro271Ala)	TM3 - TM4	Zelinger et al. (2015)	Likely pathogenic
Exon 8	c.811C>A	p.(Pro271Thr)	TM3 - TM4	This study	Likely pathogenic

10981004, 2022, 7, Downloaded from https://onlinelibrary.wiley.com/doi/10.1002/humu.24371, Wiley Online Library on [09/12/2024]. See the Terms and Conditions (https://onlinelibrary.wiley.com/terms-and-conditions) on Wiley Online Library for rules of use; OA articles are governed by the applicable Creative Commons License

TABLE 2 (Continued)

Location *CNGA3*	Alteration nucleotide sequence[a]	Alteration polypeptide	Location protein domain[b]	References	ACMG/AMP classification
Exon 8	c.811C>T	p.(Pro271Ser)	TM3 - TM4	Georgiou et al. (2019)	Likely pathogenic
Exon 8	c.822G>T	p.(Arg274Ser)	TM4	Azam et al. (2010)	Likely pathogenic
Exon 8	c.821G>A	p.(Arg274Lys)	TM4	Li et al. (2014)	Likely pathogenic
Exon 8	c.827A>G	p.(Asn276Ser)	TM4	Saqib et al. (2011)	Likely pathogenic
Exon 8	c.829C>T	p.(Arg277Cys)	TM4	Wissinger et al. (2001)	Pathogenic
Exon 8	c.829C>G	p.(Arg277Gly)	TM4	Koeppen et al. (2010)	Likely pathogenic
Exon 8	c.830G>A	p.(Arg277His)	TM4	Wissinger et al. (2001)	Pathogenic
Exon 8	c.833T>C	p.(Leu278Pro)	TM4	Li et al. (2014)	Likely pathogenic
Exon 8	c.838A>T	p.(Lys280Ter)	TM4	Wang et al. (2019)	Likely pathogenic
Exon 8	c.847C>T	p.(Arg283Trp)	TM4	Kohl et al. (1998)	Pathogenic
Exon 8	c.848G>A	p.(Arg283Gln)	TM4	Kohl et al. (1998)	Pathogenic
Exon 8	c.851del	p.(Leu284ProfsTer78)	TM4	This study	Likely pathogenic
Exon 8	c.869G>A	p.(Arg290His)	TM4	Burkard et al. (2018)	Pathogenic
Exon 8	c.872C>G	p.(Thr291Arg)	TM4 - TM5	Kohl et al. (1998)	Pathogenic
Exon 8	c.872_873del	p.(Thr291ArgfsTer77)	TM4 - TM5	Li et al. (2014)	Likely pathogenic
Exon 8	c.902_903delinsAA	p.(Phe301Ter)	TM5	This study	Likely pathogenic
Exon 8	c.904A>G	p.(Arg302Gly)	TM5	Zelinger et al. (2015)	Likely pathogenic
Exon 8	c.906G>T	p.(Arg302Ser)	TM5	Weisschuh et al. (2020)	Likely pathogenic
Exon 8	c.907A>T	p.(Ile303Phe)	TM5	ClinVar	Likely pathogenic
Exon 8	c.940_942del	p.(Ile314del)	TM5	Wissinger et al. (2001)	Pathogenic
Exon 8	c.945C>G	p.(His315Gln)	TM5	Patel et al. (2019)	Likely pathogenic
Exon 8	c.947G>A	p.(Trp316Ter)	TM5	Wissinger et al. (2001)	Likely pathogenic
Exon 8	c.952G>A	p.(Ala318Thr)	TM5	Li et al. (2017)	Likely pathogenic
Exon 8	c.955T>C	p.(Cys319Arg)	TM5	Shaikh et al. (2015)	Pathogenic
Exon 8	c.955_963delinsACCAAT-GAAATGGAAAT	p.(Cys319ThrfsTer46)	TM5	This study	Likely pathogenic
Exon 8	c.965T>C	p.(Phe322Ser)	TM5	Li et al. (2014)	Likely pathogenic
Exon 8	c.967G>C	p.(Ala323Pro)	TM5	Carss et al. (2017)	Likely pathogenic
Exon 8	c.968C>A	p.(Ala323Asp)	TM5	Li et al. (2015)	Likely pathogenic
Exon 8	c.983T>C	p.(Ile328Thr)	TM5	This study	Likely pathogenic
Exon 8	c.985G>T	p.(Gly329Cys)	TM5 - pore helix	Genead et al. (2011)	Pathogenic
Exon 8	c.989T>C	p.(Phe330Ser)	TM5 - pore helix	Li et al. (2014)	Likely pathogenic
Exon 8	c.991G>C	p.(Gly331Arg)	TM5 - pore helix	Saqib et al. (2015)	Likely pathogenic
Exon 8	c.992G>A	p.(Gly331Glu)	TM5 - pore helix	This study	Likely pathogenic
Exon 8	c.997_998del	p.(Asp333LeufsTer35)	TM5 - pore helix	Kuniyoshi et al. (2016)	Likely pathogenic
Exon 8	c.1001C>T	p.(Ser334Phe)	TM5 - pore helix	Sundaram et al. (2014)	Likely pathogenic
Exon 8	c.1004G>A	p.(Trp335Ter)	TM5 - pore helix	This study	Likely pathogenic
Exon 8	c.1006G>T	p.(Val336Phe)	TM5 - pore helix	Liang et al. (2015)	Likely pathogenic

(Continues)

10981004, 2022, 7, Downloaded from https://onlinelibrary.wiley.com/doi/10.1002/humu.24371, Wiley Online Library on [09/12/2024]. See the Terms and Conditions (https://onlinelibrary.wiley.com/terms-and-conditions) on Wiley Online Library for rules of use; OA articles are governed by the applicable Creative Commons License

TABLE 2 (Continued)

Location *CNGA3*	Alteration nucleotide sequence[a]	Alteration polypeptide	Location protein domain[b]	References	ACMG/AMP classification
Exon 8	c.1010_1012delinsCAATCCCAGTG	p.(Tyr337SerfsTer28)	TM5 - pore helix	Li et al. (2014)	Likely pathogenic
Exon 8	c.1021T>C	p.(Ser341Pro)	TM5 - pore helix	Wissinger et al. (2001)	Pathogenic
Exon 8	c.1030G>T	p.(Glu344Ter)	TM5 - pore helix	Nishiguchi et al. (2005)	Likely pathogenic
Exon 8	c.1034A>G	p.(His345Arg)	TM5 - pore helix	ClinVar	Likely pathogenic
Exon 8	c.1039C>T	p.(Arg347Cys)	TM5 - pore helix	Sun et al. (2020)	Likely pathogenic
Exon 8	c.1048A>G	p.(Arg350Gly)	TM5 - pore helix	ClinVar	VUS
Exon 8	c.1058T>C	p.(Ile353Thr)	Pore helix	Liang et al. (2015)	Likely pathogenic
Exon 8	c.1061A>G	p.(Tyr354Cys)	Pore helix	This study	Likely pathogenic
Exon 8	c.1063A>G	p.(Ser355Gly)	Pore helix	This study	Likely pathogenic
Exon 8	c.1070A>G	p.(Tyr357Cys)	Pore helix	Vincent et al. (2011)	Likely pathogenic
Exon 8	c.1074G>A	p.(Trp358Ter)	Pore helix	Li et al. (2014)	Likely pathogenic
Exon 8	c.1076C>T	p.(Ser359Phe)	Pore helix	This study	Likely pathogenic
Exon 8	c.1085C>T	p.(Thr362Ile)	Pore helix	ClinVar	Likely pathogenic
Exon 8	c.1088T>C	p.(Leu363Pro)	Pore helix	Koeppen et al. (2010)	Pathogenic
Exon 8	c.1100G>T	p.(Gly367Val)	pore helix -TM6	Koeppen et al. (2010)	Pathogenic
Exon 8	c.1106C>G	p.(Thr369Ser)	pore helix -TM6	Wissinger et al. (2001)	Pathogenic
Exon 8	c.1114C>T	p.(Pro372Ser)	pore helix -TM6	Wissinger et al. (2001)	Pathogenic
Exon 8	c.1114C>G	p.(Pro372Ala)	pore helix -TM6	Sharon et al. (2020)	Likely pathogenic
Exon 8	c.1115C>T	p.(Pro372Leu)	pore helix -TM6	This study	Likely pathogenic
Exon 8	c.1116del	p.(Val373Ter)	pore helix -TM6	Zobor et al. (2017)	Likely pathogenic
Exon 8	c.1116dup	p.(Val373ArgfsTer4)	pore helix -TM6	Li et al. (2014)	Pathogenic
Exon 8	c.1117G>A	p.(Val373Met)	pore helix -TM6	This study	Likely pathogenic
Exon 8	c.1124A>G	p.(Asp375Gly)	TM6	Sun et al. (2020)	Likely pathogenic
Exon 8	c.1126G>A	p.(Glu376Lys)	TM6	Koeppen et al. (2010)	Pathogenic
Exon 8	c.1129_1131del	p.(Glu377del)	TM6	Fahim et al. (2013)	Likely pathogenic
Exon 8	c.1137_1139del	p.(Phe380del)	TM6	Liang et al. (2015)	Likely pathogenic
Exon 8	c.1139T>C	p.(Phe380Ser)	TM6	Wissinger et al. (2001)	Pathogenic
Exon 8	c.1146dup	p.(Val383ArgfsTer36)	TM6	Li et al. (2014)	Likely pathogenic
Exon 8	c.1163G>A	p.(Gly388Asp)	TM6	Sun et al. (2020)	Likely pathogenic
Exon 8	c.1163G>T	p.(Gly388Val)	TM6	Sun et al. (2020)	Likely pathogenic
Exon 8	c.1190G>T	p.(Gly397Val)	TM6	Ahuja et al. (2008)	Likely pathogenic
Exon 8	c.1201T>C	p.(Ser401Pro)	TM6	Nishiguchi et al. (2005)	Likely pathogenic
Exon 8	c.1217T>C	p.(Met406Thr)	TM6	Wissinger et al. (2001)	Likely pathogenic
Exon 8	c.1228C>T	p.(Arg410Trp)	TM6 - C-linker	Kohl et al. (1998)	Pathogenic
Exon 8	c.1235_1236del	p.(Glu412ValfsTer6)	TM6 - C-linker	Méjécase et al. (2019)	Likely pathogenic
Exon 8	c.1243G>C	p.(Ala415Pro)	C-linker αA'	Stone et al. (2017)	Likely pathogenic
Exon 8	c.1254T>G	p.(Asp418Glu)	C-linker αA'	ClinVar	Likely pathogenic
Exon 8	c.1255T>C	p.(Ser419Pro)	C-linker αA'	Weisschuh et al. (2020)	Likely pathogenic

10981004, 2022, 7, Downloaded from https://onlinelibrary.wiley.com/doi/10.1002/humu.24371, Wiley Online Library on [09/12/2024]. See the Terms and Conditions (https://onlinelibrary.wiley.com/terms-and-conditions) on Wiley Online Library for rules of use; OA articles are governed by the applicable Creative Commons License

TABLE 2 (Continued)

Location *CNGA3*	Alteration nucleotide sequence[a]	Alteration polypeptide	Location protein domain[b]	References	ACMG/AMP classification
Exon 8	c.1256C>T	p.(Ser419Phe)	C-linker αA'	Patel et al. (2019)	Likely pathogenic
Exon 8	c.1262del	p.(Lys421SerfsTer44)	C-linker αA'	Rim et al. (2017)	Likely pathogenic
Exon 8	c.1267dup	p.(Tyr423LeufsTer20)	C-linker αA'	Sun et al. (2020)	Likely pathogenic
Exon 8	c.1268A>C	p.(Tyr423Ser)	C-linker αA'	This study	Likely pathogenic
Exon 8	c.1270A>G	p.(Met424Val)	C-linker αA'	Kuniyoshi et al. (2016)	Pathogenic
Exon 8	c.1271T>C	p.(Met424Thr)	C-linker αA'	ClinVar	Likely pathogenic
Exon 8	c.1273C>T	p.(Gln425Ter)	C-linker αA'	This study	Likely pathogenic
Exon 8	c.1279C>T	p.(Arg427Cys)	C-linker αA' - αB'	Wissinger et al. (2001)	Pathogenic
Exon 8	c.1280G>T	p.(Arg427Leu)	C-linker αA' - αB'	ClinVar	Likely pathogenic
Exon 8	c.1286T>C	p.(Val429Ala)	C-linker αA' - αB'	Georgiou et al. (2019)	Likely pathogenic
Exon 8	c.1294G>T	p.(Asp432Tyr)	C-linker αB'	Sun et al. (2020)	Likely pathogenic
Exon 8	c.1294del	p.(Asp432ThrfsTer33)	C-linker αB'	Zelinger et al. (2015)	Likely pathogenic
Exon 8	c.1298T>G	p.(Leu433Trp)	C-linker αB'	Koeppen et al. (2008)	Pathogenic
Exon 8	c.1306C>T	p.(Arg436Trp)	C-linker αB'	Wissinger et al. (2001)	Pathogenic
Exon 8	c.1307G>A	p.(Arg436Gln)	C-linker αB'	Li et al. (2014)	Likely pathogenic
Exon 8	c.1315C>T	p.(Arg439Trp)	C-linker αB'	Reuter et al. (2008)	Pathogenic
Exon 8	c.1319G>C	p.(Trp440Ser)	C-linker αB'	Georgiou et al. (2019)	Likely pathogenic
Exon 8	c.1320del	p.(Trp440CysfsTer25)	C-linker αB'	This study	Pathogenic
Exon 8	c.1319G>A	p.(Trp440Ter)	C-linker αB'	Li et al. (2014)	Likely pathogenic
Exon 8	c.1320G>A	p.(Trp440Ter)	C-linker αB'	Wissinger et al. (2001)	Likely pathogenic
Exon 8	c.1351dup	p.(Val451GlyfsTer3)	C-linker αB' - αC'	Wissinger et al. (2001)	Likely pathogenic
Exon 8	c.1360A>T	p.(Lys454Ter)	C-linker αC'	Sundaram et al. (2014)	Likely pathogenic
Exon 8	c.1366del	p.(Val456CysfsTer9)	C-linker αC'	This study	Likely pathogenic
Exon 8	c.1379del	p.(Leu460ProfsTer5)	C-linker αC' - αD'	This study	Likely pathogenic
Exon 8	c.1391T>G	p.(Leu464Arg)	C-linker αD'	Greenberg et al. (2014)	Likely pathogenic
Exon 8	c.1395_1412del	p.(Lys465_Ile470del)	C-linker αD'	This study	Likely pathogenic
Exon 8	c.1405G>A	p.(Ala469Thr)	C-linker αD'	Reuter et al. (2008)	Pathogenic
Exon 8	c.1435_1436delinsGT	p.(Lys479Val)	C-linker αE'	Sun et al. (2020)	VUS
Exon 8	c.1443dup	p.(Ile482HisfsTer6)	C-linker αF'	Johnson et al. (2004)	Likely pathogenic
Exon 8	c.1454A>T	p.(Asp485Val)	C-linker αF'	Wissinger et al. (2001)	Likely pathogenic
Exon 8	c.1457G>A	p.(Cys486Tyr)	C-linker αF' - CNBD αA	Abouelhoda et al. (2016)	Likely pathogenic
Exon 8	c.1466G>T	p.(Gly489Val)	CNBD αA	This study	Likely pathogenic
Exon 8	c.1495C>T	p.(Arg499Ter)	CNBD β1	Burgueño-Montañés et al. (2014)	Likely pathogenic
Exon 8	c.1513C>G	p.(Pro505Ala)	CNBD β1 - β2	Huang et al. (2016)	Likely pathogenic
Exon 8	c.1519del	p.(Asp507IlefsTer47)	CNBD β1 - β2	This study	Likely pathogenic
Exon 8	c.1520A>G	p.(Asp507Gly)	CNBD β1 - β2	LOVD	Likely pathogenic
Exon 8	c.1529G>C	p.(Cys510Ser)	CNBD β2	Wissinger et al. (2001)	Pathogenic

(Continues)

10981004, 2022, 7, Downloaded from https://onlinelibrary.wiley.com/doi/10.1002/humu.24371, Wiley Online Library on [09/12/2024]. See the Terms and Conditions (https://onlinelibrary.wiley.com/terms-and-conditions) on Wiley Online Library for rules of use; OA articles are governed by the applicable Creative Commons License

TABLE 2 (Continued)

Location *CNGA3*	Alteration nucleotide sequence[a]	Alteration polypeptide	Location protein domain[b]	References	ACMG/AMP classification
Exon 8	c.1535A>T	p.(Lys512Met)	CNBD β2 - β3	Carrigan et al. (2016)	Likely pathogenic
Exon 8	c.1537G>C	p.(Gly513Arg)	CNBD β2 - β3	Huang et al. (2016)	Likely pathogenic
Exon 8	c.1537G>A	p.(Gly513Arg)	CNBD β2 - β3	This study	Likely pathogenic
Exon 8	c.1538G>A	p.(Gly513Glu)	CNBD β2 - β3	Wissinger et al. (2001)	Pathogenic
Exon 8	c.1540G>A	p.(Asp514Asn)	CNBD β2 - β3	Arshad et al. (2019)	Likely pathogenic
Exon 8	c.1541A>T	p.(Asp514Val)	CNBD β2 - β3	Genead et al. (2011)	Likely pathogenic
Exon 8	c.1547G>A	p.(Gly516Glu)	CNBD β2 - β3	Wissinger et al. (2001)	Pathogenic
Exon 8	c.1556T>C	p.(Met519Thr)	CNBD β3	Huang et al. (2016)	Likely pathogenic
Exon 8	c.1557G>A	p.(Met519Ile)	CNBD β3	Ellingford et al. (2016)	Likely pathogenic
Exon 8	c.1565T>C	p.(Ile522Thr)	CNBD β3	Wissinger et al. (2001)	Likely pathogenic
Exon 8	c.1569_1577del	p.(Asn523_Gly525del)	CNBD β3	Sun et al. (2020)	VUS
Exon 8	c.1573G>A	p.(Gly525Ser)	CNBD β3 - β4	Patel et al. (2016)	Likely pathogenic
Exon 8	c.1574G>A	p.(Gly525Asp)	CNBD β3 - β4	Wissinger et al. (2001)	Pathogenic
Exon 8	c.1579C>A	p.(Leu527Met)	CNBD β4	Wang et al. (2011)	Likely pathogenic
Exon 8	c.1580T>G	p.(Leu527Arg)	CNBD β4	Lam et al. (2011)	Likely pathogenic
Exon 8	c.1585G>A	p.(Val529Met)	CNBD β4	Kohl et al. (1998)	Pathogenic
Exon 8	c.1597G>C	p.(Asp533His)	CNBD β4 - β5	Li et al. (2014)	Pathogenic
Exon 8	c.1609C>T	p.(Gln537Ter)	CNBD β4 - β5	Wissinger et al. (2001)	Likely pathogenic
Exon 8	c.1621C>T	p.(Leu541Phe)	CNBD β5	Greenberg et al. (2014)	Likely pathogenic
Exon 8	c.1627_1635del	p.(Asp543_Ser545del)	CNBD β5/β5 - β6	Li et al. (2014)	VUS
Exon 8	c.1640T>G	p.(Phe547Cys)	CNBD β6	Zelinger et al. (2015)	Likely pathogenic
Exon 8	c.1641C>A	p.(Phe547Leu)	CNBD β6	Kohl et al. (1998)	Pathogenic
Exon 8	c.1642G>A	p.(Gly548Arg)	CNBD β6	Johnson et al. (2004)	Pathogenic
Exon 8	c.1645G>T	p.(Glu549Ter)	CNBD β6	This study	Likely pathogenic
Exon 8	c.1658T>A	p.(Leu553Gln)	CNBD β6 - β7	This study	Likely pathogenic
Exon 8	c.1669G>A	p.(Gly557Arg)	CNBD β6 - β7	Kohl et al. (1998)	Pathogenic
Exon 8	c.1679C>T	p.(Ser560Leu)	CNBD β6 - β7	ClinVar	Likely pathogenic
Exon 8	c.1682G>A	p.(Gly561Glu)	CNBD β6 - β7	Zobor et al. (2017)	Likely pathogenic
Exon 8	c.1682_1683insACGCG	p.(Asn562ArgfsTer47)	CNBD β6 - β7	This study	Likely pathogenic
Exon 8	c.1686C>A	p.(Asn562Lys)	CNBD β6 - β7	ClinVar	Likely pathogenic
Exon 8	c.1687C>T	p.(Arg563Cys)	CNBD β6 - β7	Koeppen et al. (2008)	Pathogenic
Exon 8	c.1688G>A	p.(Arg563His)	CNBD β6 - β7	Wissinger et al. (2001)	Pathogenic
Exon 8	c.1694C>T	p.(Thr565Met)	CNBD β6 - β7	Wissinger et al. (2001)	Pathogenic
Exon 8	c.1705C>T	p.(Arg569Cys)	CNBD β7	This study	Likely pathogenic
Exon 8	c.1706G>A	p.(Arg569His)	CNBD β7	Wissinger et al. (2001)	Pathogenic
Exon 8	c.1708A>G	p.(Ser570Gly)	CNBD β7	This study	Likely pathogenic
Exon 8	c.1709G>A	p.(Ser570Asn)	CNBD β7	Li et al. (2014)	Likely pathogenic
Exon 8	c.1709G>T	p.(Ser570Ile)	CNBD β7	Thiadens et al. (2010)	Likely pathogenic
Exon 8	c.1712T>C	p.(Ile571Thr)	CNBD β7 - β8	Jinda et al. (2021)	Likely pathogenic

10981004, 2022, 7, Downloaded from https://onlinelibrary.wiley.com/doi/10.1002/humu.24371, Wiley Online Library on [09/12/2024]. See the Terms and Conditions (https://onlinelibrary.wiley.com/terms-and-conditions) on Wiley Online Library for rules of use; OA articles are governed by the applicable Creative Commons License

TABLE 2 (Continued)

Location *CNGA3*	Alteration nucleotide sequence[a]	Alteration polypeptide	Location protein domain[b]	References	ACMG/AMP classification
Exon 8	c.1717T>C	p.(Tyr573His)	CNBD β7 - β8	This study	Likely pathogenic
Exon 8	c.1718A>G	p.(Tyr573Cys)	CNBD β7 - β8	Wissinger et al. (2001)	Pathogenic
Exon 8	c.1719C>G	p.(Tyr573Ter)	CNBD β7 - β8	Holtan et al. (2020)	Likely pathogenic
Exon 8	c.1736T>G	p.(Leu579Arg)	CNBD β8	This study	Likely pathogenic
Exon 8	c.1768G>A	p.(Glu590Lys)	CNBD αB	Nishiguchi et al. (2005)	Pathogenic
Exon 8	c.1771T>C	p.(Tyr591His)	CNBD αB - αC	This study	Likely pathogenic
Exon 8	c.1775C>T	p.(Pro592Leu)	CNBD αB - αC	This study	Likely pathogenic
Exon 8	c.1777G>A	p.(Glu593Lys)	CNBD αC	Wissinger et al. (2001)	Pathogenic
Exon 8	c.1793T>G	p.(Leu598Arg)	CNBD αC	Sun et al. (2020)	VUS
Exon 8	c.1805G>A	p.(Gly602Glu)	CNBD αC	Georgiou et al. (2019)	Likely pathogenic
Exon 8	c.1810C>T	p.(Gln604Ter)	CNBD αC	Taylor et al. (2017)	Likely pathogenic
Exon 8	c.1811del	p.(Gln604ArgfsTer3)	CNBD αC	Sun et al. (2020)	Likely pathogenic
Exon 8	c.1898T>C	p.(Leu633Pro)	CLZ	Goto-Omoto et al. (2006)	Likely pathogenic
Exon 8	c.1931T>C	p.(Phe644Ser)	CLZ	Ellingford et al. (2016)	VUS
Exon 8	c.1937G>A	p.(Arg646His)	CLZ	Li et al. (2014)	VUS
Exon 8	c.1949A>C	p.(Glu650Ala)	CLZ	LOVD	VUS
Exon 8	c.1963C>T	p.(Gln655Ter)	CLZ	Wissinger et al. (2001)	Likely pathogenic
Exon 8	c.1975A>T	p.(Lys659Ter)	CLZ	Li et al. (2014)	Likely pathogenic
Exon 8	c.1981C>A	p.(Arg661Ser)	CLZ	Yang et al. (2014)	Likely pathogenic
Exon 8	c.1982G>A	p.(Arg661His)	CLZ	Sun et al. (2020)	Likely pathogenic
Variants of uncertain significance					
Exon 2	c.68G>A[c]	p.(Arg23Gln)	N-Term.	ClinVar	VUS
Exon 2	c.80G>A[c]	p.(Arg27His)	N-Term.	ClinVar	VUS
Exon 3	c.110C>T[c]	p.(Ser37Leu)	N-Term.	ClinVar	VUS
Exon 3	c.154A>G[c]	p.(Met52Val)	N-Term.	ClinVar	VUS
Exon 3	c.211G>A[c]	p.(Ala71Thr)	N-Term.	ClinVar	VUS
Exon 4	c.316G>A[c]	p.(Glu106Lys)	N-Term.	Sharon et al. (2020)	VUS
Exon 4	c.358A>G[c]	p.(Asn120Asp)	N-Term.	Li et al. (2014)	VUS
Exon 5	c.440C>G[c]	p.(Thr147Arg)	N-Term.	LOVD	VUS
Exon 6	c.471T>G[c]	p.(Asp157Glu)	N-Term.	ClinVar	VUS
Exon 6	c.473C>T[c]	p.(Ala158Val)	N-Term.	LOVD	VUS
Exon 6	c.553C>G	p.(Leu185Val)	TM1	Kim et al. (2019)	VUS
Exon 7	c.587A>G	p.(Gln196Arg)	TM1 - TM2	Sun et al. (2020)	VUS
Exon 7	c.625T>C	p.(Ser209Pro)	TM2	Weisschuh et al. (2020)	VUS
Exon 7	c.664G>C	p.(Ala222Pro)	TM2	Reuter et al. (2008)	VUS
Exon 7	c.670A>G	p.(Thr224Ala)	TM2 - TM3	This study	VUS
Exon 7	c.671C>T	p.(Thr224Ile)	TM2 - TM3	Li et al. (2014)	VUS
Exon 8	c.743A>G	p.(Gln248Arg)	TM3	This study	VUS
Exon 8	c.784G>C	p.(Ala262Pro)	TM3	Zobor et al. (2017)	VUS

(Continues)

10981004, 2022, 7, Downloaded from https://onlinelibrary.wiley.com/doi/10.1002/humu.24371, Wiley Online Library on [09/12/2024]. See the Terms and Conditions (https://onlinelibrary.wiley.com/terms-and-conditions) on Wiley Online Library for rules of use; OA articles are governed by the applicable Creative Commons License

TABLE 2 (Continued)

Location *CNGA3*	Alteration nucleotide sequence[a]	Alteration polypeptide	Location protein domain[b]	References	ACMG/AMP classification
Exon 8	c.796G>A	p.(Val266Met)	TM3 - TM4	Thiadens et al. (2010)	VUS
Exon 8	c.1343A>G	p.(Lys448Arg)	C-linker αB' - αC'	This study	VUS
Exon 8	c.1615G>A[d]	p.(Val539Met)	CNBD β5	This study	VUS
Exon 8	c.1784A>G[c]	p.(Lys595Arg)	CNBD αC	ClinVar	VUS
Exon 8	c.1845G>T[c]	p.(Glu615Asp)	CNBD αC - CLZ	ClinVar	VUS
Exon 8	c.1877T>G	p.(Leu626Arg)	CLZ	Huang et al. (2016)	VUS
Exon 8	c.1889T>C	p.(Val630Ala)	CLZ	This study	VUS
Exon 8	c.1968G>A[c]	p.(Met656Ile)	CLZ	ClinVar	VUS
Exon 8	c.2005G>C[c]	p.(Val669Leu)	CLZ	ClinVar	VUS
Exon 8	c.2050G>A[c]	p.(Gly684Arg)	C-Term.	Patel et al. (2016)	VUS
Likely benign variants					
Exon 2	c.59C>T	p.(Thr20Ile)	N-Term.	ClinVar	Benign
Exon 2	c.66C>T	p.(=)	N-Term.	This study	VUS
Exon 2	c.72T>C	p.(=)	N-Term.	This study	Benign
Exon 2	c.81C>T	p.(=)	N-Term.	Nishiguchi et al. (2005)	Likely benign
Intron 2	c.102-16A>G	p.(?)	-	This study	Benign
Exon 3	c.129G>A	p.(=)	N-Term.	ClinVar	Likely benign
Exon 3	c.143C>T	p.(Pro48Leu)	N-Term.	Nishiguchi et al. (2005)	Benign
Intron 3	c.215+11A>G	p.(?)	-	LOVD	Benign
Intron 3	c.215+151T>C	p.(?)	-	This study	Benign
Exon 3	c.198C>T	p.(=)	N-Term.	This study	Likely benign
Exon 3b[e]	c.336G>A[e]	p.(Met112Ile)	-	This study	n.a.
Exon 3b[e]	c.360C>T[e]	p.(=)	-	This study	n.a.
Intron Exon 3b[e]	c.215+46T>G[e]	p.(?)	-	This study	n.a.
Intron Exon 3b[e]	c.216-60A>T[e]	p.(?)	-	This study	n.a.
Exon 4	c.225C>T	p.(=)	N-Term.	ClinVar	VUS
Exon 4	c.238C>T	p.(=)	N-Term.	ClinVar	VUS
Exon 4	c.284C>T[f]	p.(Pro95Leu)	N-Term.	Thiadens et al. (2010)	VUS
Exon 4	c.353A>G[d]	p.(Gln118Arg)	N-Term.	This study	Likely benign
Intron 4	c.395+9C>T	p.(?)	-	ClinVar	VUS
Intron 4	c.396-4G>A	p.(?)	-	ClinVar	Benign
Intron 5	c.449+13A>G	p.(?)	-	ClinVar	VUS
Exon 6	c.458C>T	p.(Thr153Met)	N-Term.	Kohl et al. (1998)	Benign
Intron 6	c.566+6C>T	p.(?)	-	ClinVar	Likely benign
Intron 6	c.566+14G>A	p.(?)	-	ClinVar	VUS
Exon 7	c.592G>A	p.(Glu198Lys)	TM2	This study	Benign
Exon 8	c.715C>T	p.(=)	TM2 - TM3	ClinVar	VUS

10981004, 2022, 7, Downloaded from https://onlinelibrary.wiley.com/doi/10.1002/humu.24371, Wiley Online Library on [09/12/2024]. See the Terms and Conditions (https://onlinelibrary.wiley.com/terms-and-conditions) on Wiley Online Library for rules of use; OA articles are governed by the applicable Creative Commons License

TABLE 2 (Continued)

Location *CNGA3*	Alteration nucleotide sequence[a]	Alteration polypeptide	Location protein domain[b]	References	ACMG/AMP classification
Exon 8	c.734C>T[f]	p.(Thr245Met)	TM2 - TM3	Johnson et al. (2004)	VUS
Exon 8	c.740C>T	p.(Thr247Met)	TM3	Li et al. (2014)	Likely benign
Exon 8	c.777C>A	p.(=)	TM3	ClinVar	VUS
Exon 8	c.1116C>T	p.(=)	pore helix - TM6	ClinVar	Likely benign
Exon 8	c.1347G>A	p.(=)	C-linker αB' - αC'	This study	VUS
Exon 8	c.1412A>G[f]	p.(Asn471Ser)	C-linker αD'	Wissinger et al. (2001)	VUS
Exon 8	c.1413C>T	p.(=)	C-linker αD'	Nishiguchi et al. (2005)	VUS
Exon 8	c.1569C>T	p.(=)	CNBD β3	Nishiguchi et al. (2005)	Likely benign
Exon 8	c.1611G>A	p.(=)	CNBD β4 - β5	ClinVar	VUS
Exon 8	c.1618G>A[f]	p.(Val540Ile)	CNBD β5	Thiadens et al. (2010)	VUS
Exon 8	c.1626C>T	p.(=)	CNBD β5	ClinVar	Benign
Exon 8	c.1695G>A	p.(=)	CNBD β6 - β7	Nishiguchi et al. (2005)	Likely benign
Exon 8	c.1746C>T	p.(=)	CNBD αB	LOVD	Likely benign
Exon 8	c.1767C>T	p.(=)	CNBD αB	LOVD	Likely benign
Exon 8	c.1856C>T[f]	p.(Ala619Val)	CNBD αC - CLZ	Thiadens et al. (2010)	VUS
Exon 8	c.1862C>A[f]	p.(Ala621Glu)	CNBD αC - CLZ	Wiszniewski et al. (2007)	VUS
Exon 8	c.1863G>A	p.(=)	CNBD αC - CLZ	LOVD	Likely benign
Exon 8	c.1866C>T	p.(=)	CNBD αC - CLZ	ClinVar	VUS

Note: All 316 variants were classified following ACMG/AMP criteria and subsequently revised manually and expert-categorized into "likely benign," "VUS," and "likely disease-causing."

Abbreviation: ACHM, achromatopsia.

[a]Variant designation is based on NM_001298.2 (GRCh38/hg38).

[b]Functional domains of CNGA3 according to Gofman et al., 2014 and Shuart et al., 2011: N-Term., N-terminus; TM1 to TM6, transmembrane domains; C-linker having six alpha helices (αA'–αF'); CNBD, cyclic-nucleotide binding domain having three alpha helices (αA–αC) and eight beta-sheets (β1–β8); CLZ, C-terminal leucin zipper; C-Term., C-terminus; -, intermediate amino acid residue between two domains.

[c]Variants classified as VUS: no genotype could be established from the literature or database data.

[d]Variants observed in an affected individual with an *OPN1MW/OPN1LW*-associated genotype indicative for and compatible with a clinical diagnosis of blue cone monochromatism, X-linked.

[e]Variant designation of variants located in the alternate exon 3b (formerly named exon 2b (Wissinger et al., 2001), now renamed exon 3b) and its flanking intronic sequences is based on XM_011510554.2 (GRCh38/hg38).

[f]Variants only observed in a heterozygous state in the absence of a second likely disease-causing allele.

was identified in compound heterozygous state with the variant c.847C>A/p.(Arg283Trp) on the second allele in one patient. Following the standard variant screening, the variant c.847C>A/p.(Arg283Trp) was initially identified apparent homozygously in this index patient. Segregation analysis failed to detect the variant in the father of the patient. Microsatellite marker analysis confirmed paternity and deletion mapping via PCR and primer walking identified the heterozygous 5.19 kb deletion.

Copy number variations (CNVs) are an important mutation type associated with ACHM and are commonly seen in the *CNGB3* gene as well as in *GNAT2* and *ATF6*. Whereas ten out of 98 disease-associated *CNGB3* variants identified in a large cohort of ACHM patients are CNVs, the mutation spectrum of *ATF6* and *GNAT2* includes two CNVs each (Felden et al., 2019; Kohl et al., 2002; Lee et al., 2020; Mayer et al., 2017). In contrast, it seems that this kind of structural variation is not common in *CNGA3*. This notion is further supported by the fact, that the gene had not been pinpointed by a CNV-study focusing on genes in inherited retinal dystrophies (Van Schil et al., 2018). In addition, single heterozygous cases are rarely found in *CNGA3* compared to the *CNGB3* gene where 44 out of 552 patients with *CNGB3* variants were identified to harbor only a single heterozygous pathogenic variant following standard variant screening and CNV analysis (Mayer et al., 2017). This further suggests that most variants in *CNGA3* are exonic indicating that there are not many hidden pathogenic variants—such as deep intronic variants—left.

10981004, 2022, 7, Downloaded from https://onlinelibrary.wiley.com/doi/10.1002/humu.24371, Wiley Online Library on [09/12/2024]. See the Terms and Conditions (https://onlinelibrary.wiley.com/terms-and-conditions) on Wiley Online Library for rules of use; OA articles are governed by the applicable Creative Commons License

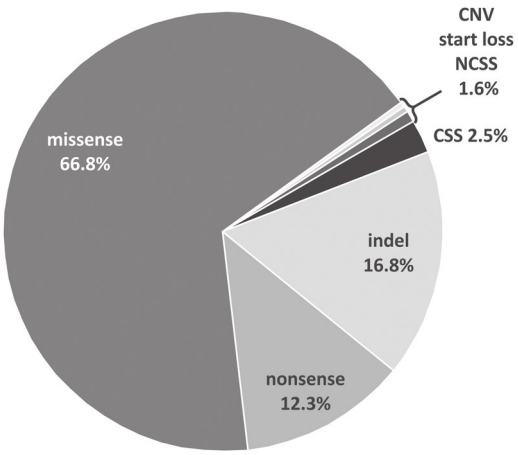


FIGURE 2 Frequencies of "likely disease-causing" variant types within the *CNGA3* variant database. The *CNGA3* variant database contains 244 "likely disease-causing" variants. The vast majority are missense variants (66.8%) followed by small indels (16.8%), and nonsense variants (12.3%). Splice variants affecting canonical splice sites (CSS) (2.5%), noncanonical splice site (NCSS) variants (0.8%), copy number variations (CNV) (0.4%), and start loss variants (0.4%) are the minority of the identified variants.

Regarding the localization of "likely disease-causing" *CNGA3* variants, 236 sequence alterations are located in the coding exons whereas only eight variants are located in the intronic sequences of the gene (Figure 3). Of these intronic variants, seven variants represent single nucleotide substitutions affecting either the canonical splice sites (i.e., the first two and last two nucleotides of an intron) ($n = 5$) or are located in the vicinity of a highly conserved splice acceptor site ($n = 2$). All variants affecting the canonical splice sites are predicted to lead to the loss of the respective donor or acceptor site based on five *in silico* algorithms. Additionally, the previously published variant c.396-11C>G/p.(?) and the novel sequence alteration c.450-15T>G/p.(?), both located in the vicinity of a highly conserved splice acceptor site, are predicted to activate an intronic cryptic acceptor site potentially affecting splicing (SpliceAI Δ scores: acceptor loss 0.87 and 0.65, respectively; acceptor gain 0.70 and 0.53, respectively; Table S3). Furthermore, one small duplication is localized at the exon/intron border of exon 5 (c.396-2_398dup/p.(?)). Although only one of the *in silico* tools predicts a minor effect on transcript splicing, the variant is still considered to be "likely disease-causing" (SpliceAI Δ score: acceptor loss 0.00; acceptor gain 0.22). The novel missense variant c.566G>A/p.(Arg189Lys) affecting the last nucleotide of exon 6 was also predicted to have an effect—though minor—on transcript splicing (SpliceAI Δ score: donor loss 0.08; donor gain 0.32). Consequently, it remains unclear whether this variant needs to be considered a splicing or missense variant, as it may also act both ways.

The majority of the exonic ACHM-associated *CNGA3* variants classified as "likely disease-causing" within the *CNGA3* variant database are located in exon 8 including 140 missense substitutions, 46 nonsense/small indel variants, and the single copy number variation (deletion of complete exon 8) (Table 2 and Figure 3). The remaining 49 variants are distributed across exon 2 to exon 7, with exons 6 and 7 (encoding TM1 and TM2) each harboring triple the number of variants as exons 2 to exon 5. On protein level, the majority of CNGA3 variants ($n = 82$) are spread across the six transmembrane domains and their connecting loops. Another major group of "likely disease-causing" CNGA3 variants ($n = 57$) clusters within the CNBD whereas only few variants ($n = 8$) reside in the adjacent CLZ domain more closely located to the C-terminus. The C-linker of the CNGA3 subunit and the pore region harbor a similar fraction of "likely disease-causing" CNGA3 variants ($n = 36$ and $n = 30$, respectively). The pore region spanning around 46 amino acids, is thereby rendered to have the highest mutation density within the CNGA3 subunit. Whereas the overall majority of variants within the CNGA3 protein are missense substitutions, the sequence changes within the N-terminal region mainly comprise nonsense variants or small indels (17 out of 22) (Figure 3). Of 163 "likely disease-causing" missense variants listed in our database, 94 affect amino acid positions which are completely conserved across CNGA3 orthologues and its rod equivalent CNGA1 (Table S3 and Figure S2).

3.3 | Prevalence of *CNGA3* variants in ACHM

From our in-house genetic investigations, we report disease-associated *CNGA3* variants in 385 affected individuals descending from 304 independent families representing 36.3% of our ACHM cohort which predominantly comprises Western European and North American patients (Figure S1). This observation is in line with our previous and other studies reporting a prevalence of 5%–41% for *CNGA3* variants in cohorts of Dutch and British ACHM patients making *CNGA3* the second most frequently mutated gene in European ACHM patients or patients of European descent (Johnson et al., 2004; Thiadens et al., 2009; Wissinger et al., 2001).

The vast majority of all "likely disease-causing" *CNGA3* variants listed in our *CNGA3* database represent amino acid substitutions (66.8%) which are completely in line with several previously conducted studies where missense variants showed a frequency of 61.5%–71.4% (Li et al., 2014; Liang et al., 2015; Wissinger et al., 2001). In contrast, 16 out of 98 sequence changes (16%) in the CNGB3 subunit of the cone photoreceptor CNG channel identified in a large cohort of ACHM patients are missense variants (Mayer et al., 2017). This high prevalence of missense substitutions in the *CNGA3* gene may indicate a reduced tolerance of CNGA3 for amino acid substitutions regarding the functional maintenance of the channel protein.

All "likely disease-causing" variants listed in our *CNGA3* database except the c.682G>A/p.(Glu228Lys) variant have a minor allele frequency (MAF) lower than 0.1% in gnomAD (Table S3). In contrast, the mentioned variant displays a MAF of 0.13% (Table S3). In the South Asian population, the c.682G>A/p.(Glu228Lys) variant displays an even higher allele frequency of

10981004, 2022, 7, Downloaded from https://onlinelibrary.wiley.com/doi/10.1002/humu.24371, Wiley Online Library on [09/12/2024]. See the Terms and Conditions (https://onlinelibrary.wiley.com/terms-and-conditions) on Wiley Online Library for rules of use; OA articles are governed by the applicable Creative Commons License

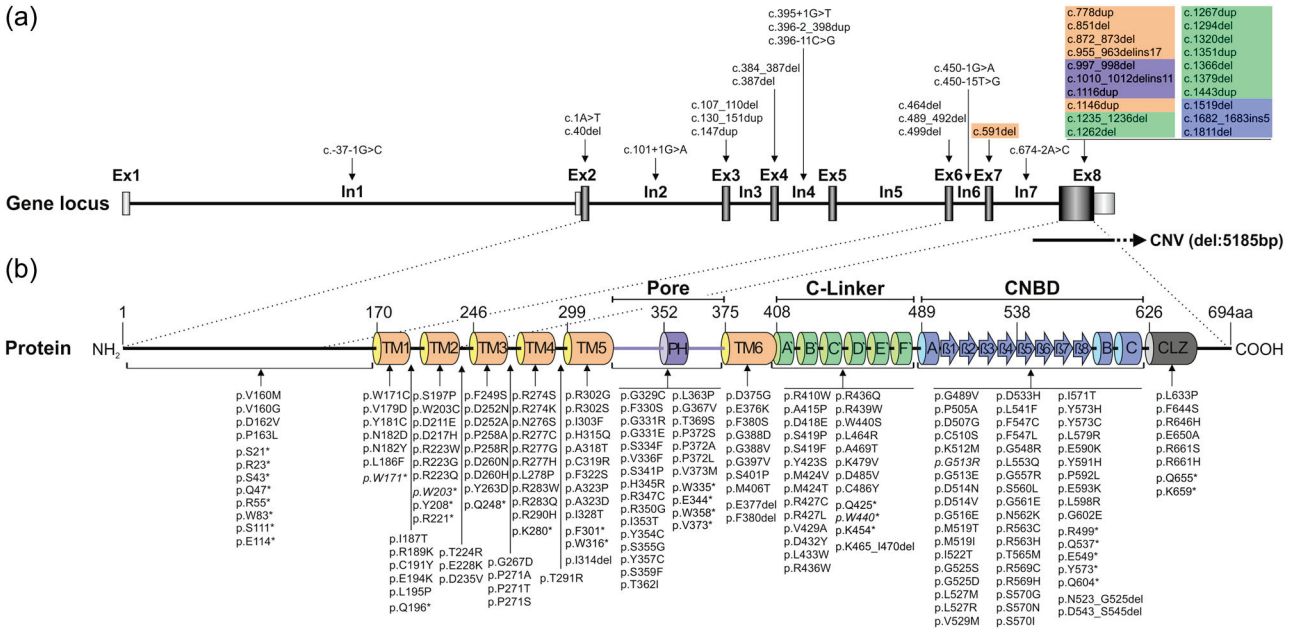


FIGURE 3 Localization of "likely disease-causing" *CNGA3* variants identified in the ACHM cohort genetically characterized in Tübingen, mutation databases, and in the literature. (a) The *CNGA3* gene locus with its eight exons (GRCh38/hg38, NM_001298.2) (alternatively spliced exon 3b is not shown) is depicted. Noncoding exonic regions are indicated by small light gray rectangles and coding exonic regions by dark gray rectangles. Introns are depicted by a black line. The location of canonical and noncanonical splice site variants, start loss variants and small insertion, duplication, deletions, and indel variants resulting in frameshift with premature termination codon are depicted above the *CNGA3* gene. Variants are color-coded with respect to their location within functional domains of the CNGA3 protein. The copy number variation (CNV) is indicated by a horizontal line under exon 8. The right breakpoint of the CNV extending beyond the 3′UTR of the *CNGA3* gene locus is marked by a dashed line. (b) The CNGA3 polypeptide with its structural and functional domains is shown. CNGA3 comprises six transmembrane helices (TM1–TM6), a pore region including the pore helix (PH), the C-linker formed by six α helices (αA′–αF′), the CNBD consisting of three α helices (αA–αC) and eight β sheets (β1–β8) and the CLZ. The location of missense, nonsense, and in-frame deletion variants are given below the protein. Protein variants originating from different nucleotide variants are depicted in italic. Functional domains of CNGA3 are annotated according to Gofman et al., 2014 and Shuart et al., 2011. aa, amino acids; ACHM, achromatopsia; bp, base pairs; CNBD, cyclic nucleotide-binding domain; CLZ, C-terminal leucine zipper; del, deletion; dup, duplication; Ex, exon; In, intron; ins, insertion; PH, pore helix; 3′UTR, 3′ untranslated region.

0.99% in concordance with *CNGA3* variants being more common here than in the European population. The c.682G>A/p.(Glu228Lys) variant has been observed in four patients from two families of South Asian origin in our cohort, but since it is part of complex alleles in these patients (homozygous for c.[67C>T;682G>A] or c.[682G>A;1315C>T]) the contribution of the c.682G>A/p.(Glu228Lys) variant to the ACHM phenotype in these families remains unclear—it may exert a cumulative effect (Table S2). In addition, one ACHM patient carrying the c.682G>A/p.(Glu228Lys) variant homozygously was described in a previously published study (Sun & Zhang, 2019). Furthermore, the variant was described to be part of a triallelic inheritance pattern involving the *CNGB3* c.1208G>A/p.(Arg403Gln) variant (Burkard et al., 2018; Thiadens et al., 2010). Due to the deleterious effect predicted by two out of three *in silico* analysis tools and functional studies demonstrating impaired functionality of CNG channels harboring $CNGA3_{Glu228Lys}$ subunits (Reuter et al., 2008; Täger et al., 2021), we classified this variant as "likely disease-causing." A complete overview of the outcomes of the *in silico* prediction algorithms and previously published functional studies are included in Table S3.

3.4 | Functional studies on CNGA3 variants

As a first gene therapy trial for ACHM resulting from defects in *CNGA3* has already been completed (Fischer et al., 2020), and several trials are ongoing (ClinicalTrials.gov Identifier: NCT02610582, NCT03278873, NCT03758404, and NCT02935517), the genotypes of patients with *CNGA3* missense variants classified as "VUS" unfortunately hamper the inclusion of such patients eligible for these gene therapeutic trials. Therefore, functional studies are needed to validate the possible pathogenic effect of the respective variants. Commonly used methods to characterize the functionality of mutant CNG channels involve calcium imaging and patch-clamp recordings of heterologously expressed mutant channels (Burkard et al., 2018; Dai & Varnum, 2013; Koeppen et al., 2008, 2010; Kuniyoshi et al., 2016; Liu & Varnum, 2005; Matveev et al., 2010; Meighan et al., 2015; Muraki-Oda et al., 2007; Patel et al., 2005; Reuter et al., 2008; Shaikh et al., 2015; Täger et al., 2018; Tränkner et al., 2004). Furthermore, a recently developed functional assay proposes a fluorescence-based, high-throughput calcium influx-based approach for analyzing mutant CNGA3 channels (Jacobson

10981004, 2022, 7, Downloaded from https://onlinelibrary.wiley.com/doi/10.1002/humu.24371, Wiley Online Library on [09/12/2024]. See the Terms and Conditions (https://onlinelibrary.wiley.com/terms-and-conditions) on Wiley Online Library for rules of use; OA articles are governed by the applicable Creative Commons License

et al., 2019). In total, 54 missense substitutions, two nonsense and one canonical splice site variant have already been functionally characterized (Table S3), and this information was used to classify 44 variants as pathogenic, 11 as likely pathogenic, one as VUS—due to contradictory results in functional approaches—and one as benign according to ACMG/AMP guidelines.

Following functional characterization of heterologously expressed mutant channels in previously conducted studies, 27 out of 54 missense variants completely abolished formation of functional channels (Koeppen et al., 2008, 2010; Liu & Varnum, 2005; Matveev et al., 2010; Muraki-Oda et al., 2007; Patel et al., 2005; Shaikh et al., 2015; Tränkner et al., 2004). Seventeen previously analyzed missense substitutions allowed the formation of functional channels but with impaired/altered functionality such as impaired protein folding and/or channel trafficking or altered biophysical properties, for example, altered apparent cGMP-sensitivity or ion selectivity (Burkard et al., 2018; Dai & Varnum, 2013; Koeppen et al., 2008; Liu & Varnum, 2005; Meighan et al., 2015; Muraki-Oda et al., 2007; Patel et al., 2005; Reuter et al., 2008; Tränkner et al., 2004). Furthermore, an improvement in the mutant channel functionality was achieved in a total of ten missense variants by using chemical chaperones or co-expressing the CNGB3 subunit and/or reducing the cell cultivation temperature from the standard 37°C to 27/28°C, a procedure that is known to enhance protein folding and trafficking (Koeppen et al., 2010; Kuniyoshi et al., 2016; Patel et al., 2005; Reuter et al., 2008). A complete overview of *CNGA3* variants previously analyzed in functional studies and the respective channel functionality is summarized in Table S3.

4 | CLINICAL AND DIAGNOSTIC ASPECTS OF ACHM

ACHM usually becomes clinically manifest at early infancy. The most typical signs and symptoms are marked photosensitivity, nystagmus, severely reduced visual acuity, and the inability to discriminate colors. The presented nystagmus is mostly of low amplitude and in many affected individuals improves with older age. However, the most pronounced and subjectively difficult symptom photophobia usually remains for the lifetime of the patient.

In a complete achromat, the best-corrected visual acuity is stable at around 20/200. Patients suffering from incomplete ACHM present with a milder phenotype with retained residual color discrimination, better visual acuity, and/or residual photopic ERG responses (Hirji et al., 2018; Michalakis et al., 2017; Sun & Zhang, 2019).

ACHM is clinically diagnosed in childhood due to the typical symptoms of nystagmus, photophobia, and low vision. Parents of affected children usually notice nystagmus in the first months of life, but in some patients the diagnosis is only made in preschool age. In the case of incomplete achromats, the diagnosis is occasionally made even later (Felden et al., 2019; Weisschuh et al., 2018).

The differential diagnosis of ACHM also includes treatable ophthalmological diseases of infancy, but due to the low cooperation of children at ophthalmological examination, the final confirmation is usually given by molecular genetic testing. The most important differential diagnoses for ACHM not only include other rare genetic retinal diseases such as blue cone monochromacy, bradyopsia, or early onset cone dystrophy, but also include other diseases of early childhood connected to photophobia such as juvenile glaucoma or neuroophthalmological causes of nystagmus.

ACHM is genetically heterogeneous encompassing six known causative genes, but the multimodal ophthalmological diagnostics, especially retinal imaging, almost always reveal a very similar clinical picture: a funduscopic normal-appearing retina (Figure 4d) with a normal or close to normal fundus autofluorescence pattern (Figure 4e). In some patients, changes in the foveal autofluorescence are obvious, corresponding to granular changes in the ellipsoid zone of the cones or fovea thinning (Felden et al., 2019; Zobor et al., 2017). Optical coherence tomography (OCT) shows a normal layering of the central retina, especially in children and young adults (Figure 4a), but disruptions of the outer segments become obvious with increasing age (Figures 4b,c). Furthermore, hypoplasia of the fovea has been described in many ACHM patients. However, the image quality is frequently diminished due to nystagmus (Tekavcic Pompe et al., 2021; Zobor et al., 2017).

Achromatopsia has been classically considered to be a stationary disease. But nowadays using high-resolution retinal imaging we know that progressive cone cell loss and degenerative changes occur in the retinal morphology in ACHM patients (Georgiou et al., 2020; Thiadens et al., 2010; Thomas et al., 2012). Four stages of morphological degenerative changes have been described in ACHM patients using high-resolution OCT (Tekavcic Pompe et al., 2021; Zobor et al., 2017): preserved inner segment ellipsoid, disrupted inner segment ellipsoid, inner segment ellipsoid loss, and inner segment & retinal pigment epithelium loss (Figure 4a–c).

Another very important tool for the diagnostics of ACHM is retinal functional testing. As already mentioned above, the best-corrected visual acuity is usually in the range of 20/400–20/200 but can be higher in incomplete achromats. Color vision testing supporting the subjective loss of color discrimination shows a rod-dominated mixed color perception disorder (Zobor et al., 2017). Cone-driven perimetric and microperimetric techniques reveal reduced light sensitivity especially in the macular region (Zobor et al., 2017).

Essential diagnostic tests are also those that can reliably and objectively distinguish between rod and cone function thereby detecting normal rod functionality while revealing missing or markedly reduced cone functionality. Thus, the full-field ERG (ffERG) is a well-established diagnostic tool for ACHM. In ffERG the scotopic responses, especially the rod-driven dark-adapted flash-elicited responses, are in the normal range, but the standard mixed flashes (3 and 10 cd/m2) can elicit either reduced or close to normal responses (Maguire et al., 2018; Zobor et al., 2017). The standard photopic recordings in the ffERG including the 30 Hz flicker are

10981004, 2022, 7, Downloaded from https://onlinelibrary.wiley.com/doi/10.1002/humu.24371, Wiley Online Library on [09/12/2024]. See the Terms and Conditions (https://onlinelibrary.wiley.com/terms-and-conditions) on Wiley Online Library for rules of use; OA articles are governed by the applicable Creative Commons License



FIGURE 4 Examples of typical findings obtained with retinal imaging in achromatopsia patients. (a), (b), and (c) show spectral domain optical coherence tomography images of the central retina in three different stages: (a) Foveal structures with preserved inner segment ellipsoid, (b) foveal inner segment ellipsoid loss, (c) Inner segment & retinal pigment epithelium loss. In (d) fundus photography shows a typically normal retinal image, (e) illustrates a fundus autofluorescence image with typically roughly normal finding, although slight changes of the perifoveal autofluorescence (i.e., a decent perifoveal hyperfluorescence is shown here) are possible.

reduced below the noise level and therefore clinically not measurable. However, in some incomplete achromats reduced photopic responses can be observed (Maguire et al., 2018; Tekavcic Pompe et al., 2021; Zobor et al., 2017). A recent study using time-frequency analysis of the standard ffERG in ACHM patients compared to age-matched controls showed a strongly reduced but not absent activity of oscillatory potentials in a frequency range mostly driven by cones and only in a small part by rods (Righetti et al., 2021). This manifestation of the lack of cone modulation on the retinal network gives insights into interactions between both types of photoreceptors and the inner retinal network (Righetti et al., 2021). Similarly, pupillometric measures are objective tests of the retinal function that are able to address cones and rods independently from each other and can reveal reduced cone functionality and preserved or increased rod function due to the missing interaction of cones and rods in the retina of ACHM patients (Kelbsch et al., 2019; Lisowska et al., 2017). Due to the lack of rod inhibition by cones, as is the case in normal eyes, the affected individuals experience severe photophobia. Rods are not directly affected by defects in ACHM genes and accordingly the dark-adapted thresholds are also in a normal range, not only for white and blue stimuli, but also for red stimuli (Zobor et al., 2017).

5 | ANIMAL MODELS OF *CNGA3*-ASSOCIATED ACHM

Both small and large animal models of *CNGA3*-associated ACHM exist enabling the characterization of the pathogenesis of the disease. The first described small animal model was the *Cnga3* knockout (KO) mouse which was generated by a targeted deletion of exon 7 of the murine *Cnga3* gene (Biel et al., 1999). Furthermore, a naturally occurring mouse model of ACHM, the so-called *cpfl5* mouse, was discovered harboring a missense variant c.493A>G/p.(Thr165Ala) in exon 5 of the murine *Cnga3* gene (Pang et al., 2012). Both mouse models exhibited a similar ocular phenotype including the selective loss of cone-mediated light responses which was accompanied by a progressive degeneration of cone photoreceptors. Additionally, both mouse models presented a defect in the cone opsin transport by failing to target cone opsins to the outer segments. In contrast, the rod photoreceptors remained both structurally and functionally intact (Biel et al., 1999; Pang et al., 2012). A recent study exploring the disease mechanism in *Cnga3* KO mice revealed an accumulation of cGMP in *Cnga3* KO cones and a transient upregulation of the cGMP-dependent protein kinase 2 (Prkg2). Knockout of *Prkg2* counteracted the cone degeneration by normalizing the endoplasmic reticulum

10981004, 2022, 7, Downloaded from https://onlinelibrary.wiley.com/doi/10.1002/humu.24371, Wiley Online Library on [09/12/2024]. See the Terms and Conditions (https://onlinelibrary.wiley.com/terms-and-conditions) on Wiley Online Library for rules of use; OA articles are governed by the applicable Creative Commons License

homeostasis thereby pinpointing *Prkg2* as a novel key mediator of cone degeneration (Koch et al., 2020).

A large animal model of ACHM includes the naturally occurring Awassi sheep model presenting with congenital day blindness and severely diminished cone function (Ezra-Elia et al., 2014; Shamir et al., 2010). The affected lambs are homozygous for a nonsense variant p.(Arg236Ter) in the ovine *CNGA3* gene (Reicher et al., 2010). Furthermore, the day-blind sheep show no responses to bright red light in chromatic pupil light reflex measurement underlining the loss of cone function (Ross et al., 2020). Similar to human ACHM patients, the scotopic responses are unaffected (Shamir et al., 2010). In addition, a second Awassi sheep model was described by Gootwine and colleagues harboring a missense variant in *CNGA3* (c.1618G>A/p.(Gly540Ser)) resulting in day blindness (Gootwine et al., 2017).

Finally, two naturally occurring canine models of *CNGA3*-associated channelopathy were described. German Shepherds were identified to carry the missense variant c.1270C>T/p.(Arg424Trp) homozygously in the canine *CNGA3* gene whereas Labrador Retrievers presented with a three-nucleotide deletion in exon 7 of *CNGA3* (c.1931_1933del/p.(Val644del)) in a homozygous state (Tanaka et al., 2015). Both canine models were characterized by a complete loss of cone function at 8–10 weeks of age, further underlined by the lack of light-induced cone responses under photopic conditions. In contrast, the scotopic ERG remained unaffected indicating normal rod function (Tanaka et al., 2015).

6 | CONCLUSIONS AND FUTURE DIRECTIONS

In conclusion, the present study provides a comprehensive overview of the *CNGA3* variant spectrum by combining variants identified in our large cohort of 889 independent families with ACHM, including variants retrieved from 216 unpublished families, as well as all previously published *CNGA3* variants, both in literature and mutation databases. We thereby expand the allele spectrum of *CNGA3* variants by 48 novel "likely disease-causing" variants to a total of 316 variants emphasizing the role of *CNGA3* as a major disease-causing gene for ACHM. We further provide data on the extensive *in silico* analysis demonstrating the importance of *in silico* variant assessment and provide ACMG/AMP classification for 312 *CNGA3* variants. Furthermore, we summarize clinical and diagnostic aspects of ACHM and provide an overview of several animal models of *CNGA3*-associated ACHM. However, our study demonstrates the need for functional assays to finalize the pathogenicity assessment of variants still assigned as "VUS." This would contribute to the improvement of genetic diagnostics and facilitate the selection of patients with *CNGA3*-associated ACHM eligible for future gene therapeutic trials.

WEB RESOURCES

Mutalyzer name checker tool: https://mutalyzer.nl/name-checker

PubMed®: https://pubmed.ncbi.nlm.nih.gov/

Human Gene Mutation Database (HGMD®): http://www.hgmd.cf.ac.uk/ac/index.php

Leiden Open Variation Database (LOVD) for *CNGA3*: https://www.lovd.nl/CNGA3

ClinVar: https://www.ncbi.nlm.nih.gov/clinvar/

Combined Annotation Dependent Depletion (CADD): https://cadd.gs.washington.edu/

Sorting Intolerant From Tolerant (SIFT): http://sift.bii.a-star.edu.sg/

MutationTaster: http://www.mutationtaster.org/

Align-GVGD: https://agvgd.iarc.fr/index.php

Clustal Omega: https://www.ebi.ac.uk/Tools/msa/clustalo/

BoxShade version 3.21: https://embnet.vital-it.ch/software/BOX_form.html

Genome Aggregation Database (gnomAD): https://gnomad.broadinstitute.org/

SpliceAI: https://spliceailookup.broadinstitute.org/

Franklin by Genoox Ltd: https://franklin.genoox.com/

ACKNOWLEDGMENTS

The authors would like to thank all patients and their families for participating in this study. We would also like to acknowledge the contributions of Agnes Farkas (Budapest, Hungary) and the deceased Christian Hamel (Montpellier, France). Jana Moravíková performed segregation analysis in samples of Czech origin. This study was funded by the Deutsche Forschungsgemeinschaft as part of the SPP 2127: Gene and cell-based therapies to counteract neuroretinal degeneration, project numbers: KO 2176/3-1, 398539671 to S. Kohl and STI 727/1-1, 399487883 to K. Stingl. In addition, S. Kohl has received reimbursement for CNGA3 variant deposition at the LOVD, which is supported by a Research Core Award of the Foundation Fighting Blindness Inc. (award number BR-GE-0120-0775-LUMC) to J. T. den Dunnen, F. P. M. Cremers, I. F. A. C. Fokkema, and S. Roosing. S. Kohl, K. Stingl, I. Audo, I. Meunier, H. Dollfus, E. De Baere, P. Liskova, and B. Lorenz are members of ERN-EYE. This study was supported by the Instituto de Salud Carlos III (ISCIII) of the Spanish Ministry of Health (FIS PI19/00321). I. Audo was supported by LabEx LifeSenses, IHU FOReSIGHT, and Foundation Fighting Blindness grant (BR-GE-0619-0761-INSERM). Samples from I. Audo originate from NeuroSensCol, a biobank for research in neuroscience (PI: J. A. Sahel, coPI I. Audo, partner with Centre Hospitalier National d'Ophtalmologie des Quinze-Vingts, INSERM, and CNRS). The authors are thankful to the patients and family members participating in the study and clinical staff from the Centre d'Investigation Clinique CIC1438. P. L. was supported by the Ministry of Health of the Czech Republic (AZV NU20-07-00182 research grant). Open access funding enabled and organized by Projekt DEAL.

CONFLICTS OF INTEREST

S. H. Tsang is salaried by the National Institute of Health 5P30CA013696, U01 EY030580, R01EY033770, R01EY018213, R01EY024698, R24EY028758, R24EY027285, 5P30EY019007, U54OD020351, and R21AG050437. S. H. Tsang receives grant support from Abeona

10981004, 2022, 7, Downloaded from https://onlinelibrary.wiley.com/doi/10.1002/humu.24371, Wiley Online Library on [09/12/2024]. See the Terms and Conditions (https://onlinelibrary.wiley.com/terms-and-conditions) on Wiley Online Library for rules of use; OA articles are governed by the applicable Creative Commons License

Therapeutics, Inc and Emendo. He is also the founder of Rejuvitas and is on the scientific and clinical advisory board for Nanoscope Therapeutics. The other authors declared no conflict of interest.

DATA AVAILABILITY STATEMENT

The data that support the findings of this study are openly available in ClinVar at https://www.ncbi.nlm.nih.gov/clinvar/, reference number SCV001571262 to SCV001571322 and will be submitted to the Global Variome shared LOVD database at databases.lovd.nl/shared.

ORCID

Maria Solaki http://orcid.org/0000-0002-7965-9865
Peggy Reuter http://orcid.org/0000-0001-6880-9437
Isabelle Audo http://orcid.org/0000-0003-0698-5309
Ghassan Balousha http://orcid.org/0000-0002-0260-1577
Francesco Benedicenti http://orcid.org/0000-0002-9458-0688
David Birch http://orcid.org/0000-0002-6594-2897
Pierre Bitoun http://orcid.org/0000-0001-6557-6826
Delphine Blain http://orcid.org/0000-0002-9275-5827
Jaume Català-Mora http://orcid.org/0000-0003-2152-8579
Roberto Giorda http://orcid.org/0000-0001-8175-9606
Irina Golovleva http://orcid.org/0000-0001-8741-0616
Kaylie Jones http://orcid.org/0000-0003-2818-5097
Herbert Jägle http://orcid.org/0000-0001-6353-2651
Andreas R. Janecke http://orcid.org/0000-0001-7155-0315
Ulrich Kellner http://orcid.org/0000-0001-5221-4631
Petra Liskova http://orcid.org/0000-0001-7834-8486
Birgit Lorenz http://orcid.org/0000-0002-9737-8127
Loreto Martorell-Sampol http://orcid.org/0000-0003-0898-7332
André Messias http://orcid.org/0000-0002-5328-9608
Fernanda Belga Ottoni Porto http://orcid.org/0000-0002-4308-1766
Eleni Papageorgiou http://orcid.org/0000-0003-1931-4168
Astrid S. Plomp http://orcid.org/0000-0002-4903-8232
Thomas Rosenberg http://orcid.org/0000-0003-0095-8991
Günther Rudolph http://orcid.org/0000-0002-9399-730X
Paul A. Sieving http://orcid.org/0000-0002-2918-577X
Franco Stanzial http://orcid.org/0000-0001-8762-9255
Stephen H. Tsang http://orcid.org/0000-0001-9082-2427
Balázs Varsanyi http://orcid.org/0000-0002-3891-3839
Richard G. Weleber http://orcid.org/0000-0003-0001-0367
Ditta Zobor http://orcid.org/0000-0001-7187-5558
Bernd Wissinger http://orcid.org/0000-0001-8964-5953
Susanne Kohl http://orcid.org/0000-0002-6438-6331

REFERENCES

Abdelkader, E., Brandau, O., Bergmann, C., AlSalamah, N., Nowilaty, S., & Schatz, P. (2018). Novel causative variants in patients with achromatopsia. *Ophthalmic Genetics*, *39*(6), 678–683. https://doi.org/10.1080/13816810.2018.1522653

Abouelhoda, M., Sobahy, T., El-Kalioby, M., Patel, N., Shamseldin, H., Monies, D., Al-Tassan, N., Ramzan, K., Imtiaz, F., Shaheen, R., & Alkuraya, F. S. (2016). Clinical genomics can facilitate countrywide estimation of autosomal recessive disease burden. *Genetics in Medicine*, *18*(12), 1244–1249. https://doi.org/10.1038/gim.2016.37

Ahuja, Y., Kohl, S., & Traboulsi, E. I. (2008). CNGA3 mutations in two United Arab Emirates families with achromatopsia. *Molecular Vision*, *14*, 1293–1297.

Aligianis, I. A., Forshew, T., Johnson, S., Michaelides, M., Johnson, C. A., Trembath, R. C., & Maher, E. R. (2002). Mapping of a novel locus for achromatopsia (ACHM4) to 1p and identification of a germline mutation in the alpha subunit of cone transducin (GNAT2). *Journal of Medical Genetics*, *39*(9), 656–660. https://doi.org/10.1136/jmg.39.9.656

Ansar, M., Santos-Cortez, R. L., Saqib, M. A., Zulfiqar, F., Lee, K., Ashraf, N. M., & Leal, S. M. (2015). Mutation of ATF6 causes autosomal recessive achromatopsia. *Human Genetics*, *134*(9), 941–950. https://doi.org/10.1007/s00439-015-1571-4

Arshad, M. W., Lee, Y., Malik, M. A., Khan, J., Khan, A., Kareem, A., Kang, C., & Shabbir, M. I. (2019). Identification of novel mutation in CNGA3 gene by whole-exome sequencing and in-silico analyses for genotype-phenotype assessment with autosomal recessive achromatopsia in Pakistani families. *The Journal of the Pakistan Medical Association*, *69*(2), 183–189.

Azam, M., Collin, R. W., Shah, S. T., Shah, A. A., Khan, M. I., Hussain, A., Sadeque, A., Strom, T. M., Thiadens, A. A., Roosing, S., den Hollander, A. I., Cremers, F. P., & Qamar, R. (2010). Novel CNGA3 and CNGB3 mutations in two Pakistani families with achromatopsia. *Molecular Vision*, *16*, 774–781.

Barret, D. C. A., Schertler, G. F. X., Benjamin Kaupp, U., & Marino, J. (2022). The structure of the native CNGA1/CNGB1 CNG channel from bovine retinal rods. *Nature Structural & Molecular Biology*, *29*(1), 32–39. https://doi.org/10.1038/s41594-021-00700-8

Biel, M., & Michalakis, S. (2009). Cyclic nucleotide-gated channels. *Handbook of Experimental Pharmacology*, *191*, 111–136. https://doi.org/10.1007/978-3-540-68964-5_7

Biel, M., Seeliger, M., Pfeifer, A., Kohler, K., Gerstner, A., Ludwig, A., & Hofmann, F. (1999). Selective loss of cone function in mice lacking the cyclic nucleotide-gated channel CNG3. *Proceedings of the National Academy of Sciences of the United States of America*, *96*(13), 7553–7557. https://doi.org/10.1073/pnas.96.13.7553

Burkard, M., Kohl, S., Kratzig, T., Tanimoto, N., Brennenstuhl, C., Bausch, A. E., & Ruth, P. (2018). Accessory heterozygous mutations in cone photoreceptor CNGA3 exacerbate CNG channel-associated retinopathy. *Journal of Clinical Investigation*, *128*(12), 5663–5675. https://doi.org/10.1172/JCI96098

Burgueño-Montañés, C., Colunga Cueva, M., & Costales Álvarez, C. (2014). Una nueva mutación en el gen CNGA3 causante de acromatopsia incompleta. *Archivos de La Sociedad Española de Oftalmología*, *89*(3), 107–109. https://doi.org/10.1016/j.oftal.2012.07.019

Carrigan, M., Duignan, E., Malone, C. P. G., Stephenson, K., Saad, T., McDermott, C., Green, A., Keegan, D., Humphries, P., Kenna, P. F., & Farrar, G. J. (2016). Panel-based population next-generation sequencing for inherited retinal degenerations. *Scientific Reports*, *6*(1), 33248. https://doi.org/10.1038/srep33248

Carss, K. J., Arno, G., Erwood, M., Stephens, J., Sanchis-Juan, A., Hull, S., Megy, K., Grozeva, D., Dewhurst, E., Malka, S., Plagnol, V., Penkett, C., Stirrups, K., Rizzo, R., Wright, G., Josifova, D., Bitner-Glindzicz, M., Scott, R. H., Clement, E., & Yu, P. (2017). Comprehensive rare variant analysis via whole-genome sequencing to determine the molecular pathology of inherited retinal disease. *The American Journal of Human Genetics*, *100*(1), 75–90. https://doi.org/10.1016/j.ajhg.2016.12.003

Chang, B., Grau, T., Dangel, S., Hurd, R., Jurklies, B., Sener, E. C., & Wissinger, B. (2009). A homologous genetic basis of the murine cpfl1 mutant and human achromatopsia linked to mutations in the PDE6C gene. *Proceedings of the National Academy of Sciences of the United*

10981004, 2022, 7, Downloaded from https://onlinelibrary.wiley.com/doi/10.1002/humu.24371, Wiley Online Library on [09/12/2024]. See the Terms and Conditions (https://onlinelibrary.wiley.com/terms-and-conditions) on Wiley Online Library for rules of use; OA articles are governed by the applicable Creative Commons License

States of America, *106*(46), 19581–19586. https://doi.org/10.1073/pnas.0907720106

Dai, G., Peng, C., Liu, C., & Varnum, M. D. (2013). Two structural components in CNGA3 support regulation of cone CNG channels by phosphoinositides. *Journal of General Physiology*, *141*(4), 413–430. https://doi.org/10.1085/jgp.201210944

Dai, G., & Varnum, M. D. (2013). CNGA3 achromatopsia-associated mutation potentiates the phosphoinositide sensitivity of cone photoreceptor CNG channels by altering intersubunit interactions. *American Journal of Physiology: Cell Physiology*, *305*(2), C147–C159. https://doi.org/10.1152/ajpcell.00037.2013

Dubis, A. M., Cooper, R. F., Aboshiha, J., Langlo, C. S., Sundaram, V., Liu, B., Collison, F., Fishman, G. A., Moore, A. T., Webster, A. R., Dubra, A., Carroll, J., & Michaelides, M. (2014). Genotype-dependent variability in residual cone structure in achromatopsia: Toward developing metrics for assessing cone health. *Investigative Opthalmology & Visual Science*, *55*(11), 7303–7311. https://doi.org/10.1167/iovs.14-14225

Duricka, D. L., Brown, R. L., & Varnum, M. D. (2012). Defective trafficking of cone photoreceptor CNG channels induces the unfolded protein response and ER-stress-associated cell death. *Biochemical Journal*, *441*(2), 685–696. https://doi.org/10.1042/BJ20111004

Ellingford, J. M., Barton, S., Bhaskar, S., O'Sullivan, J., Williams, S. G., Lamb, J. A., Panda, B., Sergouniotis, P. I., Gillespie, R. L., Daiger, S. P., Hall, G., Gale, T., Lloyd, I. C., Bishop, P. N., Ramsden, S. C., & Black, G. C. M. (2016). Molecular findings from 537 individuals with inherited retinal disease. *Journal of Medical Genetics*, *53*(11), 761–767. https://doi.org/10.1136/jmedgenet-2016-103837

Ezquerra-Inchausti, M., Anasagasti, A., Barandika, O., Garay-Aramburu, G., Galdós, M., López de Munain, A., Irigoyen, C., & Ruiz-Ederra, J. (2018). A new approach based on targeted pooled DNA sequencing identifies novel mutations in patients with Inherited Retinal Dystrophies. *Scientific Reports*, *8*(1). https://doi.org/10.1038/s41598-018-33810-3

Ezra-Elia, R., Banin, E., Honig, H., Rosov, A., Obolensky, A., Averbukh, E., & Ofri, R. (2014). Flicker cone function in normal and day blind sheep: A large animal model for human achromatopsia caused by CNGA3 mutation. *Documenta Ophthalmologica*, *129*(3), 141–150. https://doi.org/10.1007/s10633-014-9458-6

Fahim, A. T., Khan, N. W., Zahid, S., Schachar, I. H., Branham, K., Kohl, S., Wissinger, B., Elner, V. M., Heckenlively, J. R., & Jayasundera, T. (2013). Diagnostic fundus autofluorescence patterns in achromatopsia. *American Journal of Ophthalmology*, *156*(6), 1211–1219. https://doi.org/10.1016/j.ajo.2013.06.033

Felden, J., Baumann, B., Ali, M., Audo, I., Ayuso, C., Bocquet, B., & Kohl, S. (2019). Mutation spectrum and clinical investigation of achromatopsia patients with mutations in the GNAT2 gene. *Human Mutation*, *40*(8), 1145–1155. https://doi.org/10.1002/humu.23768

Fischer, M. D., Michalakis, S., Wilhelm, B., Zobor, D., Muehlfriedel, R., Kohl, S., & Wissinger, B. (2020). Safety and vision outcomes of subretinal gene therapy targeting cone photoreceptors in achromatopsia: A nonrandomized controlled trial. *JAMA Ophthalmol*, *138*(6), 643–651. https://doi.org/10.1001/jamaophthalmol.2020.1032

François, J. (1961). *Heredity in ophthalmology*. Mosby.

Georgiou, M., Litts, K. M., Kalitzeos, A., Langlo, C. S., Kane, T., Singh, N., Kassilian, M., Hirji, N., Kumaran, N., Dubra, A., Carroll, J., & Michaelides, M. (2019). Adaptive optics retinal imaging in CNGA3-associated achromatopsia: Retinal characterization, interocular symmetry, and intrafamilial variability. *Investigative Opthalmology & Visual Science*, *60*(1), 383. https://doi.org/10.1167/iovs.18-25880

Genead, M. A., Fishman, G. A., Rha, J., Dubis, A. M., Bonci, D. M. O., Dubra, A., Stone, E. M., Neitz, M., & Carroll, J. (2011). Photoreceptor structure and function in patients with congenital achromatopsia. *Investigative Opthalmology & Visual Science*, *52*(10), 7298–7308. https://doi.org/10.1167/iovs.11-7762

Georgiou, M., Singh, N., Kane, T., Zaman, S., Hirji, N., Aboshiha, J., & Michaelides, M. (2020). Long-term investigation of retinal function in patients with achromatopsia. *Investigative Ophthalmology and Visual Science*, *61*(11), 38. https://doi.org/10.1167/iovs.61.11.38

Gofman, Y., Scharfe, C., Marks, D. S., Haliloglu, T., & Ben-Tal, N. (2014). Structure, dynamics and implied gating mechanism of a human cyclic nucleotide-gated channel. *PLoS Computational Biology*, *10*(12), e1003976. https://doi.org/10.1371/journal.pcbi.1003976

Gootwine, E., Abu-Siam, M., Obolensky, A., Rosov, A., Honig, H., Nitzan, T., & Seroussi, E. (2017). Gene augmentation therapy for a missense substitution in the cGMP-binding domain of ovine CNGA3 gene restores vision in day-blind sheep. *Investigative Ophthalmology and Visual Science*, *58*(3), 1577–1584. https://doi.org/10.1167/iovs.16-20986

Goto-Omoto, S., Hayashi, T., Gekka, T., Kubo, A., Takeuchi, T., & Kitahara, K. (2006). Compound heterozygous CNGA3 mutations (R436W, L633P) in a Japanese patient with congenital achromatopsia. *Visual Neuroscience*, *23*(3–4), 395–402. https://doi.org/10.1017/s095252380623308x

Grantham, R. (1974). Amino acid difference formula to help explain protein evolution. *Science*, *185*(4154), 862–864. https://doi.org/10.1126/science.185.4154.862

Greenberg, J. P., Sherman, J., Zweifel, S. A., Chen, R. W. S., Duncker, T., Kohl, S., Baumann, B., Wissinger, B., Yannuzzi, L. A., & Tsang, S. H. (2014). Spectral-domain optical coherence tomography staging and autofluorescence imaging in achromatopsia. *JAMA Ophthalmology*, *132*(4), 437–445. https://doi.org/10.1001/jamaophthalmol.2013.7987

Hirji, N., Aboshiha, J., Georgiou, M., Bainbridge, J., & Michaelides, M. (2018). Achromatopsia: Clinical features, molecular genetics, animal models and therapeutic options. *Ophthalmic Genetics*, *39*(2), 149–157. https://doi.org/10.1080/13816810.2017.1418389

Holtan, J. P., Selmer, K. K., Heimdal, K. R., & Bragadóttir, R. (2020). Inherited retinal disease in Norway – A characterization of current clinical and genetic knowledge. *Acta Ophthalmologica*, *98*(3), 286–295. https://doi.org/10.1111/aos.14218

Huang, L., Xiao, X., Li, S., Jia, X., Wang, P., Sun, W., Xu, Y., Xin, W., Guo, X., & Zhang, Q. (2016). Molecular genetics of cone-rod dystrophy in Chinese patients: New data from 61 probands and mutation overview of 163 probands. *Experimental Eye Research*, *146*, 252–258. https://doi.org/10.1016/j.exer.2016.03.015

Hull, S., Kiray, G., Chiang, J. P., & Vincent, A. L. (2020). Molecular and phenotypic investigation of a New Zealand cohort of childhood-onset retinal dystrophy. *American Journal of Medical Genetics Part C: Seminars in Medical Genetics*, *184*(3), 708–717. https://doi.org/10.1002/ajmg.c.31836

Jacobson, M. A., Jones, L. J., Colussi, D. J., & Tanaka, J. C. (2019). High-throughput Ca(2+) flux assay to monitor cyclic nucleotide-gated channel activity and characterize achromatopsia mutant channel function. *ACS Chemical Neuroscience*, *10*(8), 3662–3670. https://doi.org/10.1021/acschemneuro.9b00231

Jaganathan, K., Kyriazopoulou Panagiotopoulou, S., McRae, J. F., Darbandi, S. F., Knowles, D., Li, Y. I., & Farh, K. K. (2019). Predicting splicing from primary sequence with deep learning. *Cell*, *176*(3), 535–548. https://doi.org/10.1016/j.cell.2018.12.015

Jinda, W., Tuekprakhon, A., Thongnoppakhun, W., Limwongse, C., Trinavarat, A., & Atchaneeyasakul, L. (2021). Molecular and clinical characterization of Thai patients with achromatopsia: Identification of three novel disease-associated variants in the CNGA3 and CNGB3 genes. *International Ophthalmology*, *41*(1), 121–134. https://doi.org/10.1007/s10792-020-01559-2

Johnson, S., Michaelides, M., Aligianis, I. A., Ainsworth, J. R., Mollon, J. D., Maher, E. R., & Hunt, D. M. (2004). Achromatopsia caused by novel

10981004, 2022, 7, Downloaded from https://onlinelibrary.wiley.com/doi/10.1002/humu.24371, Wiley Online Library on [09/12/2024]. See the Terms and Conditions (https://onlinelibrary.wiley.com/terms-and-conditions) on Wiley Online Library for rules of use; OA articles are governed by the applicable Creative Commons License

mutations in both CNGA3 and CNGB3. *Journal of Medical Genetics*, *41*(2), e20. https://doi.org/10.1136/jmg.2003.011437

Kaupp, U. B., & Seifert, R. (2002). Cyclic nucleotide-gated ion channels. *Physiological Reviews*, *82*(3), 769–824. https://doi.org/10.1152/physrev.00008.2002

Kelbsch, C., Stingl, K., Kempf, M., Strasser, T., Jung, R., Kuehlewein, L., & Stingl, K. (2019). Objective measurement of local rod and cone function using gaze-controlled chromatic pupil campimetry in healthy subjects. *Translational Vision Science & Technology*, *8*(6), 19. https://doi.org/10.1167/tvst.8.6.19

Kim, M. S., Joo, K., Seong, M.-W., Kim, M. J., Park, K. H., Park, S. S., & Woo, S. J. (2019). Genetic mutation profiles in Korean patients with inherited retinal diseases. *Journal of Korean Medical Science*, *34*(21), e161. https://doi.org/10.3346/jkms.2019.34.e161

Kircher, M., Witten, D. M., Jain, P., O'Roak, B. J., Cooper, G. M., & Shendure, J. (2014). A general framework for estimating the relative pathogenicity of human genetic variants. *Nature Genetics*, *46*(3), 310–315. https://doi.org/10.1038/ng.2892

Koch, M., Scheel, C., Ma, H., Yang, F., Stadlmeier, M., Gluck, A. F., & Michalakis, S. (2020). The cGMP-dependent protein kinase 2 contributes to cone photoreceptor degeneration in the Cnga3-deficient mouse model of achromatopsia. *International Journal of Molecular Sciences*, *22*(1). https://doi.org/10.3390/ijms22010052

Koeppen, K., Reuter, P., Kohl, S., Baumann, B., Ladewig, T., & Wissinger, B. (2008). Functional analysis of human CNGA3 mutations associated with colour blindness suggests impaired surface expression of channel mutants A3(R427C) and A3(R563C). *European Journal of Neuroscience*, *27*(9), 2391–2401. https://doi.org/10.1111/j.1460-9568.2008.06195.x

Koeppen, K., Reuter, P., Ladewig, T., Kohl, S., Baumann, B., Jacobson, S. G., & Wissinger, B. (2010). Dissecting the pathogenic mechanisms of mutations in the pore region of the human cone photoreceptor cyclic nucleotide-gated channel. *Human Mutation*, *31*(7), 830–839. https://doi.org/10.1002/humu.21283

Kohl, S., Baumann, B., Broghammer, M., Jagle, H., Sieving, P., Kellner, U., & Wissinger, B. (2000). Mutations in the CNGB3 gene encoding the beta-subunit of the cone photoreceptor cGMP-gated channel are responsible for achromatopsia (ACHM3) linked to chromosome 8q21. *Human Molecular Genetics*, *9*(14), 2107–2116. https://doi.org/10.1093/hmg/9.14.2107

Kohl, S., Baumann, B., Rosenberg, T., Kellner, U., Lorenz, B., Vadala, M., & Wissinger, B. (2002). Mutations in the cone photoreceptor G-protein alpha-subunit gene GNAT2 in patients with achromatopsia. *American Journal of Human Genetics*, *71*(2), 422–425. https://doi.org/10.1086/341835

Kohl, S., Coppieters, F., Meire, F., Schaich, S., Roosing, S., Brennenstuhl, C., & Wissinger, B. (2012). A nonsense mutation in PDE6H causes autosomal-recessive incomplete achromatopsia. *American Journal of Human Genetics*, *91*(3), 527–532. https://doi.org/10.1016/j.ajhg.2012.07.006

Kohl, S., Marx, T., Giddings, I., Jagle, H., Jacobson, S. G., Apfelstedt-Sylla, E., & Wissinger, B. (1998). Total colourblindness is caused by mutations in the gene encoding the alpha-subunit of the cone photoreceptor cGMP-gated cation channel. *Nature Genetics*, *19*(3), 257–259. https://doi.org/10.1038/935

Kohl, S., Zobor, D., Chiang, W. C., Weisschuh, N., Staller, J., Gonzalez Menendez, I., & Lin, J. H. (2015). Mutations in the unfolded protein response regulator ATF6 cause the cone dysfunction disorder achromatopsia. *Nature Genetics*, *47*(7), 757–765. https://doi.org/10.1038/ng.3319

Kumar, P., Henikoff, S., & Ng, P. C. (2009). Predicting the effects of coding non-synonymous variants on protein function using the SIFT algorithm. *Nature Protocols*, *4*(7), 1073–1081. https://doi.org/10.1038/nprot.2009.86

Kuniyoshi, K., Muraki-Oda, S., Ueyama, H., Toyoda, F., Sakuramoto, H., Ogita, H., & Shimomura, Y. (2016). Novel mutations in the gene for alpha-subunit of retinal cone cyclic nucleotide-gated channels in a Japanese patient with congenital achromatopsia. *Japanese Journal of Ophthalmology*, *60*(3), 187–197. https://doi.org/10.1007/s10384-016-0424-6

Lam, K., Guo, H., Wilson, G. A., Kohl, S., & Wong, F. (2011). Identification of variants in CNGA3 as cause for achromatopsia by exome sequencing of a single patient. *Archives of Ophthalmology*, *129*(9), 1212–1217. https://doi.org/10.1001/archophthalmol.2011.254

Landrum, M. J., Lee, J. M., Riley, G. R., Jang, W., Rubinstein, W. S., Church, D. M., & Maglott, D. R. (2014). ClinVar: Public archive of relationships among sequence variation and human phenotype. *Nucleic Acids Res*, *42*(Database issue), D980–D985. https://doi.org/10.1093/nar/gkt1113

Lee, E. J., Chiang, W. J., Kroeger, H., Bi, C. X., Chao, D. L., Skowronska-Krawczyk, D., & Lin, J. H. (2020). Multiexon deletion alleles of ATF6 linked to achromatopsia. *JCI Insight*, *5*(7), e136041. https://doi.org/10.1172/jci.insight.136041

Li, L., Chen, Y., Jiao, X., Jin, C., Jiang, D., Tanwar, M., Ma, Z., Huang, L., Ma, X., Sun, W., Chen, J., Ma, Y., M'hamdi, O., Govindarajan, G., Cabrera, P. E., Li, J., Gupta, N., Naeem, M. A., Khan, S. N., & Hejtmancik, J. F. (2017). Homozygosity mapping and genetic analysis of autosomal recessive retinal dystrophies in 144 consanguineous Pakistani families. *Investigative Opthalmology & Visual Science*, *58*(4), 2218–2238. https://doi.org/10.1167/iovs.17-21424

Li, F.-F., Huang, X.-F., Chen, J., Yu, X.-D., Zheng, M.-Q., Lu, F., Jin, Z.-B., & Gan, D.-K. (2015). Identification of novel mutations by targeted exome sequencing and the genotype-phenotype assessment of patients with achromatopsia. *Journal of Translational Medicine*, *13*(1), 334. https://doi.org/10.1186/s12967-015-0694-7

Li, S., Huang, L., Xiao, X., Jia, X., Guo, X., & Zhang, Q. (2014). Identification of CNGA3 mutations in 46 families: Common cause of achromatopsia and cone-rod dystrophies in Chinese patients. *JAMA Ophthalmology*, *132*(9), 1076–1083. https://doi.org/10.1001/jamaophthalmol.2014.1032

Liang, X., Dong, F., Li, H., Li, H., Yang, L., & Sui, R. (2015). Novel CNGA3 mutations in Chinese patients with achromatopsia. *British Journal of Ophthalmology*, *99*(4), 571–576. https://doi.org/10.1136/bjophthalmol-2014-305432

Lisowska, J., Lisowski, L., Kelbsch, C., Maeda, F., Richter, P., Kohl, S., & Consortium, R.-C. (2017). Development of a Chromatic Pupillography Protocol for the First Gene Therapy Trial in Patients With CNGA3-Linked Achromatopsia. *Investigative Ophthalmology and Visual Science*, *58*(2), 1274–1282. https://doi.org/10.1167/iovs.16-20505

Liu, C., & Varnum, M. D. (2005). Functional consequences of progressive cone dystrophy-associated mutations in the human cone photoreceptor cyclic nucleotide-gated channel CNGA3 subunit. *American Journal of Physiology: Cell Physiology*, *289*(1), C187–C198. https://doi.org/10.1152/ajpcell.00490.2004

Maguire, J., McKibbin, M., Khan, K., Kohl, S., Ali, M., & McKeefry, D. (2018). CNGB3 mutations cause severe rod dysfunction. *Ophthalmic Genetics*, *39*(1), 108–114. https://doi.org/10.1080/13816810.2017.1368087

Matveev, A. V., Fitzgerald, J. B., Xu, J., Malykhina, A. P., Rodgers, K. K., & Ding, X. Q. (2010). The disease-causing mutations in the carboxyl terminus of the cone cyclic nucleotide-gated channel CNGA3 subunit alter the local secondary structure and interfere with the channel active conformational change. *Biochemistry*, *49*(8), 1628–1639. https://doi.org/10.1021/bi901960u

Mayer, A. K., Van Cauwenbergh, C., Rother, C., Baumann, B., Reuter, P., De Baere, E., & Group, A. S. (2017). CNGB3 mutation spectrum including copy number variations in 552 achromatopsia patients.

10981004, 2022, 7, Downloaded from https://onlinelibrary.wiley.com/doi/10.1002/humu.24371, Wiley Online Library on [09/12/2024]. See the Terms and Conditions (https://onlinelibrary.wiley.com/terms-and-conditions) on Wiley Online Library for rules of use; OA articles are governed by the applicable Creative Commons License

Human Mutation, *38*(11), 1579–1591. https://doi.org/10.1002/humu.23311

Meighan, P. C., Peng, C., & Varnum, M. D. (2015). Inherited macular degeneration-associated mutations in CNGB3 increase the ligand sensitivity and spontaneous open probability of cone cyclic nucleotide-gated channels. *Frontiers in Physiology*, *6*, 177. https://doi.org/10.3389/fphys.2015.00177

Méjécase, C., Hummel, A., Mohand-Saïd, S., Andrieu, C., El Shamieh, S., Antonio, A., Condroyer, C., Boyard, F., Foussard, M., Blanchard, S., Letexier, M., Saraiva, J.-P., Sahel, J.-A., Zeitz, C., & Audo, I. (2019). Whole exome sequencing resolves complex phenotype and identifies CC2D2A mutations underlying non-syndromic rod-cone dystrophy. *Clinical Genetics*, *95*(2), 329–333. https://doi.org/10.1111/cge.13453

Michalakis, S., Schon, C., Becirovic, E., & Biel, M. (2017). Gene therapy for achromatopsia. *Journal of Gene Medicine*, *19*(3), e2944. https://doi.org/10.1002/jgm.2944

Muraki-Oda, S., Toyoda, F., Okada, A., Tanabe, S., Yamade, S., Ueyama, H., & Ohji, M. (2007). Functional analysis of rod monochromacy-associated missense mutations in the CNGA3 subunit of the cone photoreceptor cGMP-gated channel. *Biochemical and Biophysical Research Communications*, *362*(1), 88–93. https://doi.org/10.1016/j.bbrc.2007.07.152

Nishiguchi, K. M., Sandberg, M. A., Gorji, N., Berson, E. L., & Dryja, T. P. (2005). Cone cGMP-gated channel mutations and clinical findings in patients with achromatopsia, macular degeneration, and other hereditary cone diseases. *Human Mutation*, *25*(3), 248–258. https://doi.org/10.1002/humu.20142

Pang, J. J., Deng, W. T., Dai, X., Lei, B., Everhart, D., Umino, Y., & Hauswirth, W. W. (2012). AAV-mediated cone rescue in a naturally occurring mouse model of CNGA3-achromatopsia. *PLoS One*, *7*(4), e35250. https://doi.org/10.1371/journal.pone.0035250

Patel, N., Aldahmesh, M. A., Alkuraya, H., Anazi, S., Alsharif, H., Khan, A. O., Sunker, A., Al-mohsen, S., Abboud, E. B., Nowilaty, S. R., Alowain, M., Al-Zaidan, H., Al-Saud, B., Alasmari, A., Abdel-Salam, G. M. H., Abouelhoda, M., Abdulwahab, F. M., Ibrahim, N., Naim, E., & Alkuraya, F. S. (2016). Expanding the clinical, allelic, and locus heterogeneity of retinal dystrophies. *Genetics in Medicine*, *18*(6), 554–562. https://doi.org/10.1038/gim.2015.127

Patel, K. A., Bartoli, K. M., Fandino, R. A., Ngatchou, A. N., Woch, G., Carey, J., & Tanaka, J. C. (2005). Transmembrane S1 mutations in CNGA3 from achromatopsia 2 patients cause loss of function and impaired cellular trafficking of the cone CNG channel. *Investigative Ophthalmology and Visual Science*, *46*(7), 2282–2290. https://doi.org/10.1167/iovs.05-0179

Patel, A., Hayward, J. D., Tailor, V., Nyanhete, R., Ahlfors, H., Gabriel, C., Jannini, T. B., Abbou-Rayyah, Y., Henderson, R., Nischal, K. K., Islam, L., Bitner-Glindzicz, M., Hurst, J., Valdivia, L. E., Zanolli, M., Moosajee, M., Brookes, J., Papadopoulos, M., Khaw, P. T., & Sowden, J. C. (2019). The oculome panel test: Next-generation sequencing to diagnose a diverse range of genetic developmental eye disorders. *Ophthalmology*, *126*(6), 888–907. https://doi.org/10.1016/j.ophtha.2018.12.050

Pertea, M., Lin, X., & Salzberg, S. L. (2001). GeneSplicer: a new computational method for splice site prediction. *Nucleic Acids Research*, *29*(5), 1185–1190. https://doi.org/10.1093/nar/29.5.1185

Pollard, K. S., Hubisz, M. J., Rosenbloom, K. R., & Siepel, A. (2010). Detection of nonneutral substitution rates on mammalian phylogenies. *Genome Research*, *20*(1), 110–121. https://doi.org/10.1101/gr.097857.109

Reese, M. G., Eeckman, F. H., Kulp, D., & Haussler, D. (1997). Improved splice site detection in Genie. *Journal of Computational Biology*, *4*(3), 311–323. https://doi.org/10.1089/cmb.1997.4.311

Reichel, F. F., Michalakis, S., Wilhelm, B., Zobor, D., Muehlfriedel, R., Kohl, S., & Fischer, D. (2021). Three-year results of phase I retinal gene therapy trial for CNGA3-mutated achromatopsia: results of a non randomised controlled trial. *British Journal of Ophthalmology*. https://doi.org/10.1136/bjophthalmol-2021-319067

Reicher, S., Seroussi, E., & Gootwine, E. (2010). A mutation in gene CNGA3 is associated with day blindness in sheep. *Genomics*, *95*(2), 101–104. https://doi.org/10.1016/j.ygeno.2009.10.003

Rentzsch, P., Schubach, M., Shendure, J., & Kircher, M. (2021). CADD-Splice-improving genome-wide variant effect prediction using deep learning-derived splice scores. *Genome Medicine*, *13*(1), 31. https://doi.org/10.1186/s13073-021-00835-9

Reuter, P., Koeppen, K., Ladewig, T., Kohl, S., Baumann, B., & Wissinger, B., Achromatopsia Clinical Study Group. (2008). Mutations in CNGA3 impair trafficking or function of cone cyclic nucleotide-gated channels, resulting in achromatopsia. *Human Mutation*, *29*(10), 1228–1236. https://doi.org/10.1002/humu.20790

Richards, S., Aziz, N., Bale, S., Bick, D., Das, S., Gastier-Foster, J., & Committee, A. L. Q. A. (2015). Standards and guidelines for the interpretation of sequence variants: A joint consensus recommendation of the American College of Medical Genetics and Genomics and the Association for Molecular Pathology. *Genetics in Medicine*, *17*(5), 405–424. https://doi.org/10.1038/gim.2015.30

Righetti, G., Kempf, M., Braun, C., Jung, R., Kohl, S., Wissinger, B., & Stingl, K. (2021). Oscillatory potentials in achromatopsia as a tool for understanding cone retinal functions. *International Journal of Molecular Sciences*, *22*(23), 12717. https://doi.org/10.3390/ijms222312717

Rim, J. H., Lee, S.-T., Gee, H. Y., Lee, B. J., Choi, J. R., Park, H. W., Han, S.-H., & Han, J. (2017). Accuracy of next-generation sequencing for molecular diagnosis in patients with infantile nystagmus syndrome. *JAMA Ophthalmology*, *135*(12), 1376–1385. https://doi.org/10.1001/jamaophthalmol.2017.4859

Ross, M., Ofri, R., Aizenberg, I., Abu-Siam, M., Pe'er, O., Arad, D., & Gantz, L. (2020). Naturally-occurring myopia and loss of cone function in a sheep model of achromatopsia. *Scientific Reports*, *10*(1), 19314. https://doi.org/10.1038/s41598-020-76205-z

Van Schil, K., Naessens, S., Van de Sompele, S., Carron, M., Aslanidis, A., Van Cauwenbergh, C., & De Baere, E. (2018). Mapping the genomic landscape of inherited retinal disease genes prioritizes genes prone to coding and noncoding copy-number variations. *Genetics in Medicine*, *20*(2), 202–213. https://doi.org/10.1038/gim.2017.97

Saqib, M. A. N., Awan, B. M., Sarfraz, M., Khan, M. N., Rashid, S., & Ansar, M. (2011). Genetic analysis of four Pakistani families with achromatopsia and a novel S4 motif mutation of CNGA3. *Japanese Journal of Ophthalmology*, *55*(6), 676–680. https://doi.org/10.1007/s10384-011-0070-y

Saqib, M. A. N., Nikopoulos, K., Ullah, E., Sher Khan, F., Iqbal, J., Bibi, R., Jarral, A., Sajid, S., Nishiguchi, K. M., Venturini, G., Ansar, M., & Rivolta, C. (2015). Homozygosity mapping reveals novel and known mutations in Pakistani families with inherited retinal dystrophies. *Scientific Reports*, *5*(1), 9965. https://doi.org/10.1038/srep09965

Schwarz, J. M., Rodelsperger, C., Schuelke, M., & Seelow, D. (2010). MutationTaster evaluates disease-causing potential of sequence alterations. *Nature Methods*, *7*(8), 575–576. https://doi.org/10.1038/nmeth0810-575

Shaikh, R. S., Reuter, P., Sisk, R. A., Kausar, T., Shahzad, M., Maqsood, M. I., & Ahmed, Z. M. (2015). Homozygous missense variant in the human CNGA3 channel causes cone-rod dystrophy. *European Journal of Human Genetics*, *23*(4), 473–480. https://doi.org/10.1038/ejhg.2014.136

Shamir, M. H., Ofri, R., Bor, A., Brenner, O., Reicher, S., Obolensky, A., & Gootwine, E. (2010). A novel day blindness in sheep: epidemiological, behavioural, electrophysiological and histopathological studies.

10981004, 2022, 7, Downloaded from https://onlinelibrary.wiley.com/doi/10.1002/humu.24371, Wiley Online Library on [09/12/2024]. See the Terms and Conditions (https://onlinelibrary.wiley.com/terms-and-conditions) on Wiley Online Library for rules of use; OA articles are governed by the applicable Creative Commons License

Veterinary Journal, *185*(2), 130–137. https://doi.org/10.1016/j.tvjl.2009.05.029

Shapiro, M. B., & Senapathy, P. (1987). RNA splice junctions of different classes of eukaryotes: sequence statistics and functional implications in gene expression. *Nucleic Acids Research*, *15*(17), 7155–7174. https://doi.org/10.1093/nar/15.17.7155

Sharon, D., Ben-Yosef, T., Goldenberg-Cohen, N., Pras, E., Gradstein, L., Soudry, S., Mezer, E., Zur, D., Abbasi, A. H., Zeitz, C., Cremers, F. P. M., Khan, M. I., Levy, J., Rotenstreich, Y., Birk, O. S., Ehrenberg, M., Leibu, R., Newman, H., Shomron, N., & Perlman, I. (2020). A nationwide genetic analysis of inherited retinal diseases in Israel as assessed by the Israeli inherited retinal disease consortium (IIRDC). *Human Mutation*, *41*(1), 140–149. https://doi.org/10.1002/humu.23903

Shuart, N. G., Haitin, Y., Camp, S. S., Black, K. D., & Zagotta, W. N. (2011). Molecular mechanism for 3:1 subunit stoichiometry of rod cyclic nucleotide-gated ion channels. *Nature Communications*, *2*, 457. https://doi.org/10.1038/ncomms1466

Sievers, F., Wilm, A., Dineen, D., Gibson, T. J., Karplus, K., Li, W., & Higgins, D. G. (2011). Fast, scalable generation of high-quality protein multiple sequence alignments using Clustal Omega. *Molecular Systems Biology*, *7*, 539. https://doi.org/10.1038/msb.2011.75

Stenson, P. D., Mort, M., Ball, E. V., Evans, K., Hayden, M., Heywood, S., & Cooper, D. N. (2017). The Human Gene Mutation Database: Towards a comprehensive repository of inherited mutation data for medical research, genetic diagnosis and next-generation sequencing studies. *Human Genetics*, *136*(6), 665–677. https://doi.org/10.1007/s00439-017-1779-6

Stone, E. M., Andorf, J. L., Whitmore, S. S., DeLuca, A. P., Giacalone, J. C., Streb, L. M., Braun, T. A., Mullins, R. F., Scheetz, T. E., Sheffield, V. C., & Tucker, B. A. (2017). Clinically focused molecular investigation of 1000 consecutive families with inherited retinal disease. *Ophthalmology*, *124*(9), 1314–1331. https://doi.org/10.1016/j.ophtha.2017.04.008

Sun, W., Li, S., Xiao, X., Wang, P., & Zhang, Q. (2020). Genotypes and phenotypes of genes associated with achromatopsia: A reference for clinical genetic testing. *Molecular Vision*, *26*, 588–602. https://www.ncbi.nlm.nih.gov/pubmed/32913385

Sun, W., & Zhang, Q. (2019). Diseases associated with mutations in CNGA3: Genotype-phenotype correlation and diagnostic guideline. *Progress in Molecular Biology and Translational Science*, *161*, 1–27. https://doi.org/10.1016/bs.pmbts.2018.10.002

Sundaram, V., Wilde, C., Aboshiha, J., Cowing, J., Han, C., Langlo, C. S., Chana, R., Davidson, A. E., Sergouniotis, P. I., Bainbridge, J. W., Ali, R. R., Dubra, A., Rubin, G., Webster, A. R., Moore, A. T., Nardini, M., Carroll, J., & Michaelides, M. (2014). Retinal structure and function in achromatopsia: Implications for gene therapy. *Ophthalmology*, *121*(1), 234–245. https://doi.org/10.1016/j.ophtha.2013.08.017

Sundin, O. H., Yang, J. M., Li, Y., Zhu, D., Hurd, J. N., Mitchell, T. N., & Maumenee, I. H. (2000). Genetic basis of total colourblindness among the Pingelapese islanders. *Nature Genetics*, *25*(3), 289–293. https://doi.org/10.1038/77162

Täger, J., Kohl, S., Birch, D. G., Wheaton, D. K. H., Wissinger, B., & Reuter, P. (2018). An early nonsense mutation facilitates the expression of a short isoform of CNGA3 by alternative translation initiation. *Experimental Eye Research*, *171*, 48–53. https://doi.org/10.1016/j.exer.2018.02.027

Täger, J., Wissinger, B., Kohl, S., & Reuter, P. (2021). Identification of chemical and pharmacological chaperones for correction of trafficking-deficient mutant cyclic nucleotide-gated A3 channels. *Molecular Pharmacology*, *99*(6), 460–468. https://doi.org/10.1124/molpharm.120.000180

Tanaka, N., Dutrow, E. V., Miyadera, K., Delemotte, L., MacDermaid, C. M., Reinstein, S. L., & Guziewicz, K. E. (2015). Canine CNGA3 gene mutations provide novel insights into human achromatopsia-associated channelopathies and treatment. *PLoS One*, *10*(9), e0138943. https://doi.org/10.1371/journal.pone.0138943

Taylor, R. L., Parry, N. R. A., Barton, S. J., Campbell, C., Delaney, C. M., Ellingford, J. M., Hall, G., Hardcastle, C., Morarji, J., Nichol, E. J., Williams, L. C., Douzgou, S., Clayton-Smith, J., Ramsden, S. C., Sharma, V., Biswas, S., Lloyd, I. C., Ashworth, J. L., Black, G. C., & Sergouniotis, P. I. (2017). Panel-based clinical Genetic Testing in 85 Children with Inherited Retinal disease. *Ophthalmology*, *124*(7), 985–991. https://doi.org/10.1016/j.ophtha.2017.02.005

Tavtigian, S. V., Deffenbaugh, A. M., Yin, L., Judkins, T., Scholl, T., Samollow, P. B., & Thomas, A. (2006). Comprehensive statistical study of 452 BRCA1 missense substitutions with classification of eight recurrent substitutions as neutral. *Journal of Medical Genetics*, *43*(4), 295–305. https://doi.org/10.1136/jmg.2005.033878

Tekavcic Pompe, M., Vrabic, N., Volk, M., Meglic, A., Jarc-Vidmar, M., Peterlin, B., & Fakin, A. (2021). Disease progression in CNGA3 and CNGB3 retinopathy; characteristics of slovenian cohort and proposed OCT staging based on pooled data from 126 patients from 7 studies. *Current Issues in Molecular Biology*, *43*(2), 941–957. https://doi.org/10.3390/cimb43020067

Thiadens, A. A., den Hollander, A. I., Roosing, S., Nabuurs, S. B., Zekveld-Vroon, R. C., Collin, R. W., & Klaver, C. C. (2009). Homozygosity mapping reveals PDE6C mutations in patients with early-onset cone photoreceptor disorders. *American Journal of Human Genetics*, *85*(2), 240–247. https://doi.org/10.1016/j.ajhg.2009.06.016

Thiadens, A. A., Roosing, S., Collin, R. W., van Moll-Ramirez, N., van Lith-Verhoeven, J. J., van Schooneveld, M. J., & Klaver, C. C. (2010). Comprehensive analysis of the achromatopsia genes CNGA3 and CNGB3 in progressive cone dystrophy. *Ophthalmology*, *117*(4), 825–830. https://doi.org/10.1016/j.ophtha.2009.09.008

Thiadens, A. A., Slingerland, N. W., Roosing, S., van Schooneveld, M. J., van Lith-Verhoeven, J. J., van Moll-Ramirez, N., & Klaver, C. C. (2009). Genetic etiology and clinical consequences of complete and incomplete achromatopsia. *Ophthalmology*, *116*(10), 1984–1989. https://doi.org/10.1016/j.ophtha.2009.03.053

Thiadens, A. A., Somervuo, V., van den Born, L. I., Roosing, S., van Schooneveld, M. J., Kuijpers, R. W., & Klaver, C. C. (2010). Progressive loss of cones in achromatopsia: an imaging study using spectral-domain optical coherence tomography. *Investigative Ophthalmology and Visual Science*, *51*(11), 5952–5957. https://doi.org/10.1167/iovs.10-5680

Thomas, M. G., McLean, R. J., Kohl, S., Sheth, V., & Gottlob, I. (2012). Early signs of longitudinal progressive cone photoreceptor degeneration in achromatopsia. *British Journal of Ophthalmology*, *96*(9), 1232–1236. https://doi.org/10.1136/bjophthalmol-2012-301737

Tränkner, D., Jagle, H., Kohl, S., Apfelstedt-Sylla, E., Sharpe, L. T., Kaupp, U. B., & Wissinger, B. (2004). Molecular basis of an inherited form of incomplete achromatopsia. *Journal of Neuroscience*, *24*(1), 138–147. https://doi.org/10.1523/JNEUROSCI.3883-03.2004

Varsányi, B., Wissinger, B., Kohl, S., Koeppen, K., & Farkas, A. (2005). Clinical and genetic features of Hungarian achromatopsia patients. *Molecular Vision*, *11*, 996–1001. https://www.ncbi.nlm.nih.gov/pubmed/16319819

Vihinen, M. (2013). Guidelines for reporting and using prediction tools for genetic variation analysis. *Human Mutation*, *34*(2), 275–282. https://doi.org/10.1002/humu.22253

Vincent, A., Wright, T., Billingsley, G., Westall, C., & Héon, E. (2011). Oligocone trichromacy is part of the spectrum of CNGA3-related cone system disorders. *Ophthalmic Genetics*, *32*(2), 107–113. https://doi.org/10.3109/13816810.2010.544366

10981004, 2022, 7, Downloaded from https://onlinelibrary.wiley.com/doi/10.1002/humu.24371, Wiley Online Library on [09/12/2024]. See the Terms and Conditions (https://onlinelibrary.wiley.com/terms-and-conditions) on Wiley Online Library for rules of use; OA articles are governed by the applicable Creative Commons License

Wang, X., Wang, H., Cao, M., Li, Z., Chen, X., Patenia, C., Gore, A., Abboud, E. B., Al-Rajhi, A. A., Lewis, R., Lupski, J. R., Mardon, G., Zhang, K., Muzny, D., Gibbs, R. A., & Chen, R. (2011). Whole-exome sequencing identifies ALMS1, IQCB1, CNGA3, and MYO7A mutations in patients with Leber congenital amaurosis. *Human Mutation*, *32*(12), 1450–1459. https://doi.org/10.1002/humu.21587

Wang, P., Li, S., Sun, W., Xiao, X., Jia, X., Liu, M., Xu, L., Long, Y., & Zhang, Q. (2019). An ophthalmic targeted exome sequencing panel as a powerful tool to Identify Causative Mutations in Patients Suspected of Hereditary Eye diseases. *Translational Vision Science & Technology*, *8*(2), 21. https://doi.org/10.1167/tvst.8.2.21

Weisschuh, N., Stingl, K., Audo, I., Biskup, S., Bocquet, B., Branham, K., & Kohl, S. (2018). Mutations in the gene PDE6C encoding the catalytic subunit of the cone photoreceptor phosphodiesterase in patients with achromatopsia. *Human Mutation*, *39*(10), 1366–1371. https://doi.org/10.1002/humu.23606

Wissinger, B., Gamer, D., Jagle, H., Giorda, R., Marx, T., Mayer, S., & Kohl, S. (2001). CNGA3 mutations in hereditary cone photoreceptor disorders. *American Journal of Human Genetics*, *69*(4), 722–737. https://doi.org/10.1086/323613

Weisschuh, N., Obermaier, C. D., Battke, F., Bernd, A., Kuehlewein, L., Nasser, F., Zobor, D., Zrenner, E., Weber, E., Wissinger, B., Biskup, S., Stingl, K., & Kohl, S. (2020). Genetic architecture of inherited retinal degeneration in Germany: A large cohort study from a single diagnostic center over a 9-year period. *Human Mutation*, *41*(9), 1514–1527. https://doi.org/10.1002/humu.24064

Wiszniewski, W., Lewis, R. A., & Lupski, J. R. (2007). Achromatopsia: The CNGB3 p.T383fsX mutation results from a founder effect and is responsible for the visual phenotype in the original report of uniparental disomy 14. *Human Genetics*, *121*(3–4), 433–439. https://doi.org/10.1007/s00439-006-0314-y

Xu, M., Gelowani, V., Eblimit, A., Wang, F., Young, M. P., Sawyer, B. L., & Chen, R. (2015). ATF6 is mutated in early onset photoreceptor degeneration with macular involvement. *Investigative Ophthalmology and Visual Science*, *56*(6), 3889–3895. https://doi.org/10.1167/iovs.15-16778

Yang, P., Michaels, K. V., Courtney, R. J., Wen, Y., Greninger, D. A., Reznick, L., Karr, D. J., Wilson, L. B., Weleber, R. G., & Pennesi, M. E. (2014). Retinal morphology of patients with achromatopsia during early childhood: Implications for gene therapy. *JAMA Ophthalmology*, *132*(7), 823–831. https://doi.org/10.1001/jamaophthalmol.2014.685

Yeo, G., & Burge, C. B. (2004). Maximum entropy modeling of short sequence motifs with applications to RNA splicing signals. *Journal of Computational Biology*, *11*(2-3), 377–394. https://doi.org/10.1089/1066527041410418

Zagotta, W. N., & Siegelbaum, S. A. (1996). Structure and function of cyclic nucleotide-gated channels. *Annual Review of Neuroscience*, *19*, 235–263. https://doi.org/10.1146/annurev.ne.19.030196.001315

Zelinger, L., Cideciyan, A. V., Kohl, S., Schwartz, S. B., Rosenmann, A., Eli, D., & Sharon, D. (2015). Genetics and disease expression in the CNGA3 form of achromatopsia: Steps on the path to gene therapy. *Ophthalmology*, *122*(5), 997–1007. https://doi.org/10.1016/j.ophtha.2014.11.025

Zheng, X., Hu, Z., Li, H., & Yang, J. (2022). Structure of the human cone photoreceptor cyclic nucleotide-gated channel. *Nature Structural & Molecular Biology*, *29*(1), 40–46. https://doi.org/10.1038/s41594-021-00699-y

Zhong, H., Molday, L. L., Molday, R. S., & Yau, K. W. (2002). The heteromeric cyclic nucleotide-gated channel adopts a 3A:1B stoichiometry. *Nature*, *420*(6912), 193–198. https://doi.org/10.1038/nature01201

Zobor, D., Werner, A., Stanzial, F., Benedicenti, F., Rudolph, G., Kellner, U., & Consortium, R.-C. (2017). The clinical phenotype of CNGA3-related achromatopsia: pretreatment characterization in preparation of a gene replacement therapy trial. *Investigative Ophthalmology and Visual Science*, *58*(2), 821–832. https://doi.org/10.1167/iovs.16-20427

SUPPORTING INFORMATION

Additional supporting information can be found online in the Supporting Information section at the end of this article.

How to cite this article: Solaki, M., Baumann, B., Reuter, P., Andreasson, S., Audo, I., Ayuso, C., Balousha, G., Benedicenti, F., Birch, D., Bitoun, P., Blain, D., Bocquet, B., Branham, K., Català-Mora, J., De Baere, E., Dollfus, H., Falana, M., Giorda, R., Golovleva, I., … Kohl, S. (2022). Comprehensive variant spectrum of the *CNGA3* gene in patients affected by achromatopsia. *Human Mutation*, 43, 832–858. https://doi.org/10.1002/humu.24371

10981004, 2022, 7, Downloaded from https://onlinelibrary.wiley.com/doi/10.1002/humu.24371, Wiley Online Library on [09/12/2024]. See the Terms and Conditions (https://onlinelibrary.wiley.com/terms-and-conditions) on Wiley Online Library for rules of use; OA articles are governed by the applicable Creative Commons License

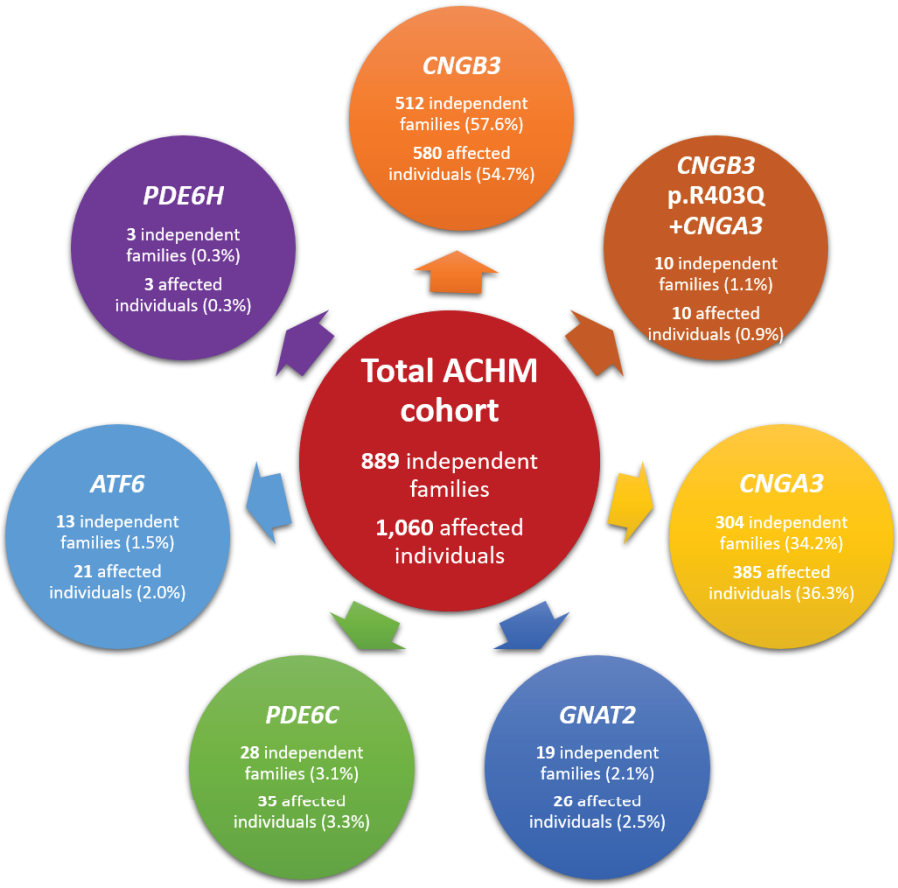
Supplementary material

Solaki et al.

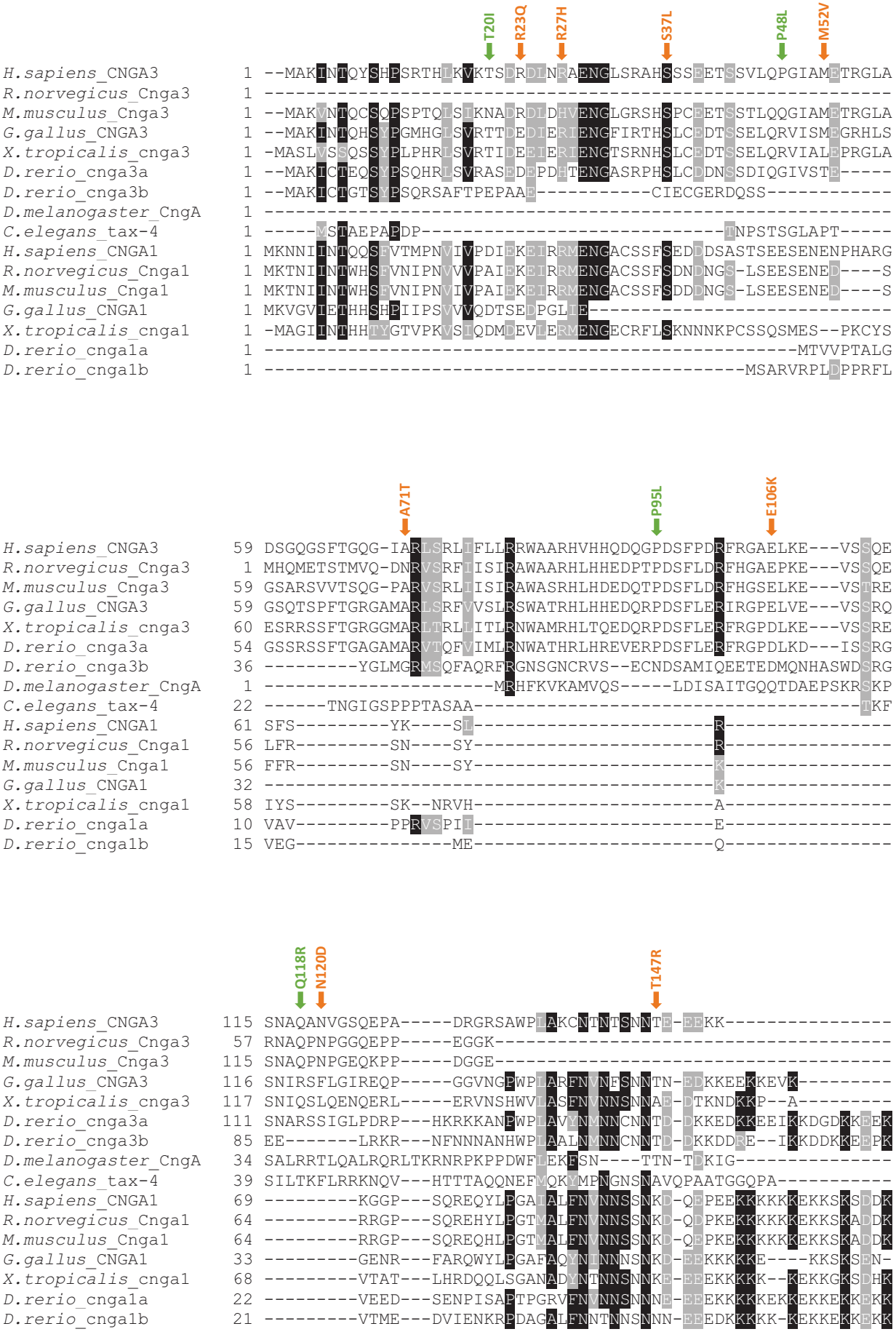
Comprehensive variant spectrum of the *CNGA3* gene in patients affected by achromatopsia

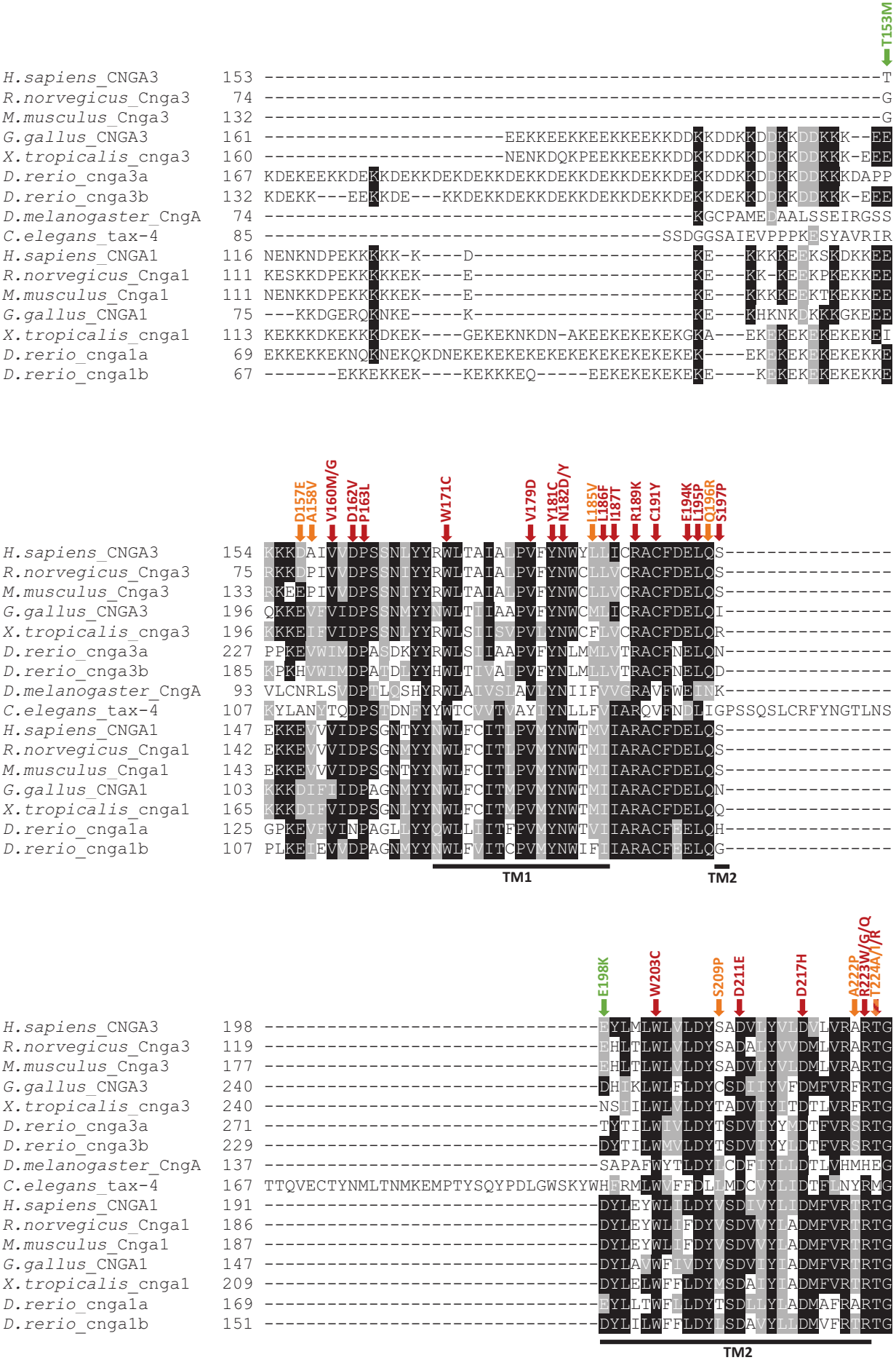
Supplementary material includes three figures, two tables and references.

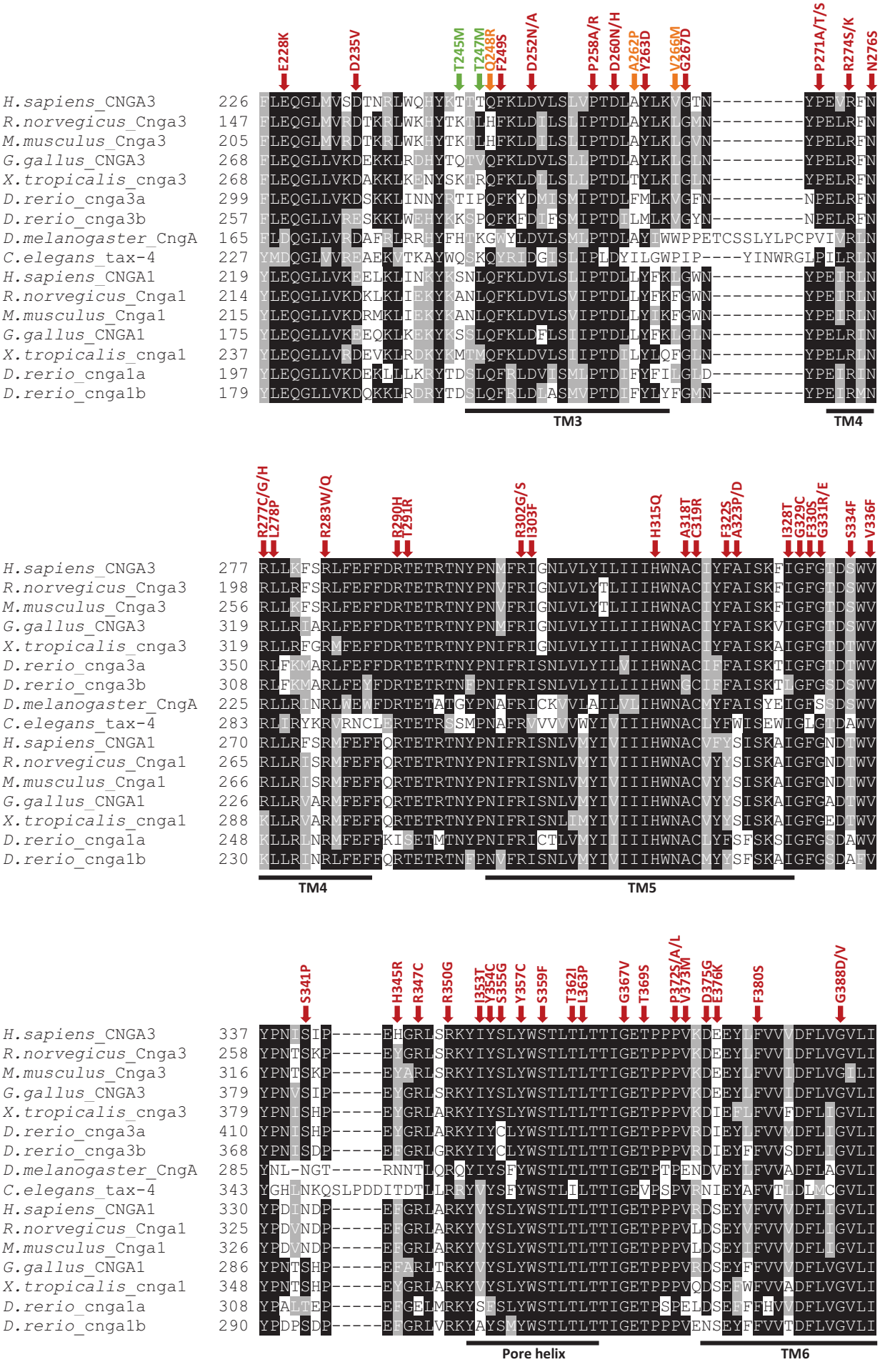
Figures

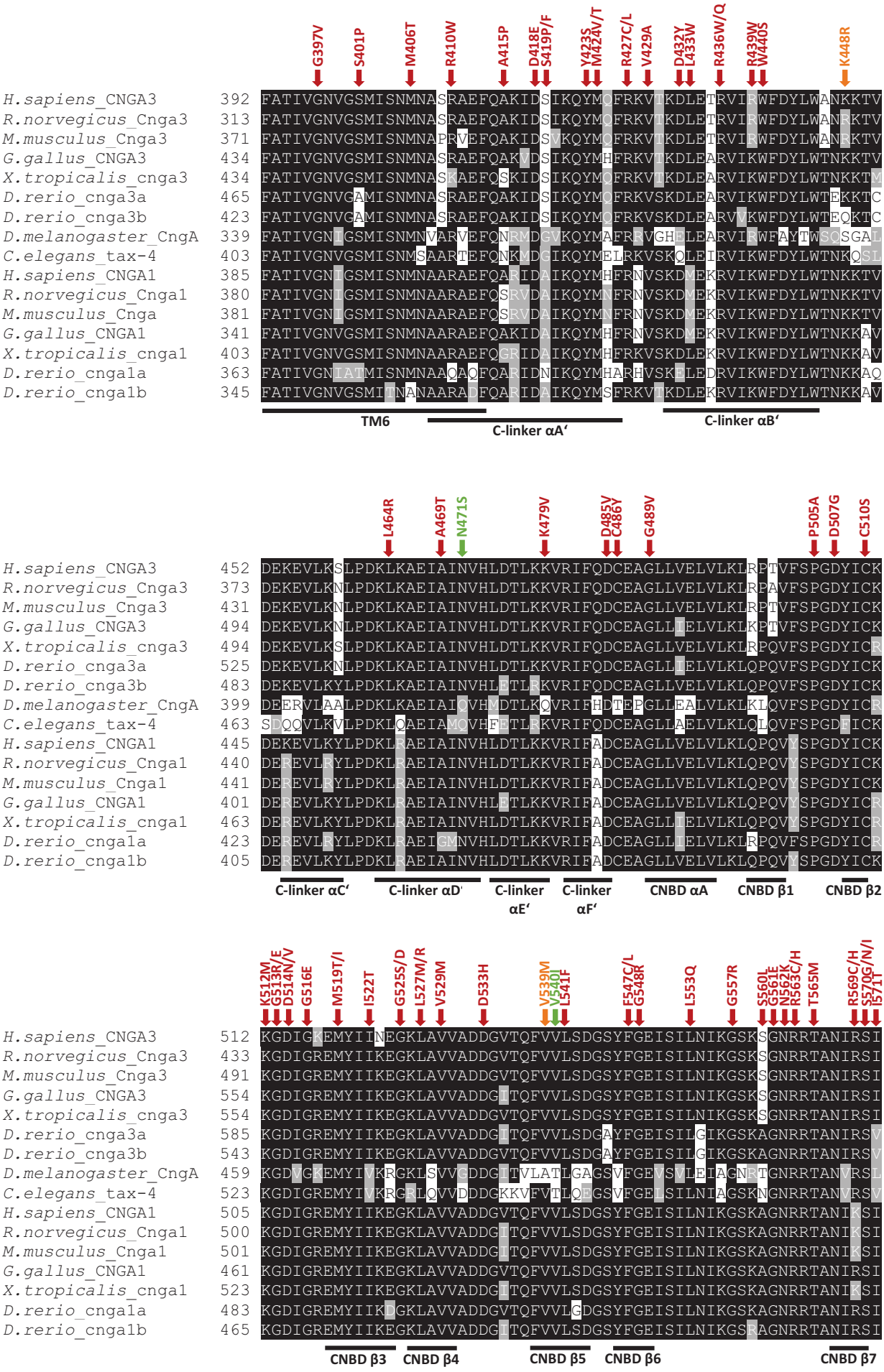


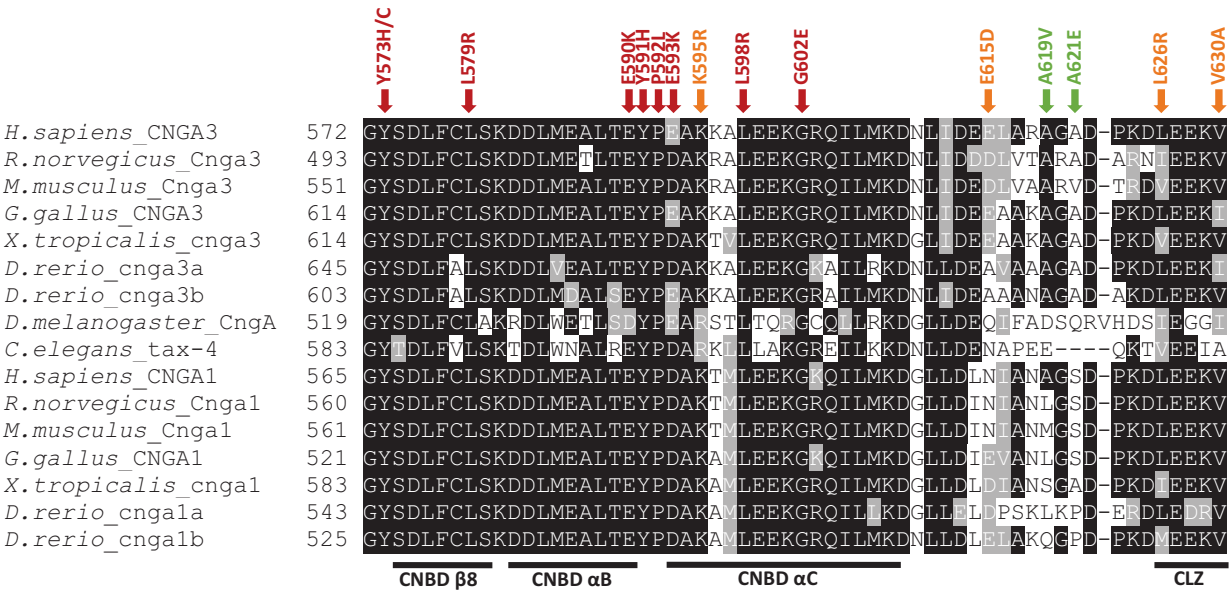
Supp. Figure S1: Overview of the total ACHM study cohort genetically characterized in Tübingen, and subdivision into numbers of genetically solved independent families and affected individuals regarding the causative genes associated with ACHM. The total Tübingen ACHM cohort comprises 1,060 genetically solved affected individuals of 889 independent families. Disease-associated variants in the *CNGA3* gene were observed in 385 patients descending from 304 distinct families. Genetic analysis revealed an additional heterozygous mutant *CNGA3* allele in 10 affected individuals who were homozygous or (compound-)heterozygous for the c.1208G>A/p.(Arg403Gln) variant in *CNGB3*.

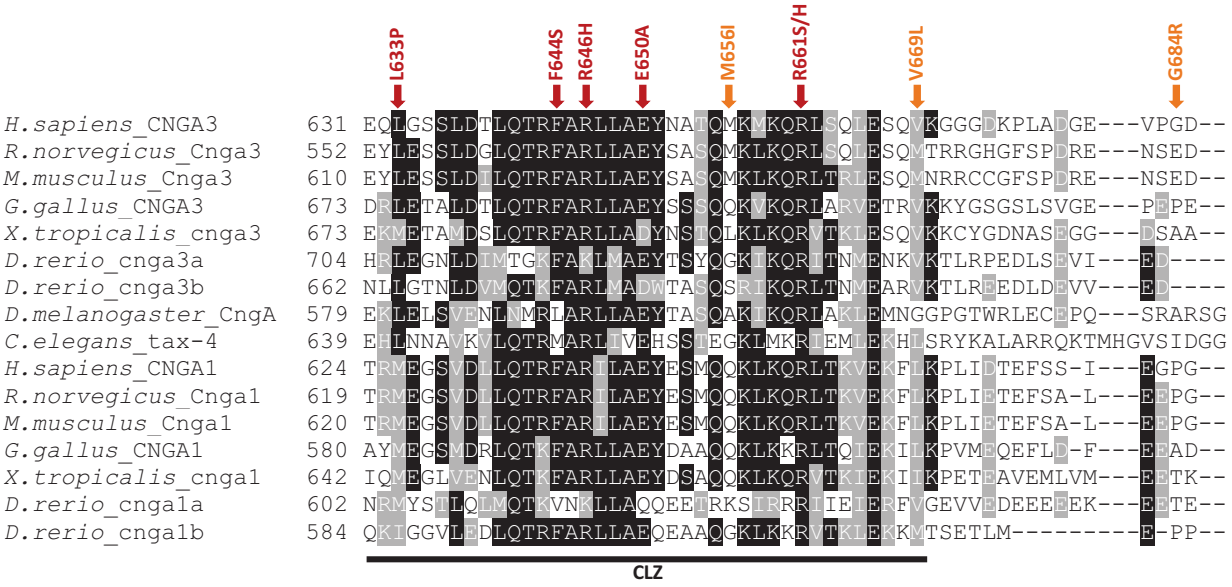

T20I
R23Q
R27H
S37L
P48L
M52V
A71T
P95L
E106K
Q118R
N120D
T147R
H.sapiens_CNGA3
R.norvegicus_Cnga3
M.musculus_Cnga3
G.gallus_CNGA3
X.tropicalis_cnga3
D.rerio_cnga3a
D.rerio_cnga3b
D.melanogaster_CngA
C.elegans_tax-4
H.sapiens_CNGA1
R.norvegicus_Cnga1
M.musculus_Cnga1
G.gallus_CNGA1
X.tropicalis_cnga1
D.rerio_cnga1a
D.rerio_cnga1b

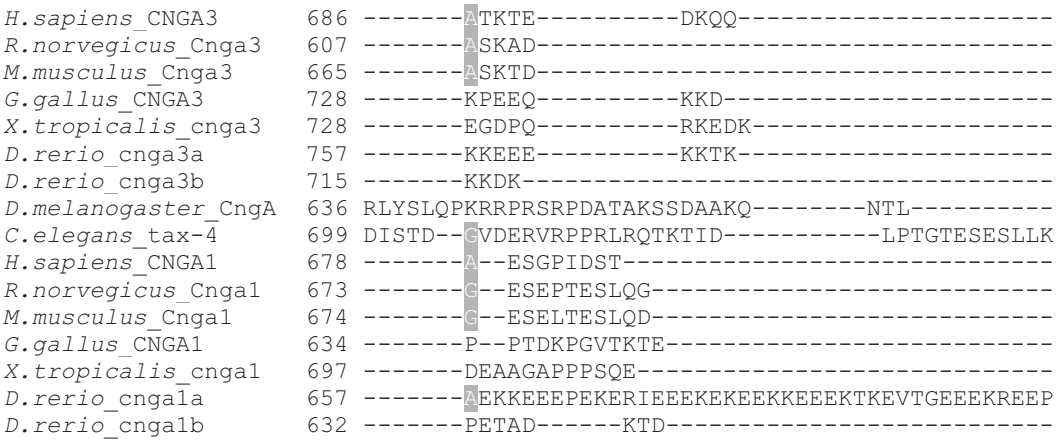

T153M
H.sapiens_CNGA3 153
R.norvegicus_Cnga3 74
M.musculus_Cnga3 132
G.gallus_CNGA3 161
X.tropicalis_cnga3 160
D.rerio_cnga3a 167
D.rerio_cnga3b 132
D.melanogaster_CngA 74
C.elegans_tax-4 85
H.sapiens_CNGA1 116
R.norvegicus_Cnga1 111
M.musculus_Cnga1 111
G.gallus_CNGA1 75
X.tropicalis_cnga1 113
D.rerio_cnga1a 69
D.rerio_cnga1b 67
D157E
A158V
V160M/G
D162V
P163L
W171C
V179D
Y181C
N182D/Y
L185V
L186F
I187T
R189K
C191Y
E194K
L195P
Q196R
S197P
H.sapiens_CNGA3 154
R.norvegicus_Cnga3 75
M.musculus_Cnga3 133
G.gallus_CNGA3 196
X.tropicalis_cnga3 196
D.rerio_cnga3a 227
D.rerio_cnga3b 185
D.melanogaster_CngA 93
C.elegans_tax-4 107
H.sapiens_CNGA1 147
R.norvegicus_Cnga1 142
M.musculus_Cnga1 143
G.gallus_CNGA1 103
X.tropicalis_cnga1 165
D.rerio_cnga1a 125
D.rerio_cnga1b 107
TM1
TM2
E198K
W203C
S209P
D211E
D217H
A222P
R223W/G/Q
T224A/I/R
H.sapiens_CNGA3 198
R.norvegicus_Cnga3 119
M.musculus_Cnga3 177
G.gallus_CNGA3 240
X.tropicalis_cnga3 240
D.rerio_cnga3a 271
D.rerio_cnga3b 229
D.melanogaster_CngA 137
C.elegans_tax-4 167
H.sapiens_CNGA1 191
R.norvegicus_Cnga1 186
M.musculus_Cnga1 187
G.gallus_CNGA1 147
X.tropicalis_cnga1 209
D.rerio_cnga1a 169
D.rerio_cnga1b 151
TM2


E228K
D235V
T245M
T247M
Q248R
F249S
D252N/A
P258A/R
D260N/H
A262P
Y263D
V266M
G267D
P271A/T/S
R274S/K
N276S
H.sapiens_CNGA3 226 FLEQGLMVSDTNRLWQHYKTTTQFKLDVLSLVPTDLAYLKVGTN---------YPEVRFN
R.norvegicus_Cnga3 147 FLEQGLMVRDTKRLWKHYTKILHFKLDILSLIPTDLAYLKLGVN---------YPELRFN
M.musculus_Cnga3 205 FLEQGLMVRDTKRLWKHYTKILHFKLDILSLIPTDLAYLKLGVN---------YPELRFN
G.gallus_CNGA3 268 FLEQGLLVKDEKKLRDHYTQTVQFKLDVLSLLPTDLAYLKLGLN---------YPELRFN
X.tropicalis_cnga3 268 FLEQGLLVKDAKKLKENYSKIRQFKLDLLSLLPTDLTYLKLGLN---------YPELRFN
D.rerio_cnga3a 299 FLEQGLLVKDSKKLINNYRTIPQFKYDMISMIPTDLFMLKVGFN---------NPELRFN
D.rerio_cnga3b 257 FLEQGLLVRESKKLWEHYKKSPQFKFDIFSMIPTDILMLKVGYN---------NPELRFN
D.melanogaster_CngA 165 FLLQGLLVRDAFRLRRHYFHIKGWYLDVLSMLPTDLAYIWWPPETCSSLYLPCPVIVRLN
C.elegans_tax-4 227 YMDQGLVVREAEKVTKAYWQSKQYRIDGISLIPLDYILGWPIP----YINWRGLPILRLN
H.sapiens_CNGA1 219 YLEQGLLVKEELKLINKYKSNLQFKLDVLSLIPTDLLYFKLGWN---------YPEIRLN
R.norvegicus_Cnga1 214 YLEQGLLVKDKLKLIEKYKANLQFKLDVLSVIPTDLLYFKFGWN---------YPEIRLN
M.musculus_Cnga1 215 YLEQGLLVKDRMKLIEKYKANLQFKLDVLSVIPTDLLYIKFGWN---------YPEIRLN
G.gallus_CNGA1 175 YLEQGLLVKEEQKLKEKYKSSLQFKLDFLSIIPTDLLYFKLGLN---------YPELRIN
X.tropicalis_cnga1 237 YLEQGLLVRDEVKLRDKYKMTMQFKLDVLSIIPTDILYLQFGLN---------YPELRLN
D.rerio_cnga1a 197 YLEQGLLVKDEKLLLKRYTDSLQFRLDVISMLPTDIFYFILGLD---------YPEIRIN
D.rerio_cnga1b 179 YLEQGLLVKDQKKLRDRYTDSLQFRLDLASMVPTDIFYLYFGMN---------YPEIRMN
TM3
TM4
R277C/G/H
L278P
R283W/Q
R290H
T291R
R302G/S
I303F
H315Q
A318T
C319R
F322S
A323P/D
I328T
G329C
F330S
G331R/E
S334F
V336F
H.sapiens_CNGA3 277 RLLKFSRLFEFFDRTETRTNYPNMFRIGNLVLYILIIIHWNACIYFAISKFIGFGTDSWV
R.norvegicus_Cnga3 198 RLLRFSRLFEFFDRTETRTNYPNVFRIGNLVLYTLIIIHWNACIYFAISKFIGFGTDSWV
M.musculus_Cnga3 256 RLLKFSRLFEFFDRTETRTNYPNVFRIGNLVLYTLIIIHWNACIYFAISKFIGFGTDSWV
G.gallus_CNGA3 319 RLLRIARLFEFFDRTETRTNYPNMFRIGNLVLYILIIIHWNACIYFAISKVIGFGTDSWV
X.tropicalis_cnga3 319 RLLRFGRMFEFFDRTETRTNYPNIFRIGNLVLYILIIIHWNACIYFAISKAIGFGTDTWV
D.rerio_cnga3a 350 RLFKMARLFEFFDRTETRTNYPNIFRISNLVLYILVIIHWNACIFFAISKTIGFGTDTWV
D.rerio_cnga3b 308 RLFKMARLFEYFDRTETRTNFPNIFRISNLVLYILIIIHWNGCIFFAISKTLGFGSDSWV
D.melanogaster_CngA 225 RLLRINRLWEWFDRTETATGYPNAFRICKVVLAILVLIHWNACMYFAISYEIGFSSDSWV
C.elegans_tax-4 283 RLIRYKRVRNCLERTETRSSMPNAFRVVVVVWYIVIIIHWNACIYFWISEWIGLGIDAWV
H.sapiens_CNGA1 270 RLLRFSRMFEFFQRTETRTNYPNIFRISNLVMYIVIIIHWNACVFYSISKAIGFGNDTWV
R.norvegicus_Cnga1 265 RLLRISRMFEFFQRTETRTNYPNIFRISNLVMYIVIIIHWNACVYYSISKAIGFGNDTWV
M.musculus_Cnga1 266 RLLRISRMFEFFQRTETRTNYPNIFRISNLVMYIVIIIHWNACVYYSISKAIGFGNDTWV
G.gallus_CNGA1 226 RLLRVARMFEFFQRTETRTNYPNIFRISNLVMYIVIIIHWNACVYYSISKAIGFGADTWV
X.tropicalis_cnga1 288 KLLRVARMFEFFQRTETRTNYPNIFRISNLIMYIVIIIHWNACVYYSISKAIGFGEDTWV
D.rerio_cnga1a 248 KLLRINRMFEFFKISETMTNYPNIFRICTLVMYIIIIIHWNACLYFSFSKSIGFGSDAWV
D.rerio_cnga1b 230 KLLRINRLFEFFQRTETRTNFPNVFRISNLVMYIVIIIHWNACMYYSFSKAIGFGSDAFV
TM4
TM5
S341P
H345R
R347C
R350G
I353T
Y354C
S355G
Y357C
S359F
T362I
L363P
G367V
T369S
P372S/A/L
V373M
D375G
E376K
F380S
G388D/V
H.sapiens_CNGA3 337 YPNISIP-----EHGRLSRKYIYSLYWSTLTLTTIGETPPPVKDEEYLFVVVDFLVGVLI
R.norvegicus_Cnga3 258 YPNTSKP-----EYGRLSRKYIYSLYWSTLTLTTIGETPPPVKDEEYLFVVIDFLVGVLI
M.musculus_Cnga3 316 YPNTSKP-----EYARLSRKYIYSLYWSTLTLTTIGETPPPVKDEEYLFVVIDFLVGILI
G.gallus_CNGA3 379 YPNVSIP-----EYGRLSRKYIYSLYWSTLTLTTIGETPPPVKDEEYLFVVIDFLVGVLI
X.tropicalis_cnga3 379 YPNISHP-----EYGRLARKYIYSLYWSTLTLTTIGETPPPVKDIEFLFVVFDFLIGVLI
D.rerio_cnga3a 410 YPNISHP-----EYGRLARKYIYCLYWSTLTLTTIGETPPPVRDIEYLFVVMDFLIGVLI
D.rerio_cnga3b 368 YPNISDP-----EFGRLGRKYIYCLYWSTLTLTTIGETPPPVRDIEYFFVVSDFLIGVLI
D.melanogaster_CngA 285 YNL-NGT-----RNNTLQRQYIYSFYWSTLTLTTIGETPTPENDVEYLFVVADFLAGVLI
C.elegans_tax-4 343 YGHLNKQSLPDDITDTLLRRYVYSFYWSTLILTTIGEVPSPVRNIEYAFVTLDLMCGVLI
H.sapiens_CNGA1 330 YPDINDP-----EFGRLARKYVYSLYWSTLTLTTIGETPPPVRDSEYVFVVVDFLIGVLI
R.norvegicus_Cnga1 325 YPDVNDP-----EFGRLARKYVYSLYWSTLTLTTIGETPPPVLDSEYVFVVVDFLIGVLI
M.musculus_Cnga1 326 YPDVNDP-----EFGRLARKYVYSLYWSTLTLTTIGETPPPVLDSEYIFVVVDFLIGVLI
G.gallus_CNGA1 286 YPNTSHP-----EFARLTRKYVYSLYWSTLTLTTIGETPPPVRDSEYFFVVVDFLVGVLI
X.tropicalis_cnga1 348 YPNTSHP-----EYGRLARKYVYSLYWSTLTLTTIGETPPPVQDSEFWFVVADFLVGVLI
D.rerio_cnga1a 308 YPALTEP-----EFGELMRKYSFSLYWSTLTLTTIGETPSPELDSEFFFHVVDFLVGVLI
D.rerio_cnga1b 290 YPDPSDP-----EFGRLVRKYAYSMYWSTLTLTTIGETPPPVENSEYFFVVTDFLVGVLI
Pore helix
TM6


G397V
S401P
M406T
R410W
A415P
D418E
S419P/F
Y423S
M424V/T
R427C/L
V429A
D432Y
L433W
R436W/Q
R439W
W440S
K448R
H.sapiens_CNGA3 392 FATIVGNVGSMISNMNASRAEFQAKIDSIKQYMQFRKVTKDLETRVIRWFDYLWANKKTV
R.norvegicus_Cnga3 313 FATIVGNVGSMISNMNASRAEFQAKIDSIKQYMQFRKVTKDLETRVIRWFDYLWANRKTV
M.musculus_Cnga3 371 FATIVGNVGSMISNMNAPRVEFQAKIDSVKQYMQFRKVTKDLETRVIRWFDYLWANRKTV
G.gallus_CNGA3 434 FATIVGNVGSMISNMNASRAEFQAKVDSIKQYMHFRKVTKDLEARVIKWFDYLWTNKKTV
X.tropicalis_cnga3 434 FATIVGNVGSMISNMNASKAEFQSKIDSIKQYMQFRKVTKDLEARVIKWFDYLWTNKKTM
D.rerio_cnga3a 465 FATIVGNVGAMISNMNASRAEFQAKIDSIKQYMQFRKVSKDLEARVIKWFDYLWTEKKTC
D.rerio_cnga3b 423 FATIVGNVGAMISNMNASRAEFQAKIDSIKQYMQFRKVSKDLEARVVKWFDYLWTEQKTC
D.melanogaster_CngA 339 FATIVGNIGSMISNMNVARVEFQNRMDGVKQYMAFRRVGHELEARVIRWFAYTWSQSGAL
C.elegans_tax-4 403 FATIVGNVGSMISNMSAARTEFQNKMDGIKQYMELRKVSKQLEIRVIKWFDYLWTNKQSL
H.sapiens_CNGA1 385 FATIVGNIGSMISNMNAARAEFQARIDAIKQYMHFRNVSKDMEKRVIKWFDYLWTNKKTV
R.norvegicus_Cnga1 380 FATIVGNIGSMISNMNAARAEFQSRVDAIKQYMNFRNVSKDMEKRVIKWFDYLWTNKKTV
M.musculus_Cnga 381 FATIVGNIGSMISNMNAARAEFQSRVDAIKQYMNFRNVSKDMEKRVIKWFDYLWTNKKTV
G.gallus_CNGA1 341 FATIVGNVGSMISNMNAARAEFQAKIDAIKQYMHFRNVSKDMEKRVIKWFDYLWTNKKAV
X.tropicalis_cnga1 403 FATIVGNVGSMISNMNAARAEFQGRIDAIKQYMHFRKVSKDLEKRVIKWFDYLWTNKKAV
D.rerio_cnga1a 363 FATIVGNIATMISNMNAAQAQFQARIDNIKQYMHARHVSKELEDRVIKWFDYLWTNKKAQ
D.rerio_cnga1b 345 FATIVGNVGSMITNANAARADFQARIDAIKQYMSFRKVTKDLEKRVIKWFDYLWTNKKAV
TM6
C-linker αA'
C-linker αB'
L464R
A469T
N471S
K479V
D485V
C486Y
G489V
P505A
D507G
C510S
H.sapiens_CNGA3 452 DEKEVLKSLPDKLKAEIAINVHLDTLKKVRIFQDCEAGLLVELVLKLRPTVFSPGDYICK
R.norvegicus_Cnga3 373 DEKEVLKNLPDKLKAEIAINVHLDTLKKVRIFQDCEAGLLVELVLKLRPAVFSPGDYICK
M.musculus_Cnga3 431 DEKEVLKNLPDKLKAEIAINVHLDTLKKVRIFQDCEAGLLVELVLKLRPTVFSPGDYICK
G.gallus_CNGA3 494 DEKEVLKNLPDKLKAEIAINVHLDTLKKVRIFQDCEAGLLIELVLKLKPTVFSPGDYICK
X.tropicalis_cnga3 494 DEKEVLKSLPDKLKAEIAINVHLDTLKKVRIFQDCEAGLLVELVLKLRPQVFSPGDYICR
D.rerio_cnga3a 525 DEKEVLKNLPDKLKAEIAINVHLDTLKKVRIFQDCEAGLLIELVLKLQPQVFSPGDYICK
D.rerio_cnga3b 483 DEKEVLKYLPDKLKAEIAINVHLETLRKVRIFQDCEAGLLVELVLKLQPQVFSPGDYICK
D.melanogaster_CngA 399 DEERVLAALPDKLKAEIAIQVHMDTLKQVRIFHDTEPGLLEALVLKLKLQVFSPGDYICR
C.elegans_tax-4 463 SDQQVLKVLPDKLQAEIAMQVHFETLRKVRIFQDCEAGLLAELVLKLQLQVFSPGDFICK
H.sapiens_CNGA1 445 DEKEVLKYLPDKLRAEIAINVHLDTLKKVRIFADCEAGLLVELVLKLQPQVYSPGDYICK
R.norvegicus_Cnga1 440 DEREVLRYLPDKLRAEIAINVHLDTLKKVRIFADCEAGLLVELVLKLQPQVYSPGDYICK
M.musculus_Cnga1 441 DEREVLRYLPDKLRAEIAINVHLDTLKKVRIFADCEAGLLVELVLKLQPQVYSPGDYICK
G.gallus_CNGA1 401 DEREVLKYLPDKLRAEIAINVHLETLKKVRIFADCEAGLLVELVLKLQPQVYSPGDYICR
X.tropicalis_cnga1 463 DEREVLKYLPDKLRAEIAINVHLDTLKKVRIFADCEAGLLIELVLKLQPQVYSPGDYICR
D.rerio_cnga1a 423 DEREVLRYLPDKLRAEIGMNVHLDTLKKVRIFADCEAGLLIELVLKLRPQVFSPGDYICR
D.rerio_cnga1b 405 DEREVLKYLPDKLRAEIAINVHLDTLKKVRIFADCEAGLLVELVLKLQPQVYSPGDYICK
C-linker αC'
C-linker αD'
C-linker αE'
C-linker αF'
CNBD αA
CNBD β1
CNBD β2
K512M
G513R/E
D514N/V
G516E
M519T/I
I522T
G525S/D
L527M/R
V529M
D533H
V539M
V540I
L541F
F547C/L
G548R
L553Q
G557R
S560L
G561E
N562K
R563C/H
T565M
R569C/H
S570G/N/I
I571T
H.sapiens_CNGA3 512 KGDIGKEMYIINEGKLAVVADDGVTQFVVLSDGSYFGEISILNIKGSKSGNRRTANIRSI
R.norvegicus_Cnga3 433 KGDIGREMYIIKEGKLAVVADDGVTQFVVLSDGSYFGEISILNIKGSKSGNRRTANIRSI
M.musculus_Cnga3 491 KGDIGREMYIIKEGKLAVVADDGVTQFVVLSDGSYFGEISILNIKGSKSGNRRTANIRSI
G.gallus_CNGA3 554 KGDIGREMYIIKEGKLAVVADDGITQFVVLSDGSYFGEISILNIKGSKSGNRRTANIRSI
X.tropicalis_cnga3 554 KGDIGREMYIIKEGKLAVVADDGVTQFVVLSDGSYFGEISILNIKGSKSGNRRTANIRSI
D.rerio_cnga3a 585 KGDIGREMYIIKEGKLAVVADDGITQFVVLSDGAYFGEISILGIKGSKAGNRRTANIRSV
D.rerio_cnga3b 543 KGDIGREMYIIKEGKLAVVADDGVTQFVVLSDGAYFGEISILGIKGSKAGNRRTANIRSV
D.melanogaster_CngA 459 KGDVGKEMYIVKRGKLSVVGDDGITVLATLGAGSVFGEVSVLEIAGNRTGNRRTANVRSL
C.elegans_tax-4 523 KGDIGREMYIVKRGRLQVVDDDGKKVFVTLQEGSVFGELSILNIAGSKNGNRRTANVRSV
H.sapiens_CNGA1 505 KGDIGREMYIIKEGKLAVVADDGVTQFVVLSDGSYFGEISILNIKGSKAGNRRTANIKSI
R.norvegicus_Cnga1 500 KGDIGREMYIIKEGKLAVVADDGITQFVVLSDGSYFGEISILNIKGSKAGNRRTANIKSI
M.musculus_Cnga1 501 KGDIGREMYIIKEGKLAVVADDGITQFVVLSDGSYFGEISILNIKGSKAGNRRTANIKSI
G.gallus_CNGA1 461 KGDIGREMYIIKEGKLAVVADDGVTQFVVLSDGSYFGEISILNIKGSKAGNRRTANIRSI
X.tropicalis_cnga1 523 KGDIGREMYIIKEGKLAVVADDGITQFVVLSDGSYFGEISILNIKGSKAGNRRTANIKSI
D.rerio_cnga1a 483 KGDIGREMYIIKDGKLAVVADDGVTQFVVLGDGSYFGEISILNIKGSKAGNRRTANIRSI
D.rerio_cnga1b 465 KGDIGREMYIIKEGKLAVVADDGITQFVVLSDGSYFGEISILNIKGSRAGNRRTANIRSI
CNBD β3
CNBD β4
CNBD β5
CNBD β6
CNBD β7


Y573H/C
L579R
E590K
Y591H
P592L
E593K
K595R
L598R
G602E
E615D
A619V
A621E
L626R
V630A
H.sapiens_CNGA3 572 GYSDLFCLSKDDLMEALTEYPEAKKALEEKGRQILMKDNLIDEELARAGAD-PKDLEEKV
R.norvegicus_Cnga3 493 GYSDLFCLSKDDLMETLTEYPDAKRALEEKGRQILMKDNLIDDDLVTARAD-ARNIEEKV
M.musculus_Cnga3 551 GYSDLFCLSKDDLMEALTEYPDAKRALEEKGRQILMKDNLIDEDLVAARVD-TRDVEEKV
G.gallus_CNGA3 614 GYSDLFCLSKDDLMEALTEYPEAKKALEEKGRQILMKDNLIDEEAAKAGAD-PKDLEEKI
X.tropicalis_cnga3 614 GYSDLFCLSKDDLMEALTEYPDAKTVLEEKGRQILMKDGLIDEEAAKAGAD-PKDVEEKV
D.rerio_cnga3a 645 GYSDLFALSKDDLVEALTEYPDAKKALEEKGKAILRKDNLLDEAVAAAGAD-PKDLEEKI
D.rerio_cnga3b 603 GYSDLFALSKDDLMDALSEYPEAKKALEEKGRAILMKDNLIDEAAANAGAD-AKDLEEKV
D.melanogaster_CngA 519 GYSDLFCLAKRDLWETLSDYPEARSTLTQRGCQLLRKDGLLDEQIFADSQRVHDSIEGGI
C.elegans_tax-4 583 GYTDLFVLSKTDLWNALREYPDARKLLLAKGREILKKDNLLDENAPEE-----QKTVEEIA
H.sapiens_CNGA1 565 GYSDLFCLSKDDLMEALTEYPDAKTMLEEKGKQILMKDGLLDLNIANAGSD-PKDLEEKV
R.norvegicus_Cnga1 560 GYSDLFCLSKDDLMEALTEYPDAKTMLEEKGRQILMKDGLLDINIANLGSD-PKDLEEKV
M.musculus_Cnga1 561 GYSDLFCLSKDDLMEALTEYPDAKTMLEEKGRQILMKDGLLDINIANMGSD-PKDLEEKV
G.gallus_CNGA1 521 GYSDLFCLSKDDLMEALTEYPDAKAMLEEKGKQILMKDGLLDIEVANLGSD-PKDLEEKV
X.tropicalis_cnga1 583 GYSDLFCLSKDDLMEALTEYPDAKAMLEEKGRQILMKDGLLDLDIANSGAD-PKDTEEKV
D.rerio_cnga1a 543 GYSDLFCLSKDDLMEALTEYPDAKAMLEEKGRQILIKDGLLELDPSKLKPD-ERDLEDRV
D.rerio_cnga1b 525 GYSDLFCLSKDDLMEALTEYPDAKAMLEEKGRQILMKDNLLDLEIAKQGPD-PKDVEEKV
CNBD β8
CNBD αB
CNBD αC
CLZ


L633P
F644S
R646H
E650A
M656I
R661S/H
V669L
G684R
H.sapiens_CNGA3 631 EQLGSSLDTLQTRFARLLAEYNATQMKMKQRLSQLESQVKGGGDKPLADGE---VPGD--
R.norvegicus_Cnga3 552 EYLESSLDGLQTRFARLLAEYSASQMKLKQRLSQLESQMTRRGHGFSPDRE---NSED--
M.musculus_Cnga3 610 EYLESSLDILQTRFARLLAEYSASQMKLKQRLTRLESQMNRRCCGFSPDRE---NSED--
G.gallus_CNGA3 673 DRLETALDTLQTRFARLLAEYSSSQQKVKQRLARVETRVKKYGSGSLSVGE---PEPE--
X.tropicalis_cnga3 673 EKMETAMDSLQTRFARLLADYNSTQLKLKQRVTKLESQVKKCYGDNASEGG---DSAA--
D.rerio_cnga3a 704 HRLEGNLDIMTGKFAKLMAEYTSYQGKIKQRITNMENKVKTLRPEDLSEVI---ED----
D.rerio_cnga3b 662 NILGTNLDVMQTKFARLMADWTASQSRIKQRLTNMEARVKTLREEDLDEVV---ED----
D.melanogaster_CngA 579 EKLELSVENLNMRLARLLAEYTASQAKIKQRLAKLEMNGGPGTWRLECEPQ---SRARSG
C.elegans_tax-4 639 EHLNNAVKVLQTRMARLIVEHSSTEGKLMKRIEMLEKHLSRYKALARRQKTMHGVSIDGG
H.sapiens_CNGA1 624 TRMEGSVDLLQTRFARLLAEYESMQQKLKQRLTKVEKFLKPLIDTEFSS-I---EGPG--
R.norvegicus_Cnga1 619 TRMEGSVDLLQTRFARLLAEYESMQQKLKQRLTKVEKFLKPLIETEFSA-L---EEPG--
M.musculus_Cnga1 620 TRMEGSVDLLQTRFARLLAEYESMQQKLKQRLTKVEKFLKPLIETEFSA-L---EEPG--
G.gallus_CNGA1 580 AYMEGSMDRLQTKFARLLAEYDAAQQKLKKRLTQIEKILKPVMEQEFLD-F---EEAD--
X.tropicalis_cnga1 642 IQMEGLVENLQTKFARLLAEYDSAQQKLKQRVTKIEKIIKPETEAVEMLVM---EETK--
D.rerio_cnga1a 602 NRMYSILQLMQTKVNKLLAQQEETRKSIRRRIIEIERFVGEVVEDEEEEEK---EETE--
D.rerio_cnga1b 584 QKIGGVLEDLQTRFARLLAEQEAAQGKLKKRVTKLEKKMTSETLM---------E-PP--
CLZ


H.sapiens_CNGA3 686 -------ATKTE----------DKQQ----------
R.norvegicus_Cnga3 607 -------ASKAD----------
M.musculus_Cnga3 665 -------ASKTD----------
G.gallus_CNGA3 728 -------KPEEQ----------KKD----------
X.tropicalis_cnga3 728 -------EGDPQ----------RKEDK----------
D.rerio_cnga3a 757 -------KKEEE----------KKTK----------
D.rerio_cnga3b 715 -------KKDK----------
D.melanogaster_CngA 636 RLYSLQPKRRPRSRPDATAKSSDAAKQ--------NTL----------
C.elegans_tax-4 699 DISTD--CVDERVRPPRLRQTKTID----------LPTGTESESLLK
H.sapiens_CNGA1 678 -------A--ESGPIDST----------
R.norvegicus_Cnga1 673 -------G--ESEPTESLQG----------
M.musculus_Cnga1 674 -------G--ESELTESLQD----------
G.gallus_CNGA1 634 -------P--PTDKPGVTKTE----------
X.tropicalis_cnga1 697 -------DEAAGAPPPSQE----------
D.rerio_cnga1a 657 -------AEKKEEEPEKERIEEEKEKEEKKEEEKTKEVTGEEEKREEP
D.rerio_cnga1b 632 -------PETAD------KTD----------

Supp. Figure S2: Conservation of CNGA3 and CNGA1 orthologues across various species and location of the 204 missense variants identified in the ACHM study cohort genetically characterized in Tübingen, in mutation databases and in the literature summarized in our *CNGA3* variant database (see Supp. Table S3). Protein sequence alignment of *Homo sapiens* CNGA3 and its orthologues from seven other species, the *Homo sapiens* CNGA1 protein and its orthologues from additional five species was established using Clustal Omega (https://www.ebi.ac.uk/Tools/msa/clustalo/) and BoxShade (https://embnet.vital-it.ch/software/BOX_form.html). The mutated amino acid residues are indicated by an arrow and the amino acid substitution is given above the variant amino acid residue. Red arrows indicate residues affected by amino acid substitutions which were classified as "likely disease-causing", orange arrows indicate residues affected by amino acid substitutions which were classified as "variants of uncertain significance", and green arrows denote residues affected by amino acid substitutions which were classified as "likely benign". Functional domains of the human CNGA3 subunit according to Gofman et al., 2014 and Shuart et al., 2011 are highlighted by black bars below the alignment. Reference sequences were taken from NCBI or Ensembl and are as follows: CNGA3: *H. sapiens* NP_001289.1, *R. norvegicus* NP_445947.1, *M. musculus* NP_001268939.1, *G. gallus* NP_990552.1, *X. tropicalis* XP_031752880.1, *D. rerio* (cnga3a) XP_005166141.1, *D. rerio* (cnga3b) ENSDART00000027050 (Zebrafish Assembly Jul.2010 (Zv9/danRer7)), *D. melanogaster* NP_477116.1, *C. elegans* NP_499033.1. CNGA1: *H. sapiens* NP_001366199.1, *R. norvegicus* NP_445949.2, *M. musculus* NP_031749.2, *G. gallus* NP_990551.1, *X. tropicalis* XP_017950934.1, *D. rerio* (cnga1a) ENSDART00000134649.4, *D. rerio* (cnga1b) XP_701036.4. CLZ – C-terminal leucine-zipper, CNBD – cyclic nucleotide-binding domain, TM – transmembrane domain, α – α-sheet, β – β-sheet.

Tables

Supp. Table S1: List of all oligonucleotides used as PCR and sequencing primers for the genetic analysis of the *CNGA3* gene in this study.

***CNGA3* PCR primers**

Exon	Primer forward 5‘-3‘	Primer reverse 5‘-3‘
2	gcagcaggaactacaagag	agctgtggaaatgaccagag
3&3b	cctgggatgaggatctgtg	gctggagtacggatgtca
4	cccttgagacagacagagag	ggctgtagagcatgtagtgc
5	cccgaggtaactaatcaca	gggagcaggagcactaa
6	catgtgactcccttgagact	gctgtccaggtgaagctc
7	attacatgatccagcgtctt	aaggtcatacagcttgttgg
8	tcagagtgcatttcctgtagt	gctttcaaagggtgagtaga

***CNGA3* Sequencing primers**

Exon	Orientation	Sequencing primer 5‘-3‘
2	forward	gtagcccttgcccttga
3 & 3b	forward	gtggctttccctgctaag
	forward	ggggtggagttgagttgaagatt
4	forward	ggggtttgggggtgtgg
5	forward	cccgaggtaactaatcaca
6	forward	ggctctctaaaaccctcca
7	reverse	tgtccaagggttccgtgtag
8	forward	gcatactgtgtagccgtgagg
	forward	atgtttgaattctttgaccgca
	forward	gtgggcaatgtgggctcc
	forward	tggcagctacttcggggagat

Supp. Table S2: Allele compositions of *CNGA3* gene variants and their observed absolute frequencies in the ACHM cohort genetically characterized in Tübingen.

Supp. Table S2 is provided as a separate file (.xlsx file).

Supp. Table S3: *CNGA3* variant database. Summary of all classified "likely disease-causing" variants, "variants of uncertain significance" and "likely benign" variants in the *CNGA3* gene identified in the ACHM study cohort genetically characterized in Tübingen, mutation databases and in the literature, including location of variant in polypeptide and functional or structural domain, information of previous functional testing, ClinVar and dbSNP IDs, minor allele frequency in gnomAD, allele count, conservation scoring and *in silico* predictions for missense variants (i.e. SIFT, MutationTaster, AlignGVGD, CADD, PhyloP, Grantham distance) and splice site variants (i.e. SpliceSiteFinder-like, MaxEntScan, NNSplice, GeneSplicer and SpliceAI), as well as ACMG/AMP classification.

Supp. Table S3 is provided as a separate file (.xlsx file).

References Supplementary Material

Abdelkader, E., Brandau, O., Bergmann, C., AlSalamah, N., Nowilaty, S., & Schatz, P. (2018). Novel causative variants in patients with achromatopsia. *Ophthalmic Genet, 39*(6), 678-683. doi:10.1080/13816810.2018.1522653

Abouelhoda, M., Sobahy, T., El-Kalioby, M., Patel, N., Shamseldin, H., Monies, D., . . . Alkuraya, F. S. (2016). Clinical genomics can facilitate countrywide estimation of autosomal recessive disease burden. *Genet Med, 18*(12), 1244-1249. doi:10.1038/gim.2016.37

Ahuja, Y., Kohl, S., & Traboulsi, E. I. (2008). CNGA3 mutations in two United Arab Emirates families with achromatopsia. *Mol Vis, 14*, 1293-1297. Retrieved from https://www.ncbi.nlm.nih.gov/pubmed/18636117

Arshad, M. W., Lee, Y., Malik, M. A., Khan, J., Khan, A., Kareem, A., . . . Shabbir, M. I. (2019). Identification of Novel Mutation in CNGA3 gene by Whole-Exome Sequencing and In-Silico

Analyses for Genotype-Phenotype Assessment with Autosomal Recessive Achromatopsia in Pakistani families. *J Pak Med Assoc, 69*(2), 183-189. Retrieved from https://www.ncbi.nlm.nih.gov/pubmed/30804581

Azam, M., Collin, R. W., Shah, S. T., Shah, A. A., Khan, M. I., Hussain, A., . . . Qamar, R. (2010). Novel CNGA3 and CNGB3 mutations in two Pakistani families with achromatopsia. *Mol Vis, 16*, 774-781. Retrieved from https://www.ncbi.nlm.nih.gov/pubmed/20454696

Burgueño-Montañés, C., Colunga Cueva, M., & Costales Alvarez, C. (2014). [A novel mutation in the CNGA3 gene responsible for incomplete achromatopsia]. *Arch Soc Esp Oftalmol, 89*(3), 107-109. doi:10.1016/j.oftal.2012.07.019

Burkard, M., Kohl, S., Kratzig, T., Tanimoto, N., Brennenstuhl, C., Bausch, A. E., . . . Ruth, P. (2018). Accessory heterozygous mutations in cone photoreceptor CNGA3 exacerbate CNG channel-associated retinopathy. *J Clin Invest, 128*(12), 5663-5675. doi:10.1172/JCI96098

Carrigan, M., Duignan, E., Malone, C. P., Stephenson, K., Saad, T., McDermott, C., . . . Farrar, G. J. (2016). Panel-Based Population Next-Generation Sequencing for Inherited Retinal Degenerations. *Sci Rep, 6*, 33248. doi:10.1038/srep33248

Carss, K. J., Arno, G., Erwood, M., Stephens, J., Sanchis-Juan, A., Hull, S., . . . Raymond, F. L. (2017). Comprehensive Rare Variant Analysis via Whole-Genome Sequencing to Determine the Molecular Pathology of Inherited Retinal Disease. *Am J Hum Genet, 100*(1), 75-90. doi:10.1016/j.ajhg.2016.12.003

Dai, G., & Varnum, M. D. (2013). CNGA3 achromatopsia-associated mutation potentiates the phosphoinositide sensitivity of cone photoreceptor CNG channels by altering intersubunit interactions. *Am J Physiol Cell Physiol, 305*(2), C147-159. doi:10.1152/ajpcell.00037.2013

Dubis, A. M., Cooper, R. F., Aboshiha, J., Langlo, C. S., Sundaram, V., Liu, B., . . . Michaelides, M. (2014). Genotype-dependent variability in residual cone structure in achromatopsia: toward developing metrics for assessing cone health. *Invest Ophthalmol Vis Sci, 55*(11), 7303-7311. doi:10.1167/iovs.14-14225

Ellingford, J. M., Barton, S., Bhaskar, S., O'Sullivan, J., Williams, S. G., Lamb, J. A., . . . Black, G. C. M. (2016). Molecular findings from 537 individuals with inherited retinal disease. *J Med Genet, 53*(11), 761-767. doi:10.1136/jmedgenet-2016-103837

Ezquerra-Inchausti, M., Anasagasti, A., Barandika, O., Garay-Aramburu, G., Galdos, M., Lopez de Munain, A., . . . Ruiz-Ederra, J. (2018). A new approach based on targeted pooled DNA sequencing identifies novel mutations in patients with Inherited Retinal Dystrophies. *Sci Rep, 8*(1), 15457. doi:10.1038/s41598-018-33810-3

Fahim, A. T., Khan, N. W., Zahid, S., Schachar, I. H., Branham, K., Kohl, S., . . . Jayasundera, T. (2013). Diagnostic fundus autofluorescence patterns in achromatopsia. *Am J Ophthalmol, 156*(6), 1211-1219 e1212. doi:10.1016/j.ajo.2013.06.033

Genead, M. A., Fishman, G. A., Rha, J., Dubis, A. M., Bonci, D. M., Dubra, A., . . . Carroll, J. (2011). Photoreceptor structure and function in patients with congenital achromatopsia. *Invest Ophthalmol Vis Sci, 52*(10), 7298-7308. doi:10.1167/iovs.11-7762

Georgiou, M., Litts, K. M., Kalitzeos, A., Langlo, C. S., Kane, T., Singh, N., . . . Michaelides, M. (2019). Adaptive Optics Retinal Imaging in CNGA3-Associated Achromatopsia: Retinal Characterization, Interocular Symmetry, and Intrafamilial Variability. *Invest Ophthalmol Vis Sci, 60*(1), 383-396. doi:10.1167/iovs.18-25880

Gofman, Y., Scharfe, C., Marks, D. S., Haliloglu, T., & Ben-Tal, N. (2014). Structure, dynamics and implied gating mechanism of a human cyclic nucleotide-gated channel. *PLoS Comput Biol, 10*(12), e1003976. doi:10.1371/journal.pcbi.1003976

Goto-Omoto, S., Hayashi, T., Gekka, T., Kubo, A., Takeuchi, T., & Kitahara, K. (2006). Compound heterozygous CNGA3 mutations (R436W, L633P) in a Japanese patient with congenital achromatopsia. *Vis Neurosci, 23*(3-4), 395-402. doi:10.1017/S095252380623308X

Greenberg, J. P., Sherman, J., Zweifel, S. A., Chen, R. W., Duncker, T., Kohl, S., . . . Tsang, S. H. (2014). Spectral-domain optical coherence tomography staging and autofluorescence imaging in achromatopsia. *JAMA Ophthalmol, 132*(4), 437-445. doi:10.1001/jamaophthalmol.2013.7987

Holtan, J. P., Selmer, K. K., Heimdal, K. R., & Bragadottir, R. (2020). Inherited retinal disease in Norway - a characterization of current clinical and genetic knowledge. *Acta Ophthalmol, 98*(3), 286-295. doi:10.1111/aos.14218

Huang, L., Xiao, X., Li, S., Jia, X., Wang, P., Sun, W., . . . Zhang, Q. (2016). Molecular genetics of cone-rod dystrophy in Chinese patients: New data from 61 probands and mutation overview of 163 probands. *Exp Eye Res, 146*, 252-258. doi:10.1016/j.exer.2016.03.015

Hull, S., Kiray, G., Chiang, J. P., & Vincent, A. L. (2020). Molecular and phenotypic investigation of a New Zealand cohort of childhood-onset retinal dystrophy. *Am J Med Genet C Semin Med Genet, 184*(3), 708-717. doi:10.1002/ajmg.c.31836

Jinda, W., Tuekprakhon, A., Thongnoppakhun, W., Limwongse, C., Trinavarat, A., & Atchaneeyasakul, L. O. (2021). Molecular and clinical characterization of Thai patients with achromatopsia: identification of three novel disease-associated variants in the CNGA3 and CNGB3 genes. *Int Ophthalmol, 41*(1), 121-134. doi:10.1007/s10792-020-01559-2

Johnson, S., Michaelides, M., Aligianis, I. A., Ainsworth, J. R., Mollon, J. D., Maher, E. R., . . . Hunt, D. M. (2004). Achromatopsia caused by novel mutations in both CNGA3 and CNGB3. *J Med Genet, 41*(2), e20. doi:10.1136/jmg.2003.011437

Kim, M. S., Joo, K., Seong, M. W., Kim, M. J., Park, K. H., Park, S. S., & Woo, S. J. (2019). Genetic Mutation Profiles in Korean Patients with Inherited Retinal Diseases. *J Korean Med Sci, 34*(21), e161. doi:10.3346/jkms.2019.34.e161

Koeppen, K., Reuter, P., Kohl, S., Baumann, B., Ladewig, T., & Wissinger, B. (2008). Functional analysis of human CNGA3 mutations associated with colour blindness suggests impaired surface expression of channel mutants A3(R427C) and A3(R563C). *Eur J Neurosci, 27*(9), 2391-2401. doi:10.1111/j.1460-9568.2008.06195.x

Koeppen, K., Reuter, P., Ladewig, T., Kohl, S., Baumann, B., Jacobson, S. G., . . . Wissinger, B. (2010). Dissecting the pathogenic mechanisms of mutations in the pore region of the human cone photoreceptor cyclic nucleotide-gated channel. *Hum Mutat, 31*(7), 830-839. doi:10.1002/humu.21283

Kohl, S., Marx, T., Giddings, I., Jagle, H., Jacobson, S. G., Apfelstedt-Sylla, E., . . . Wissinger, B. (1998). Total colourblindness is caused by mutations in the gene encoding the alpha-subunit of the cone photoreceptor cGMP-gated cation channel. *Nat Genet, 19*(3), 257-259. doi:10.1038/935

Kuniyoshi, K., Muraki-Oda, S., Ueyama, H., Toyoda, F., Sakuramoto, H., Ogita, H., . . . Shimomura, Y. (2016). Novel mutations in the gene for alpha-subunit of retinal cone cyclic nucleotide-gated channels in a Japanese patient with congenital achromatopsia. *Jpn J Ophthalmol, 60*(3), 187-197. doi:10.1007/s10384-016-0424-6

Lam, K., Guo, H., Wilson, G. A., Kohl, S., & Wong, F. (2011). Identification of variants in CNGA3 as cause for achromatopsia by exome sequencing of a single patient. *Arch Ophthalmol, 129*(9), 1212-1217. doi:10.1001/archophthalmol.2011.254

Li, F. F., Huang, X. F., Chen, J., Yu, X. D., Zheng, M. Q., Lu, F., . . . Gan, D. K. (2015). Identification of novel mutations by targeted exome sequencing and the genotype-phenotype assessment of patients with achromatopsia. *J Transl Med, 13*, 334. doi:10.1186/s12967-015-0694-7

Li, L., Chen, Y., Jiao, X., Jin, C., Jiang, D., Tanwar, M., . . . Hejtmancik, J. F. (2017). Homozygosity Mapping and Genetic Analysis of Autosomal Recessive Retinal Dystrophies in 144 Consanguineous Pakistani Families. *Invest Ophthalmol Vis Sci, 58*(4), 2218-2238. doi:10.1167/iovs.17-21424

Li, S., Huang, L., Xiao, X., Jia, X., Guo, X., & Zhang, Q. (2014). Identification of CNGA3 mutations in 46 families: common cause of achromatopsia and cone-rod dystrophies in Chinese patients. *JAMA Ophthalmol, 132*(9), 1076-1083. doi:10.1001/jamaophthalmol.2014.1032

Liang, X., Dong, F., Li, H., Li, H., Yang, L., & Sui, R. (2015). Novel CNGA3 mutations in Chinese patients with achromatopsia. *Br J Ophthalmol, 99*(4), 571-576. doi:10.1136/bjophthalmol-2014-305432

Liu, C., & Varnum, M. D. (2005). Functional consequences of progressive cone dystrophy-associated mutations in the human cone photoreceptor cyclic nucleotide-gated channel CNGA3 subunit. *Am J Physiol Cell Physiol, 289*(1), C187-198. doi:10.1152/ajpcell.00490.2004

Matveev, A. V., Fitzgerald, J. B., Xu, J., Malykhina, A. P., Rodgers, K. K., & Ding, X. Q. (2010). The disease-causing mutations in the carboxyl terminus of the cone cyclic nucleotide-gated channel CNGA3 subunit alter the local secondary structure and interfere with the channel active conformational change. *Biochemistry, 49*(8), 1628-1639. doi:10.1021/bi901960u

Meighan, P. C., Peng, C., & Varnum, M. D. (2015). Inherited macular degeneration-associated mutations in CNGB3 increase the ligand sensitivity and spontaneous open probability of cone cyclic nucleotide-gated channels. *Front Physiol, 6*, 177. doi:10.3389/fphys.2015.00177

Méjécase, C., Hummel, A., Mohand-Said, S., Andrieu, C., El Shamieh, S., Antonio, A., . . . Audo, I. (2019). Whole exome sequencing resolves complex phenotype and identifies CC2D2A mutations underlying non-syndromic rod-cone dystrophy. *Clin Genet, 95*(2), 329-333. doi:10.1111/cge.13453

Muraki-Oda, S., Toyoda, F., Okada, A., Tanabe, S., Yamade, S., Ueyama, H., . . . Ohji, M. (2007). Functional analysis of rod monochromacy-associated missense mutations in the CNGA3 subunit of the cone photoreceptor cGMP-gated channel. *Biochem Biophys Res Commun, 362*(1), 88-93. doi:10.1016/j.bbrc.2007.07.152

Nishiguchi, K. M., Sandberg, M. A., Gorji, N., Berson, E. L., & Dryja, T. P. (2005). Cone cGMP-gated channel mutations and clinical findings in patients with achromatopsia, macular degeneration, and other hereditary cone diseases. *Hum Mutat, 25*(3), 248-258. doi:10.1002/humu.20142

Patel, A., Hayward, J. D., Tailor, V., Nyanhete, R., Ahlfors, H., Gabriel, C., . . . Sowden, J. C. (2019). The Oculome Panel Test: Next-Generation Sequencing to Diagnose a Diverse Range of Genetic Developmental Eye Disorders. *Ophthalmology, 126*(6), 888-907. doi:10.1016/j.ophtha.2018.12.050

Patel, K. A., Bartoli, K. M., Fandino, R. A., Ngatchou, A. N., Woch, G., Carey, J., & Tanaka, J. C. (2005). Transmembrane S1 mutations in CNGA3 from achromatopsia 2 patients cause loss of function and impaired cellular trafficking of the cone CNG channel. *Invest Ophthalmol Vis Sci, 46*(7), 2282-2290. doi:10.1167/iovs.05-0179

Patel, N., Aldahmesh, M. A., Alkuraya, H., Anazi, S., Alsharif, H., Khan, A. O., . . . Alkuraya, F. S. (2016). Expanding the clinical, allelic, and locus heterogeneity of retinal dystrophies. *Genet Med, 18*(6), 554-562. doi:10.1038/gim.2015.127

Reuter, P., Koeppen, K., Ladewig, T., Kohl, S., Baumann, B., Wissinger, B., & Achromatopsia Clinical Study, G. (2008). Mutations in CNGA3 impair trafficking or function of cone cyclic nucleotide-gated channels, resulting in achromatopsia. *Hum Mutat, 29*(10), 1228-1236. doi:10.1002/humu.20790

Rim, J. H., Lee, S. T., Gee, H. Y., Lee, B. J., Choi, J. R., Park, H. W., . . . Han, J. (2017). Accuracy of Next-Generation Sequencing for Molecular Diagnosis in Patients With Infantile Nystagmus Syndrome. *JAMA Ophthalmol, 135*(12), 1376-1385. doi:10.1001/jamaophthalmol.2017.4859

Saqib, M. A., Awan, B. M., Sarfraz, M., Khan, M. N., Rashid, S., & Ansar, M. (2011). Genetic analysis of four Pakistani families with achromatopsia and a novel S4 motif mutation of CNGA3. *Jpn J Ophthalmol, 55*(6), 676-680. doi:10.1007/s10384-011-0070-y

Saqib, M. A., Nikopoulos, K., Ullah, E., Sher Khan, F., Iqbal, J., Bibi, R., . . . Rivolta, C. (2015). Homozygosity mapping reveals novel and known mutations in Pakistani families with inherited retinal dystrophies. *Sci Rep, 5*, 9965. doi:10.1038/srep09965

Shaikh, R. S., Reuter, P., Sisk, R. A., Kausar, T., Shahzad, M., Maqsood, M. I., . . . Ahmed, Z. M. (2015). Homozygous missense variant in the human CNGA3 channel causes cone-rod dystrophy. *Eur J Hum Genet, 23*(4), 473-480. doi:10.1038/ejhg.2014.136

Sharon, D., Ben-Yosef, T., Goldenberg-Cohen, N., Pras, E., Gradstein, L., Soudry, S., . . . Perlman, I. (2020). A nationwide genetic analysis of inherited retinal diseases in Israel as assessed by the Israeli inherited retinal disease consortium (IIRDC). *Hum Mutat, 41*(1), 140-149. doi:10.1002/humu.23903

Shuart, N. G., Haitin, Y., Camp, S. S., Black, K. D., & Zagotta, W. N. (2011). Molecular mechanism for 3:1 subunit stoichiometry of rod cyclic nucleotide-gated ion channels. *Nat Commun, 2*, 457. doi:10.1038/ncomms1466

Stone, E. M., Andorf, J. L., Whitmore, S. S., DeLuca, A. P., Giacalone, J. C., Streb, L. M., . . . Tucker, B. A. (2017). Clinically Focused Molecular Investigation of 1000 Consecutive Families with Inherited Retinal Disease. *Ophthalmology, 124*(9), 1314-1331. doi:10.1016/j.ophtha.2017.04.008

Sun, W., Li, S., Xiao, X., Wang, P., & Zhang, Q. (2020). Genotypes and phenotypes of genes associated with achromatopsia: A reference for clinical genetic testing. *Mol Vis, 26*, 588-602. Retrieved from https://www.ncbi.nlm.nih.gov/pubmed/32913385

Sundaram, V., Wilde, C., Aboshiha, J., Cowing, J., Han, C., Langlo, C. S., . . . Michaelides, M. (2014). Retinal structure and function in achromatopsia: implications for gene therapy. *Ophthalmology, 121*(1), 234-245. doi:10.1016/j.ophtha.2013.08.017

Täger, J., Kohl, S., Birch, D. G., Wheaton, D. K. H., Wissinger, B., & Reuter, P. (2018). An early nonsense mutation facilitates the expression of a short isoform of CNGA3 by alternative translation initiation. *Exp Eye Res, 171*, 48-53. doi:10.1016/j.exer.2018.02.027

Taylor, R. L., Parry, N. R. A., Barton, S. J., Campbell, C., Delaney, C. M., Ellingford, J. M., . . . Sergouniotis, P. I. (2017). Panel-Based Clinical Genetic Testing in 85 Children with Inherited Retinal Disease. *Ophthalmology, 124*(7), 985-991. doi:10.1016/j.ophtha.2017.02.005

Thiadens, A. A., Roosing, S., Collin, R. W., van Moll-Ramirez, N., van Lith-Verhoeven, J. J., van Schooneveld, M. J., . . . Klaver, C. C. (2010). Comprehensive analysis of the achromatopsia genes CNGA3 and CNGB3 in progressive cone dystrophy. *Ophthalmology, 117*(4), 825-830 e821. doi:10.1016/j.ophtha.2009.09.008

Thiadens, A. A., Somervuo, V., van den Born, L. I., Roosing, S., van Schooneveld, M. J., Kuijpers, R. W., . . . Klaver, C. C. (2010). Progressive loss of cones in achromatopsia: an imaging study using spectral-domain optical coherence tomography. *Invest Ophthalmol Vis Sci, 51*(11), 5952-5957. doi:10.1167/iovs.10-5680

Thomas, M. G., McLean, R. J., Kohl, S., Sheth, V., & Gottlob, I. (2012). Early signs of longitudinal progressive cone photoreceptor degeneration in achromatopsia. *Br J Ophthalmol, 96*(9), 1232-1236. doi:10.1136/bjophthalmol-2012-301737

Tränkner, D., Jagle, H., Kohl, S., Apfelstedt-Sylla, E., Sharpe, L. T., Kaupp, U. B., . . . Wissinger, B. (2004). Molecular basis of an inherited form of incomplete achromatopsia. *J Neurosci, 24*(1), 138-147. doi:10.1523/JNEUROSCI.3883-03.2004

Vincent, A., Wright, T., Billingsley, G., Westall, C., & Heon, E. (2011). Oligocone trichromacy is part of the spectrum of CNGA3-related cone system disorders. *Ophthalmic Genet, 32*(2), 107-113. doi:10.3109/13816810.2010.544366

Wang, P., Li, S., Sun, W., Xiao, X., Jia, X., Liu, M., . . . Zhang, Q. (2019). An Ophthalmic Targeted Exome Sequencing Panel as a Powerful Tool to Identify Causative Mutations in Patients Suspected of Hereditary Eye Diseases. *Transl Vis Sci Technol, 8*(2), 21. doi:10.1167/tvst.8.2.21

Wang, X., Wang, H., Cao, M., Li, Z., Chen, X., Patenia, C., . . . Chen, R. (2011). Whole-exome sequencing identifies ALMS1, IQCB1, CNGA3, and MYO7A mutations in patients with Leber congenital amaurosis. *Hum Mutat, 32*(12), 1450-1459. doi:10.1002/humu.21587

Weisschuh, N., Obermaier, C. D., Battke, F., Bernd, A., Kuehlewein, L., Nasser, F., . . . Kohl, S. (2020). Genetic architecture of inherited retinal degeneration in Germany: A large cohort study from a single diagnostic center over a 9-year period. *Hum Mutat, 41*(9), 1514-1527. doi:10.1002/humu.24064

Wissinger, B., Gamer, D., Jagle, H., Giorda, R., Marx, T., Mayer, S., . . . Kohl, S. (2001). CNGA3 mutations in hereditary cone photoreceptor disorders. *Am J Hum Genet, 69*(4), 722-737. doi:10.1086/323613

Wiszniewski, W., Lewis, R. A., & Lupski, J. R. (2007). Achromatopsia: the CNGB3 p.T383fsX mutation results from a founder effect and is responsible for the visual phenotype in the original report of uniparental disomy 14. *Hum Genet, 121*(3-4), 433-439. doi:10.1007/s00439-006-0314-y

Yang, P., Michaels, K. V., Courtney, R. J., Wen, Y., Greninger, D. A., Reznick, L., . . . Pennesi, M. E. (2014). Retinal morphology of patients with achromatopsia during early childhood: implications for gene therapy. *JAMA Ophthalmol, 132*(7), 823-831. doi:10.1001/jamaophthalmol.2014.685

Zelinger, L., Cideciyan, A. V., Kohl, S., Schwartz, S. B., Rosenmann, A., Eli, D., . . . Sharon, D. (2015). Genetics and Disease Expression in the CNGA3 Form of Achromatopsia: Steps on the Path to Gene Therapy. *Ophthalmology, 122*(5), 997-1007. doi:10.1016/j.ophtha.2014.11.025

Zobor, D., Werner, A., Stanzial, F., Benedicenti, F., Rudolph, G., Kellner, U., . . . Consortium, R.-C. (2017). The Clinical Phenotype of CNGA3-Related Achromatopsia: Pretreatment Characterization in Preparation of a Gene Replacement Therapy Trial. *Invest Ophthalmol Vis Sci, 58*(2), 821-832. doi:10.1167/iovs.16-20427

Supp. Table S2: Allele compositions of *CNGA3* gene variants and their observed absolute frequencies in the ACHM cohort genetically characterized in Tübingen.

Allele 1†	Allele 2†	Number of independent families	Number of affected individuals	Segregation analysis		
				Both parents	One parent or other relatives	No segregation analysis possible
c.1641C>A	c.1641C>A	20	23	7	6	10
c.847C>T	c.847C>T‡	12	22	10	11	1
c.1114C>T	c.1114C>T	7	8	5	2	1
c.1306C>T	c.1306C>T	7	8	2	1	5
c.847C>T	c.829C>T	6	6	1	1	4
c.1495C>T	c.1495C>T	5	6	4	1	1
c.1641C>A	c.847C>T	5	6	4	0	2
c.1641C>A	c.829C>T	4	4	1	0	3
c.848G>A	c.848G>A	3	5	3	2	0
c.947G>A	c.947G>A	3	5	2	2	1
c.1100G>T	c.1100G>T	3	4	3	0	1
c.1114C>T	c.811C>G	3	4	2	1	1
c.667C>T	c.667C>T	3	4	1	2	1
c.829C>T	c.1279C>T	3	4	2	0	2
c.830G>A	c.830G>A	3	4	2	0	2
c.542A>G	c.542A>G	3	3	0	1	2
c.488C>T	c.488C>T	2	5	3	2	0
c.1279C>T	c.667C>T	2	3	2	1	0
c.1641C>A	c.1279C>T	2	3	0	3	0
c.829C>T	c.1405G>A	2	3	0	2	1
c.829C>T	c.829C>T	2	3	2	0	1
c.847C>T	c.488C>T‡	2	3	3	0	0
c.940_942del	c.940_942del	2	3	1	2	0
c.1228C>T	c.1228C>T	2	2	2	0	0
c.1306C>T	c.1688G>A	2	2	1	0	1
c.670A>G	c.670A>G	2	2	2	0	0
c.829C>T	c.572G>A	2	2	0	2	0
c.829C>T	c.1315C>T	2	2	0	1	1
c.985G>T	c.985G>T	1	6	6	0	0
c.1126G>A	c.1126G>A	1	3	2	1	0
c.1190G>T	c.1190G>T	1	3	0	3	0
c.1320G>A	c.1547G>A	1	3	3	0	0
c.1641C>A	c.1688G>A	1	3	0	3	0
c.1694C>T	c.1717T>C	1	3	0	3	0
c.[458C>T;1585G>A]	c.1228C>T	1	2	0	2	0
c.[67C>T;682G>A]	c.[67C>T;682G>A]¥	1	2	0	2	0
c.[682G>A;1315C>T]	c.[682G>A;1315C>T]¥	1	2	2	0	0
c.1088T>C	c.1088T>C	1	2	2	0	0
c.1279C>T	c.107_110del	1	2	2	0	0
c.1279C>T	c.1642G>A	1	2	0	2	0
c.1279C>T	c.1706G>A	1	2	2	0	0
c.1391T>G	c.1621C>T	1	2	2	0	0
c.147dup	c.947G>A	1	2	2	0	0
c.1574G>A	c.1694C>T	1	2	0	2	0
c.162_163insT	c.1405G>A	1	2	0	2	0
c.1641C>A	c.872C>G	1	2	2	0	0
c.1641C>A	c.1004G>A	1	2	2	0	0
c.499del	c.1669G>A	1	2	2	0	0
c.542A>G	c.851del	1	2	0	2	0
c.667C>T	c.668G>A	1	2	0	2	0
c.671C>G	c.1106C>G	1	2	2	0	0
c.67C>T	c.1030G>T	1	2	2	0	0
c.754G>A	c.754G>A	1	2	2	0	0
c.784G>C	c.1708A>G	1	2	2	0	0
c.800G>A	c.1963C>T	1	2	2	0	0
c.829C>T	c.1981C>A	1	2	2	0	0
c.829C>T	c.1580T>G	1	2	2	0	0
c.847C>T	c.746T>C	1	2	2	0	0
c.847C>T	c.1114C>T	1	2	2	0	0
c.847C>T	c.1279C>T	1	2	2	0	0
c.847C>T	c.674-1935_*1838del	1	2	2	0	0
c.847C>T	c.1190G>T	1	2	0	2	0
c.847C>T	c.1538G>A	1	2	2	0	0
c.940_942del	c.1454A>T	1	2	0	2	0
c.1004G>A(;)1641C>A	c.947G>A	1	1	0	0	1
c.1021T>C	c.1273C>T	1	1	0	0	1
c.1030G>T	c.1694C>T	1	1	0	1	0
c.1061A>G	c.1070A>G	1	1	1	0	0
c.1074G>A	c.1889T>C	1	1	0	0	1
c.1114C>T	c.572G>A	1	1	0	0	1
c.1114C>T	c.1981C>A	1	1	0	0	1
c.1116del	c.1579C>A	1	1	1	0	0
c.1139T>C	c.1768G>A	1	1	0	0	1
c.1279C>T	c.940_942del	1	1	0	0	1
c.1279C>T	c.661C>T	1	1	0	1	0
c.1279C>T	c.67C>T	1	1	1	0	0
c.1279C>T	c.1351dup	1	1	1	0	0
c.1279C>T	c.1319G>C	1	1	0	0	1
c.1279C>T	c.1495C>T	1	1	0	0	1
c.1279C>T	c.332_333delinsAA	1	1	0	0	1
c.1306C>T	c.1126G>A	1	1	0	0	1
c.1306C>T	c.1A>T	1	1	1	0	0
c.1306C>T	c.1114C>T	1	1	1	0	0
c.1306C>T	c.743A>G	1	1	1	0	0
c.1306C>T	c.668G>A	1	1	1	0	0
c.1306C>T	c.667C>T	1	1	0	0	1
c.1306C>T	c.848G>A	1	1	0	1	0
c.1306C>T	c.1279C>T	1	1	0	0	1
c.1306C>T	c.488C>T	1	1	1	0	0
c.1306C>T	c.1320del	1	1	0	1	0
c.1306C>T	c.1579C>A	1	1	0	0	1
c.1315C>T	c.1315C>T	1	1	1	0	0
c.1366del	c.1669G>A	1	1	1	0	0

c.1379del	c.1557G>A	1	1	1	0	0
c.1391T>G	c.1391T>G	1	1	1	0	0
c.1395_1412del	c.1565T>C	1	1	0	0	1
c.1443dup	c.1642G>A	1	1	0	0	1
c.1443dup	c.1771T>C	1	1	1	0	0
c.1457G>A	c.1585G>A	1	1	1	0	0
c.1495C>T	c.139C>T	1	1	0	1	0
c.1495C>T	c.450-15T>G	1	1	0	1	0
c.1495C>T	c.332_333delinsAA	1	1	0	0	1
c.1495C>T	c.625T>C	1	1	1	0	0
c.1495C>T	c.1201T>C	1	1	0	0	1
c.1529G>C	c.1529G>C	1	1	0	0	1
c.1538G>A	c.1706G>A	1	1	1	0	0
c.1585G>A	c.1585G>A	1	1	1	0	0
c.1641C>A	c.784G>C	1	1	0	0	1
c.1641C>A	c.955_963delinsACCAATGAAATGGAAAT	1	1	0	0	1
c.1641C>A	c.340G>T	1	1	1	0	0
c.1641C>A	c.580G>A	1	1	1	0	0
c.1641C>A	c.591del	1	1	1	0	0
c.1641C>A	c.1682G>A	1	1	0	1	0
c.1641C>A	c.1706G>A	1	1	1	0	0
c.1641C>A	c.778G>A	1	1	1	0	0
c.1641C>A	c.1565T>C	1	1	0	0	1
c.1641C>A	c.1391T>G	1	1	0	0	1
c.1641C>A	c.544A>T	1	1	0	0	1
c.1641C>A	c.1682_1683insACGCG	1	1	0	0	1
c.1641C>A	c.67C>T	1	1	1	0	0
c.1641C>A	c.830G>A	1	1	1	0	0
c.1641C>A	c.1228C>T	1	1	0	0	1
c.1641C>A	c.1306C>T	1	1	0	1	0
c.1641C>A	c.1255T>C	1	1	1	0	0
c.1641C>A	c.479T>G	1	1	1	0	0
c.1641C>A	c.1585G>A	1	1	1	0	0
c.1642G>A	c.1642G>A	1	1	1	0	0
c.1669G>A	c.1669G>A	1	1	1	0	0
c.1688G>A	c.1688G>A	1	1	1	0	0
c.1694C>T	c.1694C>T	1	1	0	0	1
c.1705C>T	c.1709G>T	1	1	0	0	1
c.1775C>T	c.1775C>T	1	1	0	0	1
c.1810C>T	c.1810C>T	1	1	0	0	1
c.353A>G	c.1615G>A¶	1	1	0	0	1
c.384_387del	c.513G>A	1	1	0	0	1
c.387del	c.387del	1	1	0	0	1
c.396-2_398dup	c.396-2_398dup	1	1	0	0	1
c.464del	c.464del	1	1	0	0	1
c.485A>T	c.778G>A	1	1	0	0	1
c.513G>A	c.1557G>A	1	1	1	0	0
c.513G>A	c.772C>G	1	1	1	0	0
c.513G>A	c.983T>C	1	1	1	0	0
c.544A>G	c.668G>A	1	1	0	0	1
c.572G>A	c.572G>A	1	1	1	0	0
c.572G>A	c.1706G>A	1	1	1	0	0
c.572G>A	c.902_903delinsAA	1	1	1	0	0
c.572G>A	c.1585G>A	1	1	0	0	1
c.609G>T	c.1106C>G	1	1	0	0	1
c.625T>C	c.625T>C	1	1	0	0	1
c.661C>T	c.967G>C	1	1	0	0	1
c.664G>C	c.1669G>A	1	1	0	0	1
c.667C>T	c.1706G>A	1	1	1	0	0
c.667C>T	c.1768G>A	1	1	1	0	0
c.667C>T	c.830G>A	1	1	0	0	1
c.667C>T	c.848G>A	1	1	0	0	1
c.667C>T	c.1021T>C	1	1	1	0	0
c.671C>G	c.1645G>T	1	1	1	0	0
c.67C>T	c.811C>A	1	1	0	1	0
c.704A>T	c.1706G>A	1	1	0	1	0
c.742C>T	c.1115C>T	1	1	0	0	1
c.778G>A	c.778G>A	1	1	0	1	0
c.778G>A	c.1228C>T	1	1	0	0	1
c.778G>A	c.1115C>T	1	1	0	0	1
c.778G>A	c.1557G>A	1	1	0	0	1
c.778G>C	c.778G>C	1	1	1	0	0
c.784G>C	c.1736T>G	1	1	0	0	1
c.811C>G	c.1076C>T	1	1	0	0	1
c.822G>T	c.822G>T	1	1	1	0	0
c.829C>G	c.1021T>C	1	1	0	0	1
c.829C>T	c.778G>A	1	1	0	1	0
c.829C>T	c.556C>T	1	1	0	1	0
c.829C>T	c.566G>A	1	1	0	0	1
c.829C>T	c.661C>T	1	1	0	0	1
c.829C>T	c.667C>T	1	1	1	0	0
c.829C>T	c.1609C>T	1	1	0	1	0
c.829C>T	c.1718A>G	1	1	0	0	1
c.829C>T	c.1669G>A	1	1	1	0	0
c.829C>T	c.1306C>T	1	1	1	0	0
c.829C>T	c.1687C>T	1	1	0	0	1
c.829C>T	c.1585G>A	1	1	0	0	1
c.829C>T	c.1466G>T	1	1	0	0	1
c.829C>T	c.1228C>T	1	1	0	0	1
c.829C>T	c.1537G>A	1	1	0	0	1
c.829C>T	c.1343A>G(;)1658T>A	1	1	0	0	1
c.829C>T	c.1117G>A	1	1	1	0	0
c.829C>T	c.1694C>T	1	1	0	0	1
c.830G>A	c.746T>C	1	1	0	1	0
c.830G>A	c.1585G>A	1	1	0	1	0
c.830G>A	c.1129_1131del	1	1	1	0	0
c.830G>A	c.1070A>G	1	1	0	0	1
c.830G>A	c.1706G>A	1	1	0	0	1
c.830G>A	c.1694C>T	1	1	1	0	0
c.830G>A	c.1320del	1	1	0	0	1
c.847C>T	c.830G>A	1	1	1	0	0

c.847C>T	c.1139T>C	1	1	0	0	1
c.847C>T	c.1688G>A	1	1	0	0	1
c.847C>T	c.1694C>T	1	1	1	0	0
c.847C>T	c.1574G>A	1	1	1	0	0
c.847C>T	c.1306C>T	1	1	1	0	0
c.847C>T	c.1519del	1	1	1	0	0
c.847C>T	c.1669G>A	1	1	0	0	1
c.847C>T	c.1495C>T	1	1	1	0	0
c.847C>T	c.1268A>C	1	1	0	0	1
c.847C>T	c.940_942del	1	1	1	0	0
c.847C>T	c.1768G>A	1	1	0	0	1
c.847C>T	c.332_333delinsAA	1	1	0	0	1
c.848G>A	c.450-1G>A	1	1	1	0	0
c.848G>A	c.830G>A	1	1	0	0	1
c.848G>A	c.1669G>A	1	1	1	0	0
c.848G>A	c.1298T>G	1	1	1	0	0
c.848G>A	c.1706G>A	1	1	0	1	0
c.848G>A	c.1063A>G	1	1	1	0	0
c.848G>A	c.1116del	1	1	1	0	0
c.848G>A	unknown§	1	1	0	0	1
c.906G>T	c.1319G>C	1	1	1	0	0
c.952G>A	c.1706G>A	1	1	0	0	1
c.967G>C	c.1706G>A	1	1	0	0	1
c.967G>C	c.1687C>T	1	1	0	0	1
c.967G>C	c.967G>C	1	1	0	0	1
c.992G>A	c.992G>A	1	1	0	0	1
c.992G>A	c.1201T>C	1	1	1	0	0
		304 (306§ ¶)	385 (387§ ¶)	181	88	118 (116§ ¶)

†Variant designation is based on NM_001298.2 (GRCh38/hg38).

‡One family showed pseudo-dominant inheritance: the mother is homozygous for c.847C>T whereas the two affected children are compound-heterozygous for c.488C>T and c.847C>T.

§One affected individual carries only a single heterozygous *CNGA3* variant; screening of all other ACHM-associated genes did not identify any other likely causative mutations and the case is therefore referred to as unsolved.

¶Genetic reanalysis of the affected individual harboring the above-mentioned *CNGA3* genotype revealed an *OPN1MW* /*OPN1LW* -associated genotype indicative for and compatible with a clinical diagnosis of blue cone monochromatism, X-linked.

¥Complex alleles associated with c.682G>A/p.(Glu228Lys).

Supp. Table S3: *CNGA3* variant database. Summary of all classified "likely disease-causing" variants, "variants of uncertain significance" and "likely benign" variants in the *CNGA3* gene identified in the ACHM study cohort genetically characterized in Tübingen, mutation databases and in the literature, including location of variant in polypeptide and functional or structural domain, information of previous functional testing, ClinVar and dbSNP IDs, minor allele frequency in gnomAD, allele count, conservation scoring and *in silico* predictions for missense variants (i.e. SIFT, MutationTaster, AlignGVGD, CADD, PhyloP, Grantham distance) and splice site variants (i.e. SpliceSiteFinder-like, MaxEntScan, NNSplice, GeneSplicer and SpliceAI), as well as ACMG/AMP classification.

Location *CNGA3*	Alteration gDNA level †	Alteration Nucleotide Sequence †	Alteration Polypeptide	Location Protein Domain$	Reference	Functional Analysis# Reference	Functional Analysis# Functional response#	ClinVar Variation ID	dbSNP	Minor allele frequency gnomAD	Allele count in the ACHM cohort genetically characterized in Tübingen	Conservation of amino acid residue ††	*In silico* missense variant predictions£ SIFT	*In silico* missense variant predictions£ MutationTaster	*In silico* missense variant predictions£ Align-GVGD	CADD score (GRCh38-v1.6)£	PhyloP	Grantham distance	*In silico* splicing predictions£ SpliceSite Finder-like [0-100]	*In silico* splicing predictions£ MaxEntScan [0-12]a; [0-16]b	*In silico* splicing predictions£ NNSplice [0-1]	*In silico* splicing predictions£ GeneSplicer [0-15]	*In silico* splicing predictions£ SpliceAI Δ score [0-1]	ACMG/AMP criteria	ACMG/AMP classification
Likely disease-causing variants																									
Intron 1	g.98369938G>C	c.-37-1G>C	p.(?)	-	Burkard et al., 2018	Burkard et al., 2018	- (Splicing Assay)	503559	rs1553447991	no entry	0	-	n.a.	n.a.	n.a.	33.0 (damaging)	n.a.	n.a.	3' score reference: 76.95; mutant: 0 (-100%)	3' score reference: 6.59; mutant: 0 (-100%)	3' score reference: 0.61; mutant: 0 (-100%)	3' score reference: 7.45; mutant: 0 (-100%)	acceptor loss: 0.96 acceptor gain: 0.10	PVS1;PM2;PP5;PS3	Pathogenic
Exon 2	g.98369976A>T	c.1A>T	p.(?)	N-Term.	This study	n.d.	n.d.	no entry	no entry	no entry	1	-	n.a.	n.a.	n.a.	23.0 (damaging)	n.a.	n.a.	3' score reference: 0; mutant: 0 (no effect)	3' score reference: 0; mutant: 0 (no effect)	3' score reference: 0; mutant: 0 (no effect)	3' score reference: 0; mutant: 0 (no effect)	acceptor loss: 0.01 acceptor gain: 0.02	PM2;PVS1	VUS
Exon 2	g.98370015del	c.40del	p.(Thr14ProfsTer5)	N-Term.	Liang et al., 2015	n.d.	n.d.	no entry	no entry	no entry	0	-	n.a.	n.a.	n.a.	n.a.	n.a.	n.a.	n.a.	n.a.	n.a.	n.a.	n.a.	PP1;PVS1;PM2	Pathogenic
Exon 2	g.98370037C>G	c.62C>G	p.(Ser21Ter)	N-Term.	Li et al., 2014	n.d.	n.d.	no entry	no entry	0.0020%	0	-	n.a.	n.a.	n.a.	23.1 (damaging)	n.a.	n.a.	n.a.	n.a.	n.a.	n.a.	n.a.	PP1;PVS1;PM2	Pathogenic
Exon 2	g.98370042C>T	c.67C>T	p.(Arg23Ter)	N-Term.	Johnson et al., 2004	Täger et al., 2018	+ (Aequorin-Bioassay)	337652	rs777509481	0.0033%	9	-	n.a.	n.a.	n.a.	31.0 (damaging)	n.a.	n.a.	n.a.	n.a.	n.a.	n.a.	n.a.	PVS1;PM2;PP5;PP1;PS3	Pathogenic
Intron 2	g.98370077G>A	c.101+1G>A	p.(?)	-	Abdelkader et al., 2018	n.d.	n.d.	208567	rs147118493	0.024%	0	-	n.a.	n.a.	n.a.	33.0 (damaging)	n.a.	n.a.	5' score reference: 94.67; mutant: 0 (-100%)	5' score reference: 10.77; mutant: 0 (-100%)	5' score reference: 0.98; mutant: 0 (-100%)	5' score reference: 8.33; mutant: 0 (-100%)	donor loss: 0.99 donor gain: 0.00	PVS1;PM2;PP5;PP3	Pathogenic
Exon 3	g.98377692_98377695del	c.107_110del	p.(His36ArgfsTer136)	N-Term.	Thomas et al.,2012	n.d.	n.d.	438155	rs749036398	no entry	2	-	n.a.	n.a.	n.a.	n.a.	n.a.	n.a.	n.a.	n.a.	n.a.	n.a.	n.a.	PS4;PVS1;PM2;PP5;PP1	Pathogenic
Exon 3	g.98377713C>A	c.128C>A	p.(Ser43Ter)	N-Term.	Sun et al., 2020	n.d.	n.d.	no entry	no entry	no entry	0	-	n.a.	n.a.	n.a.	35.0 (damaging)	n.a.	n.a.	n.a.	n.a.	n.a.	n.a.	n.a.	PVS1;PM2	Likely pathogenic
Exon 3	g.98377715_98377736dup	c.130_151dup	p.(Ala51ValfsTer16)	N-Term.	Zelinger et al.,2015	n.d.	n.d.	599216	no entry	no entry	0	-	n.a.	n.a.	n.a.	n.a.	n.a.	n.a.	n.a.	n.a.	n.a.	n.a.	n.a.	PVS1;PM2;PP5;PP1	Pathogenic
Exon 3	g.98377724C>T	c.139C>T	p.(Gln47Ter)	N-Term.	Zobor et al., 2017	n.d.	n.d.	no entry	no entry	no entry	1	-	n.a.	n.a.	n.a.	36.0 (damaging)	n.a.	n.a.	n.a.	n.a.	n.a.	n.a.	n.a.	PVS1;PM2	Likely pathogenic
Exon 3	g.98377732dup	c.147dup	p.(Ile50AspfsTer10)	N-Term.	Wissinger et al., 2001	n.d.	n.d.	no entry	no entry	no entry	2	-	n.a.	n.a.	n.a.	n.a.	n.a.	n.a.	n.a.	n.a.	n.a.	n.a.	n.a.	PVS1;PM2	Likely pathogenic
Exon 3	g.98377747_98377748insT	c.162_163insT	p.(Arg55Ter)	N-Term.	Ezquerra-Inchausti et al., 2018	n.d.	n.d.	no entry	no entry	no entry	2	-	n.a.	n.a.	n.a.	n.a.	n.a.	n.a.	n.a.	n.a.	n.a.	n.a.	n.a.	PVS1;PM2;PP1	Pathogenic
Exon 4	g.98380207G>A	c.248G>A	p.(Trp83Ter)	N-Term.	Ellingford et al., 2016	n.d.	n.d.	236461	rs757470958	0.00041%	0	-	n.a.	n.a.	n.a.	36.0 (damaging)	n.a.	n.a.	n.a.	n.a.	n.a.	n.a.	n.a.	PVS1;PM2;PP5	Pathogenic
Exon 4	g.98380291_98380292delinsAA	c.332_333delinsAA	p.(Ser111Ter)	N-Term.	This study	n.d.	n.d.	866218	no entry	no entry	3	-	n.a.	n.a.	n.a.	n.a.	n.a.	n.a.	n.a.	n.a.	n.a.	n.a.	n.a.	PVS1;PM2;PP5	Pathogenic
Exon 4	g.98380299G>T	c.340G>T	p.(Glu114Ter)	N-Term.	This study	n.d.	n.d.	860884	no entry	no entry	1	-	n.a.	n.a.	n.a.	36.0 (damaging)	n.a.	n.a.	n.a.	n.a.	n.a.	n.a.	n.a.	PVS1;PM2;PP5	Pathogenic
Exon 4	g.98380343_98380346del	c.384_387del	p.(Asp128GlufsTer44)	N-Term.	This study	n.d.	n.d.	no entry	no entry	no entry	1	-	n.a.	n.a.	n.a.	n.a.	n.a.	n.a.	n.a.	n.a.	n.a.	n.a.	n.a.	PVS1;PM2	Likely pathogenic
Exon 4	g.98380346del	c.387del	p.(Arg131GlufsTer42)	N-Term.	This study	n.d.	n.d.	no entry	no entry	no entry	2	-	n.a.	n.a.	n.a.	n.a.	n.a.	n.a.	n.a.	n.a.	n.a.	n.a.	n.a.	PVS1;PM2	Likely pathogenic
Intron 4	g.98380355G>T	c.395+1G>T	p.(?)	-	Abdelkader et al., 2018	n.d.	n.d.	no entry	no entry	no entry	0	-	n.a.	n.a.	n.a.	34.0 (damaging)	n.a.	n.a.	5' score reference: 94.67; mutant: 0 (-100%)	5' score reference: 10.51; mutant: 0 (-100%)	5' score reference: 1.00; mutant: 0 (-100%)	5' score reference: 8.85; mutant: 0 (-100%)	donor loss: 0.99 donor gain: 0.02	PVS1;PM2;PP3	Likely pathogenic
Intron 4	g.98383386_98383390dup	c.396-2_398dup	p.(?)	-	This study	n.d.	n.d.	no entry	no entry	no entry	2	-	n.a.	n.a.	n.a.	n.a.	n.a.	n.a.	3' score reference: 78.80; mutant: 78.80 (no effect)	3' score reference: 11.35; mutant: 11.35 (no effect)	3' score reference: 0.90; mutant: 0.95 (+6%)	3' score reference: 12.40; mutant: 12.80 (+3%)	acceptor loss: 0.00 acceptor gain: 0.22	PVS1;PM2;BP4	Likely pathogenic
Intron 4	g.98383377C>G	c.396-11C>G	p.(?)	-	Li et al., 2014	n.d.	n.d.	no entry	rs545114991	no entry	0	-	n.a.	n.a.	n.a.	25.3 (damaging)	n.a.	n.a.	3' score reference: 78.80; mutant: 0 (-100%)	3' score reference: 11.35; mutant: 5.31 (-53%)	3' score reference: 0.90; mutant: 0.80 (-12%)	3' score reference: 12.40; mutant: 7.24 (-42%)	acceptor loss: 0.87 acceptor gain: 0.70	PP1;PM2;PP3	VUS
Intron 5	g.98389657G>A	c.450-1G>A	p.(?)	-	Georgiou et al., 2019	n.d.	n.d.	no entry	rs754158805	0.0012%	1	-	n.a.	n.a.	n.a.	33.0 (damaging)	n.a.	n.a.	3' score reference: 82.49; mutant: 0 (-100%)	3' score reference: 8.60; mutant: 0 (-100%)	3' score reference: 0.82; mutant: 0 (-100%)	3' score reference: 7.32; mutant: 0 (-100%)	acceptor loss: 0.95 acceptor gain: 0.01	PVS1;PM2;PP3	Likely pathogenic
Intron 5	g.98389643T>G	c.450-15T>G	p.(?)	-	This study	n.d.	n.d.	no entry	no entry	no entry	1	-	n.a.	n.a.	n.a.	22.6 (damaging)	n.a.	n.a.	3' score reference: 82.49; mutant: 82.49 (no effect)	3' score reference: 8.60; mutant: 4.68 (-46%)	3' score reference: 0.82; mutant: 0.63 (-24%)	3' score reference: 7.31; mutant: 2.57 (-65%)	acceptor loss: 0.65 acceptor gain: 0.53	PM2;PP3	VUS
Exon 6	g.98389672del	c.464del	p.(Lys155ArgfsTer18)	N-Term.	This study	n.d.	n.d.	no entry	no entry	no entry	2	-	n.a.	n.a.	n.a.	n.a.	n.a.	n.a.	n.a.	n.a.	n.a.	n.a.	n.a.	PVS1;PM2;PP1	Pathogenic
Exon 6	g.98389686G>A	c.478G>A	p.(Val160Met)	N-Term.	ClinVar	n.d.	n.d.	898383	rs373542579	0.0042%	0	conserved	DELETERIOUS (score: 0.05, median: 3.38)	disease causing (prob: 0.753)	Class C0 (GV: 141.80 GD: 0.00)	22.9 (damaging)	2.80	21	n.a.	n.a.	n.a.	n.a.	n.a.	PM2;PM1;PP2;PP3	VUS
Exon 6	g.98389687T>G	c.479T>G	p.(Val160Gly)	N-Term.	This study	n.d.	n.d.	no entry	no entry	no entry	1	conserved	DELETERIOUS (score: 0.02, median: 3.38)	disease causing (prob: 1)	Class C0 (GV: 141.80 GD: 29.38)	25.3 (damaging)	6.95	109	n.a.	n.a.	n.a.	n.a.	n.a.	PM2;PM1;PP2;PP3	VUS
Exon 6	g.98389693A>T	c.485A>T	p.(Asp162Val)	N-Term.	Wissinger et al., 2001	Muraki-Oda et al., 2007	- (Ephys)	no entry	rs747447519	0.0097%	1	conserved	DELETERIOUS (score: 0, median: 3.38)	disease causing (prob: 1)	Class C65 (GV: 0.00 GD: 152.22)	24.9 (damaging)	3.96	152	n.a.	n.a.	n.a.	n.a.	n.a.	PS3;PM2;PM1;PP2;PP3	Likely pathogenic
Exon 6	g.98389696C>T	c.488C>T	p.(Pro163Leu)	N-Term.	Kohl et al., 1998	Muraki-Oda et al., 2007	- (Ephys)	9473	rs104893612	0.0016%	14	completely conserved	DELETERIOUS (score: 0, median: 3.38)	disease causing (prob: 1)	Class C65 (GV: 0.00 GD: 97.78)	24.8 (damaging)	7.53	98	n.a.	n.a.	n.a.	n.a.	n.a.	PP1;PS3;PM2;PM1;PP2;PP3;PP5	Pathogenic
Exon 6	g.98389697_98389700del	c.489_492del	p.(Ser164AlafsTer8)	N-Term.	LOVD	n.d.	n.d.	987365	no entry	no entry	0	-	n.a.	n.a.	n.a.	n.a.	n.a.	n.a.	n.a.	n.a.	n.a.	n.a.	n.a.	PVS1;PM2;PP5	Pathogenic
Exon 6	g.98389707del	c.499del	p.(Leu167CysfsTer6)	N-Term.	Weisschuh et al., 2020	n.d.	n.d.	813039	no entry	no entry	2	-	n.a.	n.a.	n.a.	n.a.	n.a.	n.a.	n.a.	n.a.	n.a.	n.a.	n.a.	PP1;PVS1;PM2;PP5	Pathogenic
Exon 6	g.98389720G>A	c.512G>A	p.(Trp171Ter)	TM1	Li et al., 2014	Täger et al., 2018	- (Aequorin-Bioassay)	no entry	no entry	no entry	0	-	n.a.	n.a.	n.a.	38.0 (damaging)	n.a.	n.a.	n.a.	n.a.	n.a.	n.a.	n.a.	PVS1;PM2;PS3	Pathogenic
Exon 6	g.98389721G>T	c.513G>T	p.(Trp171Cys)	TM1	Li et al., 2014	n.d.	n.d.	no entry	rs762773298	0.00041%	0	completely conserved	DELETERIOUS (score: 0, median: 3.38)	disease causing (prob: 1)	Class C65 (GV: 0.00 GD: 214.36)	32.0 (damaging)	9.55	215	n.a.	n.a.	n.a.	n.a.	n.a.	PM2;PM1;PP2;PP3	VUS
Exon 6	g.98389721G>A	c.513G>A	p.(Trp171Ter)	TM1	This study	Täger et al., 2018	- (Aequorin-Bioassay)	488683	rs762773298	0.00081%	4	-	n.a.	n.a.	n.a.	38.0 (damaging)	n.a.	n.a.	n.a.	n.a.	n.a.	n.a.	n.a.	PVS1;PM2;PP5;PS3	Pathogenic
Exon 6	g.98389744T>A	c.536T>A	p.(Val179Asp)	TM1	Dubis et al., 2014	n.d.	n.d.	no entry	no entry	no entry	0	conserved	DELETERIOUS (score: 0.01, median: 3.38)	disease causing (prob: 1)	Class C35 (GV: 53.69 GD: 140.23)	25.3 (damaging)	7.64	152	n.a.	n.a.	n.a.	n.a.	n.a.	PM2;PM1;PP2;PP3	VUS
Exon 6	g.98389750A>G	c.542A>G	p.(Tyr181Cys)	TM1	Wissinger et al., 2001	Patel et al., 2005 Patel et al., 2005 Muraki-Oda et al., 2007	- (Ephys) + (Ephys, with glycerol) - (Ephys)	no entry	no entry	no entry	8	completely conserved	DELETERIOUS (score: 0, median: 3.38)	disease causing (prob: 1)	Class C65 (GV: 0.00 GD: 193.72)	26.1 (damaging)	8.90	194	n.a.	n.a.	n.a.	n.a.	n.a.	PP1;PS3;PM2;PM1;PP2;PP3	Pathogenic
Exon 6	g.98389752A>G	c.544A>G	p.(Asn182Asp)	TM1	This study	n.d.	n.d.	no entry	no entry	no entry	1	completely conserved	DELETERIOUS (score: 0, median: 3.38)	disease causing (prob: 1)	Class C15 (GV: 0.00 GD: 23.01)	25.3 (damaging)	8.90	23	n.a.	n.a.	n.a.	n.a.	n.a.	PM2;PM1;PP2;PM5;PP3	Likely pathogenic
Exon 6	g.98389752A>T	c.544A>T	p.(Asn182Tyr)	TM1	Wissinger et al., 2001	Patel et al., 2005 Muraki-Oda et al., 2007	- (Ephys) - (Ephys)	no entry	no entry	no entry	1	completely conserved	DELETERIOUS (score: 0, median: 3.38)	disease causing (prob: 1)	Class C65 (GV: 0.00 GD: 142.23)	25.4 (damaging)	8.90	143	n.a.	n.a.	n.a.	n.a.	n.a.	PS3;PM2;PM1;PP2;PP3	Likely pathogenic
Exon 6	g.98389764C>T	c.556C>T	p.(Leu186Phe)	TM1	Wissinger et al., 2001	Patel et al., 2005 Patel et al., 2005 Muraki-Oda et al., 2007	- (Ephys) + (Ephys, with glycerol) - (Ephys)	no entry	no entry	no entry	1	not conserved	DELETERIOUS (score: 0.04, median: 3.38)	disease causing (prob: 1)	Class C0 (GV: 30.92 GD: 21.28)	24.2 (damaging)	1.52	22	n.a.	n.a.	n.a.	n.a.	n.a.	PS3;PM2;PM1;PP2;PP3	Likely pathogenic
Exon 6	g.98389768T>C	c.560T>C	p.(Ile187Thr)	TM1 - TM2	Taylor et al., 2017	n.d.	n.d.	no entry	no entry	no entry	0	conserved	DELETERIOUS (score: 0.01, median: 3.38)	disease causing (prob: 0.982)	Class C25 (GV: 28.68 GD: 69.84)	23.2 (damaging)	7.64	89	n.a.	n.a.	n.a.	n.a.	n.a.	PP5;PM2;PM1;PP2;PP3	Likely pathogenic
Exon 6	g.98389774G>A	c.566G>A	p.(Arg189Lys)	TM1 - TM2	This study	n.d.	n.d.	no entry	no entry	no entry	1	completely conserved	DELETERIOUS (score: 0, median: 3.38)	disease causing (prob: 1)	Class C25 (GV: 0.00 GD: 26.00)	33.0 (damaging)	9.55	26	5' score reference: 94.22; mutant: 82.09 (-13%)	5' score reference: 9.88; mutant: 7.47 (-24%)	5' score reference: 0.99; mutant: 0.69 (-30%)	5' score reference: 11.93; mutant: 8.08 (-32%)	donor loss: 0.08 donor gain: 0.32	PM2;PM1;PP2;PP3	VUS
Exon 7	g.98391869G>A	c.572G>A	p.(Cys191Tyr)	TM1 - TM2	Wissinger et al., 2001	Patel et al., 2005 Muraki-Oda et al., 2007	+ (Ephys) - (Ephys)	866560	rs761554853	0.0022%	8	conserved	DELETERIOUS (score: 0.01, median: 3.38)	disease causing (prob: 1)	Class C0 (GV: 191.39 GD: 51.90)	25.4 (damaging)	6.41	194	n.a.	n.a.	n.a.	n.a.	n.a.	PP5;PM2;PP3;PP2	Likely pathogenic
Exon 7	g.98391877G>A	c.580G>A	p.(Glu194Lys)	TM1 - TM2	Wissinger et al., 2001	Muraki-Oda et al., 2007	- (Ephys)	no entry	no entry	no entry	1	conserved	DELETERIOUS (score: 0.02, median: 3.38)	disease causing (prob: 1)	Class C15 (GV: 44.60 GD: 56.87)	24.6 (damaging)	7.63	56	n.a.	n.a.	n.a.	n.a.	n.a.	PS3;PM2;PP3;PP2	Likely pathogenic
Exon 7	g.98391881T>C	c.584T>C	p.(Leu195Pro)	TM1 - TM2	ClinVar	n.d.	n.d.	898385	no entry	no entry	0	conserved	DELETERIOUS (score: 0, median: 3.38)	disease causing (prob: 1)	Class C65 (GV: 4.86 GD: 95.38)	27.5 (damaging)	7.52	98	n.a.	n.a.	n.a.	n.a.	n.a.	PM2;PP3;PP2	VUS
Exon 7	g.98391883C>T	c.586C>T	p.(Gln196Ter)	TM1 - TM2	Johnson et al., 2004	n.d.	n.d.	no entry	no entry	0.00041%	0	-	n.a.	n.a.	n.a.	39.0 (damaging)	n.a.	n.a.	n.a.	n.a.	n.a.	n.a.	n.a.	PVS1;PM2	Likely pathogenic
Exon 7	g.98391886T>C	c.589T>C	p.(Ser197Pro)	TM2	ClinVar	n.d.	n.d.	829838	rs1330263985	no entry	0	not conserved	TOLERATED (score: 0.27, median: 3.38)	disease causing (prob: 0.594)	Class C0 (GV: 201.18 GD: 0.00)	18.36 (tolerated)	0.91	74	n.a.	n.a.	n.a.	n.a.	n.a.	PM2;PP2;PP5	Likely pathogenic
Exon 7	g.98391888del	c.591del	p.(Glu198SerfsTer3)	TM2	This study	n.d.	n.d.	no entry	no entry	no entry	1	-	n.a.	n.a.	n.a.	n.a.	n.a.	n.a.	n.a.	n.a.	n.a.	n.a.	n.a.	PVS1;PM2	Likely pathogenic
Exon 7	g.98391905G>A	c.608G>A	p.(Trp203Ter)	TM2	Georgiou et al., 2019	n.d.	n.d.	no entry	no entry	no entry	0	-	n.a.	n.a.	n.a.	38.0 (damaging)	n.a.	n.a.	n.a.	n.a.	n.a.	n.a.	n.a.	PVS1;PM2	Likely pathogenic
Exon 7	g.98391906G>A	c.609G>A	p.(Trp203Ter)	TM2	Sun et al., 2020	n.d.	n.d.	no entry	no entry	no entry	0	-	n.a.	n.a.	n.a.	37.0 (damaging)	n.a.	n.a.	n.a.	n.a.	n.a.	n.a.	n.a.	PVS1;PM2	Likely pathogenic
Exon 7	g.98391906G>T	c.609G>T	p.(Trp203Cys)	TM2	This study	n.d.	n.d.	no entry	rs757650055	0.0011%	1	completely conserved	DELETERIOUS (score: 0, median: 3.38)	disease causing (prob: 1)	Class C65 (GV: 0.00 GD: 214.36)	26.8 (damaging)	9.55	215	n.a.	n.a.	n.a.	n.a.	n.a.	PM2;PP3;PP2	VUS
Exon 7	g.98391921C>G	c.624C>G	p.(Tyr208Ter)	TM2	Hull et al., 2020	n.d.	n.d.	no entry	no entry	no entry	0	-	n.a.	n.a.	n.a.	34.0 (damaging)	n.a.	n.a.	n.a.	n.a.	n.a.	n.a.	n.a.	PVS1;PM2	Likely pathogenic
Exon 7	g.98391930T>A	c.633T>A	p.(Asp211Glu)	TM2	Liang et al., 2015	n.d.	n.d.	no entry	rs553995770	0.00041%	0	completely conserved	DELETERIOUS (score: 0, median: 3.38)	disease causing (prob: 0.907)	Class C35 (GV: 0.00 GD: 44.60)	15.25 (tolerated)	-0.96	45	n.a.	n.a.	n.a.	n.a.	n.a.	PM2;PP2	VUS
Exon 7	g.98391946G>C	c.649G>C	p.(Asp217His)	TM2	ClinVar	n.d.	n.d.	867035	no entry	no entry	0	completely conserved	DELETERIOUS (score: 0, median: 3.38)	disease causing (prob: 1)	Class C65 (GV: 0.00 GD: 81.24)	27.6 (damaging)	9.29	81	n.a.	n.a.	n.a.	n.a.	n.a.	PM2;PP2;PP3	VUS
Exon 7	g.98391958C>T	c.661C>T	p.(Arg221Ter)	TM2	Johnson et al., 2004	n.d.	n.d.	962966	rs770713600	0.0018%	3	-	n.a.	n.a.	n.a.	36.0 (damaging)	n.a.	n.a.	n.a.	n.a.	n.a.	n.a.	n.a.	PVS1;PP5;PM2	Pathogenic
Exon 7	g.98391964C>T	c.667C>T	p.(Arg223Trp)	TM2	Wissinger et al., 2001	Muraki-Oda et al., 2007	- (Ephys)	498768	rs138958917	0.0076%	20	conserved	DELETERIOUS (score: 0, median: 3.38)	disease causing (prob: 1)	Class C35 (GV: 28.82 GD: 98.36)	25.4 (damaging)	0.89	101	n.a.	n.a.	n.a.	n.a.	n.a.	PP1;PS3;PP5;PM2;PM5;PP3;PP2	Pathogenic
Exon 7	g.98391964C>G	c.667C>G	p.(Arg223Gly)	TM2	Wiszniewski et al., 2007	n.d.	n.d.	812278	rs138958917	0.0033%	0	conserved	DELETERIOUS (score: 0.02, median: 3.38)	disease causing (prob: 1)	Class C35 (GV: 28.82 GD: 97.11)	24.3 (damaging)	0.89	125	n.a.	n.a.	n.a.	n.a.	n.a.	PM2;PM5;PP3;PP2;PP5	Likely pathogenic
Exon 7	g.98391965G>A	c.668G>A	p.(Arg223Gln)	TM2	Li et al., 2014; Greenberg et al., 2014	n.d.	n.d.	865874	rs762668060	0.0049%	4	conserved	DELETERIOUS (score: 0.04, median: 3.38)	disease causing (prob: 1)	Class C0 (GV: 28.82 GD: 19.90)	29.1 (damaging)	9.55	43	n.a.	n.a.	n.a.	n.a.	n.a.	PP5;PP1;PM2;PM5;PP3;PP2	Pathogenic
Exon 7	g.98391968C>G	c.671C>G	p.(Thr224Arg)	TM2 - TM3	Wissinger et al., 2001	Tränkner et al., 2004 Muraki-Oda et al., 2007	- (Imaging & Ephys) - (Ephys)	no entry	no entry	no entry	3	completely conserved	TOLERATED (score: 0.08, median: 3.38)	disease causing (prob: 1)	Class C0 (GV: 131.86 GD: 19.25)	27.0 (damaging)	7.53	71	5' score reference: 95.64; mutant: 92.58 (-3%)	5' score reference: 10.67; mutant: 10.03 (-6%)	5' score reference: 0.99; mutant: 0.99 (no effect)	5' score reference: 14.19; mutant: 11.95 (-16%)	donor loss: 0.00 donor gain: 0.00	PP1;PS3;PM2;PP3;PP2	Likely pathogenic
Intron 7	g.98395842A>C	c.674-2A>C	p.(?)	-	Li et al., 2014	n.d.	n.d.	no entry	no entry	no entry	0	-	n.a.	n.a.	n.a.	34.0 (damaging)	n.a.	n.a.	3' score reference: 87.76; mutant: 0 (-100%)	3' score reference: 12.24; mutant: 0 (-100%)	3' score reference: 1.00; mutant: 0 (-100%)	3' score reference: 11.42; mutant: 0 (-100%)	acceptor loss: 0.99 acceptor gain: 0.84	PVS1;PM2;PP3	Likely pathogenic
Exon 8	g.98393909_98399093del	c.674-1935_*1838del (Deletion Ex 8)	p.(?)	-	This study	n.d.	n.d.	no entry	no entry	no entry	2	-	n.a.	n.a.	n.a.	n.a.	n.a.	n.a.	n.a.	n.a.	n.a.	n.a.	n.a.	PVS1;PM2;PP1	Pathogenic
Exon 8	g.98395852G>A	c.682G>A	p.(Glu228Lys)	TM2 - TM3	Reuter et al., 2008	Reuter et al., 2008	+ (Imaging & Ephys)	337659	rs147415641	0.13%	8	conserved	DELETERIOUS (score: 0.03, median: 3.38)	disease causing (prob: 1)	Class C15 (GV: 44.60 GD: 56.87)	24.0 (damaging)	9.60	56	n.a.	n.a.	n.a.	n.a.	n.a.	PP1;PS3;PP5;PP3;PP2;BS1	Pathogenic
Exon 8	g.98395874A>T	c.704A>T	p.(Asp235Val)	TM2 - TM3	Weisschuh et al., 2020	n.d.	n.d.	813041	no entry	no entry	1	conserved	DELETERIOUS (score: 0, median: 3.38)	disease causing (prob: 1)	Class C35 (GV: 44.60 GD: 121.34)	24.5 (damaging)	8.95	152	n.a.	n.a.	n.a.	n.a.	n.a.	PM2;PP3;PP2;PP5	VUS
Exon 8	g.98395912C>T	c.742C>T	p.(Gln248Ter)	TM3	This study	n.d.	n.d.	no entry	no entry	no entry	1	-	n.a.	n.a.	n.a.	35.0 (damaging)	n.a.	n.a.	n.a.	n.a.	n.a.	n.a.	n.a.	PVS1;PM2	Likely pathogenic
Exon 8	g.98395916T>C	c.746T>C	p.(Phe249Ser)	TM3	Nishiguchi et al., 2005	n.d.	n.d.	no entry	no entry	no entry	3	conserved	DELETERIOUS (score: 0.01, median: 3.38)	disease causing (prob: 1)	Class C35 (GV: 43.96 GD: 140.15)	26.0 (damaging)	7.67	155	n.a.	n.a.	n.a.	n.a.	n.a.	PP1;PM2;PP3;PP2	VUS
Exon 8	g.98395924G>A	c.754G>A	p.(Asp252Asn)	TM3	Koeppen et al., 2008	Koeppen et al., 2008	- (Imaging)	no entry	no entry	no entry	4	completely conserved	DELETERIOUS (score: 0, median: 3.38)	disease causing (prob: 1)	Class C15 (GV: 0.00 GD: 23.01)	27.5 (damaging)	9.60	23	n.a.	n.a.	n.a.	n.a.	n.a.	PP1;PS3;PM2;PP3;PP2	Likely pathogenic
Exon 8	g.98395925A>C	c.755A>C	p.(Asp252Ala)	TM3	Sun et al., 2020	n.d.	n.d.	no entry	no entry	no entry	0	completely conserved	DELETERIOUS (score: 0, median: 3.36)	disease causing (prob: 1)	Class C65 (GV: 0.00 GD: 125.75)	27.0 (damaging)	8.76	126	n.a.	n.a.	n.a.	n.a.	n.a.	PM2;PP3;PP2	VUS
Exon 8	g.98395942C>G	c.772C>G	p.(Pro258Ala)	TM3	This study	n.d.	n.d.	no entry	no entry	no entry	1	completely conserved	DELETERIOUS (score: 0, median: 3.38)	disease causing (prob: 1)	Class C25 (GV: 0.00 GD: 26.87)	24.2 (damaging)	7.57	27	n.a.	n.a.	n.a.	n.a.	n.a.	PM2;PM5;PP3;PP2	VUS
Exon 8	g.98395943C>G	c.773C>G	p.(Pro258Arg)	TM3	Li et al., 2014	n.d.	n.d.	no entry	no entry	no entry	0	completely conserved	DELETERIOUS (score: 0, median: 3.38)	disease causing (prob: 1)	Class C65 (GV: 0.00 GD: 102.71)	25.2 (damaging)	7.57	103	n.a.	n.a.	n.a.	n.a.	n.a.	PM2;PP3;PP2	VUS
Exon 8	g.98395948G>A	c.778G>A	p.(Asp260Asn)	TM3	Wissinger et al., 2001	Muraki-Oda et al., 2007	- (Ephys)	689726	rs374258471	0.0029%	8	completely conserved	DELETERIOUS (score: 0, median: 3.38)	disease causing (prob: 1)	Class C15 (GV: 0.00 GD: 23.01)	27.2 (damaging)	9.60	23	n.a.	n.a.	n.a.	n.a.	n.a.	PP1;PS3;PP5;PM2;PP3;PP2	Pathogenic
Exon 8	g.98395948G>C	c.778G>C	p.(Asp260His)	TM3	This study	n.d.	n.d.	no entry	rs374258471	0.00081%	2	completely conserved	DELETERIOUS (score: 0, median: 3.38)	disease causing (prob: 1)	Class C65 (GV: 0.00 GD: 81.24)	26.7 (damaging)	9.60	81	n.a.	n.a.	n.a.	n.a.	n.a.	PM2;PM5;PP3;PP2	Likely pathogenic
Exon 8	g.98395948dup	c.778dup	p.(Asp260GlyfsTer27)	TM3	LOVD	n.d.	n.d.	987366	rs756172609	0.00040%	0	-	n.a.	n.a.	n.a.	n.a.	n.a.	n.a.	n.a.	n.a.	n.a.	n.a.	n.a.	PVS1;PP5;PM2	Pathogenic
Exon 8	g.98395957T>G	c.787T>G	p.(Tyr263Asp)	TM3	Nishiguchi et al., 2005	n.d.	n.d.	866862	rs943314733	no entry	0	conserved	DELETERIOUS (score: 0, median: 3.38)	disease causing (prob: 0.998)	Class C35 (GV: 37.91 GD: 146.11)	25.9 (damaging)	4.47	160	n.a.	n.a.	n.a.	n.a.	n.a.	PM2;PP5;PP3;PP2	Likely pathogenic
Exon 8	g.98395970G>A	c.800G>A	p.(Gly267Asp)	TM3 - TM4	Wissinger et al., 2001	Muraki-Oda et al., 2007	- (Ephys)	no entry	rs781673067	no entry	2	conserved	TOLERATED (score: 0.23, median: 3.38)	disease causing (prob: 1)	Class C0 (GV: 146.93 GD: 78.25)	26.0 (damaging)	9.60	94	n.a.	n.a.	n.a.	n.a.	n.a.	PP1;PS3;PM1;PP2;PM2;PP3	Pathogenic
Exon 8	g.98395981C>G	c.811C>G	p.(Pro271Ala)	TM3 - TM4	Zelinger et al., 2015	n.d.	n.d.	598143	rs149802213	0.012%	5	conserved	DELETERIOUS (score: 0, median: 3.38)	disease causing (prob: 1)	Class C25 (GV: 0.00 GD: 26.87)	23.8 (damaging)	7.57	27	n.a.	n.a.	n.a.	n.a.	n.a.	PP1;PP5;PM1;PP2;PM2;PP3	Likely pathogenic
Exon 8	g.98395981C>A	c.811C>A	p.(Pro271Thr)	TM3 - TM4	This study	n.d.	n.d.	no entry	rs149802213	0.00041%	1	conserved	DELETERIOUS (score: 0, median: 3.38)	disease causing (prob: 1)	Class C35 (GV: 0.00 GD: 37.56)	24.3 (damaging)	7.57	38	n.a.	n.a.	n.a.	n.a.	n.a.	PM1;PP2;PM2;PM5;PP3	Likely pathogenic
Exon 8	g.98395981C>T	c.811C>T	p.(Pro271Ser)	TM3 - TM4	Georgiou et al., 2019	n.d.	n.d.	no entry	no entry	no entry	0	conserved	DELETERIOUS (score: 0, median: 3.38)	disease causing (prob: 1)	Class C65 (GV: 0.00 GD: 73.35)	24.3 (damaging)	7.57	74	n.a.	n.a.	n.a.	n.a.	n.a.	PM1;PP2;PM2;PM5;PP3	Likely pathogenic
Exon 8	g.98395992G>T	c.822G>T	p.(Arg274Ser)	TM4	Azam et al., 2010	n.d.	n.d.	800820	rs368513591	0.0032%	2	completely conserved	DELETERIOUS (score: 0, median: 3.38)	disease causing (prob: 1)	Class C65 (GV: 0.00 GD: 109.21)	23.8 (damaging)	-0.01	110	n.a.	n.a.	n.a.	n.a.	n.a.	PM1;PP2;PM2;PP3;PM5	Likely pathogenic
Exon 8	g.98395991G>A	c.821G>A	p.(Arg274Lys)	TM4	Li et al., 2014	n.d.	n.d.	no entry	no entry	no entry	0	completely conserved	DELETERIOUS (score: 0, median: 3.38)	disease causing (prob: 1)	Class C25 (GV: 0.00 GD: 26.00)	26.5 (damaging)	9.60	26	n.a.	n.a.	n.a.	n.a.	n.a.	PM1;PP2;PM2;PP3	Likely pathogenic
Exon 8	g.98395997A>G	c.827A>G	p.(Asn276Ser)	TM4	Saqib et al., 2011	n.d.	n.d.	156335	rs199474697	no entry	0	completely conserved	DELETERIOUS (score: 0, median: 3.38)	disease causing (prob: 1)	Class C45 (GV: 0.00 GD: 46.24)	24.9 (damaging)	8.95	46	n.a.	n.a.	n.a.	n.a.	n.a.	PM1;PP1;PP2;PM2;PP3	Likely pathogenic
Exon 8	g.98395999C>T	c.829C>T	p.(Arg277Cys)	TM4	Wissinger et al., 2001	Liu and Varnum, 2005 Muraki-Oda et al., 2007	- (Ephys) - (Ephys)	9481	rs104893620	0.011%	48	conserved	DELETERIOUS (score: 0, median: 3.38)	disease causing (prob: 1)	Class C65 (GV: 0.00 GD: 179.53)	26.8 (damaging)	3.58	180	n.a.	n.a.	n.a.	n.a.	n.a.	PP1;PS3;PP5;PM1;PP2;PM2;PM5;PP3	Pathogenic
Exon 8	g.98395999C>G	c.829C>G	p.(Arg277Gly)	TM4	Koeppen et al., 2010	n.d.	n.d.	no entry	no entry	no entry	1	conserved	DELETERIOUS (score: 0, median: 3.38)	disease causing (prob: 1)	Class C65 (GV: 0.00 GD: 125.13)	25.3 (damaging)	3.58	125	n.a.	n.a.	n.a.	n.a.	n.a.	PS1;PM5;PM1;PP2;PM2;PP3	Likely pathogenic
Exon 8	g.98396000G>A	c.830G>A	p.(Arg277His)	TM4	Wissinger et al., 2001	Muraki-Oda et al., 2007	- (Ephys)	800983	rs778114016	0.0024%	19	conserved	DELETERIOUS (score: 0, median: 3.38)	disease causing (prob: 1)	Class C25 (GV: 0.00 GD: 28.82)	27.6 (damaging)	7.81	29	n.a.	n.a.	n.a.	n.a.	n.a.	PP1;PS3;PP5;PS1;PM5;PM1;PP2;PM2;PP3	Pathogenic
Exon 8	g.98396003T>C	c.833T>C	p.(Leu278Pro)	TM4	Li et al., 2014	n.d.	n.d.	no entry	rs763421555	0.00041%	0	completely conserved	DELETERIOUS (score: 0, median: 3.38)	disease causing (prob: 1)	Class C65 (GV: 0.00 GD: 97.78)	27.4 (damaging)	7.67	98	n.a.	n.a.	n.a.	n.a.	n.a.	PM1;PP2;PM2;PP3	Likely pathogenic
Exon 8	g.98396008A>T	c.838A>T	p.(Lys280Ter)	TM4	Wang et al., 2019	n.d.	n.d.	no entry	no entry	no entry	0	-	n.a.	n.a.	n.a.	36.0 (damaging)	n.a.	n.a.	n.a.	n.a.	n.a.	n.a.	n.a.	PVS1;PM2	Likely pathogenic
Exon 8	g.98396017C>T	c.847C>T	p.(Arg283Trp)	TM4	Kohl et al., 1998	Muraki-Oda et al., 2007	- (Ephys)	9474	rs104893613	0.011%	84	completely conserved	DELETERIOUS (score: 0, median: 3.38)	disease causing (prob: 1)	Class C65 (GV: 0.00 GD: 101.29)	25.4 (damaging)	0.55	101	n.a.	n.a.	n.a.	n.a.	n.a.	PP1;PS3;PP5;PS1;PM5;PM1;PP2;PM2;PP3	Pathogenic

Exon 8	g.98396636G>T	c.1466G>T	p.(Gly489Val)	CNBD αA	This study	n.d.	n.d.	no entry	no entry	no entry	1	completely conserved	DELETERIOUS (score: 0, median: 3.38)	disease causing (prob: 1)	Class C0 (GV: 206.04 GD: 97.05)	26.7 (damaging)	9.60	109	n.a.	n.a.	n.a.	n.a.	n.a.	PM1;PP2;PM2;PP3	Likely pathogenic
Exon 8	g.98396665C>T	c.1495C>T	p.(Arg499Ter)	CNBD β1	Burgueño-Montañés et al., 2014	n.d.	n.d.	no entry	no entry	0.0011%	19	-	n.a.	n.a.	n.a.	36.0 (damaging)	n.a.	n.a.	n.a.	n.a.	n.a.	n.a.	n.a.	PP1;PVS1;PM2	Likely pathogenic
Exon 8	g.98396683C>G	c.1513C>G	p.(Pro505Ala)	CNBD β1 - β2	Huang et al., 2016	n.d.	n.d.	no entry	no entry	no entry	0	completely conserved	DELETERIOUS (score: 0, median: 3.38)	disease causing (prob: 1)	Class C0 (GV: 208.63 GD: 1.62)	24.7 (damaging)	7.57	27	n.a.	n.a.	n.a.	n.a.	n.a.	PM1;PP2;PM2;PP3	Likely pathogenic
Exon 8	g.98396689del	c.1519del	p.(Asp507IlefsTer47)	CNBD β1 - β2	This study	n.d.	n.d.	no entry	no entry	no entry	1	-	n.a.	n.a.	n.a.	n.a.	n.a.	n.a.	n.a.	n.a.	n.a.	n.a.	n.a.	PVS1;PM2	Likely pathogenic
Exon 8	g.98396690A>G	c.1520A>G	p.(Asp507Gly)	CNBD β1 - β2	LOVD	n.d.	n.d.	959907	no entry	0.0016%	0	completely conserved	DELETERIOUS (score: 0, median: 3.38)	disease causing (prob: 1)	Class C0 (GV: 213.16 GD: 64.73)	28.0 (damaging)	8.94	94	n.a.	n.a.	n.a.	n.a.	n.a.	PM1;PP2;PM2;PP3	Likely pathogenic
Exon 8	g.98396699G>C	c.1529G>C	p.(Cys510Ser)	CNBD β2	Wissinger et al., 2001	Muraki-Oda et al., 2007	- (Ephys)	no entry	no entry	0.00041%	2	completely conserved	DELETERIOUS (score: 0, median: 3.38)	disease causing (prob: 1)	Class C0 (GV: 213.42 GD: 59.88)	26.8 (damaging)	9.60	112	n.a.	n.a.	n.a.	n.a.	n.a.	PS3;PM1;PP2;PM2;PP3	Pathogenic
Exon 8	g.98396705A>T	c.1535A>T	p.(Lys512Met)	CNBD β2 - β3	Carrigan et al., 2016	n.d.	n.d.	no entry	no entry	no entry	0	completely conserved	DELETERIOUS (score: 0, median: 3.38)	disease causing (prob: 1)	Class C0 (GV: 238.71 GD: 90.63)	26.0 (damaging)	7.16	95	n.a.	n.a.	n.a.	n.a.	n.a.	PM1;PP2;PM2;PP3	Likely pathogenic
Exon 8	g.98396707G>C	c.1537G>C	p.(Gly513Arg)	CNBD β2 - β3	Huang et al., 2016	n.d.	n.d.	no entry	no entry	no entry	0	completely conserved	DELETERIOUS (score: 0, median: 3.38)	disease causing (prob: 1)	Class C15 (GV: 206.04 GD: 124.98)	27.9 (damaging)	9.60	125	n.a.	n.a.	n.a.	n.a.	n.a.	PM1;PP2;PM2;PM5;PP3	Likely pathogenic
Exon 8	g.98396707G>A	c.1537G>A	p.(Gly513Arg)	CNBD β2 - β3	This study	n.d.	n.d.	no entry	rs764918448	0.00041%	1	completely conserved	DELETERIOUS (score: 0, median: 3.38)	disease causing (prob: 1)	Class C15 (GV: 206.04 GD: 124.98)	28.2 (damaging)	9.60	125	n.a.	n.a.	n.a.	n.a.	n.a.	PM1;PP2;PM2;PM5;PP3	Likely pathogenic
Exon 8	g.98396708G>A	c.1538G>A	p.(Gly513Glu)	CNBD β2 - β3	Wissinger et al., 2001	Muraki-Oda et al., 2007	- (Ephys)	no entry	no entry	no entry	3	completely conserved	DELETERIOUS (score: 0, median: 3.38)	disease causing (prob: 1)	Class C0 (GV: 206.04 GD: 97.07)	27.0 (damaging)	9.60	98	n.a.	n.a.	n.a.	n.a.	n.a.	PP1;PS3;PM1;PP2;PM2;PP3	Pathogenic
Exon 8	g.98396710G>A	c.1540G>A	p.(Asp514Asn)	CNBD β2 - β3	Arshad et al., 2019	n.d.	n.d.	no entry	no entry	no entry	0	completely conserved	DELETERIOUS (score: 0, median: 3.38)	disease causing (prob: 1)	Class C0 (GV: 213.16 GD: 22.75)	28.3 (damaging)	9.60	23	n.a.	n.a.	n.a.	n.a.	n.a.	PP1;PM1;PP2;PM2;PP3	Likely pathogenic
Exon 8	g.98396711A>T	c.1541A>T	p.(Asp514Val)	CNBD β2 - β3	Genead et al., 2011	n.d.	n.d.	no entry	rs767904913	no entry	0	completely conserved	DELETERIOUS (score: 0, median: 3.38)	disease causing (prob: 1)	Class C15 (GV: 213.16 GD: 119.12)	27.2 (damaging)	8.94	152	n.a.	n.a.	n.a.	n.a.	n.a.	PM1;PP2;PM2;PP3	Likely pathogenic
Exon 8	g.98396717G>A	c.1547G>A	p.(Gly516Glu)	CNBD β2 - β3	Wissinger et al., 2001	Muraki-Oda et al., 2007	- (Ephys)	no entry	no entry	no entry	3	completely conserved	DELETERIOUS (score: 0, median: 3.38)	disease causing (prob: 1)	Class C0 (GV: 206.04 GD: 97.07)	27.0 (damaging)	9.60	98	n.a.	n.a.	n.a.	n.a.	n.a.	PP1;PS3;PM1;PP2;PM2;PP3	Pathogenic
Exon 8	g.98396726T>C	c.1556T>C	p.(Met519Thr)	CNBD β3	Huang et al., 2016	n.d.	n.d.	no entry	no entry	no entry	0	completely conserved	DELETERIOUS (score: 0, median: 3.38)	disease causing (prob: 1)	Class C0 (GV: 231.87 GD: 46.93)	25.6 (damaging)	7.67	81	n.a.	n.a.	n.a.	n.a.	n.a.	PM1;PP2;PM2;PP3	Likely pathogenic
Exon 8	g.98396727G>A	c.1557G>A	p.(Met519Ile)	CNBD β3	Ellingford et al., 2016	n.d.	n.d.	236463	rs199655686	0.0058%	3	completely conserved	DELETERIOUS (score: 0, median: 3.38)	disease causing (prob: 1)	Class C0 (GV: 231.87 GD: 10.12)	26.5 (damaging)	9.60	10	n.a.	n.a.	n.a.	n.a.	n.a.	PM1;PP2;PM2;PP3	Likely pathogenic
Exon 8	g.98396735T>C	c.1565T>C	p.(Ile522Thr)	CNBD β3	Wissinger et al., 2001	Koeppen et al., 2008 Muraki-Oda et al., 2007	- (Imaging) - (Ephys)	no entry	no entry	no entry	2	conserved	DELETERIOUS (score: 0.01, median: 3.38)	disease causing (prob: 1)	Class C0 (GV: 234.99 GD: 43.70)	26.2 (damaging)	7.67	89	n.a.	n.a.	n.a.	n.a.	n.a.	PS3;PM2;PP3;PP2	Likely pathogenic
Exon 8	g.98396739_98396747del	c.1569_1577del	p.(Asn523_Gly525del)	CNBD β3	Sun et al., 2020	n.d.	n.d.	no entry	no entry	no entry	0	-	n.a.	n.a.	n.a.	n.a.	n.a.	n.a.	n.a.	n.a.	n.a.	n.a.	n.a.	PM2;PM4	VUS
Exon 8	g.98396743G>A	c.1573G>A	p.(Gly525Ser)	CNBD β3 - β4	Patel et al., 2016	n.d.	n.d.	191122	rs786205532	no entry	0	completely conserved	DELETERIOUS (score: 0, median: 3.38)	disease causing (prob: 1)	Class C0 (GV: 206.04 GD: 29.56)	26.4 (damaging)	9.60	56	n.a.	n.a.	n.a.	n.a.	n.a.	PM1;PP2;PM2;PP3;PP5	Likely pathogenic
Exon 8	g.98396744G>A	c.1574G>A	p.(Gly525Asp)	CNBD β3 - β4	Wissinger et al., 2001	Koeppen et al., 2008 Muraki-Oda et al., 2007	- (Imaging) - (Ephys)	no entry	no entry	no entry	3	completely conserved	DELETERIOUS (score: 0, median: 3.38)	disease causing (prob: 1)	Class C0 (GV: 206.04 GD: 82.83)	26.1 (damaging)	9.60	94	n.a.	n.a.	n.a.	n.a.	n.a.	PP1;PS3;PM1;PP2;PM2;PM5;PP3	Pathogenic
Exon 8	g.98396749C>A	c.1579C>A	p.(Leu527Met)	CNBD β4	Wang et al., 2011	n.d.	n.d.	988792	no entry	no entry	2	completely conserved	DELETERIOUS (score: 0, median: 3.38)	disease causing (prob: 1)	Class C0 (GV: 234.72 GD: 12.95)	23.1 (damaging)	1.36	15	n.a.	n.a.	n.a.	n.a.	n.a.	PM1;PP2;PM2;PM5;PP3;PP5	Likely pathogenic
Exon 8	g.98396750T>G	c.1580T>G	p.(Leu527Arg)	CNBD β4	Lam et al., 2011	n.d.	n.d.	no entry	rs779023431	0.00081%	2	completely conserved	DELETERIOUS (score: 0, median: 3.38)	disease causing (prob: 1)	Class C0 (GV: 234.72 GD: 91.58)	26.3 (damaging)	7.67	102	n.a.	n.a.	n.a.	n.a.	n.a.	PP1;PM1;PP2;PM2;PM5;PP3	Likely pathogenic
Exon 8	g.98396755G>A	c.1585G>A	p.(Val529Met)	CNBD β4	Kohl et al., 1998	Muraki-Oda et al., 2007	- (Ephys)	9480	rs104893619	0.0065%	9	completely conserved	DELETERIOUS (score: 0, median: 3.38)	disease causing (prob: 1)	Class C0 (GV: 223.30 GD: 20.52)	25.7 (damaging)	9.60	21	n.a.	n.a.	n.a.	n.a.	n.a.	PP1;PS3;PP5;PM1;PP2;PM2;PP3	Pathogenic
Exon 8	g.98396767G>C	c.1597G>C	p.(Asp533His)	CNBD β4 - β5	Li et al., 2014	n.d.	n.d.	282547	rs775332304	0.00081%	0	completely conserved	DELETERIOUS (score: 0, median: 3.38)	disease causing (prob: 1)	Class C0 (GV: 213.16 GD: 59.84)	25.8 (damaging)	9.60	81	n.a.	n.a.	n.a.	n.a.	n.a.	PP5;PM1;PP2;PM2;PP3	Pathogenic
Exon 8	g.98396779C>T	c.1609C>T	p.(Gln537Ter)	CNBD β4 - β5	Wissinger et al., 2001	n.d.	n.d.	no entry	no entry	no entry	1	-	n.a.	n.a.	n.a.	39.0 (damaging)	n.a.	n.a.	n.a.	n.a.	n.a.	n.a.	n.a.	PVS1;PM2	Likely pathogenic
Exon 8	g.98396791C>T	c.1621C>T	p.(Leu541Phe)	CNBD β5	Greenberg et al., 2014	n.d.	n.d.	no entry	no entry	no entry	2	completely conserved	DELETERIOUS (score: 0, median: 3.38)	disease causing (prob: 1)	Class C15 (GV: 0.00 GD: 21.82)	24.6 (damaging)	4.07	22	n.a.	n.a.	n.a.	n.a.	n.a.	PP1;PM2;PM1;PP2;PP3	Likely pathogenic
Exon 8	g.98396797_98396805del	c.1627_1635del	p.(Asp543_Ser545del)	CNBD β5/β5 - β6	Li et al., 2014	n.d.	n.d.	no entry	no entry	no entry	0	-	n.a.	n.a.	n.a.	n.a.	n.a.	n.a.	n.a.	n.a.	n.a.	n.a.	n.a.	PM2;PM4;PM1	VUS
Exon 8	g.98396810T>G	c.1640T>G	p.(Phe547Cys)	CNBD β6	Zelinger et al., 2015	n.d.	n.d.	no entry	no entry	no entry	0	completely conserved	DELETERIOUS (score: 0, median: 3.38)	disease causing (prob: 1)	Class C65 (GV: 0.00 GD: 204.39)	26.2 (damaging)	7.67	205	n.a.	n.a.	n.a.	n.a.	n.a.	PP1;PS1;PM5;PM1;PP2;PM2;PP3;PP5	Likely pathogenic
Exon 8	g.98396811C>A	c.1641C>A	p.(Phe547Leu)	CNBD β6	Kohl et al., 1998	Reuter et al., 2008 Reuter et al., 2008 Muraki-Oda et al., 2007 Matveev et al., 2010	- (Imaging, 37°C) + (Imaging & Ephys, 27°C) - (Ephys) - (Imaging & Ephys)	9478	rs104893617	0.016%	86	completely conserved	DELETERIOUS (score: 0, median: 3.38)	disease causing (prob: 1)	Class C15 (GV: 0.00 GD: 21.82)	20.3 (damaging)	0.03	22	n.a.	n.a.	n.a.	n.a.	n.a.	PP1;PS3;PP5;PS1;PM5;PM1;PP2;PM2;PP3	Pathogenic
Exon 8	g.98396812G>A	c.1642G>A	p.(Gly548Arg)	CNBD β6	Johnson et al., 2004	n.d.	n.d.	812283	rs781227859	0.0024%	5	completely conserved	DELETERIOUS (score: 0, median: 3.38)	disease causing (prob: 1)	Class C65 (GV: 0.00 GD: 125.13)	26.2 (damaging)	9.60	125	n.a.	n.a.	n.a.	n.a.	n.a.	PP1;PP5;PM1;PP2;PM2;PP3	Pathogenic
Exon 8	g.98396815G>T	c.1645G>T	p.(Glu549Ter)	CNBD β6	This study	n.d.	n.d.	no entry	no entry	0.00041%	1	-	n.a.	n.a.	n.a.	41.0 (damaging)	n.a.	n.a.	n.a.	n.a.	n.a.	n.a.	n.a.	PVS1;PM2	Likely pathogenic
Exon 8	g.98396828T>A	c.1658T>A	p.(Leu553Gln)	CNBD β6 - β7	This study	n.d.	n.d.	no entry	rs745779023	0.00040%	1	completely conserved	DELETERIOUS (score: 0, median: 3.38)	disease causing (prob: 1)	Class C65 (GV: 0.00 GD: 112.44)	26.9 (damaging)	7.67	113	n.a.	n.a.	n.a.	n.a.	n.a.	PM1;PP2;PM2;PP3	Likely pathogenic
Exon 8	g.98396839G>A	c.1669G>A	p.(Gly557Arg)	CNBD β6 - β7	Kohl et al., 1998	Reuter et al., 2008 Muraki-Oda et al., 2007	+ (Imaging & Ephys) + (Ephys)	9476	rs104893615	0.015%	9	completely conserved	DELETERIOUS (score: 0, median: 3.38)	disease causing (prob: 1)	Class C65 (GV: 0.00 GD: 125.13)	27.7 (damaging)	9.60	125	n.a.	n.a.	n.a.	n.a.	n.a.	PP1;PS3;PM1;PP2;PM2;PP3;PP5	Pathogenic
Exon 8	g.98396849C>T	c.1679C>T	p.(Ser560Leu)	CNBD β6 - β7	ClinVar	n.d.	n.d.	337664	rs370911601	0.0032%	0	not conserved	DELETERIOUS (score: 0.02, median: 3.38)	disease causing (prob: 0.999)	Class C0 (GV: 116.80 GD: 72.45)	23.2 (damaging)	2.21	145	n.a.	n.a.	n.a.	n.a.	n.a.	PM1;PP2;PM2;PP3	Likely pathogenic
Exon 8	g.98396852G>A	c.1682G>A	p.(Gly561Glu)	CNBD β6 - β7	Zobor et al., 2017	n.d.	n.d.	no entry	no entry	no entry	1	completely conserved	DELETERIOUS (score: 0, median: 3.38)	disease causing (prob: 1)	Class C65 (GV: 0.00 GD: 97.85)	27.2 (damaging)	9.60	98	n.a.	n.a.	n.a.	n.a.	n.a.	PM1;PP2;PM2;PP3	Likely pathogenic
Exon 8	g.98396852_98396853insACGCG	c.1682_1683insACGCG	p.(Asn562ArgfsTer47)	CNBD β6 - β7	This study	n.d.	n.d.	no entry	no entry	no entry	1	-	n.a.	n.a.	n.a.	n.a.	n.a.	n.a.	n.a.	n.a.	n.a.	n.a.	n.a.	PVS1;PM2	Likely pathogenic
Exon 8	g.98396856C>A	c.1686C>A	p.(Asn562Lys)	CNBD β6 - β7	ClinVar	n.d.	n.d.	865797	no entry	no entry	0	completely conserved	DELETERIOUS (score: 0, median: 3.38)	disease causing (prob: 1)	Class C65 (GV: 0.00 GD: 93.88)	23.6 (damaging)	1.50	94	n.a.	n.a.	n.a.	n.a.	n.a.	PM1;PP2;PM2;PP3;PP5	Likely pathogenic
Exon 8	g.98396857C>T	c.1687C>T	p.(Arg563Cys)	CNBD β6 - β7	Koeppen et al., 2008	Koeppen et al., 2008	+ (Imaging & Ephys)	596480	rs150153987	0.0022%	2	completely conserved	DELETERIOUS (score: 0, median: 3.38)	disease causing (prob: 1)	Class C65 (GV: 0.00 GD: 179.53)	27.1 (damaging)	1.56	180	n.a.	n.a.	n.a.	n.a.	n.a.	PS3;PM1;PP2;PM2;PM5;PP3;PP5	Pathogenic
Exon 8	g.98396858G>A	c.1688G>A	p.(Arg563His)	CNBD β6 - β7	Wissinger et al., 2001	Liu and Varnum, 2005 Muraki-Oda et al., 2007 Muraki-Oda et al., 2007	+ (Ephys) - (Ephys) ++ (Ephys, +B3)	265467	rs552069173	0.0072%	8	completely conserved	DELETERIOUS (score: 0, median: 3.38)	disease causing (prob: 1)	Class C25 (GV: 0.00 GD: 28.82)	29.4 (damaging)	9.60	29	n.a.	n.a.	n.a.	n.a.	n.a.	PS4;PP1;PS3;PP5;PM1;PP2;PM2;PM5;PP3	Pathogenic
Exon 8	g.98396864C>T	c.1694C>T	p.(Thr565Met)	CNBD β6 - β7	Wissinger et al., 2001	Muraki-Oda et al., 2007	+ (Ephys)	867082	rs201747279	0.017%	11	completely conserved	DELETERIOUS (score: 0, median: 3.38)	disease causing (prob: 1)	Class C65 (GV: 0.00 GD: 81.04)	25.6 (damaging)	7.57	81	n.a.	n.a.	n.a.	n.a.	n.a.	PP1;PS3;PP5;PM1;PP2;PM2;PP3	Pathogenic
Exon 8	g.98396875C>T	c.1705C>T	p.(Arg569Cys)	CNBD β7	This study	n.d.	n.d.	862038	rs757167624	0.0011%	1	conserved	DELETERIOUS (score: 0, median: 3.38)	disease causing (prob: 1)	Class C65 (GV: 0.00 GD: 179.53)	23.9 (damaging)	1.28	180	n.a.	n.a.	n.a.	n.a.	n.a.	PM1;PP2;PM2;PM5;PP3	Likely pathogenic
Exon 8	g.98396876G>A	c.1706G>A	p.(Arg569His)	CNBD β7	Wissinger et al., 2001	Koeppen et al., 2008 Muraki-Oda et al., 2007	- (Imaging) - (Ephys)	861698	rs201782746	0.0022%	11	conserved	DELETERIOUS (score: 0, median: 3.38)	disease causing (prob: 1)	Class C25 (GV: 0.00 GD: 28.82)	26.0 (damaging)	5.62	29	n.a.	n.a.	n.a.	n.a.	n.a.	PP1;PS3;PP5;PM1;PP2;PM2;PP3	Pathogenic
Exon 8	g.98396878A>G	c.1708A>G	p.(Ser570Gly)	CNBD β7	This study	n.d.	n.d.	no entry	no entry	no entry	2	completely conserved	DELETERIOUS (score: 0, median: 3.38)	disease causing (prob: 1)	Class C55 (GV: 0.00 GD: 55.27)	25.8 (damaging)	8.95	56	n.a.	n.a.	n.a.	n.a.	n.a.	PP1;PM1;PP2;PM2;PP3	Likely pathogenic
Exon 8	g.98396879G>A	c.1709G>A	p.(Ser570Asn)	CNBD β7	Li et al., 2014	n.d.	n.d.	no entry	no entry	no entry	0	completely conserved	DELETERIOUS (score: 0, median: 3.38)	disease causing (prob: 1)	Class C45 (GV: 0.00 GD: 46.24)	25.6 (damaging)	9.60	46	n.a.	n.a.	n.a.	n.a.	n.a.	PM1;PP2;PM2;PP3	Likely pathogenic
Exon 8	g.98396879G>T	c.1709G>T	p.(Ser570Ile)	CNBD β7	Thiadens et al., 2010	n.d.	n.d.	no entry	no entry	no entry	1	completely conserved	DELETERIOUS (score: 0, median: 3.38)	disease causing (prob: 1)	Class C65 (GV: 0.00 GD: 141.80)	26.6 (damaging)	9.60	142	n.a.	n.a.	n.a.	n.a.	n.a.	PM1;PP2;PM2;PP3	Likely pathogenic
Exon 8	g.98396882T>C	c.1712T>C	p.(Ile571Thr)	CNBD β7 - β8	Jinda et al., 2021	n.d.	n.d.	289061	rs750456621	0.00080%	0	conserved	DELETERIOUS (score: 0.01, median: 3.36)	disease causing (prob: 1)	Class C25 (GV: 30.92 GD:69.84)	25.1 (damaging)	7.53	89	n.a.	n.a.	n.a.	n.a.	n.a.	PP1;PM1;PP2;PM2;PP3	Likely pathogenic
Exon 8	g.98396887T>C	c.1717T>C	p.(Tyr573His)	CNBD β7 - β8	This study	n.d.	n.d.	no entry	no entry	0.0032%	3	completely conserved	DELETERIOUS (score: 0, median: 3.38)	disease causing (prob: 1)	Class C65 (GV: 0.00 GD: 83.33)	26.2 (damaging)	7.67	83	n.a.	n.a.	n.a.	n.a.	n.a.	PM1;PP1;PP2;PM2;PM5;PP3	Likely pathogenic
Exon 8	g.98396888A>G	c.1718A>G	p.(Tyr573Cys)	CNBD β7 - β8	Wissinger et al., 2001	Muraki-Oda et al., 2007	- (Ephys)	no entry	no entry	no entry	1	completely conserved	DELETERIOUS (score: 0, median: 3.38)	disease causing (prob: 1)	Class C65 (GV: 0.00 GD: 193.72)	27.1 (damaging)	8.95	194	n.a.	n.a.	n.a.	n.a.	n.a.	PS3;PM1;PP2;PM2;PP3	Pathogenic
Exon 8	g.98396889C>G	c.1719C>G	p.(Tyr573Ter)	CNBD β7 - β8	Holtan et al., 2020	n.d.	n.d.	no entry	no entry	no entry	0	-	n.a.	n.a.	n.a.	37.0 (damaging)	n.a.	n.a.	n.a.	n.a.	n.a.	n.a.	n.a.	PVS1;PM2	Likely pathogenic
Exon 8	g.98396906T>G	c.1736T>G	p.(Leu579Arg)	CNBD β8	This study	n.d.	n.d.	no entry	no entry	no entry	1	completely conserved	DELETERIOUS (score: 0, median: 3.38)	disease causing (prob: 1)	Class C65 (GV: 0.00 GD: 101.88)	26.1 (damaging)	7.67	102	n.a.	n.a.	n.a.	n.a.	n.a.	PM1;PP2;PM2;PP3	Likely pathogenic
Exon 8	g.98396938G>A	c.1768G>A	p.(Glu590Lys)	CNBD αB	Nishiguchi et al., 2005	Reuter et al., 2008	+ (Imaging & Ephys)	800759	rs763041373	0.00072%	3	conserved	DELETERIOUS (score: 0.02, median: 3.38)	disease causing (prob: 1)	Class C15 (GV: 44.60 GD: 56.87)	25.9 (damaging)	9.60	56	n.a.	n.a.	n.a.	n.a.	n.a.	PP1;PS3;PP5;PM1;PP2;PM2;PP3	Pathogenic
Exon 8	g.98396941T>C	c.1771T>C	p.(Tyr591His)	CNBD αB - αC	This study	n.d.	n.d.	no entry	no entry	no entry	1	completely conserved	DELETERIOUS (score: 0, median: 3.38)	disease causing (prob: 1)	Class C65 (GV: 0.00 GD: 83.33)	26.1 (damaging)	7.67	83	n.a.	n.a.	n.a.	n.a.	n.a.	PM1;PP2;PM2;PP3	Likely pathogenic
Exon 8	g.98396945C>T	c.1775C>T	p.(Pro592Leu)	CNBD αB - αC	This study	n.d.	n.d.	no entry	no entry	0.00041%	2	completely conserved	DELETERIOUS (score: 0, median: 3.38)	disease causing (prob: 1)	Class C65 (GV: 0.00 GD: 97.78)	25.4 (damaging)	7.57	98	n.a.	n.a.	n.a.	n.a.	n.a.	PM1;PP2;PM2;PP3	Likely pathogenic
Exon 8	g.98396947G>A	c.1777G>A	p.(Glu593Lys)	CNBD αC	Wissinger et al., 2001	Muraki-Oda et al., 2007	+ (Ephys)	503564	rs774676415	0.0012%	0	not conserved	TOLERATED (score: 0.06, median: 3.38)	disease causing (prob: 1)	Class C15 (GV: 44.60 GD: 56.87)	24.7 (damaging)	9.60	56	n.a.	n.a.	n.a.	n.a.	n.a.	PS3;PM1;PP2;PM2;PP3;PP5	Pathogenic
Exon 8	g.98396963T>G	c.1793T>G	p.(Leu598Arg)	CNBD αC	Sun et al., 2020	n.d.	n.d.	no entry	no entry	no entry	0	completely conserved	DELETERIOUS (score: 0, median: 3.36)	disease causing (prob: 1)	Class C65 (GV: 0.00 GD: 101.88)	28.3 (damaging)	7.53	102	n.a.	n.a.	n.a.	n.a.	n.a.	PM2;PM1;PP2;PP3	VUS
Exon 8	g.98396975G>A	c.1805G>A	p.(Gly602Glu)	CNBD αC	Georgiou et al., 2019	n.d.	n.d.	no entry	no entry	no entry	0	completely conserved	DELETERIOUS (score: 0, median: 3.38)	disease causing (prob: 1)	Class C65 (GV: 0.00 GD: 97.85)	27.8 (damaging)	9.60	98	n.a.	n.a.	n.a.	n.a.	n.a.	PP1;PM2;PM1;PP2;PP3	Likely pathogenic
Exon 8	g.98396980C>T	c.1810C>T	p.(Gln604Ter)	CNBD αC	Taylor et al., 2017	n.d.	n.d.	444512	rs753692812	0.00041%	2	-	n.a.	n.a.	n.a.	39.0 (damaging)	n.a.	n.a.	n.a.	n.a.	n.a.	n.a.	n.a.	PVS1;PM2;PP5	Likely pathogenic
Exon 8	g.98396981del	c.1811del	p.(Gln604ArgfsTer3)	CNBD αC	Sun et al., 2020	n.d.	n.d.	no entry	no entry	no entry	0	-	n.a.	n.a.	n.a.	n.a.	n.a.	n.a.	n.a.	n.a.	n.a.	n.a.	n.a.	PVS1;PM2	Likely pathogenic
Exon 8	g.98397068T>C	c.1898T>C	p.(Leu633Pro)	CLZ	Goto-Omoto et al., 2006	Dai and Varnum, 2013	+ (Ephys)	no entry	no entry	no entry	0	not conserved	DELETERIOUS (score: 0, median: 3.38)	disease causing (prob: 1)	Class C45 (GV: 14.30 GD: 86.59)	24.2 (damaging)	7.67	98	n.a.	n.a.	n.a.	n.a.	n.a.	PS3;PM2;PP3;PP2	Likely pathogenic
Exon 8	g.98397101T>C	c.1931T>C	p.(Phe644Ser)	CLZ	Ellingford et al., 2016	n.d.	n.d.	236462	rs878853359	no entry	0	conserved	DELETERIOUS (score: 0.01, median: 3.38)	disease causing (prob: 1)	Class C45 (GV: 30.27 GD: 134.86)	24.8 (damaging)	7.67	155	n.a.	n.a.	n.a.	n.a.	n.a.	PM2;PP3;PP2	VUS
Exon 8	g.98397107G>A	c.1937G>A	p.(Arg646His)	CLZ	Li et al., 2014	n.d.	n.d.	no entry	rs141577844	0.0025%	0	conserved	DELETERIOUS (score: 0.01, median: 3.38)	disease causing (prob: 1)	Class C0 (GV: 26.00 GD: 23.36)	25.3 (damaging)	2.96	29	n.a.	n.a.	n.a.	n.a.	n.a.	PM2;PP3;PP2	VUS
Exon 8	g.98397119A>C	c.1949A>C	p.(Glu650Ala)	CLZ	LOVD	n.d.	n.d.	337668	rs139368657	0.020%	0	conserved	DELETERIOUS (score: 0.02, median: 3.38)	disease causing (prob: 1)	Class C25 (GV: 44.60 GD: 95.68)	23.6 (damaging)	7.10	107	n.a.	n.a.	n.a.	n.a.	n.a.	PM2;PP3;PP2	VUS
Exon 8	g.98397133C>T	c.1963C>T	p.(Gln655Ter)	CLZ	Wissinger et al., 2001	n.d.	n.d.	no entry	no entry	no entry	2	-	n.a.	n.a.	n.a.	39.0 (damaging)	n.a.	n.a.	n.a.	n.a.	n.a.	n.a.	n.a.	PP1;PVS1;PM2	Likely pathogenic
Exon 8	g.98397145A>T	c.1975A>T	p.(Lys659Ter)	CLZ	Li et al., 2014	n.d.	n.d.	no entry	no entry	no entry	0	-	n.a.	n.a.	n.a.	41.0 (damaging)	n.a.	n.a.	n.a.	n.a.	n.a.	n.a.	n.a.	PVS1;PM2	Likely pathogenic
Exon 8	g.98397151C>A	c.1981C>A	p.(Arg661Ser)	CLZ	Yang et al., 2014	n.d.	n.d.	867037	rs183838250	0.032%	3	completely conserved	DELETERIOUS (score: 0, median: 3.38)	disease causing (prob: 1)	Class C65 (GV: 0.00 GD: 109.21)	24.9 (damaging)	1.19	110	n.a.	n.a.	n.a.	n.a.	n.a.	PP1;PP5;PM2;PP3;PP2	Likely pathogenic
Exon 8	g.98397152G>A	c.1982G>A	p.(Arg661His)	CLZ	Sun et al., 2020	n.d.	n.d.	864739	rs144715956	0.0035%	0	completely conserved	DELETERIOUS (score: 0, median: 3.36)	disease causing (prob: 1)	Class C25 (GV: 0.00 GD: 28.82)	29.5 (damaging)	9.27	29	n.a.	n.a.	n.a.	n.a.	n.a.	PM2;PM5;PP3;PP2	Likely pathogenic
Variants of uncertain significance																									
Exon 2	g.98370043G>A	c.68G>A¶	p.(Arg23Gln)	N-Term.	ClinVar	n.d.	n.d.	895316	rs746563618	0.0028%	0	not conserved	TOLERATED (score: 0.44, median: 3.37)	polymorphism (prob: 1)	Class C0 (GV: 249.02 GD: 0.00)	10.19 (tolerated)	0.67	43	n.a.	n.a.	n.a.	n.a.	n.a.	PM2;PP2;BP4	VUS
Exon 2	g.98370055G>A	c.80G>A¶	p.(Arg27His)	N-Term.	ClinVar	n.d.	n.d.	895317	rs769433253	0.0078%	0	conserved	TOLERATED (score: 0.56, median: 3.37)	polymorphism (prob: 1)	Class C0 (GV: 258.79 GD: 0.00)	0.032 (tolerated)	-1.10	29	n.a.	n.a.	n.a.	n.a.	n.a.	PM2;PP2;BP4	VUS
Exon 3	g.98377695C>T	c.110C>T¶	p.(Ser37Leu)	N-Term.	ClinVar	n.d.	n.d.	74757	rs141086649	0.022%	0	conserved	TOLERATED (score: 0.07, median: 3.38)	polymorphism (prob: 1)	Class C0 (GV: 353.86 GD: 0.00)	3.317 (tolerated)	0.08	145	n.a.	n.a.	n.a.	n.a.	n.a.	PM2;PP2;BP4	VUS
Exon 3	g.98377739A>G	c.154A>G¶	p.(Met52Val)	N-Term.	ClinVar	n.d.	n.d.	896737	rs368962370	0.00040%	0	not conserved	TOLERATED (score: 0.73, median: 3.54)	polymorphism (prob: 0.999)	Class C0 (GV: 353.86 GD: 0.00)	12.28 (tolerated)	3.27	21	n.a.	n.a.	n.a.	n.a.	n.a.	PM2;PP2;BP4	VUS
Exon 3	g.98377796G>A	c.211G>A¶	p.(Ala71Thr)	N-Term.	ClinVar	n.d.	n.d.	858875	rs61756692	0.018%	0	not conserved	TOLERATED (score: 0.5, median: 3.38)	polymorphism (prob: 0.997)	Class C0 (GV: 353.86 GD: 0.00)	6.040 (tolerated)	0.91	58	5' score reference: 87.30 mutant: 87.30 (no effect)	5' score reference: 8.63 mutant: 8.63 (no effect)	5' score reference: 0.96 mutant: 0.98 (+2%)	5' score reference: 7.58 mutant: 7.51 (-1%)	donor loss: 0.00 donor gain: 0.00	PM2;PP2;BP4	VUS
Exon 4	g.98380275G>A	c.316G>A¶	p.(Glu106Lys)	N-Term.	Sharon et al., 2020	n.d.	n.d.	812277	rs375152706	0.0024%	0	not conserved	TOLERATED (score: 0.17, median: 3.37)	disease causing (prob: 1)	Class C0 (GV: 241.23 GD: 23.30)	24.4 (damaging)	7.37	56	n.a.	n.a.	n.a.	n.a.	n.a.	PM2;PP2;PP5;PP3	VUS
Exon 4	g.98380317A>G	c.358A>G¶	p.(Asn120Asp)	N-Term.	Li et al., 2014	n.d.	n.d.	no entry	rs199859850	0.0012%	0	not conserved	TOLERATED (score: 0.65, median: 3.37)	polymorphism (prob: 1)	Class C0 (GV: 278.41 GD: 0.00)	5.544 (tolerated)	0.74	23	n.a.	n.a.	n.a.	n.a.	n.a.	PM2;PP2;BP4	VUS
Exon 5	g.98383432C>G	c.440C>G¶	p.(Thr147Arg)	N-Term.	LOVD	n.d.	n.d.	897209	rs144099488	0.028%	0	not conserved	TOLERATED (score: 0.57, median: 3.51)	polymorphism (prob: 1)	Class C0 (GV: 353.86 GD: 0.00)	12.76 (tolerated)	1.31	71	n.a.	n.a.	n.a.	n.a.	n.a.	PM2;PP2;BP4	VUS
Exon 6	g.98389679T>G	c.471T>G¶	p.(Asp157Glu)	N-Term.	ClinVar	n.d.	n.d.	898382	rs199631623	0.0057%	0	not conserved	TOLERATED (score: 1, median: 3.54)	polymorphism (prob: 1)	Class C0 (GV: 223.67 GD: 0.00)	0.001 (tolerated)	-1.45	45	n.a.	n.a.	n.a.	n.a.	n.a.	PM2;PM1;PP2;BP4	VUS
Exon 6	g.98389681C>T	c.473C>T¶	p.(Ala158Val)	N-Term.	LOVD	n.d.	n.d.	374721	rs138934573	0.038%	0	not conserved	TOLERATED (score: 1, median: 3.54)	polymorphism (prob: 1)	Class C0 (GV: 256.10 GD: 0.00)	1.383 (tolerated)	2.28	64	n.a.	n.a.	n.a.	n.a.	n.a.	PM2;PM1;PP2;BP4	VUS
Exon 6	g.98389761C>G	c.553C>G	p.(Leu185Val)	TM1	Kim et al., 2019	n.d.	n.d.	337657	rs779715055	0.00040%	0	not conserved	TOLERATED (score: 0.13, median: 3.38)	polymorphism (prob: 0.968)	Class C0 (GV: 30.27 GD: 20.52)	18.87 (tolerated)	-0.35	32	n.a.	n.a.	n.a.	n.a.	n.a.	PM2;PM1;PP2;BP4	VUS
Exon 7	g.98391884A>G	c.587A>G	p.(Gln196Arg)	TM1 - TM2	Sun et al., 2020	n.d.	n.d.	no entry	no entry	no entry	0	conserved	TOLERATED (score: 0.14, median: 3.38)	disease causing (prob: 1)	Class C0 (GV: 142.23 GD: 0.00)	23.2 (damaging)	8.76	43	n.a.	n.a.	n.a.	n.a.	n.a.	PM2;PP3;PP2	VUS
Exon 7	g.98391922T>C	c.625T>C	p.(Ser209Pro)	TM2	Weisschuh et al., 2020	n.d.	n.d.	813040	no entry	no entry	3	not conserved	TOLERATED (score: 0.14, median: 3.38)	polymorphism (prob: 1)	Class C0 (GV: 216.60 GD: 0.00)	18.64 (tolerated)	-1.03	74	n.a.	n.a.	n.a.	n.a.	n.a.	PM2;PP2;PP5;BP4	VUS
Exon 7	g.98391961G>C	c.664G>C	p.(Ala222Pro)	TM2	Reuter et al., 2008	n.d.	n.d.	no entry	no entry	no entry	1	not conserved	TOLERATED (score: 0.2, median: 3.38)	polymorphism (prob: 1)	Class C0 (GV: 158.17 GD: 0.00)	22.1 (damaging)	0.59	27	n.a.	n.a.	n.a.	n.a.	n.a.	PM2;PP2	VUS
Exon 7	g.98391967A>G	c.670A>G	p.(Thr224Ala)	TM2 - TM3	This study	n.d.	n.d.	no entry	no entry	no entry	4	conserved	TOLERATED (score: 0.19, median: 3.38)	disease causing (prob: 1)	Class C0 (GV: 131.86 GD: 30.40)	26.3 (damaging)	8.89	58	5' score reference: 95.64; mutant: 95.64 (no effect)	5' score reference: 10.67; mutant: 10.67 (no effect)	5' score reference: 0.99; mutant: 0.98 (-1%)	5' score reference: 14.19; mutant: 12.61 (-11%)	donor loss: 0.00 donor gain: 0.01	PM2;PM5;PP3;PP2	VUS
Exon 7	g.98391968C>T	c.671C>T	p.(Thr224Ile)	TM2 - TM3	Li et al., 2014	n.d.	n.d.	no entry	no entry	no entry	0	conserved	TOLERATED (score: 0.09, median: 3.38)	disease causing (prob: 1)	Class C0 (GV: 131.86 GD: 10.12)	31.0 (damaging)	7.53	89	5' score reference: 95.64; mutant: 91.51 (-4%)	5' score reference: 10.67; mutant: 8.83 (-17%)	5' score reference: 0.99; mutant: 0.99 (no effect)	5' score reference: 14.19; mutant: 15.66 (+10%)	donor loss: 0.00 donor gain: 0.01	PM2;PM5;PP3;PP2	VUS
Exon 8	g.98395913A>G	c.743A>G	p.(Gln248Arg)	TM3	This study	n.d.	n.d.	no entry	no entry	no entry	1	conserved	TOLERATED (score: 0.29, median: 3.38)	disease causing (prob: 1)	Class C0 (GV: 99.61 GD: 28.37)	16.87 (tolerated)	8.95	43	n.a.	n.a.	n.a.	n.a.	n.a.	PM2;PP2	VUS
Exon 8	g.98395954G>C	c.784G>C	p.(Ala262Pro)	TM3	Zobor et al., 2017	n.d.	n.d.	no entry	no entry	no entry	4	not conserved	TOLERATED (score: 0.15, median: 3.54)	disease causing (prob: 0.995)	Class C0 (GV: 252.82 GD: 0.00)	24.7 (damaging)	1.60	27	n.a.	n.a.	n.a.	n.a.	n.a.	PP1;PM2;PP3;PP2	VUS
Exon 8	g.98395966G>A	c.796G>A	p.(Val266Met)	TM3 - TM4	Thiadens et al., 2010	n.d.	n.d.	503560	rs536335712	0.024%	0	not conserved	DELETERIOUS (score: 0.05, median: 3.38)	polymorphism (prob: 1)	Class C0 (GV: 57.46 GD: 0.00)	10.79 (tolerated)	-1.50	21	n.a.	n.a.	n.a.	n.a.	n.a.	PM1;PP2;PM2;BP4	VUS
Exon 8	g.98396513A>G	c.1343A>G	p.(Lys448Arg)	C-linker αB' - αC'	This study	n.d.	n.d.	337662	rs190014426	0.019%	1	conserved	TOLERATED (score: 0.38, median: 3.38)	disease causing (prob: 0.876)	Class C0 (GV: 124.29 GD: 0.00)	16.0 (tolerated)	2.09	26	n.a.	n.a.	n.a.	n.a.	n.a.	PM1;PP2;PM2	VUS
Exon 8	g.98396785G>A	c.1615G>A¥	p.(Val539Met)	CNBD β5	This study	n.d.	n.d.	no entry	rs374275399	0.0016%	1	conserved	DELETERIOUS (score: 0.01, median: 3.38)	disease causing (prob: 1)	Class C0 (GV: 65.28 GD: 20.52)	25.7 (damaging)	9.60	21	n.a.	n.a.	n.a.	n.a.	n.a.	PM2;PM1;PP2;PP3	VUS
Exon 8	g.98396954A>G	c.1784A>G¶	p.(Lys595Arg)	CNBD αC	ClinVar	n.d.	n.d.	896798	no entry	0.0032%	0	conserved	TOLERATED (score: 0.52, median: 3.38)	disease causing (prob: 1)	Class C0 (GV: 26.00 GD: 0.00)	22.7 (damaging)	8.94	26	n.a.	n.a.	n.a.	n.a.	n.a.	PM2;PM1;PP2;PP3	VUS
Exon 8	g.98397015G>T	c.1845G>T¶	p.(Glu615Asp)	CNBD αC - CLZ	ClinVar	n.d.	n.d.	337666	rs886056489	no entry	0	not conserved	TOLERATED (score: 0.45, median: 3.54)	polymorphism (prob: 1)	Class C0 (GV: 236.96 GD: 0.00)	1.813 (tolerated)	-1.45	45	n.a.	n.a.	n.a.	n.a.	n.a.	PM2;PP2;BP4	VUS
Exon 8	g.98397047T>G	c.1877T>G	p.(Leu626Arg)	CLZ	Huang et al., 2016	n.d.	n.d.	no entry	no entry	no entry	0	conserved	DELETERIOUS (score: 0.01, median: 3.38)	polymorphism (prob: 1)	Class C0 (GV: 92.35 GD: 33.45)	24.9 (damaging)	3.17	102	n.a.	n.a.	n.a.	n.a.	n.a.	PP1;PM2;PP2	VUS
Exon 8	g.98397059T>C	c.1889T>C	p.(Val630Ala)	CLZ	This study	n.d.	n.d.	no entry	no entry	no entry	1	conserved	TOLERATED (score: 0.32, median: 3.38)	disease causing (prob: 0.997)	Class C0 (GV: 93.66 GD: 0.00)	22.8 (damaging)	7.45	64	n.a.	n.a.	n.a.	n.a.	n.a.	PM2;PP2;PP3	VUS
Exon 8	g.98397138G>A	c.1968G>A¶	p.(Met656Ile)	CLZ	ClinVar	n.d.	n.d.	337669	rs147293818	0.038%	0	not conserved	TOLERATED (score: 0.35, median: 3.38)	polymorphism (prob: 0.741)	Class C0 (GV: 154.67 GD: 0.00)	17.87 (tolerated)	0.32	10	n.a.	n.a.	n.a.	n.a.	n.a.	PP2;PM2;BP4	VUS

Exon 8	g.98397177 5G>C	c.2015G>C¶	p.(Val699Ala)	CLZ	ClinVar	n.d.	n.d.	897276	rs148499805	0.0007%	0	not conserved	TOLERATED (score: 0.32, median: 3.38)	disease causing (prob: 0.677)	Class C0 (GV: 140.87 GD: 30.92)	8.121 (tolerated)	0.44	32	n.a.	n.a.	n.a.	n.a.	n.a.	PM2PP2	VUS
Exon 8	g.98397220G>A	c.2050G>A¶	p.(Gly684Arg)	C-Term.	Patel et al., 2016	n.d.	n.d.	337670	rs75403692 0	0.0002%	0	not conserved	TOLERATED (score: 0.83, median: 3.38)	polymorphism (prob: 1)	Class C0 (GV: 25.11 4.0 GD: 0.00)	9.509 (tolerated)	0.51	1.25	n.a.	n.a.	n.a.	n.a.	n.a.	PM2,PP2,BP4	VUS
Likely benign variants																									
Exon 2	g.98370 034C>T	c.59 C>T	p.(Thr20Ile)	N-Term.	ClinVar	n.d.	n.d.	895315	rs143489966	0.10%	0	not conserved	TOLERATED (score: 0.42, median: 3.54)	polymorphism (prob: 1)	Class C0 (GV: 393.66 GD: 0.01)	2.152 (tolerated)	-0.27	89	n.a.	n.a.	n.a.	n.a.	n.a.	PP2,BS1,BS2,BP4,BP6	Benign
Exon 2	g.98370 041C>T	c.66 C>T	p.(=)	N-Term.	This study	n.d.	n.d.	no entry	no entry	no entry	1	-	n.a.	n.a.	n.a.	3.176 (tolerated)	n.a.	n.a.	n.a.	n.a.	n.a.	n.a.	n.a.	PM2,BP7	VUS
Exon 2	g.98370 047T>C	c.72 T>C	p.(=)	N-Term.	This study	n.d.	n.d.	257964	rs672 7412	13.23%	9	-	n.a.	n.a.	n.a.	0.378 (tolerated)	n.a.	n.a.	n.a.	n.a.	n.a.	n.a.	n.a.	BA1,BS2,BP6,BP7	Benign
Exon 2	g.98370 056G>T	c.81 C>T	p.(=)	N-Term.	Nishiguchi et al., 2005	n.d.	n.d.	711330	rs14853989 0	0.08%	0	-	n.a.	n.a.	n.a.	0.928 (tolerated)	n.a.	n.a.	n.a.	n.a.	n.a.	n.a.	n.a.	PM2,BP6,BP7	Likely benign
Intron 2	g.98377 677A>G	c.102-16A>G	p.(?)	-	This study	n.d.	n.d.	257961	rs227 6859	8.22%	7	-	n.a.	n.a.	n.a.	7.714 (tolerated)	n.a.	n.a.	3' score reference: 76.29; mutant: 76.29 (no effect)	3' score reference: 5.84; mutant: 6.46 (+11%)	3' score reference: 0.83; mutant: 0.51 (-39%)	3' score reference: 6.34; mutant: 6.29 (-1%)	acceptor loss: 0.01 acceptor gain: 0.14	BA1,BS2,BP6,BP7	Benign
Exon 3	g.98377 714G>A	c.126G>A	p.(=)	N-Term.	ClinVar	n.d.	n.d.	736219	rs3724 89647	0.0009%	0	-	n.a.	n.a.	n.a.	0.074 (tolerated)	n.a.	n.a.	n.a.	n.a.	n.a.	n.a.	n.a.	PM2,BP7,BP6	Likely benign
Exon 3	g.98377 728C>T	c.140C>T	p.(Pro48Leu)	N-Term.	Nishiguchi et al., 2005	n.d.	n.d.	288895	rs6 21503 48	0.45%	0	not conserved	TOLERATED (score: 0.24, median: 3.54)	polymorphism (prob: 1)	Class C0 (GV: 35 3.86 GD: 0.00)	4.879 (tolerated)	0.00	98	n.a.	n.a.	n.a.	n.a.	n.a.	PP2,BS1,BS2,BP4,BP6	Benign
Intron 3	g.98377 811A>G	c.215+ 11A>G	p.(?)	-	LOVD	n.d.	n.d.	337653	rs1997 55395	0.14%	0	-	n.a.	n.a.	n.a.	0.153 (tolerated)	n.a.	n.a.	5' score reference: 87.30; mutant: 87.30 (no effect)	5' score reference: 8.63; mutant: 8.63 (no effect)	5' score reference: 0.96; mutant: 0.96 (no effect)	5' score reference: 7.58; mutant: 7.90 (+4%)	donor loss: 0.00 donor gain: 0.00	BS1,BS2,BP7,BP6	Benign
Intron 3	g.98377 951T>C	c.215+151T>C	p.(?)	-	This study	n.d.	n.d.	no entry	rs937725	70.91%	35	-	n.a.	n.a.	n.a.	6.599 (tolerated)	n.a.	n.a.	5' score reference: 70.46; mutant: 0 (-100%)	5' score reference: 7.69; mutant: 0 (-100%)	5' score reference: 0.83; mutant: 0 (-100%)	5' score reference: 0; mutant: 0 (no effect)	donor loss: 0.03 donor gain: 0.00	BA1,BS2,BP7	Benign
Exon 3	g.98377 783C>T	c.198C>T	p.(=)	N-Term.	This study	n.d.	n.d.	257962	rs1395 44302	0.15%	2	-	n.a.	n.a.	n.a.	1.298 (tolerated)	n.a.	n.a.	n.a.	n.a.	n.a.	n.a.	n.a.	BS1,BP7,BP6	Likely benign
Exon 3b]	g.98378 178G>A	c.336 G>A]	p.(Met112Ile)	-	This study	n.d.	n.d.	no entry	no entry	no entry	2	-	n.a.	n.a.	n.a.	0.000 (tolerated)	n.a.	n.a.	n.a.	n.a.	n.a.	n.a.	n.a.	n.a.	n.a.
Exon 3b]	g.98378 202C>T	c.360 C>T]	p.(=)	-	This study	n.d.	n.d.	no entry	no entry	no entry	20	-	n.a.	n.a.	n.a.	0.000 (tolerated)	n.a.	n.a.	n.a.	n.a.	n.a.	n.a.	n.a.	n.a.	n.a.
Intron Exon 3b]	g.98 378 478T>G	c.215+ 467T>G]	p.(?)	-	This study	n.d.	n.d.	no entry	no entry	no entry	5	-	n.a.	n.a.	n.a.	9.299 (tolerated)	n.a.	n.a.	n.a.	n.a.	n.a.	n.a.	n.a.	n.a.	n.a.
Intron Exon 3b]	g.98377 796M>T	c.215 -93A>T]	p.(?)	-	This study	n.d.	n.d.	no entry	no entry	no entry	2	-	n.a.	n.a.	n.a.	10.48 (tolerated)	n.a.	n.a.	n.a.	n.a.	n.a.	n.a.	n.a.	n.a.	n.a.
Exon 4	g.98380 184C>T	c.225C>T	p.(=)	N-Term.	ClinVar	n.d.	n.d.	337654	rs2004 04774	0.0092%	0	-	n.a.	n.a.	n.a.	1.869 (tolerated)	n.a.	n.a.	n.a.	n.a.	n.a.	n.a.	na.	PM2BP7	VUS
Exon 4	g.98380 197C>T	c.238C>T	p.(=)	N-Term.	ClinVar	n.d.	n.d.	337655	rs5753 26068	0.049%	0	-	n.a.	n.a.	n.a.	5.259 (tolerated)	n.a.	n.a.	n.a.	n.a.	n.a.	n.a.	na.	PM2BP7	VUS
Exon 4	g.98380 243C>T¶	c.284 C>T¶	p.(Pro95Leu)	N-Term.	Thiadens et al., 2010	n.d.	n.d.	288342	rs1141 08462	0.020%	0	conserved	TOLERATED (score: 0.28, median: 3.37)	polymorphism (prob: 1)	Class C0 (GV: 257.76 GD: 0.00)	15.41 (tolerated)	1.60	98	n.a.	n.a.	n.a.	n.a.	n.a.	PM2,PP2,BP4	VUS
Exon 4	g.98380 312A>G	c.353 A>G¶	p.(Gln118Arg)	N-Term.	This study	n.d.	n.d.	712356	rs1428 37782	0.087%	1	not conserved	TOLERATED (score: 0.61, median: 3.37)	polymorphism (prob: 0.999)	Class C0 (GV: 27.2 3.3 GD: 0.00)	5.176 (tolerated)	0.98	43	n.a.	n.a.	n.a.	n.a.	n.a.	PP2,PM2,BP6,BP4	Likely benign
Intron 4	g.98380 360C>T	c.395+9 C>T	p.(?)	-	ClinVar	n.d.	n.d.	897208	rs3754 94943	0.0072%	0	-	n.a.	n.a.	n.a.	0.734 (tolerated)	n.a.	n.a.	5' score reference: 9.43; mutant: 94.67 (no effect)	5' score reference: 10.51 mutant: 10.51 (no effect)	5' score reference: 1.00 mutant: 1.00 (no effect)	5' score reference: 8.85 mutant: 8.89 (+0.4%)	donor loss: 0.00 donor gain: 0.00	PM2	VUS
Intron 4	g.98383 384G>A	c.396 -4 G>A	p.(?)	-	ClinVar	n.d.	n.d.	337656	rs1149 51127	0.18%	0	-	n.a.	n.a.	n.a.	2.067 (tolerated)	n.a.	n.a.	5' score reference: 7.63; mutant: 76.80 (no effect)	5' score reference: 11.35 mutant: 11.15 (-2%)	5' score reference: 0.90 mutant: 0.92 (+2%)	5' score reference: 12.40 mutant: 11.97 (-3%)	acceptor loss: 0.00 acceptor gain: 0.04	BS1,BP4,BP6	Benign
Intron 5	g.98383 454A>G	c.449+ 13A>G	p.(?)	-	ClinVar	n.d.	n.d.	897210	no entry	no entry	0	-	n.a.	n.a.	n.a.	7.471 (tolerated)	n.a.	n.a.	5' score reference: 7.53; mutant: 75.95 (no effect)	5' score reference: 8.57 mutant: 8.57 (no effect)	5' score reference: 0.98 mutant: 0.98 (no effect)	5' score reference: 8.21 mutant: 8.64 (+5%)	donor loss: 0.00 donor gain: 0.00	PM2BP7	VUS
Exon 6	g.98389 699C>T	c.459C> T	p.(Thr153Met)	N-Term.	Kohl et al., 1998	Tränkner et al., 2004 Meighan et al., 2015 Meiyhan et al., 2015	++ (Imaging & Ephys) ++ (Ephys) + (Ephys, +80)	285271	rs2 43142 05	0.86%	2	not conserved	TOLERATED (score: 0.1, median: 3.54)	polymorphism (prob: 0.999)	Class C0 (GV: 35 3.86 GD: 0.00)	6.577 (tolerated)	-0.69	81	n.a.	n.a.	n.a.	n.a.	n.a.	PP2,BS1,BS2,BP6,BP4	Benign
Intron 6	g.98389 780C>T	c.5 66+6C >T	p.(?)	-	ClinVar	n.d.	n.d.	337658	rs1995 58955	0.56%	0	-	n.a.	n.a.	n.a.	3.894 (tolerated)	n.a.	n.a.	5' score reference: 9.4; 2.2 mutant: 100.00 (+6%)	5' score reference: 10.86 (+51%) (insufficient)	5' score reference: 0.99 mutant: 1.00 (+0.3%)	5' score reference: 11.93 mutant: 12.76 (+7%)	donor loss: 0.01 donor gain: 0.00	PM2,BP4,BP6	Likely benign
Intron 6	g.98389 788G>A	c.566+ 14G>A	p.(?)	-	ClinVar	n.d.	n.d.	898394	rs3677 48425	0.0028%	0	-	n.a.	n.a.	n.a.	4.290 (tolerated)	n.a.	n.a.	5' score reference: 9.4; 2.2 mutant: 94.22 (no effect)	5' score reference: 9.88 mutant: 9.88 (insufficient)	5' score reference: 0.99 mutant: 0.99 (no effect)	5' score reference: 11.93 mutant: 11.60 (-3%)	donor loss: 0.00 donor gain: 0.00	PM2BP7	VUS
Exon 7	g.98391 899G>A	c.592G>A	p.(Glu198Lys)	TM2	This study	n.d.	n.d.	377069	rs227 1041	0.43%	1	not conserved	TOLERATED (score: 0.72, median: 3.38)	polymorphism (prob: 1)	Class C0 (GV: 112.26 GD: 28.94)	16.33 (tolerated)	1.96	56	n.a.	n.a.	n.a.	n.a.	n.a.	PP2,BS1,BS2,BP6,BP4	Benign
Exon 8	g.98395 889C>T	c.715C> T	p.(=)	TM2 - TM3	ClinVar	n.d.	n.d.	898396	rs7894 56172	0.00440%	0	-	n.a.	n.a.	n.a.	5.907 (tolerated)	n.a.	n.a.	n.a.	n.a.	n.a.	n.a.	na.	PM2BP7	VUS
Exon 8	g.98395 904C>T	c.734 C>T¶	p.(Thr245Met)	TM2 - TM3	Johnson et al., 2004	n.d.	n.d.	no entry	rs1435 31659	0.0058%	0	not conserved	TOLERATED (score: 0.06, median: 3.38)	polymorphism (prob: 1)	Class C0 (GV: 82.71 GD: 52.12)	13.05 (tolerated)	0.23	81	n.a.	n.a.	n.a.	n.a.	n.a.	PM2,PP2BP4	VUS
Exon 8	g.98395 910C>T	c.740C>T	p.(Thr247Met)	TM3	Liet al., 2014	n.d.	n.d.	198771	rs1496 16345	0.12%	0	not conserved	TOLERATED (score: 0.14, median: 3.38)	polymorphism (prob: 1)	Class C0 (GV: 147.31 GD: 0.00)	0.376 (tolerated)	0.36	81	n.a.	n.a.	n.a.	n.a.	n.a.	BS1,PP2,BP6,BP4	Likely benign
Exon 8	g.98395 947C>A	c.777C>A	p.(=)	TM3	ClinVar	n.d.	n.d.	337660	rs1399 21037	0.0042%	0	-	n.a.	n.a.	n.a.	0.454 (tolerated)	n.a.	n.a.	n.a.	n.a.	n.a.	n.a.	na.	PM2BP7	VUS
Exon 8	g.98396 289C>T	c.111 6C>T	p.(=)	pore helix - TM6	ClinVar	n.d.	n.d.	722716	rs2016 49850	0.028%	0	-	n.a.	n.a.	n.a.	0.030 (tolerated)	n.a.	n.a.	n.a.	n.a.	n.a.	n.a.	n.a.	PM2,BP7BP6	Likely benign
Exon 8	g.98396 517G>A	c.1347G>A	p.(=)	C-linker cdI8 - αC	This study	n.d.	n.d.	no entry	rs7762 51470	0.00081%	1	-	n.a.	n.a.	n.a.	3.541 (tolerated)	n.a.	n.a.	n.a.	n.a.	n.a.	n.a.	n.a.	PM2,BP7	VUS
Exon 8	g.98396 582A>G	c.1412A>G§	p.(Asn471Ser)	C-linker αD7	Weisinger et al., 2001	Liu and Varnum, 2013 Muraki,Okuda et al., 2017	+ (Ephys) ++ (Ephys)	no entry	rs3739 54146	0.001 2%	0	completely conserved	TOLERATED (score: 0.1, median: 3.38)	disease causing (prob: 1)	Class C0 (GV: 224.00 GD: 21.66)	19.81 (tolerated)	7.15	46	n.a.	n.a.	n.a.	n.a.	n.a.	PM1PP2,PM2	VUS
Exon 8	g.98396 583C>T	c.1413C>T	p.(=)	C-linker αD7	Nishiguchi et al., 2005	n.d.	n.d.	no entry	rs7718 39849	0.00080%	0	-	n.a.	n.a.	n.a.	4.782 (tolerated)	n.a.	n.a.	n.a.	n.a.	n.a.	n.a.	n.a.	PM2,BP7	VUS
Exon 8	g.98396 739C>T	c.1569C>T	p.(=)	CNBD β3	Nishiguchi et al., 2005	n.d.	n.d.	284151	rs6 17525 03	0.35%	0	-	n.a.	n.a.	n.a.	0.714 (tolerated)	n.a.	n.a.	n.a.	n.a.	n.a.	n.a.	n.a.	BS1,BP7,BP6	Likely benign
Exon 8	g.98396 761G>A	c.1611G>A	p.(=)	CNBD β4 - β5	ClinVar	n.d.	n.d.	866315	no entry	no entry	0	-	n.a.	n.a.	n.a.	6.115 (tolerated)	n.a.	n.a.	n.a.	n.a.	n.a.	n.a.	na.	PM2,BP7,PP5	VUS
Exon 8	g.98396 788G>A	c.1618G>A§	p.(Val540Ile)	CNBD β5	Thiadens et al., 2010	n.d.	n.d.	425212	rs1164 48158	0.13%	0	conserved	TOLERATED (score: 0.13, median: 3.38)	disease causing (prob: 1)	Class C0 (GV: 69.84 GD: 28.66)	22.8 (damaging)	3.74	29	n.a.	n.a.	n.a.	n.a.	n.a.	BS1,PP5,PM1PP2,PP3	VUS
Exon 8	g.98396 796C>T	c.1623C>T	p.(=)	CNBD β5	ClinVar	n.d.	n.d.	337663	rs7 859361 1	0.64%	0	-	n.a.	n.a.	n.a.	0.320 (tolerated)	n.a.	n.a.	n.a.	n.a.	n.a.	n.a.	n.a.	BS1,BS2,BP7,BP6	Benign
Exon 8	g.98396 865G>A	c.1693G>A	p.(=)	CNBD β6 - β7	Nishiguchi et al., 2005	n.d.	n.d.	731427	rs7643 39481	0.0035%	0	-	n.a.	n.a.	n.a.	0.259 (tolerated)	n.a.	n.a.	n.a.	n.a.	n.a.	n.a.	n.a.	PM2,BP7BP6	Likely benign
Exon 8	g.98396 916C>T	c.1746C>T	p.(=)	CNBD αB	LOVD	n.d.	n.d.	337665	rs7 7311157	0.83%	0	-	n.a.	n.a.	n.a.	0.219 (tolerated)	n.a.	n.a.	n.a.	n.a.	n.a.	n.a.	n.a.	BS2,BP6,BP7	Likely benign
Exon 8	g.98396 937C>T	c.1767C>T	p.(=)	CNBD αB	LOVD	n.d.	n.d.	896797	rs1379 93993	0.0194%	0	-	n.a.	n.a.	n.a.	0.051 (tolerated)	n.a.	n.a.	n.a.	n.a.	n.a.	n.a.	n.a.	BS2,BP7	Likely benign
Exon 8	g.98397 026C>T	c.1856C>T§	p.(Ala619Val)	CNBD αC - CLZ	Thiadens et al., 2010	n.d.	n.d.	941672	rs7703 08610	0.0016%	0	not conserved	TOLERATED (score: 0.08, median: 3.38)	polymorphism (prob: 1)	Class C0 (GV: 125.75 GD: 47.48)	11.52 (tolerated)	1.06	64	n.a.	n.a.	n.a.	n.a.	n.a.	PM2,PP2BP4	VUS
Exon 8	g.98397 032C>A	c.1862C>A§	p.(Ala621Glu)	CNBD αC - CLZ	Wiśniewski et al., 2007	n.d.	n.d.	no entry	no entry	0.0012%	0	not conserved	TOLERATED (score: 0.91, median: 3.38)	polymorphism (prob: 1)	Class C0 (GV: 13.3 0.9 GD: 0.00)	0.999 (tolerated)	-0.42	1.07	n.a.	n.a.	n.a.	n.a.	n.a.	PM2,PP2BP4	VUS
Exon 8	g.98397 033G>A	c.1863G>A	p.(=)	CNBD αC - CLZ	LOVD	n.d.	n.d.	711262	rs1819 11949	0.26%	0	-	n.a.	n.a.	n.a.	0.052 (tolerated)	n.a.	n.a.	n.a.	n.a.	n.a.	n.a.	n.a.	PM2,BP7BP6	Likely benign
Exon 8	g.98397 039C>T	c.1869C>T	p.(=)	CNBD αC - CLZ	ClinVar	n.d.	n.d.	337667	rs8993 56490	0.00071%	0	-	n.a.	n.a.	n.a.	6.880 (tolerated)	n.a.	n.a.	n.a.	n.a.	n.a.	n.a.	n.a.	PM2BP7	VUS

* Variant designation is based on NM_001128822 (GRCh38/hg38) and NC_000002.12 (GRCh38/hg38).
‡ Variant designation of variants located in the alternate exon 3b (formerly named exon 2b (Weisinger et al., 2001), now renamed exon 3b) and its flanking intronic sequences is based on XM_011151 0994.2 (GRCh 38/hg38).
¶ Variants only observed in a heterozygous state in the absence of a second likely disease-causing allele.
§ Variants classified as VUS: no genotype could be established from the literature or database data.
# Variants observed in an affected individual with an OPN1MW/OPN1MW hybrid gene, an allele associated with a clinical diagnosis of blue cone monochromatism, X-linked.
Functional analysis of mutant channels using human CNGA3/CNGB3 subunits. **: wild type-like response; *: residual altered response; -: no response; Ephys: electrophysiological recording; Imaging: calcium imaging; 37°C/28 °C/27°C: improved/impaired channel functionality by reduction of HEK293 cell cultivation temperature from standard 37°C to 27/28°C; +/0/-: improved/impaired channel functionality of mutant heteromeric channels (CNGA3+CNGB3) compared to mutant homomeric channels (CNGA3 only).
† †Conservation was assessed for missense variants only (see Supplementary Figure S2); completely conserved= residue conserved in all CNGA3/CNGA1 proteins of all species; conserved= residue conserved in the majority of the CNGA3/CNGA1 proteins of different species (>50%); not conserved= residue conserved in the minority of the CNGA3/CNGA1 proteins of different species (<50%).
§ Function al domains of CNGA3 according to Gollman et al., 2014 and Shuart et al., 2011: N-Term., N-terminus; TM1 to TM6, transmembrane domains; C-linker having six alpha helices (αA to αC) and eight beta-sheets (β1 to β8); CLZ, C-terminal leucin zipper; C-Term., C-terminus; -, intermediate amino acid residue between two domains.
$ Cutoff for deleterious as: SIFT: score >0.05 is tolerated, score ≤ 0.05 is damaging. Mutation Taster: higher score, higher probability of the prediction; Align-GVGD: C0<C25< lower probability of pathogenicity; C25<C65 <moderate probability of pathogenicity; C65<High probability of pathogenicity; CADD: C-PHD score >20 = tolerated; Splice Site Prediction by Neural Network (Berkeley Drosophila Genome Project): score ≤ -10% = predicted to affect splicing; SpliceAI: Δ score ≥0.5 = predicted to affect splicing.
* donor sites; ** acceptor sites
n.d., no functional data available; n.a., not applicable

Publication II

Functional evaluation allows ACMG/AMP-based re-classification of *CNGA3* variants associated with achromatopsia.

Solaki, M., Wissinger, B., Kohl, S.*, and Reuter, P.*

*These authors have shared last authorship.

Genetics in Medicine: Official Journal of the American College of Medical Genetics.

2023 Dec;25(12):100979.

doi: 10.1016/j.gim.2023.100979.

This article is distributed under the terms and conditions of the Creative Commons Attribution License (CC BY 4.0) (https://creativecommons.org/licenses/by/4.0/).

Genetics in Medicine (2023) 25, 100979

ELSEVIER

Genetics in Medicine
An Official Journal of the ACMG

www.journals.elsevier.com/genetics-in-medicine

ARTICLE

Functional evaluation allows ACMG/AMP-based re-classification of *CNGA3* variants associated with achromatopsia

Maria Solaki, Bernd Wissinger, Susanne Kohl*, Peggy Reuter*

Institute for Ophthalmic Research, Centre for Ophthalmology, University of Tübingen, Tübingen, Germany

ARTICLE INFO

Article history:
Received 27 April 2023
Received in revised form
30 August 2023
Accepted 30 August 2023
Available online 6 September 2023

Keywords:
Achromatopsia
ACMG/AMP-based variant re-classification
Aequorin-based bioassay
CNGA3
Cyclic nucleotide-gated channel

ABSTRACT

Purpose: *CNGA3* encoding the main subunit of the cyclic nucleotide-gated ion channel in cone photoreceptors is one of the major disease-associated genes for achromatopsia. Most *CNGA3* variants are missense variants with the majority being functionally uncharacterized and therefore hampering genetic diagnosis. In light of potential gene therapy, objective variant pathogenicity assessment is essential.

Methods: We established a medium-throughput aequorin-based luminescence bioassay allowing mutant CNGA3 channel function assessment via quantification of CNGA3 channel-mediated calcium influx in a cell culture system, thereby enabling American College of Medical Genetics and Genomics/Association for Molecular Pathology–based variant re-classification.

Results: We provide functional read-out obtained for 150 yet uncharacterized *CNGA3* missense substitutions of which 55 were previously categorized as variants of uncertain significance (VUS) identifying 25 as functionally normal and 125 as functionally abnormal. These data enabled the American College of Medical Genetics and Genomics/ Association for Molecular Pathology–based variant re-classification of 52/55 VUS as either benign, likely benign, or likely pathogenic reaching a VUS re-classification rate of 94.5%.

Conclusion: Our aequorin-based bioassay allows functionally ensured clinical variant interpretation for 150 *CNGA3* missense variants enabling and supporting VUS re-classification and assuring molecular diagnosis to patients affected by *CNGA3*-associated achromatopsia, hereby identifying patients eligible for future gene therapy trials on this disease.

© 2023 The Authors. Published by Elsevier Inc. on behalf of American College of Medical Genetics and Genomics. This is an open access article under the CC BY license (http://creativecommons.org/licenses/by/4.0/).

The Article Publishing Charge (APC) for this article was paid by Peggy Reuter.

Susanne Kohl and Peggy Reuter have shared last authorship.

*Correspondence and requests for materials should be addressed to Susanne Kohl, Molecular Genetics Laboratory, Institute for Ophthalmic Research, Centre for Ophthalmology, University Clinics Tübingen, Elfriede-Aulhorn-Strasse 5–7, 72076 Tübingen, Germany. *Email address:* susanne.kohl@med.uni-tuebingen.de OR Peggy Reuter, Molecular Genetics Laboratory, Institute for Ophthalmic Research, Centre for Ophthalmology, University Clinics Tübingen, Elfriede-Aulhorn-Strasse 5–7, 72076 Tübingen, Germany. *Email address:* peggy.reuter@med.uni-tuebingen.de

doi: https://doi.org/10.1016/j.gim.2023.100979

1098-3600/© 2023 The Authors. Published by Elsevier Inc. on behalf of American College of Medical Genetics and Genomics. This is an open access article under the CC BY license (http://creativecommons.org/licenses/by/4.0/).

Introduction

The emergence of high-throughput sequencing technologies has nowadays revolutionized the identification of disease-associated variants in patients with inherited retinal disorders (IRDs) — a clinically and genetically heterogeneous group of diseases characterized by retinal dysfunction and degeneration.[1] However, assessing the pathogenic impact of such variants remains challenging because a large proportion of variants (16.4%-42.2%) reported in previous IRD studies have been classified as variants of uncertain significance (VUS) following the standards and guidelines provided by the American College of Medical Genetics and Genomics (ACMG) and the Association for Molecular Pathology (AMP), thereby considerably hampering molecular genetic diagnosis.[2-4] This classification system assigns 5 variant classes ranging from benign, likely benign, variant of uncertain significance, likely pathogenic, to pathogenic.

Sequence variants in 6 genes have been associated with autosomal recessive achromatopsia (ACHM; rod monochromatism), a rare congenital condition characterized by cone photoreceptor dysfunction causing color blindness, reduced vision, nystagmus, and photophobia and affecting 1 in 30,000 to 50,000 people worldwide.[5-7]. The disease-associated genes — mainly coding for cone phototransduction components — include *CNGA3* (MIM# 600053),[8] *CNGB3* (MIM# 605080),[9,10] *GNAT2* (MIM# 139340),[11,12] *PDE6C* (MIM# 600827),[13,14] *PDE6H* (MIM# 601190),[15] and *ATF6* (MIM# 605537).[16-18]

The most afflicted gene in Middle Eastern (84%) and Chinese patients with ACHM (80%) and the second most common gene (5%–44%) in patients with ACHM of European origin is *CNGA3* encoding the A3 subunit of the cyclic nucleotide-gated (CNG) channel expressed in cone photoreceptor outer segments.[19-26] Cone CNG channels are ligand-activated, non-selective cation channels organized in heterotetrameric complexes of 3 CNGA3 and 1 CNGB3 subunit and play an important role in the phototransduction cascade.[27-30] The structurally homologous channel subunits thereby comprise of 6 transmembrane helices (TM1-TM6), a pore-forming region containing the pore helix located between TM5 and TM6, the cyclic nucleotide-binding domain formed by 3 α-helices (αA to αC) and 8 β-sheets (β1 to β8), and the C-linker consisting of 6 α-helices (αA' to αF') connecting the cyclic nucleotide-binding domain to TM6.[31] The subunit assembly is enabled by the C-terminal leucine zipper (CLZ), which is only present in the CNGA3 subunit.[27]

To date, the comprehensive ACHM-associated *CNGA3* variant spectrum comprises 316 sequence alterations as reported in a recent study by Solaki et al, compiling in-house ACHM cohort data with extensive literature and public database research.[32] The most frequently observed variant type are thereby missense alterations (64.6%; $n = 204$) causing single amino acid substitutions at the protein level. Other variant types such as small indels (11.4%) and nonsense variants (10.8%) leading to premature stop codons only play a minor role.[32] Similarly, high frequencies for the observation of missense variants were also reported in other systematic reviews of the *CNGA3* variant spectrum ranging from 69.8% to 72.2%, underlining their predominant role in *CNGA3*-associated retinopathy.[26,33] Of the 204 *CNGA3* missense variants compiled by Solaki et al, 54 were classified as VUS and 144 as (likely) pathogenic, whereas only a minority of variants was categorized as (likely) benign ($n = 6$), according to the ACMG/AMP classification scheme.[32]

Missense variants are often classified as VUS applying the ACMG/AMP classification scheme, which include criteria on frequency of a variant in the normal population compared with patient group, deleterious effects of the variant predicted by in silico tools, the location in functionally important domains, or availability of co-segregation of the variant with the disease within a given family.[32] Although the ACMG/AMP classification provides an initial standardized assessment of variants with respect to their disease relevance, functional studies are needed to confirm the in silico classification and providing evidence for re-classification of VUS to lower or higher classification classes (ie, benign or pathogenic).

Variants designated as VUS represent a major obstacle in molecular genetic diagnosis. In patients carrying a VUS, the genetic defect underlying disease cannot be confirmed until the clinical significance of the VUS has been functionally demonstrated. In the light of first gene therapy trials for *CNGA3*-associated achromatopsia already being completed (NCT02610582[34,35]) or in follow-up phase (NCT03758404) and additional trials ongoing (NCT02935517), the necessity to unequivocally classify such variants is highlighted because, otherwise, such patients are not eligible for clinical studies or — in case the therapeutic approach is approved — are not permitted for therapy. Therefore, functional studies are indispensable to evaluate the impact of missense variants in *CNGA3*.

Functional characterization of CNGA3 missense variants in heterologous expression systems confirming their pathogenic or benign impact has previously only been available for 54 variants, sometimes with contradictory results.[36-47]

Therefore, we further developed a medium-throughput, previously established luminescence bioassay based on the calcium-sensitive photoprotein aequorin to functionally evaluate yet uncharacterized CNGA3 missense variants, including variants classified as VUS, (likely) pathogenic, and likely benign. We here provide functional assessment for 150 CNGA3 missense variants analyzed as mutant homomeric CNGA3 channels in comparison with wild-type (WT) channels aiming for ACMG/AMP-based reclassification of variants hereby ultimately supporting the clinical variant interpretation in *CNGA3*-associated achromatopsia.

Material and Methods

Site-directed mutagenesis

The WT human *CNGA3* (NM_001298.3, GRCh38 genome assembly) expression construct in pcDNA3.1/Zeo(+) was generated as previously described.[36] Mutant *CNGA3* expression constructs were obtained by site-directed mutagenesis using the *Pfu*Ultra High-Fidelity DNA Polymerase (Agilent Technologies) and the full-length WT *CNGA3* cDNA cloned into pcDNA3.1/Zeo(+) as a template. Correct sequences of the cytomegalovirus (CMV) promoter, the *CNGA3* cDNA insert, and the bovine growth hormone polyadenylation signal were confirmed by Sanger sequencing using the BigDye Terminator v.1.1 kit (Thermo Fisher Scientific) according to the manufacturer's protocol. Sequencing reactions were resolved on an ABI PRISM 3130xl Genetic Analyzer (Applied Biosystems, Thermo Fisher Scientific). Primers used for site-directed mutagenesis and Sanger sequencing are provided in Supplemental Tables 1 and 2. Generation of 13 mutant *CNGA3* expression constructs has previously been reported (Supplemental Table 1).[36,40-42]

Generation of stable HEK293^{aequo} cells and culture conditions

HEK293^{aequo} cells stably expressing cytosolic apo-aequorin were generated using the AAVS1 Safe Harbor Targeting 2.0 Gene-of-Interest Knock-in Kit (System Biosciences [SBI], #GE622A-KIT). The AAVS1 HR donor vector GE622A-1#1_CMV-Aeq was obtained by first amplifying the CMV-apo-aequorin fragment from an expression construct for cytosolic apo-aequorin[48] using specific primers carrying 5' tails with *Bst*BI and *Mlu*I recognition sequences by overlap-extension polymerase chain reaction (PCR) (Supplemental Table 2). *Bst*BI/*Mlu*I-digested PCR fragments were subsequently cloned into the AAVS1 HR donor vector GE622A-1 (SBI) after removal of the EF1α promoter by *Bst*BI and *Mlu*I (New England Biolabs) digestion.

Transgene integration into the *AAVS1* locus was performed by co-transfecting the AAVS1 HR donor plasmid GE622A-1#1_CMV-Aeq and the AAVS1 gRNA/Cas9 expression plasmid (SBI, #CAS601A-1) into HEK293 cells (DSMZ, German Collection of Microorganisms and Cell Cultures GmbH). After puromycin selection (2 µg/ml; Thermo Fisher Scientific), monoclonal cell clones were isolated by limiting dilution, expanded, and screened for successful transgene integration by junction PCR (primers from AAVS1 Safe Harbor Targeting 2.0 Gene-of-Interest Knock-in Kit [SBI]). Transgene expression was confirmed using an aequorin-based bioassay (procedure see below) and immunocytochemical staining as previously described.[48]

HEK293^{aequo} cells were cultured in Dulbecco's modified Eagle's medium (Thermo Fisher Scientific) supplemented with 10% fetal calf serum (Thermo Fisher Scientific), 1% penicillin/streptomycin (Thermo Fisher Scientific), 1% amphotericin B (Pan Biotech), and 2 µg/ml puromycin (Thermo Fisher Scientific) at 5% CO_2 at 37 °C.

Aequorin-based bioassay

Stable HEK293^{aequo} cells were seeded at a density of $4.5*10^5$ cells/well in a 24-well plate and grown overnight. Transfection of cells with 2 µg of WT or mutant *CNGA3* expression plasmids was performed using Lipofectamine™ 2000 (Thermo Fisher Scientific) according to the manufacturer's protocol. A fraction of these transfected cells was replated in a Poly-D-lysine (Merck Millipore)-coated white opaque 96-well plate 6 hours post transfection. After overnight incubation, treatment with 3 mM sodium butyrate (Sigma-Aldrich) was performed for 24 hours, enhancing protein expression. For the reconstitution of apo-aequorin before the luminescence measurement, cells were washed with calcium imaging buffer (CI; 2 mM $CaCl_2$, 2 mM $MgCl_2$, 5 mM KCl, 150 mM NaCl, 10 mM HEPES, 30 mM glucose [pH 7.4]) and incubated in 8 µM coelenterazine (Biomol GmbH) for 4 hours at 37 °C. After incubation, cells were washed with CI and CI^{hCa} (CI buffer containing 10 mM Ca^{2+}) and the washing buffer was replaced with 190 µl of CI^{hCa}. Luminescence measurement was performed at 37 °C using the LUMIstar Omega Microplate Luminometer (BMG Labtech GmbH), thereby recording the luminescence signals 6 seconds before and 394 seconds after automatic application of 10 µl of the membrane-permeable CNG channel agonist 8-bromoguanosine-3′,5′-cyclic monophosphate (100 mM; 8-Br-cGMP; BIOLOG Life Science Institute). Each sample was measured in 3 technical replicates performing 3 to 5 independent transfections. All assay plates included cells transfected with the WT *CNGA3* expression plasmid as positive control. Untransfected cells were incorporated as negative control on 15 assay plates.

Dot blot and western blot analysis

CNGA3 protein expression was verified by dot blot analysis of whole-cell lysates in 1 biological replicate of all samples analyzed. Additionally, western blot analysis of whole-cell lysates was performed for antibody validation and verification of CNGA3 protein expression in 1 biological replicate of samples from the assay validation data set.

For protein extraction, a fraction of the transfected HEK293^{aequo} cells described above were replated on a 24-well plate followed by a 3 mM sodium butyrate treatment for 30 hours. Cells were washed with Dulbecco's phosphate buffered saline (Thermo Fisher Scientific) and lysed in lysis buffer (50 mM Tris, 150 mM NaCl, 1 mM EDTA, 1% NP-40, 0.25% sodium deoxycholate, 1 mM dithiothreitol, 1% protease inhibitor cocktail (Merck Millipore), pH 7.4) performing 4 freeze/thaw cycles in liquid nitrogen. Cell debris was removed by centrifugation at 470xg for 20 minutes at 4 °C. Protein concentration was determined by Bradford assay.

For dot blot analysis, 5 µg of total protein in a total volume of 2 µl were applied onto a dry nitrocellulose membrane (Bio-Rad Laboratories) to form a dot.

For western blot analysis, 5 µg or 30 µg of total protein were separated on a Q-PAGE™ Bis-Tris 4-12% Precast Gel (SMOBIO Technology) and transferred onto a nitrocellulose membrane by electroblotting.

All blots were blocked with 5% blotting-grade blocker (Bio-Rad Laboratories) in TBST (10 mM Tris, 150 mM NaCl, 0.1% Tween-20, pH 8.0), and immunological protein detection was performed by incubating the membranes with the rabbit anti-human CNGA3 antibody (1:750; Elabscience) or the custom-made rabbit anti-human CNGA3 antibody SA3899 (1:1000) followed by an incubation with the goat anti-rabbit horseradish peroxidase–coupled secondary antibody (1:4000; Merck Millipore). The mouse anti-actin antibody (1:4000; Merck Millipore) in combination with the goat anti-mouse horseradish peroxidase–coupled secondary antibody (1:10,000; Merck Millipore) allowed detection of beta-actin serving as a loading control in western blot analysis.

CNGA3 variant selection

A total of 24 *CNGA3* variants were selected for the validation of the aequorin-based bioassay. These comprised benign variants ($n = 9$) and the classification of being "benign" was determined as (1) missense variants displaying WT-like function of the homomeric channel in previous heterologous expression experiments and being classified as benign following the ACMG/AMP criteria,[36,49] (2) variants detected homozygously in individuals ($n \geq 4$) on the gnomAD database (https://gnomad.broadinstitute.org/) and classified as benign following the ACMG/AMP criteria, and (3) synonymous variants identified on the gnomAD database. Furthermore, we included pathogenic variants ($n = 15$) with the classification as being "pathogenic" determined by classification of the variant as pathogenic following ACMG/AMP criteria and variant channels showing aberrant or absent channel function compared with the WT in previously conducted studies.[36,39-43] This assay validation data set is summarized in Supplemental Table 3.

For functional variant assessment and re-classification, 146 functionally uncharacterized *CNGA3* missense variants and 1 missense variant showing contradictory results in previous functional approaches[37,39] were retrieved from the comprehensive *CNGA3* variant database established by Solaki et al.[32] Additional 2 missense variants currently not associated with retinal diseases and listed in the Leiden Open Variation Database (LOVD) for *CNGA3* (https://www.lovd.nl/CNGA3) and 1 missense substitution published by Brunetti-Pierri et al[50] were also included in the functional evaluation. All analyzed *CNGA3* missense variants are listed in Supplemental Table 4. Variant nomenclature was based on the NCBI reference sequence for *CNGA3* (NM_001298.3, GRCh38 genome assembly) comprising 7 coding exons.

Data Analysis

In the first step, "non-functional" variant channels were defined as variant channels that did not show an increase in the luminescence signal after application of the ligand in the bioassay. Therefore, the ratio of the average luminescence before and after ligand addition was calculated. Mutant channels displaying a ratio of >1.5 were considered to be functional, whereas mutant channels showing a ratio of <1.5 were manually revised and classified as either "functional" or "non-functional" based on the luminescence curve progression.

In the second step, variant evaluation was conducted by assessing the overall luminescence signal (area under the curve [AUC]) and the luminescence peak latency in comparison with WT channels. Both AUC and peak latency were therefore calculated by considering a specific time window after ligand addition ranging from 21 to 400 seconds using the MARS Data Analysis Software (BMG Labtech). AUC values were thereby determined for both functional and non-functional mutant channels, whereas the peak latency was only determined for mutant channels being classified as functional. Before data normalization, we applied quality control measures by excluding all technical replicates of cells transfected with the WT *CNGA3* expression plasmid from subsequent analysis, which deviated more than 15% from the AUC mean value of the WT positive control from the respective assay plate. Finally, we normalized the AUC/peak latency data of the analyzed mutant channels to the AUC/peak latency mean value of the WT channels from the respective assay plate (normalized AUC and normalized peak latency).

Determination of thresholds for both the normalized AUC and the normalized peak latency to distinguish benign from pathogenic variants was executed by performing a receiver operating characteristic (ROC) analysis based on 9 benign and 15 pathogenic *CNGA3* variants from the assay validation data set (Supplemental Table 3) using GraphPad Prism (GraphPad Software, San Diego).

Applying the established thresholds to the 150 studied *CNGA3* variants enabled classification of variants as "functionally normal" or "functionally abnormal" following the suggested terminology from Brnich et al (2019).[51]

For evaluating overall assay quality, we calculated the Z' factor based on 15 individual assay plates containing both positive and negative controls using the MARS Data Analysis Software.

ACMG/AMP-based classification of *CNGA3* missense variants

The pathogenic effect of all 150 studied CNGA3 missense substitutions was semi-automatically classified following ACMG/AMP guidelines[2] applying the web-based variant interpretation tool Franklin (Genoox Ltd, https://franklin.genoox.com/) and manually revising the applied criteria as

previously described before functional evaluation.[32] Evidence for pathogenicity/non-pathogenicity criteria that were manually selected included the following: (1) co-segregation of the variant(s) with disease in multiple affected family members (PP1), (2) deleterious (PP3) or benign (BP4) in silico predictions retrieved by CADD (https://cadd.gs.washington.edu/) and MutationTaster (http://www.mutationtaster.org/), (3) minor allele frequency of <0.039% (PM2), >0.1% (BS1), or >5% (BA1) on the gnomAD database (v.2.1.1 https://gnomad.broadinstitute.org/gene/ENSG00000144191?dataset=gnomad_r2_1), (4) *CNGA3* variant(s) observed in *cis* with another pathogenic variant in the *CNGA3* gene (BP2), and (5) variant(s) found in affected individuals with an obvious alternate cause of disease (BP5). The threshold used for PM2 was established by review of allele frequencies of *CNGA3* variants in gnomAD, and c.1279C>T p.(Arg427Cys) being the most common *CNGA3* pathogenic allele with an allele frequency of 0.039%. Finally, the criterion PP2 was manually applied only for missense variants, which are located in the structural and functional domains of the CNGA3 protein (ie, transmembrane domains, pore, C-linker, cGMP binding site) downstream of the N terminus (Met1 to Arg170; CNGA3: total 694 amino acids) because it was previously observed that benign variants were enriched in the N-terminal region.[32]

After functional variant assessment using the aequorin-based bioassay, we added the following functional evidence criteria to enable ACMG/AMP-based variant re-classification. The criterion PS3 was thereby applied to *CNGA3* missense variants proven to be "functionally abnormal" in the luminescence bioassay displaying a damaging effect on protein function whereas missense substitutions proven to be "functionally normal" encoding channels with WT-like function were assigned the criterion BS3.

Results

In a previous study, we had developed an aequorin-based bioassay to search for chemical and pharmacological chaperones improving targeting of mutant trafficking-deficient CNG channels as a variant-independent concept for therapeutic intervention in *CNGA3*-associated ACHM.[52] We further developed this assay to generate a medium-throughput platform for the functional evaluation of disease-associated variants related to IRD, specifically *CNGA3*-ACHM.

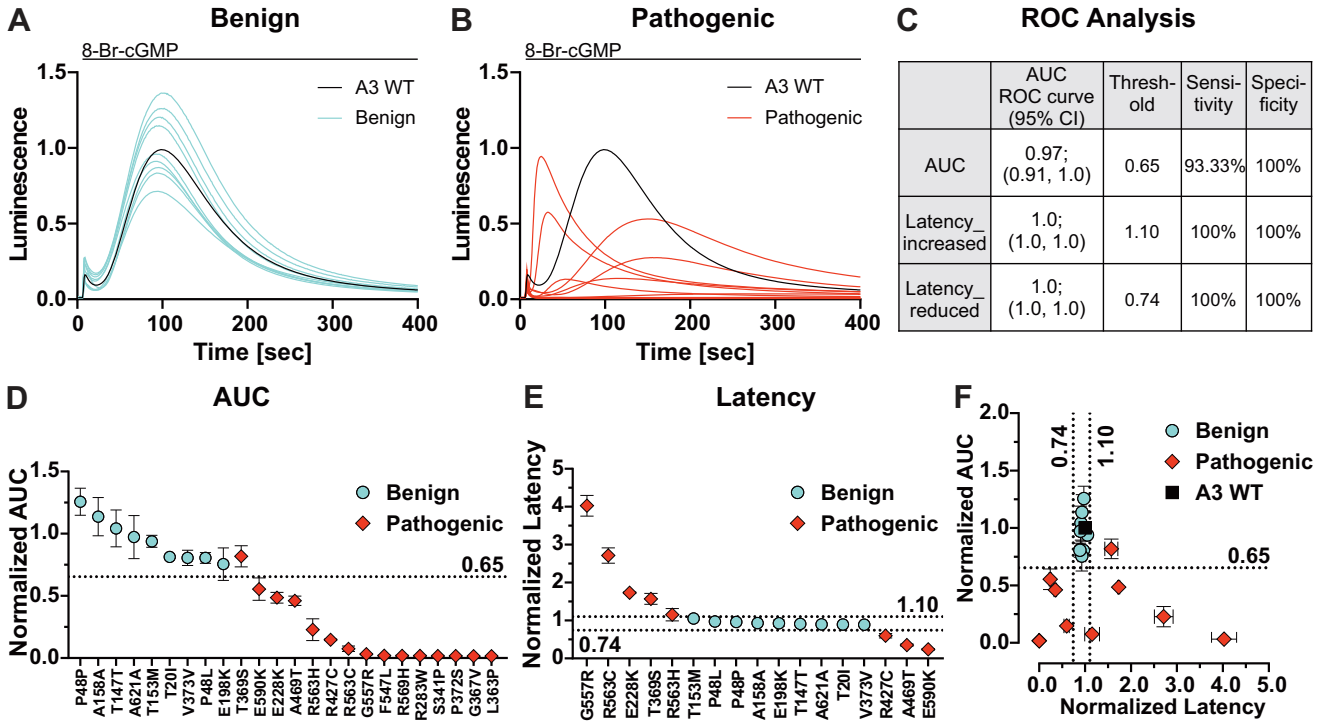
Validation of the aequorin-based bioassay

To evaluate the capability of the aequorin-based bioassay to assess mutant CNG channel function, we validated our assay by functionally testing a set of 24 *CNGA3* variants, including 9 benign and 15 pathogenic sequence alterations (Figure 1A and B, Supplemental Table 3). Our luminescence bioassay uses the calcium-sensitive photoprotein aequorin to detect the CNGA3 channel-meditated calcium influx after activation of CNG channels by the membrane-permeable ligand 8-Br-cGMP. The luminescence signal is proportional to the amount of calcium and therefore correlates with CNG channel functionality. The generated functional data were subsequently used to establish thresholds regarding both the normalized AUC and the normalized peak latency for separating functionally normal and abnormal variants (Figure 1D and E).

The 9 benign variants showed luminescence responses similar to CNGA3 WT channels (Figure 1A). For 7 variant channels from the "pathogenic" assay validation data set, we did not detect luminescence responses in our assay, which is in line with observations from previous studies on heterologous expressed mutant versus WT channels using electrophysiological recordings or calcium imaging measurements in HEK293 cells (Figure 1B).[39-43] Furthermore, the remaining 8 pathogenic variants showed altered luminescence signals in comparison with the WT. All these pathogenic variants that have been shown to mediate some residual activity in previous studies also displayed luminescence signals in our bioassay indicating a sufficient sensitivity of the assay.[36,37,39-41] ROC analysis of the normalized AUC identified a threshold of 0.65 to discriminate benign and pathogenic variants. With this threshold, our assay and analysis was not able to identify the variant p.(Thr369Ser) as pathogenic because it lies above this threshold (Figure 1D). Therefore, the sensitivity of our analysis is determined as 93.3%. The specificity was 100% as all 9 benign variants were correctly classified as functionally normal regarding the AUC (Figure 1C, Supplemental Figure 1A). In the next step, the 8 functional pathogenic and the 9 benign variants were used to establish thresholds for the luminescence peak latency. Using the ROC analysis, 2 separate thresholds were established for the normalized peak latency as 5 pathogenic CNGA3 missense variants displayed an increased peak latency and 3 CNGA3 missense variants showed a decreased peak latency compared with WT channels (Figure 1E). The pathogenicity threshold for increased peak latency was determined to be 1.10 and the threshold for decreased peak latency to be 0.74, both reaching a sensitivity and specificity of 100% (Figure 1C, Supplemental Figure 1B and C).

Combining the thresholds established with the ROC analyses, variants classified as functionally normal had a normalized AUC > 0.65 and normalized peak latency of $0.74<x<1.10$, whereas variants not meeting these criteria were classified as functionally abnormal.

Following these criteria, a clear separation of the WT, the 9 benign and the 15 pathogenic assay validation variants was achieved because all pathogenic substitutions resided outside of the functionally normal range, therefore being correctly classified as functionally abnormal in concordance with previously conducted functional studies (Figure 1F).[36,37,39-43,49]



	AUC ROC curve (95% CI)	Threshold	Sensitivity	Specificity
AUC	0.97; (0.91, 1.0)	0.65	93.33%	100%
Latency_ increased	1.0; (1.0, 1.0)	1.10	100%	100%
Latency_ reduced	1.0; (1.0, 1.0)	0.74	100%	100%

Figure 1 Validation of the aequorin-based bioassay using an assay validation data set containing 9 benign and 15 pathogenic variants in the *CNGA3* gene. A. Luminescence traces of wild-type channels (A3 WT, black line) and 9 benign variants (blue lines) normalized to A3 WT. The benign variants of the assay validation data set are listed in Supplemental Table 3, and individual normalized luminescence traces are depicted in Supplemental Figure 4. All data are represented as mean. n = 3-55 independent transfections/measurements. B. Luminescence traces of A3 WT (black line) and 15 pathogenic variants (red lines) normalized to A3 WT. The pathogenic variants of the assay validation data set are listed in Supplemental Table 3, and individual normalized luminescence traces are depicted in Supplemental Figure 4. n = 3-55 independent transfections/measurements. C. Receiver operating characteristic (ROC) analysis based on 9 benign and 15 pathogenic variants from the assay validation data set to identify thresholds for the area under the curve (AUC), increased peak latency, and reduced peak latency analysis to differentiate benign and pathogenic variants. D. Normalized overall luminescence signals (AUC) of 9 benign (blue circles) and 15 pathogenic variants (red diamonds). Threshold for discriminating between benign and pathogenic variants is displayed by a dotted line. All data are represented as mean ± standard deviation (SD). n = 3-5 independent transfections/measurements. E. Normalized peak latency of 9 benign (blue circles) and 5 still functional pathogenic variants (red diamonds). Upper and lower thresholds for discerning benign and pathogenic variants are displayed by dotted lines. All data are represented as mean ± SD. n = 3-5 independent transfections/measurements. F. Scatter plot for the normalized AUC and normalized peak latency of 9 benign (blue circles) and 15 pathogenic variants (red diamonds) in comparison with A3 WT (black square). Upper and lower thresholds for assigning functionally normal and abnormal variants are displayed by dotted lines. Thresholds for variant classification; functionally normal: normalized AUC > 0.65 and normalized peak latency 0.74 < x < 1.10; all variants not meeting the mentioned criteria are classified as functionally abnormal. All data are represented as mean ± SD. n = 3-55 independent transfections/measurements; WT, wild-type.

Seven CNGA3 missense substitutions used as pathogenic controls failed to show luminescence responses in the bioassay underlining the need to verify CNGA3 protein expression in the tested samples. Therefore, we conducted a western blot analysis of all 24 assay validation variants using whole-cell lysates, thereby validating both commercial and custom-made CNGA3 antibodies used for the analysis and finally verifying CNGA3 protein expression in all tested samples (Supplemental Figure 2).

Finally, we evaluated the overall assay quality by calculating the Z' factor based on 15 individual assay plates containing both WT and untransfected controls. The mean Z' factor was thereby 0.87 ± 0.08 (median: 0.9), indicating excellent assay quality, rendering the aequorin-based bioassay suitable for the evaluation of mutant CNG channel function (Supplemental Figure 3).

Functional evaluation of 150 CNGA3 missense variants

For the characterization of mutant CNG channel function using our established medium-throughput aequorin-based bioassay, we retrieved a total of 149 functionally uncharacterized CNGA3 missense variants and 1 CNGA3 missense substitution displaying contradictory results in previously conducted functional studies[37,39] from the *CNGA3* variant database published by Solaki et al,[32] LOVD and the literature. After luminescence measurement, we

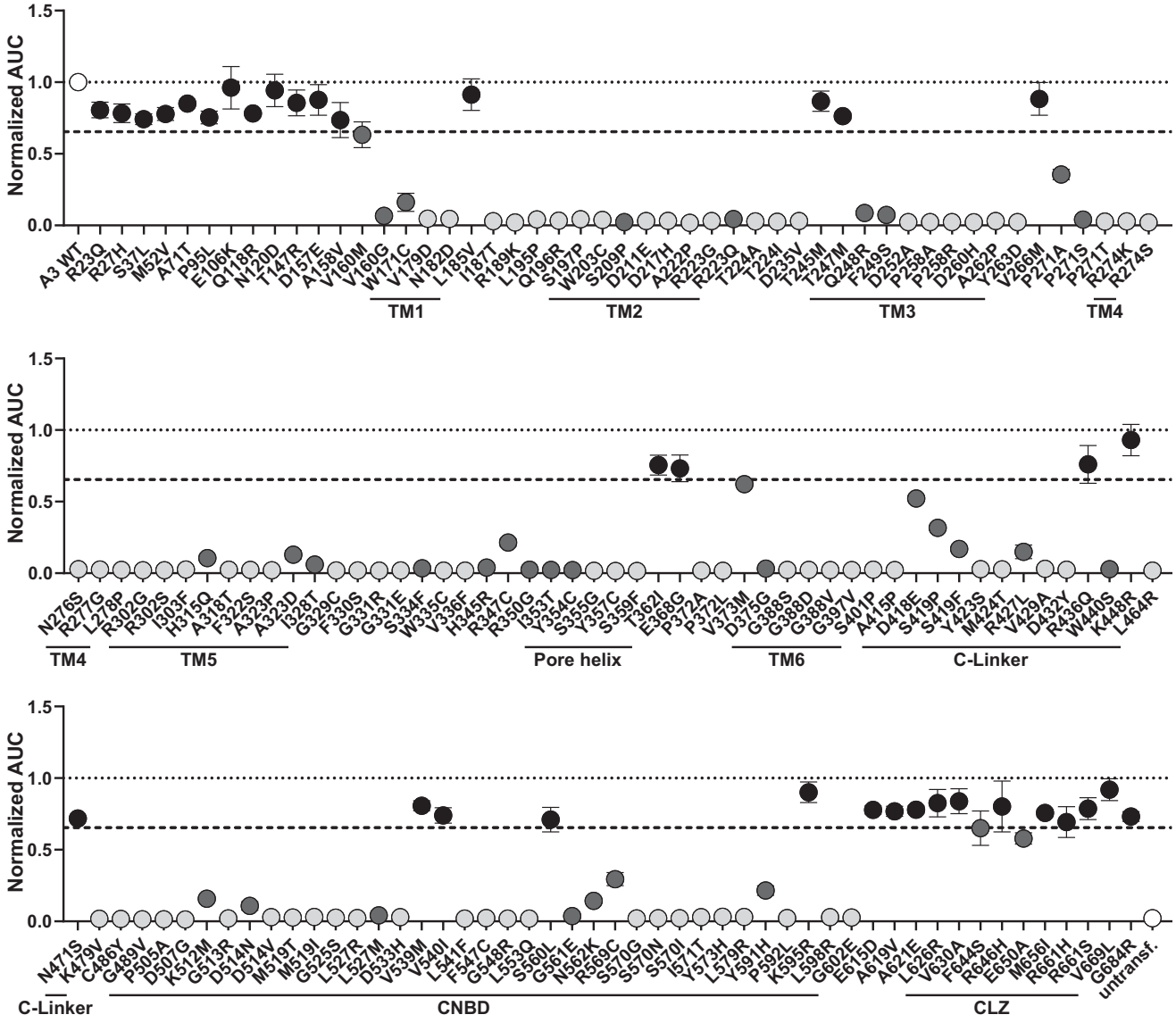


Figure 2 Normalized overall luminescence signals (AUC) of 150 analyzed CNGA3 missense variants sorted by localization on protein level. Normalized AUC value of wild-type channels (A3 WT; white circle, top panel) is exhibited as a dotted line. The threshold for assigning a damaging effect regarding the normalized AUC (0.65) is displayed by a dashed line. All missense variants that are above the threshold are depicted as black circles. 114 of 150 variants exhibited a normalized AUC below the threshold of which 80 variants did not give rise to luminescence signals after ligand application in the bioassay (depicted as light gray circles), whereas 34 variants showed reduced normalized AUC (shown as dark gray circles). Normalized AUC of untransfected control cells is shown as a white circle (bottom panel). Localization of structural and functional domains of CNGA3 are indicated by horizontal lines under the respective variants and are annotated according to Gofman et al[31] and Shuart et al.[28] All data are represented as mean ± SD. n = 3-15 independent transfections/measurements. CLZ, C-terminal leucine zipper; CNBD, cyclic-nucleotide binding domain; TM1 to TM6, transmembrane domains; untransf., untransfected control cells; WT, wild-type.

evaluated the normalized AUC and peak latency values for all analyzed CNGA3 missense variants. Individual luminescence traces of all evaluated missense substitutions are displayed in Supplemental Figure 4.

Among these 150 analyzed missense alterations, 80 gave rise to channels for which no increase in the luminescence was recorded after activation of the channels by 8-Br-cGMP. These variants were designated as nonfunctional with a high number of variants (n = 63) being located in structural/functional important protein domains (Figure 2).

Of the 70 CNGA3 variant channels showing luminescence responses, 36 surpass the pathogenicity threshold of 0.65 for the normalized AUC indicating WT-like overall luminescence signals (AUC), whereas 34 variants displayed an altered/reduced AUC compared with the WT channel (Supplemental Figure 5). Interestingly, more than half of the 36 still-functional missense substitutions displaying WT-

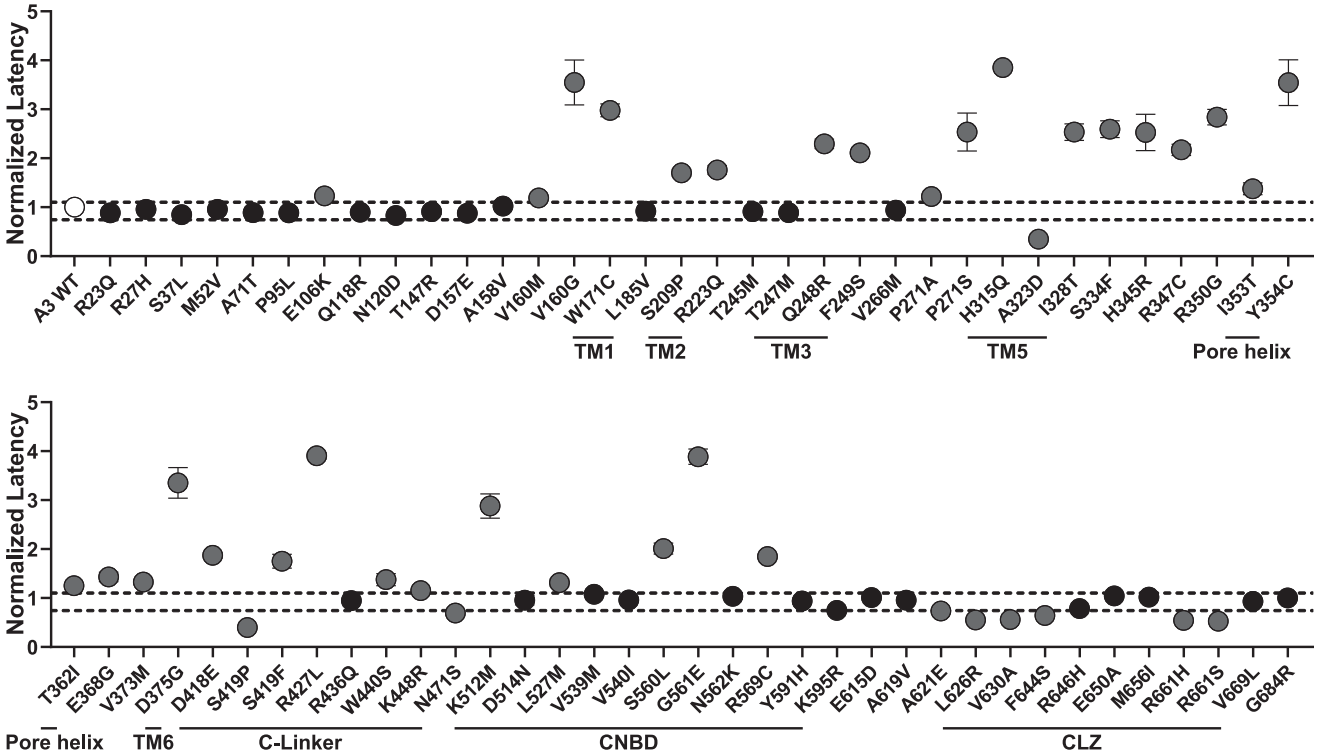


Figure 3 Normalized peak latency of 70 still functional CNGA3 missense variants sorted by localization on protein level. 32 of 70 still functional variants exhibited an increased peak latency, whereas 9 of 70 showed a reduced peak latency compared with wild-type channels (A3 WT; white circle, top panel). Upper (1.10) and lower thresholds (0.74) for assigning a damaging effect regarding the normalized peak latency are displayed by dashed lines. All missense variants that are within or outside the thresholds are shown as black or dark gray circles, respectively. Localization of structural and functional domains of CNGA3 are indicated by horizontal lines under the respective variants and are annotated according to Gofman et al[31] and Shuart et al.[28] All data are represented as mean ± SD. n = 3-5 independent transfections/measurements. CLZ, C-terminal leucine zipper; CNBD, cyclic-nucleotide binding domain; TM1 to TM6, transmembrane domains, WT, wild-type.

like normalized AUC values localize in the N-terminal and the C-terminal parts, the latter specifically in the CLZ part of the protein (n = 7 and n = 12, respectively) (Figure 2).

For all 70 still-functional variant channels, we additionally assessed the normalized peak latency to further evaluate mutant CNG channel function. After the evaluation of the normalized peak latency, we identified 32 of 70 still-functional variants exhibiting an increased peak latency (threshold: 1.10), whereas 9 of 70 showed a reduced peak latency (threshold: 0.74), 5 of which affect the CLZ domain of the CNGA3 subunit (Figure 3, Supplemental Figure 6). In contrast, 29 of 70 still-functional missense substitutions displayed a peak latency comparable to the WT channel, 11 of which are located in the N terminus of the CNGA3 protein (Figure 3, Supplemental Figure 6). Of the 36 variant channels displaying WT-like AUC characteristics, 11 showed altered normalized peak latencies. Therefore, by combining the normalized AUC and peak latency as criteria, we finally classified 25 variants as functionally normal and 125 variants as functionally abnormal (Supplemental Table 4).

Because no luminescence responses were detected after activation of the channels with the ligand 8-Br-cGMP for 53.3% of the functionally evaluated CNGA3 missense variants, we performed dot blot analysis of whole-cell lysates of all variants studied to verify expression of the variant channels in the transiently transfected HEK293^{aequo} cells. Using a commercial rabbit anti-human CNGA3 antibody, we confirmed successful expression for all variants — except the p.(Pro592Leu). Thus, reduced/absent luminescence signals in the aequorin assay are due to a functional impairment of the variant channel and are not a result of failure in, eg, cell transfection. The variant p.(Pro592Leu) was only detected using the custom-made antibody SA3899 — similarly to the variant p.(Glu590Lys) from the assay validation data set. Both variants have very likely abolished the antigen of the commercial anti-CNGA3-antibody in the CNGA3 protein and therefore were only detected with the SA3899 antibody (Supplemental Figures 2 and 7).

Re-classification of CNGA3 missense variants based on ACMG/AMP criteria and functional data

The functional data obtained by our cellular luminescence bioassay were used for ACMG/AMP-based re-classification of the 150 analyzed missense *CNGA3* variants. Initially, all variants selected for functional characterization were

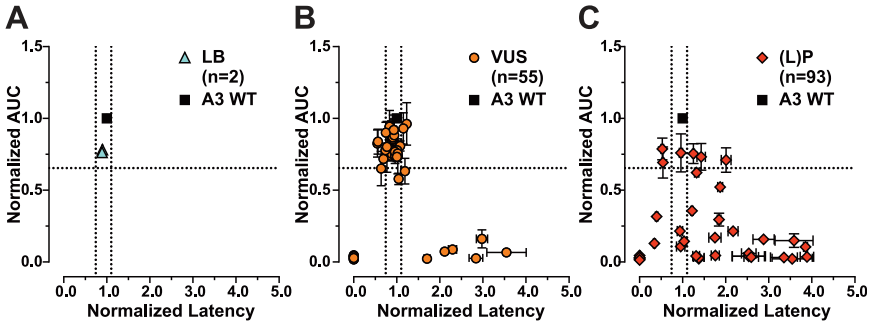


Figure 4 Comparison of variant ACMG/AMP classification class and responses of mutant channels in the aequorin-based bioassay. All 150 missense variants that were functionally characterized using our bioassay were initially classified following ACMG/AMP criteria (pre-assay). Thereby, 2 variants were classified as likely benign (A, blue triangles), 55 as VUS (B, orange circles), and 93 as (likely) pathogenic (C, red diamonds). Responses of wild-type channels (A3 WT) are shown as black squares. Thresholds for assay classification are displayed by dotted lines; functionally normal: normalized AUC > 0.65 and normalized peak latency 0.74<x<1.10; all variants not meeting the mentioned criteria are classified as functionally abnormal. All data are represented as mean ± SD. n = 3-5 independent transfections/measurements. LB, likely benign; (L)P, (likely) pathogenic; VUS, variant of uncertain significance; WT, wild-type.

classified according to ACMG/AMP guidelines without applying functional evidence (criteria BS3 or PS3). Four of 150 missense substitutions were thereby classified as pathogenic, 89 as likely pathogenic, 55 as VUS, and 2 were categorized as likely benign in the absence of protein functional data (Supplemental Table 4). To enable variant re-classification based on the ACMG/AMP guidelines, we assigned the criterion PS3_strong to all missense substitutions (125/150) deemed to be functionally abnormal after evaluation using our aequorin-based bioassay. In contrast, all variants giving rise to mutant channels categorized as functionally normal based on the determined thresholds (25/150) were assigned the criterion BS3_strong (Supplemental Table 4).

Functional variant analysis and application of all 3 pathogenicity thresholds regarding the normalized AUC and the normalized peak latency onto the obtained functional data revealed that both variants (p.(Gln118Arg) and p.(Thr247Met)) initially classified as likely benign encoded for mutant channels displaying WT-like behavior (Figure 4A). Applying the BS3_strong criterion onto the ACMG/AMP classification allowed re-classification of both variants as benign (Figure 5).

Twenty-two of 55 missense substitutions primarily categorized as VUS were identified to be functionally normal. The ACMG/AMP-based re-classification enabled 18 of the VUS to be categorized as likely benign and 1 VUS was downgraded to benign — 3 variants remained as VUS. Thirty-three VUS encoding mutant CNGA3 channels exhibiting an abnormal channel function compared with WT channels were re-classified as likely pathogenic (Figure 4B and Figure 5).

Four variants originally classified as pathogenic gave rise to channels with abnormal function in our bioassay, confirming the previous ACMG/AMP classification. Our functional screening included 89 variants that were initially categorized as likely pathogenic. One of these variants — p.(Arg436Gln) — was pinpointed as functionally normal. The application of the BS3_strong criteria had a slight effect so that the variant could be re-classified as VUS. The remaining 88 variants showed to be functionally abnormal and could be re-classified as pathogenic (Figures 4C and 5, Supplemental Table 4).

Discussion

Detection of variants in patients with inherited disease is effective using modern sequencing technologies. The main hurdle in genetic diagnosis nowadays is the interpretation and classification of the identified variants — especially missense variants — because current classification guidelines categorize this variant type typically as VUS and thus leave the clinician and patient without definite information on whether a variant or genotype is disease-relevant or not. Most variants in *CNGA3* are rare missense variants and the majority of patients with *CNGA3*-ACHM are (presumably) compound heterozygous carrying at least 1 missense variant.[26,32] Thus, functional studies assessing the effect of such CNGA3 variants onto protein function are indispensable to enhance missense variant classification and thereby molecular diagnosis.

Our current study is comprehensive and provides functional testing and ACMG/AMP-based re-classification of 150 *CNGA3* missense variants that previously lacked functional data or showed contradictory outcomes in previously conducted functional studies. The approach based on our further developed medium-throughput, aequorin-based bioassay allows clear differentiation of CNGA3 channels exhibiting WT-like function designated as "functionally normal" and altered functionality in comparison with the WT categorized as "functionally abnormal." The latter group included variant channels showing residual activity but altered responses compared with the WT, eg, reduced/enhanced latency or reduced overall luminescence signals, as well as variant channels that did not exhibit any

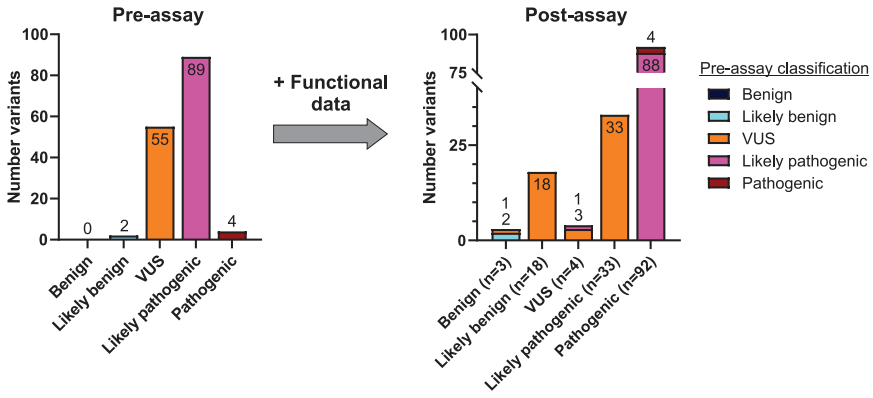


Figure 5 Influence of the functional data on the ACMG/AMP-based variant classification of 150 analyzed CNGA3 missense variants. Pre-assay ACMG/AMP classification of the 150 CNGA3 variants resulted in 2 likely benign, 55 VUS, 89 likely pathogenic, and 4 pathogenic variants (left graph). By applying the functional data obtained by our luminescence-based bioassay ACMG/AMP classification could be confirmed or revised (right graph). Two likely benign variants were re-classified as benign. Of the 55 VUS, 1 variant was re-categorized as benign, 18 variants as likely benign and 33 as likely pathogenic — only 3 variants remained as VUS. The preceding ACMG/AMP classification for all 4 pathogenic variants could be confirmed and 88 of 89 likely pathogenic variants were re-classified as pathogenic — 1 variant was re-categorized as VUS. VUS, variant of uncertain significance.

luminescence signals in our experimental setup upon ligand application. We did not intend to study how specifically a variant affects CNGA3 channel activity because this information is not necessary to classify a variant as disease-relevant or not. Therefore, we also did not further subdivide the "functionally abnormal" variant channels into loss of function, gain of function, or non-functional.

Previous studies have shown that variants in CNGA3 channels can affect ligand sensitivity, gating, ion selectivity and protein folding and/or trafficking.[36-41,44,47,49] We have selected the variants for our validation data set based on these characteristics to verify that our luminescence assay is capable of detecting impaired CNGA3 channel function independent of the defect present in the mutant channel. As examples, the variant p.(Glu228Lys) is known to have impaired surface targeting, the variants p.(Glu590Lys) and p.(Ala469Thr) have been shown to result in increased, whereas the variant p.(Gly557Arg) results in reduced apparent ligand sensitivity.[41] Overall, our assay was validated based on 9 benign and 15 pathogenic control variants in the *CNGA3* gene of which 1 benign and 15 pathogenic control variants were previously extensively studied.[36,37,39-43,49] The data obtained by the aequorin-based bioassay greatly overlapped with the data acquired by preceding calcium imaging or patch clamp recordings. Combining both the overall luminescence, as well as the peak latency as readouts, the bioassay successfully enabled reliable classification of variants from the validation data set as functionally normal or abnormal.

Furthermore, our aequorin-based bioassay displayed a sufficient dynamic range between functionally normal and functionally abnormal variants to enable the establishment of precise pathogenicity thresholds.

Finally, the functional data obtained by our medium-through-put aequorin-based calcium influx assay are highly reproducible and CNGA3 protein expression was verified using dot blot analysis of the tested samples. We did not attempt to quantify protein expression of variant CNGA3 channels in the HEK293^{aequo} cells because reduced protein amounts, eg, due to reduced protein stability would be represented as altered luminescence signals in our bioassay. In conclusion, our aequorin-based bioassay qualifies for the application as a strong line of evidence in the ACMG/AMP classification system for the re-classification of missense variants in the *CNGA3* gene related to ACHM.

The functional evaluation of 150 missense variants revealed a high number of variants coding for non-functional channels corresponding to 53.3% (n = 80 variants). This observation is in line with previously conducted functional studies in which 50% of all 54 missense variants analyzed so far dramatically impaired channel functionality, indicating that the CNGA3 polypeptide is rather sensitive toward amino acid substitutions. The majority of these variants is located in functional or structural domains of the CNGA3 protein, which are highly conserved across CNGA3 orthologs and its rod equivalent CNGA1.[32,36-40,42,43,45]

Initial ACMG/AMP-based classification of all 150 analyzed missense variants revealed that a high number of 55 variants were classified as VUS. By applying the functional evidence obtained by using our approach, we could re-classify 1of 55 as benign, 18 of 55 as likely benign, and 33 of 55 as likely pathogenic, considerably aiding clinical variant interpretation, thereby underlining the importance of functional assays for the ACMG/AMP-based re-classification of variants still assigned as VUS. One VUS re-classified as likely pathogenic is the p.(Asn471Ser) variant, which affects a completely conserved amino acid residue in the C-linker region. So far, the variant was only observed in heterozygous state in the absence of a second likely disease-associated allele in a patient diagnosed with cone dystrophy.[19] Previously conducted electrophysiological recordings

of homomeric mutant p.(Asn471Ser) channels, which were heterologously expressed in *Xenopus* oocytes or HEK293 cells delivered contradictory functional results reporting either an increased apparent cGMP sensitivity in the homomeric channels or no change compared with homomeric WT channels, respectively.[37,39] In our aequorin-based bioassay, the mutant homomeric channels carrying the p.(Asn471Ser) variant presented with an unaltered overall luminescence signal (AUC) but a reduced peak latency compared with WT channels. The latter may be because of an increase in the apparent cGMP sensitivity supporting the observation made by Liu and Varnum.[37] Therefore, we categorized the variant channels as functionally abnormal, re-classifying the missense variant p.(Asn471Ser) as likely pathogenic.

Furthermore, we identified 2 of 2 likely benign variants as functionally normal and 92 of 93 (likely) pathogenic variants as functionally abnormal, thereby upgrading or confirming their ACMG/AMP classification to benign and pathogenic, respectively. However, 1 missense substitution initially classified as likely pathogenic according to ACMG/AMP criteria — the p.(Arg436Gln) variant — could only be re-classified as VUS, although the variant displayed unaltered AUC and peak latency values in the aequorin-based bioassay and was therefore categorized as functionally normal. Initial ACMG/AMP classification as likely pathogenic was based on the localization of the variant in the C-linker region affecting a completely conserved amino acid residue, its low minor allele frequency of <0.039% in the reference population database gnomAD and the in silico prediction as having a deleterious effect on protein function. Furthermore, a known pathogenic variant p.(Arg436Trp) at the same amino acid residue position displays loss of channel functionality in previously conducted studies.[19,39,43] However, the p.(Arg436Gln) missense substitution was identified as part of a complex allele with the pathogenic p.(Phe322Ser) variant and the nonsense substitution p.(Trp440Ter) *in trans* in a patient with ACHM.[53] Because the variant was only observed as part of a complex allele, its contribution to the ACHM phenotype remains unclear. Additionally, no deleterious effect on channel function was detected using our aequorin-based bioassay approach unlike the known pathogenic p.(Arg436Trp) variant, which was previously shown to impair responsiveness of the channel to ligands and to cause cytosolic aggregation.[43] This observed differential impact of missense substitutions on the same amino acid residue emphasizes the fact that the PM5 rule of the ACMG/AMP guidelines, describing the occurrence of a missense variant at the same amino acid residue as another pathogenic variant, is only indicative for pathogenicity, further underlining the need for functional assays to assess the pathogenic impact of novel missense variants because the in silico evidence might be contradictory.

Despite utilizing functional data as strong evidence, there were still 3 VUS that could not be re-classified according to ACMG/AMP guidelines, although all 3 missense alterations were found to result in channels with normal function: p.(Lys595Arg), p.(Arg646His), and p.(Val669Leu). Initial ACMG/AMP classification as VUS was based on the minor allele frequency of the respective variants, the localization in a mutational hotspot, and the deleterious in silico prediction. However, the p.(Arg646His) variant was only observed in a heterozygous state without a second disease-associated allele. Moreover, for the p.(Lys595Arg) and the p.(Val669Leu) variants, no genotype could be established based on the ClinVar database entries.[32,53,54] Because of the provided functional evidence using our aequorin-based bioassay and the available genotype data, we suggest that these variants do not have a deleterious effect on CNGA3 protein function, even if they are still deemed to be of uncertain significance in the ACMG/AMP classification system based on inconclusive data.

In summary, our medium-throughput aequorin-based calcium influx assay represents an essential tool to characterize the impact of *CNGA3* missense variants on the function of homomeric CNGA3 channels supporting the reclassification of missense alterations assigned as VUS.

A limitation of our study might be considered the fact that we assessed the functionality of mutant homomeric CNGA3 channels that were heterologously expressed in HEK293^{aequo} cells in the absence of the modulatory CNGB3 subunit. In 5 of 54 previously extensively studied missense variants, an amelioration of the mutant channel function was observed by co-expressing the CNGB3 subunit. These mutant heteromeric channels still presented altered biophysical characteristics compared with WT channels.[37,39,41,42] In addition, besides the co-expression of the CNGB3 subunit, the cell cultivation temperature had to be lowered from the standard 37 °C to 27 °C — a commonly known method to support protein folding and trafficking — to achieve the rescue effect.[42] Thus, we do not expect that functionally abnormal CNGA3 variants from our assay would give rise to heteromeric channels with WT-like function. Therefore, assessing CNGA3 variant effects in homomeric channels appears to be sufficient and effective to assess their pathogenicity.

Using our medium-throughput aequorin-based bioassay, we functionally characterized mutant homomeric CNGA3 channels carrying a single missense substitution in the CNGA3 subunit reflecting a homozygous genotype in patients with ACHM. However, the vast majority of patients with ACHM with possibly disease-associated *CNGA3* variants are likely to harbor 2 distinct variants in the *CNGA3* gene in a compound heterozygous state as demonstrated by the studies of Sun et al and Solaki et al in which 61.8% to 79.4% of the patients with *CNGA3*-associated ACHM harbor 2 (likely compound) heterozygous variants.[26,32] Co-expressing 2 mutant CNGA3 subunits carrying 2 distinct missense variants in the heterologous HEK293^{aequo} expression system would be possible. However, the final subunit composition of these channels could not be reconstructed in the current assay setup.

Another limiting factor arising in our luminescence bioassay is the usage of a *CNGA3* cDNA expression

construct because we might miss variants acting on splicing. Three of the tested missense variants (p.(Arg189Lys), p.(Thr224Ala), and p.(Thr224Ile)) are located at the exon-intron borders possibly interfering with splicing as predicted by in silico algorithms.[32] This predicted minor effect on transcript splicing could only be confirmed for the p.(Arg189Lys) variant in a previously conducted study using a minigene assay approach, whereas both the p.(Thr224Ala) and the p.(Thr224Ile) variant exhibited no interference with transcript splicing.[55] However, all 3 missense substitutions led to the complete abolishment of channel function as shown in our aequorin-based bioassay and therefore are considered to act as missense variants because the splicing effect is negligible in all 3 cases.

To sum it up, our study highlights the medium-throughput aequorin-based bioassay as a powerful and essential tool to assess the impact of *CNGA3* variants on the functionality of mutant homomeric CNGA3 channels. Adaptation of the bioassay may also allow characterization of missense variants in the other IRD-related CNG channel genes, ie, *CNGB3* in ACHM and *CNGA1* and *CNGB1* in autosomal recessive retinitis pigmentosa. We hereby present functional data obtained by our bioassay for a total of 150 missense substitutions in the *CNGA3* gene, of which 55 were previously categorized as VUS, identifying 25 as functionally normal and 125 as functionally abnormal. These functional data were subsequently used to finalize ACMG/AMP-based variant re-classification enabling the re-classification of 52 of 55 VUS as either benign (1/52), likely benign (18/52), or likely pathogenic (33/52), reaching a high re-classification rate of 94.5%. Our study has important implications on the clinical variant interpretation of *CNGA3* missense variants thereby improving genetic diagnosis for patients with *CNGA3*-associated ACHM and supporting their selection for future gene therapeutic interventions.

Data Availability

All data that support the findings of this study are included in the article or uploaded as supplemental information.

Funding

This study was funded by the Deutsche Forschungsgemeinschaft as part of the SPP 2127: Gene and cell-based therapies to counteract neuroretinal degeneration, project number: KO 2176/3-1, 398539671 to S.K.

Author Information

Conceptualization: B.W., S.K., P.R.; Formal Analysis: M.S.; Funding Acquisition: S.K.; Investigation: M.S.; Methodology: M.S., P.R.; Supervision: B.W., S.K., P.R.; Validation: M.S.; Visualization: M.S.; Writing-original draft: M.S.; Writing-review and editing: M.S., B.W., S.K., P.R.

Ethics Declaration

Ethical approval was not required because no patient data or derived material were used in this study.

Conflict of Interest

The authors declare no conflicts of interest.

Additional Information

The online version of this article (https://doi.org/10.1016/j.gim.2023.100979) contains supplemental material, which is available to authorized users.

References

1. Broadgate S, Yu J, Downes SM, Halford S. Unravelling the genetics of inherited retinal dystrophies: past, present and future. *Prog Retin Eye Res*. 2017;59:53-96. http://doi.org/10.1016/j.preteyeres.2017.03.003
2. Richards S, Aziz N, Bale S, et al. Standards and guidelines for the interpretation of sequence variants: a joint consensus recommendation of the American College of Medical Genetics and Genomics and the Association for Molecular Pathology. *Genet Med*. 2015;17(5):405-424. http://doi.org/10.1038/gim.2015.30
3. Iancu IF, Avila-Fernandez A, Arteche A, et al. Prioritizing variants of uncertain significance for reclassification using a rule-based algorithm in inherited retinal dystrophies. *npj Genom Med*. 2021;6(1):18. http://doi.org/10.1038/s41525-021-00182-z
4. Ganapathi M, Thomas-Wilson A, Buchovecky C, et al. Clinical exome sequencing for inherited retinal degenerations at a tertiary care center. *Sci Rep*. 2022;12(1):9358. http://doi.org/10.1038/s41598-022-13026-2
5. François J. *Heredity in Ophthalmology*. St Louis: Mosby; 1961.
6. Hirji N, Aboshiha J, Georgiou M, Bainbridge J, Michaelides M. Achromatopsia: clinical features, molecular genetics, animal models and therapeutic options. *Ophthal Genet*. 2018;39(2):149-157. http://doi.org/10.1080/13816810.2017.1418389
7. Michalakis S, Gerhardt M, Rudolph G, Priglinger S, Priglinger C. Achromatopsia: genetics and gene therapy. *Mol Diagn Ther*. 2022;26(1):51-59. http://doi.org/10.1007/s40291-021-00565-z
8. Kohl S, Marx T, Giddings I, et al. Total colourblindness is caused by mutations in the gene encoding the alpha-subunit of the cone photoreceptor cGMP-gated cation channel. *Nat Genet*. 1998;19(3):257-259. http://doi.org/10.1038/935
9. Kohl S, Baumann B, Broghammer M, et al. Mutations in the CNGB3 gene encoding the beta-subunit of the cone photoreceptor cGMP-gated channel are responsible for achromatopsia (ACHM3) linked to chromosome 8q21. *Hum Mol Genet*. 2000;9(14):2107-2116. http://doi.org/10.1093/hmg/9.14.2107
10. Sundin OH, Yang JM, Li Y, et al. Genetic basis of total colourblindness among the Pingelapese islanders. *Nat Genet*. 2000;25(3):289-293. http://doi.org/10.1038/77162

11. Aligianis IA, Forshew T, Johnson S, et al. Mapping of a novel locus for achromatopsia (ACHM4) to 1p and identification of a germline mutation in the alpha subunit of cone transducin (GNAT2). *J Med Genet*. 2002;39(9):656-660. http://doi.org/10.1136/jmg.39.9.656
12. Kohl S, Baumann B, Rosenberg T, et al. Mutations in the cone photoreceptor G-protein alpha-subunit gene GNAT2 in patients with achromatopsia. *Am J Hum Genet*. 2002;71(2):422-425. http://doi.org/10.1086/341835
13. Chang B, Grau T, Dangel S, et al. A homologous genetic basis of the murine cpfl1 mutant and human achromatopsia linked to mutations in the PDE6C gene. *Proc Natl Acad Sci U S A*. 2009;106(46):19581-19586. http://doi.org/10.1073/pnas.0907720106
14. Thiadens AA, den Hollander AI, Roosing S, et al. Homozygosity mapping reveals PDE6C mutations in patients with early-onset cone photoreceptor disorders. *Am J Hum Genet*. 2009;85(2):240-247. http://doi.org/10.1016/j.ajhg.2009.06.016
15. Kohl S, Coppieters F, Meire F, et al. A nonsense mutation in PDE6H causes autosomal-recessive incomplete achromatopsia. *Am J Hum Genet*. 2012;91(3):527-532. http://doi.org/10.1016/j.ajhg.2012.07.006
16. Kohl S, Zobor D, Chiang WC, et al. Mutations in the unfolded protein response regulator ATF6 cause the cone dysfunction disorder achromatopsia. *Nat Genet*. 2015;47(7):757-765. http://doi.org/10.1038/ng.3319
17. Ansar M, Santos-Cortez RL, Saqib MA, et al. Mutation of ATF6 causes autosomal recessive achromatopsia. *Hum Genet*. 2015;134(9):941-950. http://doi.org/10.1007/s00439-015-1571-4
18. Xu M, Gelowani V, Eblimit A, et al. ATF6 is mutated in early onset photoreceptor degeneration with macular involvement. *Invest Ophthalmol Vis Sci*. 2015;56(6):3889-3895. http://doi.org/10.1167/iovs.15-16778
19. Wissinger B, Gamer D, Jägle H, et al. CNGA3 mutations in hereditary cone photoreceptor disorders. *Am J Hum Genet*. 2001;69(4):722-737. http://doi.org/10.1086/323613
20. Kaupp UB, Seifert R. Cyclic nucleotide-gated ion channels. *Physiol Rev*. 2002;82(3):769-824. http://doi.org/10.1152/physrev.00008.2002
21. Johnson S, Michaelides M, Aligianis IA, et al. Achromatopsia caused by novel mutations in both CNGA3 and CNGB3. *J Med Genet*. 2004;41(2):e20. http://doi.org/10.1136/jmg.2003.011437
22. Varsányi B, Wissinger B, Kohl S, Koeppen K, Farkas A. Clinical and genetic features of Hungarian achromatopsia patients. *Mol Vis*. 2005;11:996-1001.
23. Thiadens AA, Slingerland NW, Roosing S, et al. Genetic etiology and clinical consequences of complete and incomplete achromatopsia. *Ophthalmology*. 2009;116(10):1984-1989.e1. http://doi.org/10.1016/j.ophtha.2009.03.053
24. Zelinger L, Cideciyan AV, Kohl S, et al. Genetics and disease expression in the CNGA3 form of achromatopsia: steps on the path to gene therapy. *Ophthalmology*. 2015;122(5):997-1007. http://doi.org/10.1016/j.ophtha.2014.11.025
25. Liang X, Dong F, Li H, Li H, Yang L, Sui R. Novel CNGA3 mutations in Chinese patients with achromatopsia. *Br J Ophthalmol*. 2015;99(4):571-576. http://doi.org/10.1136/bjophthalmol-2014-305432
26. Sun W, Li S, Xiao X, Wang P, Zhang Q. Genotypes and phenotypes of genes associated with achromatopsia: a reference for clinical genetic testing. *Mol Vis*. 2020;26:588-602.
27. Zhong H, Molday LL, Molday RS, Yau KW. The heteromeric cyclic nucleotide-gated channel adopts a 3A:1B stoichiometry. *Nature*. 2002;420(6912):193-198. http://doi.org/10.1038/nature01201
28. Shuart NG, Haitin Y, Camp SS, Black KD, Zagotta WN. Molecular mechanism for 3 : 1 subunit stoichiometry of rod cyclic nucleotide-gated ion channels. *Nat Commun*. 2011;2:457. http://doi.org/10.1038/ncomms1466
29. Barret DCA, Schertler GFX, Kaupp UB, Marino J. The structure of the native CNGA1/CNGB1 CNG channel from bovine retinal rods. *Nat Struct Mol Biol*. 2022;29(1):32-39. http://doi.org/10.1038/s41594-021-00700-8
30. Zheng X, Hu Z, Li H, Yang J. Structure of the human cone photoreceptor cyclic nucleotide-gated channel. *Nat Struct Mol Biol*. 2022;29(1):40-46. http://doi.org/10.1038/s41594-021-00699-y
31. Gofman Y, Schärfe C, Marks DS, Haliloglu T, Ben-Tal N. Structure, dynamics and implied gating mechanism of a human cyclic nucleotide-gated channel. *PLOS Comput Biol*. 2014;10(12):e1003976. http://doi.org/10.1371/journal.pcbi.1003976
32. Solaki M, Baumann B, Reuter P, et al. Comprehensive variant spectrum of the CNGA3 gene in patients affected by achromatopsia. *Hum Mutat*. 2022;43(7):832-858. http://doi.org/10.1002/humu.24371
33. Sun W, Zhang Q. Diseases associated with mutations in CNGA3: genotype-phenotype correlation and diagnostic guideline. *Prog Mol Biol Transl Sci*. 2019;161:1-27. http://doi.org/10.1016/bs.pmbts.2018.10.002
34. Fischer MD, Michalakis S, Wilhelm B, et al. Safety and vision outcomes of subretinal gene therapy targeting cone photoreceptors in achromatopsia: a nonrandomized controlled trial. *JAMA Ophthalmol*. 2020;138(6):643-651. http://doi.org/10.1001/jamaophthalmol.2020.1032
35. Reichel FF, Michalakis S, Wilhelm B, et al. Three-year results of phase I retinal gene therapy trial for CNGA3-mutated achromatopsia: results of a non randomised controlled trial. *Br J Ophthalmol*. 2022;106(11):1567-1572. http://doi.org/10.1136/bjophthalmol-2021-319067
36. Tränkner D, Jägle H, Kohl S, et al. Molecular basis of an inherited form of incomplete achromatopsia. *J Neurosci*. 2004;24(1):138-147. http://doi.org/10.1523/JNEUROSCI.3883-03.2004
37. Liu C, Varnum MD. Functional consequences of progressive cone dystrophy-associated mutations in the human cone photoreceptor cyclic nucleotide-gated channel CNGA3 subunit. *Am J Physiol Cell Physiol*. 2005;289(1):C187-C198. http://doi.org/10.1152/ajpcell.00490.2004
38. Patel KA, Bartoli KM, Fandino RA, et al. Transmembrane S1 mutations in CNGA3 from achromatopsia 2 patients cause loss of function and impaired cellular trafficking of the cone CNG channel. *Invest Ophthalmol Vis Sci*. 2005;46(7):2282-2290. http://doi.org/10.1167/iovs.05-0179
39. Muraki-Oda S, Toyoda F, Okada A, et al. Functional analysis of rod monochromacy-associated missense mutations in the CNGA3 subunit of the cone photoreceptor cGMP-gated channel. *Biochem Biophys Res Commun*. 2007;362(1):88-93. http://doi.org/10.1016/j.bbrc.2007.07.152
40. Koeppen K, Reuter P, Kohl S, Baumann B, Ladewig T, Wissinger B. Functional analysis of human CNGA3 mutations associated with colour blindness suggests impaired surface expression of channel mutants A3(R427C) and A3(R563C). *Eur J Neurosci*. 2008;27(9):2391-2401. http://doi.org/10.1111/j.1460-9568.2008.06195.x
41. Reuter P, Koeppen K, Ladewig T, et al. Mutations in CNGA3 impair trafficking or function of cone cyclic nucleotide-gated channels, resulting in achromatopsia. *Hum Mutat*. 2008;29(10):1228-1236. http://doi.org/10.1002/humu.20790
42. Koeppen K, Reuter P, Ladewig T, et al. Dissecting the pathogenic mechanisms of mutations in the pore region of the human cone photoreceptor cyclic nucleotide-gated channel. *Hum Mutat*. 2010;31(7):830-839. http://doi.org/10.1002/humu.21283
43. Matveev AV, Fitzgerald JB, Xu J, Malykhina AP, Rodgers KK, Ding XQ. The disease-causing mutations in the carboxyl terminus of the cone cyclic nucleotide-gated channel CNGA3 subunit alter the local secondary structure and interfere with the channel active conformational change. *Biochemistry*. 2010;49(8):1628-1639. http://doi.org/10.1021/bi901960u
44. Dai G, Varnum MD. CNGA3 achromatopsia-associated mutation potentiates the phosphoinositide sensitivity of cone photoreceptor CNG channels by altering intersubunit interactions. *Am J Physiol Cell Physiol*. 2013;305(2):C147-C159. http://doi.org/10.1152/ajpcell.00037.2013

45. Shaikh RS, Reuter P, Sisk RA, et al. Homozygous missense variant in the human CNGA3 channel causes cone-rod dystrophy. *Eur J Hum Genet*. 2015;23(4):473-480. http://doi.org/10.1038/ejhg.2014.136
46. Kuniyoshi K, Muraki-Oda S, Ueyama H, et al. Novel mutations in the gene for alpha-subunit of retinal cone cyclic nucleotide-gated channels in a Japanese patient with congenital achromatopsia. *Jpn J Ophthalmol*. 2016;60(3):187-197. http://doi.org/10.1007/s10384-016-0424-6
47. Burkard M, Kohl S, Krätzig T, et al. Accessory heterozygous mutations in cone photoreceptor CNGA3 exacerbate CNG channel-associated retinopathy. *J Clin Invest*. 2018;128(12):5663-5675. http://doi.org/10.1172/JCI96098
48. Täger J, Kohl S, Birch DG, Wheaton DKH, Wissinger B, Reuter P. An early nonsense mutation facilitates the expression of a short isoform of CNGA3 by alternative translation initiation. *Exp Eye Res*. 2018;171:48-53. http://doi.org/10.1016/j.exer.2018.02.027
49. Meighan PC, Peng C, Varnum MD. Inherited macular degeneration-associated mutations in CNGB3 increase the ligand sensitivity and spontaneous open probability of cone cyclic nucleotide-gated channels. *Front Physiol*. 2015;6:177. http://doi.org/10.3389/fphys.2015.00177
50. Brunetti-Pierri R, Karali M, Melillo P, et al. Clinical and molecular characterization of achromatopsia patients: a longitudinal study. *Int J Mol Sci*. 2021;22(4). http://doi.org/10.3390/ijms22041681
51. Brnich SE, Abou Tayoun AN, Couch FJ, et al. Recommendations for application of the functional evidence PS3/BS3 criterion using the ACMG/AMP sequence variant interpretation framework. *Genome Med*. 2019;12(1):3. http://doi.org/10.1186/s13073-019-0690-2
52. Täger J, Wissinger B, Kohl S, Reuter P. Identification of chemical and pharmacological chaperones for correction of trafficking-deficient mutant cyclic nucleotide-gated A3 channels. *Mol Pharmacol*. 2021;99(6):460-468. http://doi.org/10.1124/molpharm.120.000180
53. Li S, Huang L, Xiao X, Jia X, Guo X, Zhang Q. Identification of CNGA3 mutations in 46 families: common cause of achromatopsia and cone-rod dystrophies in Chinese patients. *JAMA Ophthalmol*. 2014;132(9):1076-1083. http://doi.org/10.1001/jamaophthalmol.2014.1032
54. Thiadens AA, Roosing S, Collin RW, et al. Comprehensive analysis of the achromatopsia genes CNGA3 and CNGB3 in progressive cone dystrophy. *Ophthalmology*. 2010;117(4):825-830.e1-830 e821. http://doi.org/10.1016/j.ophtha.2009.09.008
55. Reuter P, Walter M, Kohl S, Weisschuh N. Systematic analysis of CNGA3 splice variants identifies different mechanisms of aberrant splicing. *Sci Rep*. 2023;13(1):2896. http://doi.org/10.1038/s41598-023-29452-9

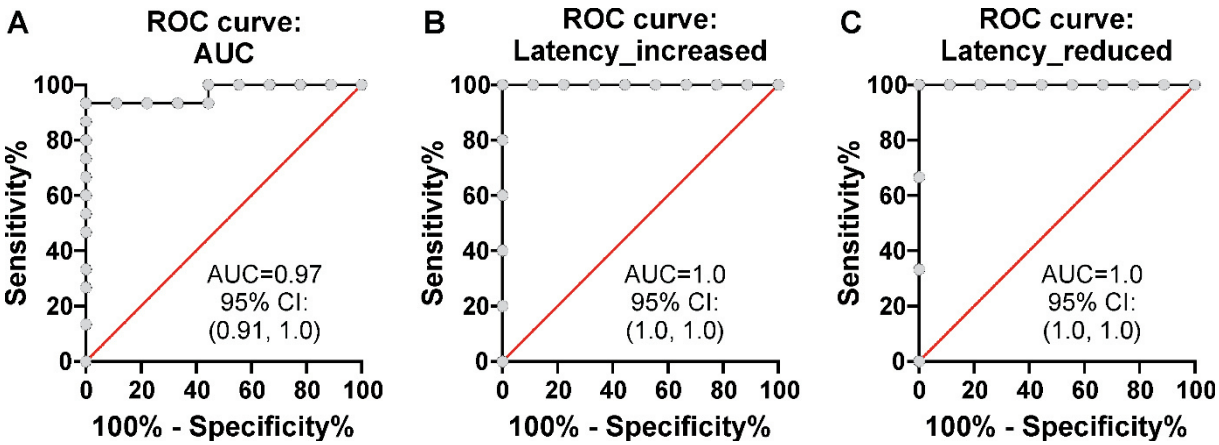
Supplementary material

Solaki et al.

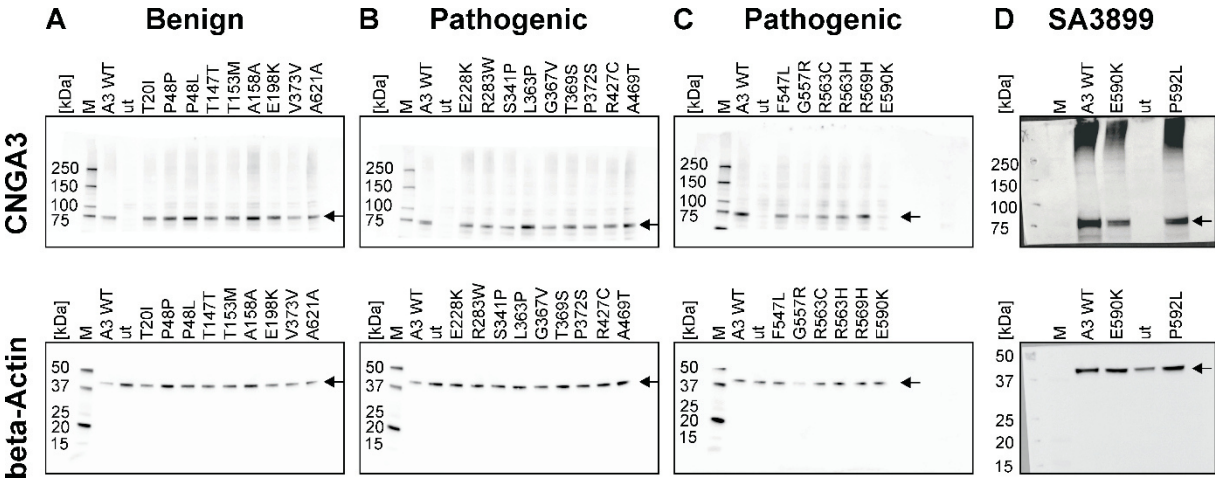
Functional evaluation allows ACMG/AMP-based re-classification of *CNGA3* variants associated with achromatopsia

Supplementary material includes seven figures, four tables and references.

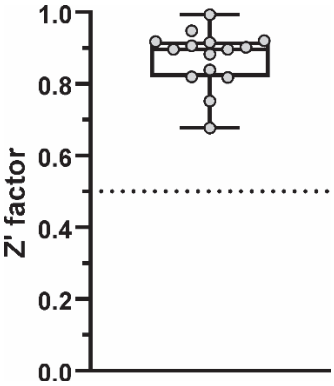
Figures



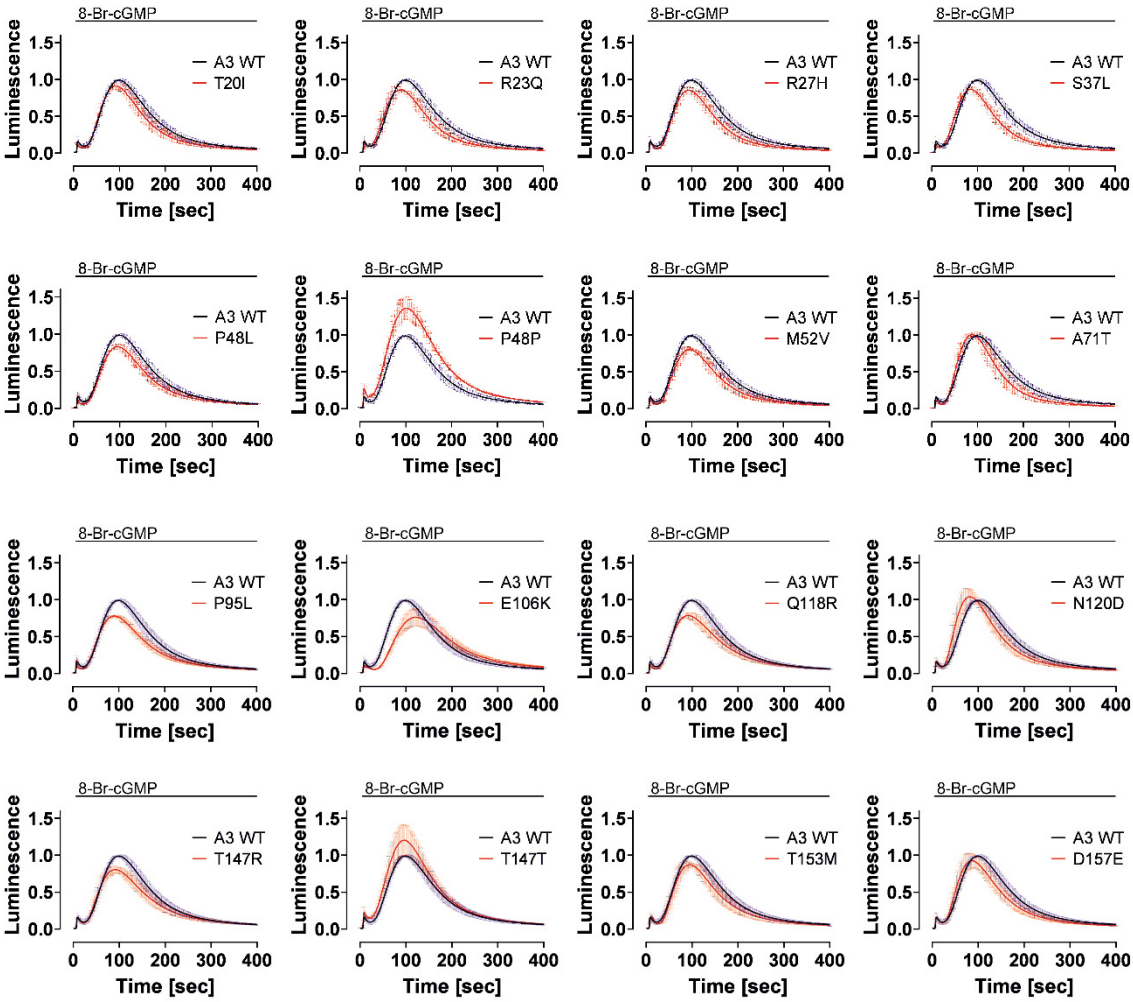
Supplemental Figure 1: Receiver operating characteristic (ROC) curve analysis for the determination of optimal thresholds for the overall luminescence signal (AUC) (A), increased peak latency (B), and reduced peak latency (C). The area under the curve (AUC) reflecting the performance of the classifier and the respective 95% confidence interval (CI) are indicated for each ROC curve.

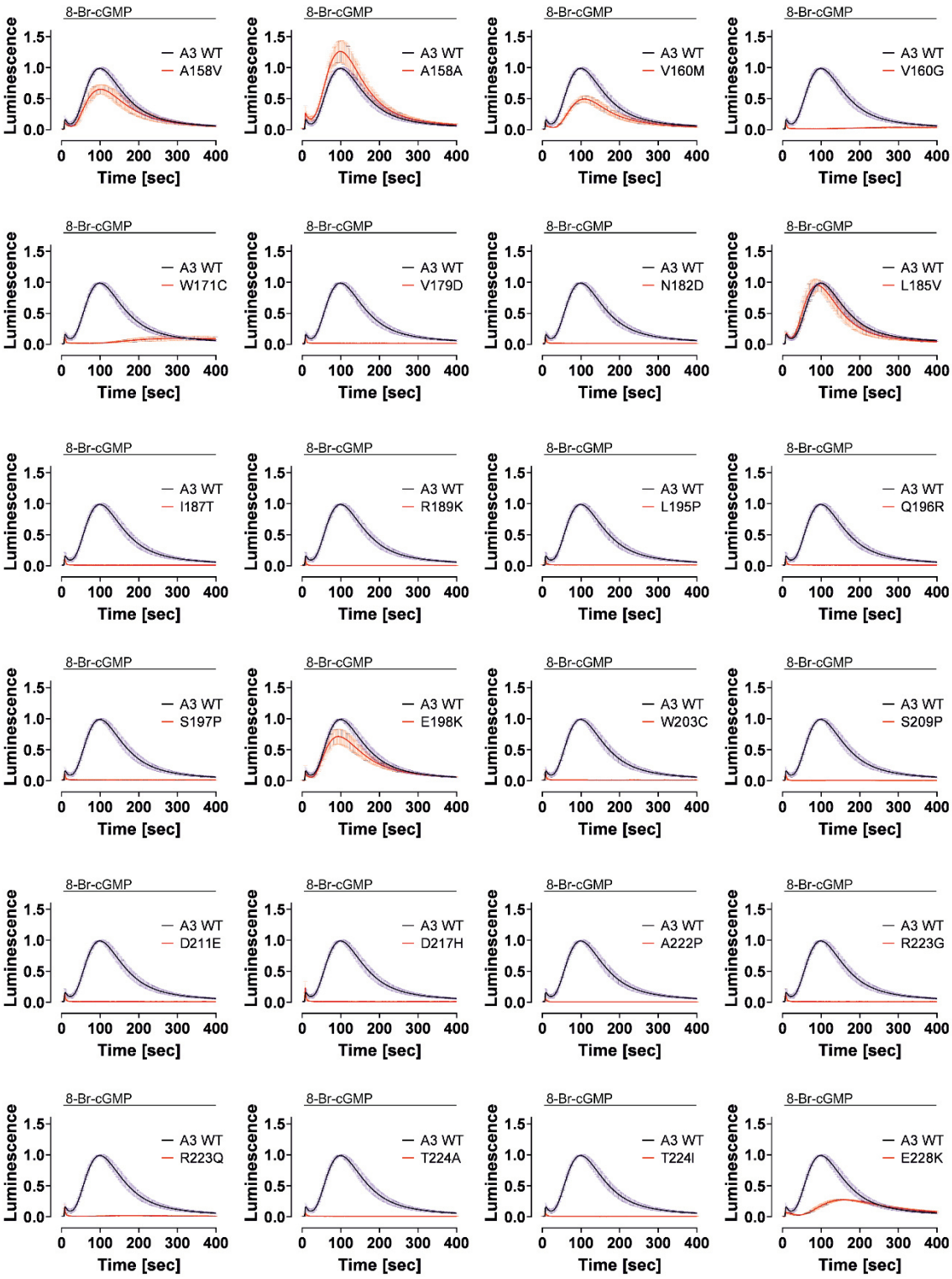


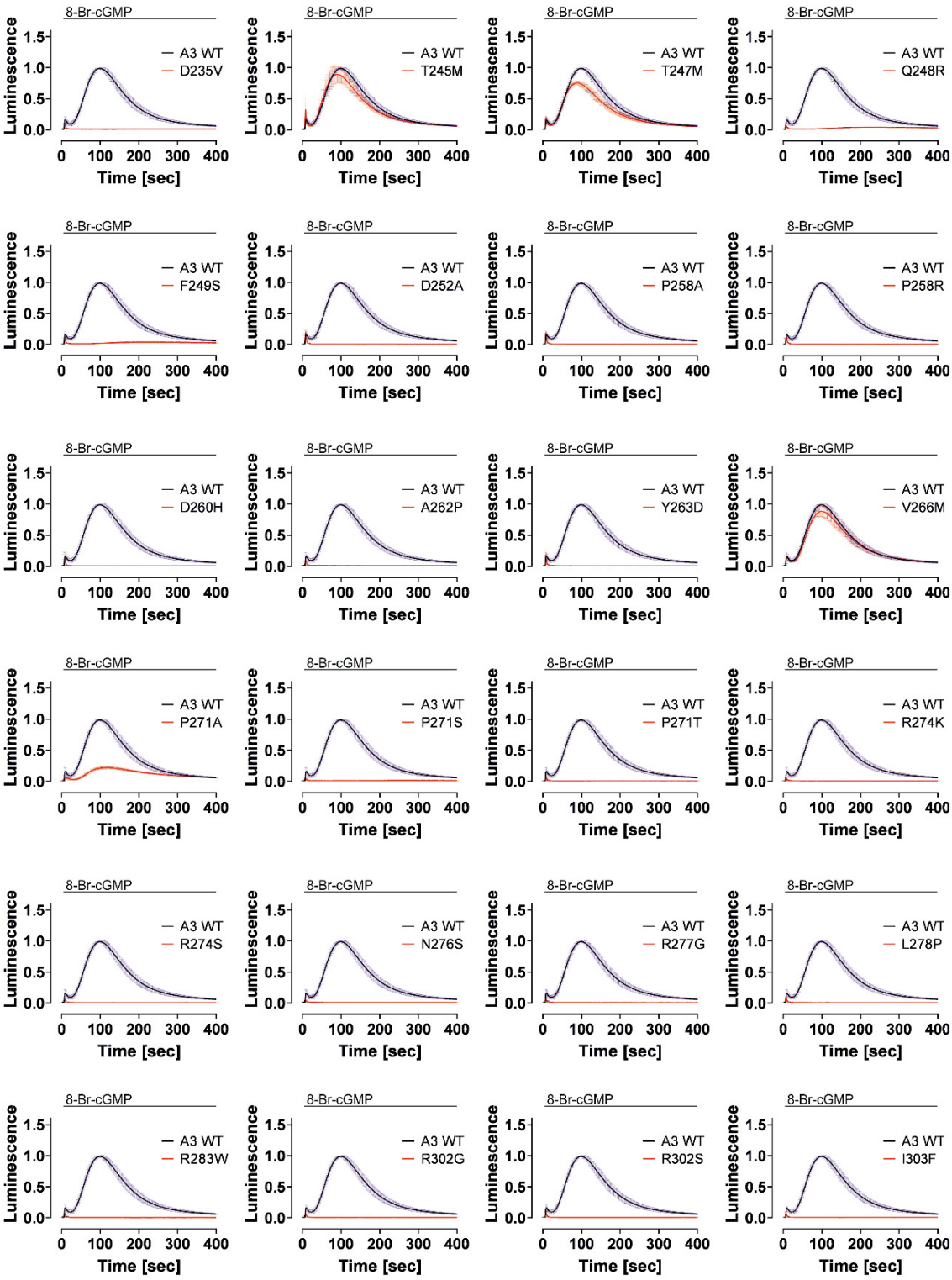
Supplemental Figure 2: Western Blot analysis of whole cell lysates performed for antibody validation and verification of CNGA3 protein expression in one biological replicate of samples from the assay validation data set. A, B, and C. CNGA3 protein expression was detected using a commercial rabbit anti-human CNGA3 antibody in whole cell lysates of HEK293^{aequo} cells transfected with wild-type or mutant *CNGA3* expression constructs carrying either benign (A; n=9 variants) or pathogenic variants (B, C; n=15 variants) from the assay validation data set. 5 µg of total protein were loaded. D. Western Blot analysis of the p.(Glu590Lys) mutant whole cell lysate was repeated using the custom-made rabbit anti-human CNGA3 antibody SA3899 since no protein band could be visualized when using the commercial rabbit anti-human CNGA3 antibody. The p.(Pro592Leu) mutant whole cell lysate was re-analyzed by Western Blotting since no CNGA3 protein expression was detected in the Dot Blot analysis (see Supplemental Figure 7). 30 µg of total protein were loaded. Endogenous levels of beta-actin were detected as loading control in Western Blotting. Whole cell lysates from cells transfected with the wild-type *CNGA3* expression construct (A3 WT) and untransfected cells were used as positive and negative controls, respectively. The protein bands of interest are indicated by an arrow. Molecular sizes of the standard protein marker were indicated on the left of each blot. M, standard protein marker; ut, whole cell lysates of untransfected cells; WT, wild-type.

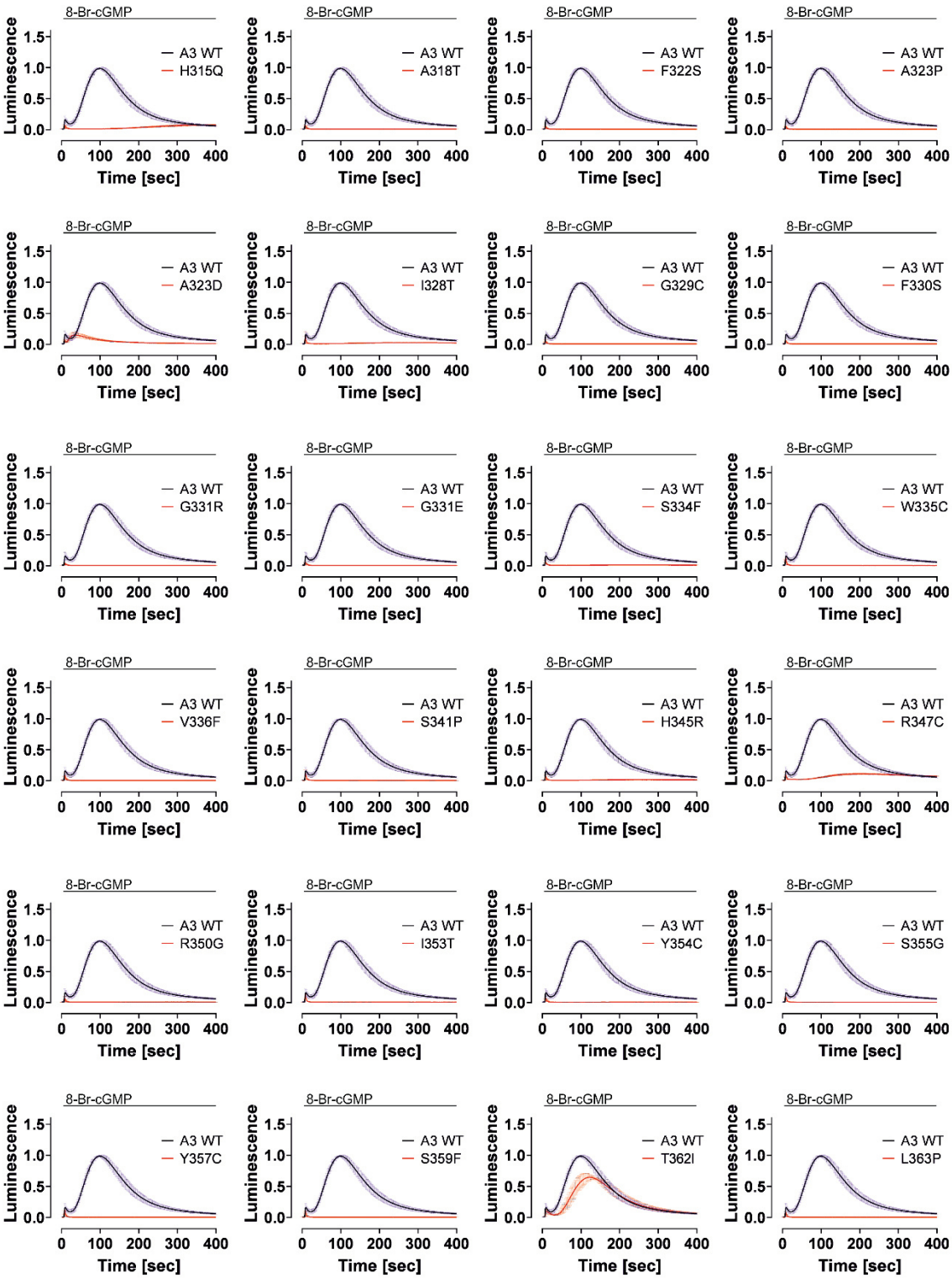


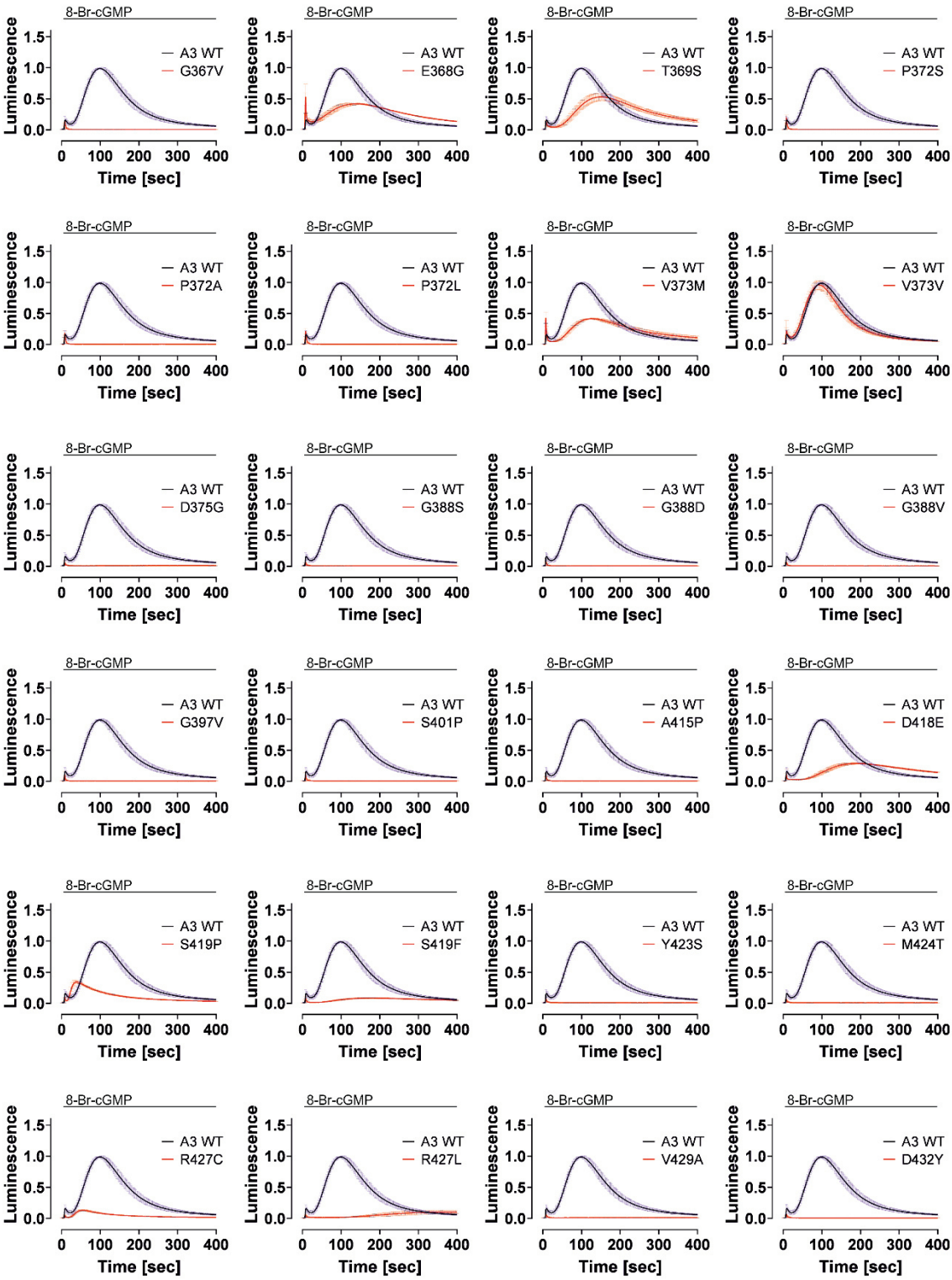
Supplemental Figure 3: Evaluation of the overall assay quality by calculating the Z' factor based on 15 individual assay plates containing both positive (HEK293^{aequo} cells transfected with the wild-type *CNGA3* expression construct) and negative controls (untransfected HEK293^{aequo} cells). The mean Z' factor was thereby 0.87±0.08 (median: 0.9) indicating excellent assay quality. Individual Z' factors of each individual assay plate used for Z' factor calculation are indicated by grey circles. Threshold of Z' factor for distinguishing between excellent and marginal assay quality is indicated by a dotted line (Z' factor between 0.5 and 1.0: excellent assay; Z' factor between 0 and 0.5: marginal assay (Zhang et al., 1999)).

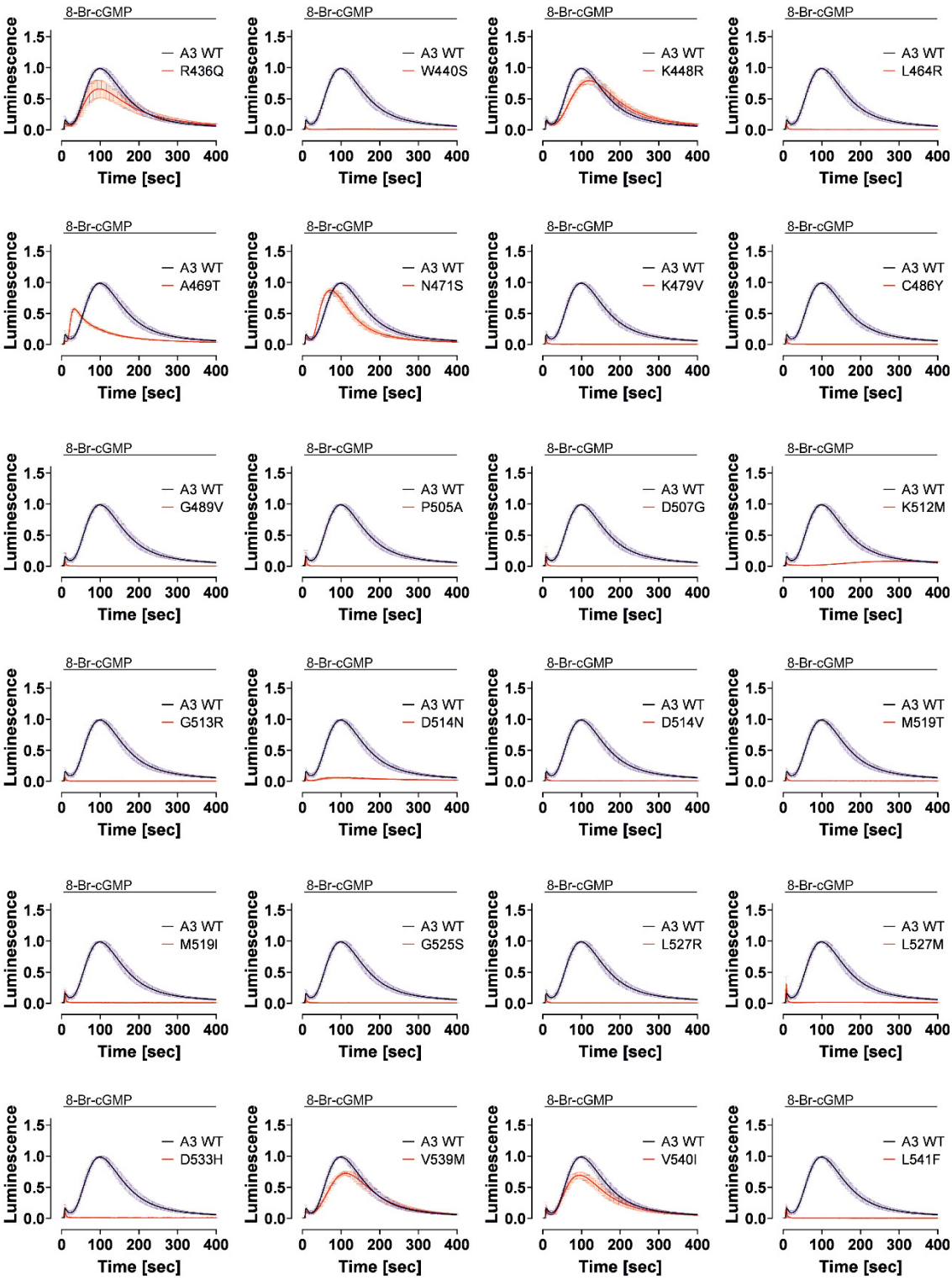


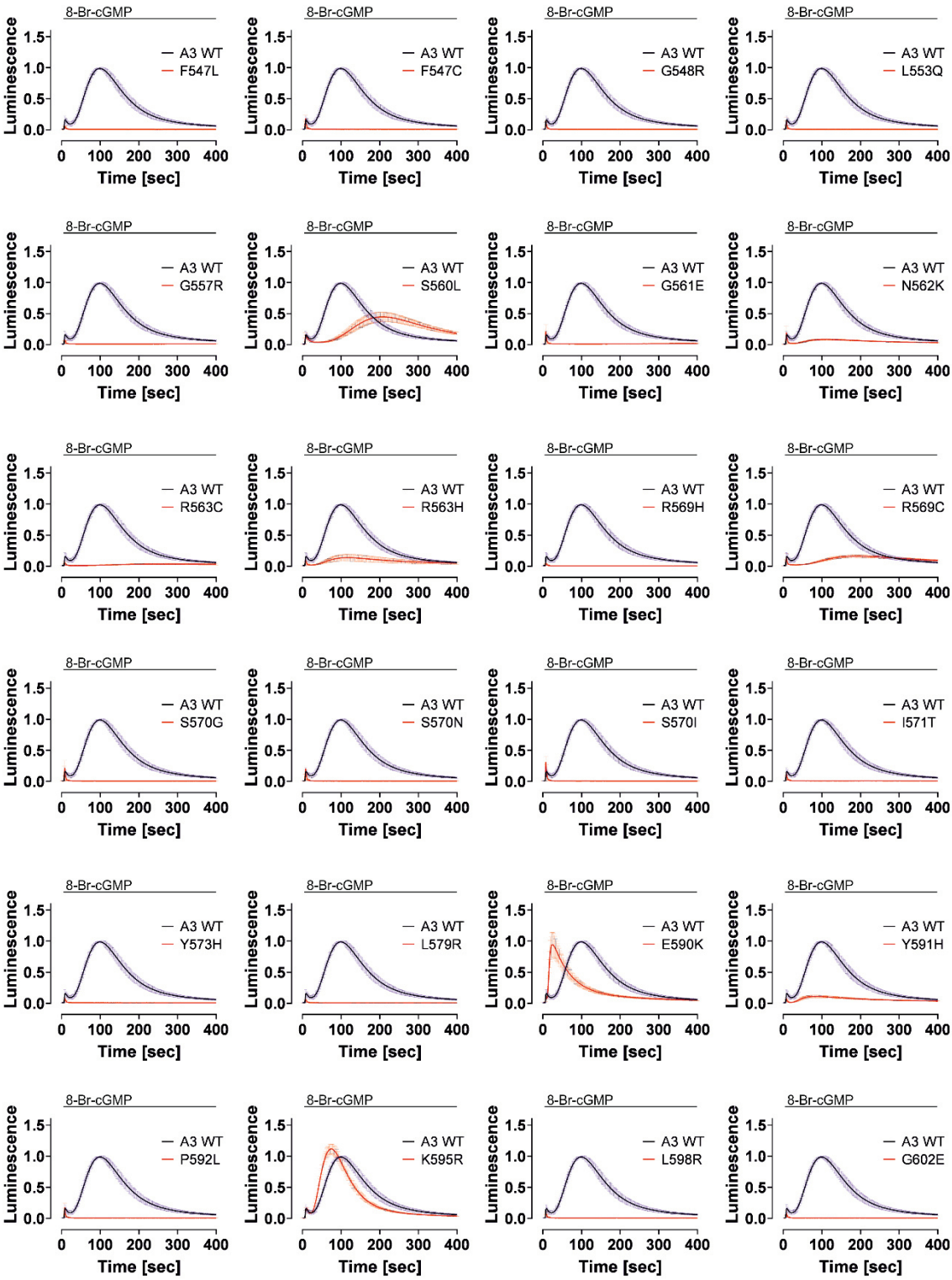

8-Br-cGMP
A3 WT
A158V
A158A
V160M
V160G
W171C
V179D
N182D
L185V
I187T
R189K
L195P
Q196R
S197P
E198K
W203C
S209P
D211E
D217H
A222P
R223G
R223Q
T224A
T224I
E228K
Luminescence
Time [sec]
0.0
0.5
1.0
1.5
0
100
200
300
400

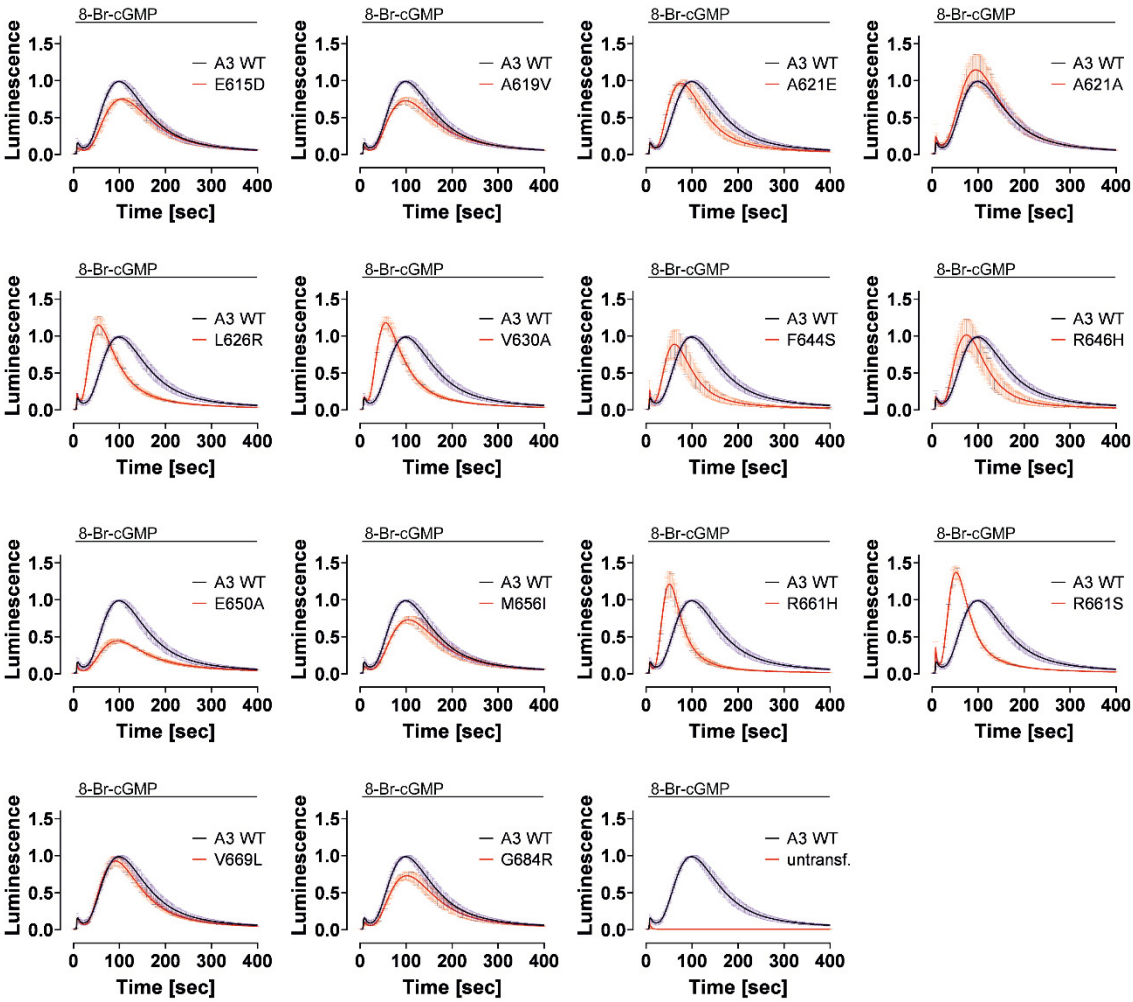

8-Br-cGMP
A3 WT
D235V
T245M
T247M
Q248R
F249S
D252A
P258A
P258R
D260H
A262P
Y263D
V266M
P271A
P271S
P271T
R274K
R274S
N276S
R277G
L278P
R283W
R302G
R302S
I303F
Luminescence
Time [sec]
0.0
0.5
1.0
1.5
0
100
200
300
400


8-Br-cGMP
A3 WT
H315Q
A318T
F322S
A323P
A323D
I328T
G329C
F330S
G331R
G331E
S334F
W335C
V336F
S341P
H345R
R347C
R350G
I353T
Y354C
S355G
Y357C
S359F
T362I
L363P
Luminescence
Time [sec]
0.0
0.5
1.0
1.5
0
100
200
300
400

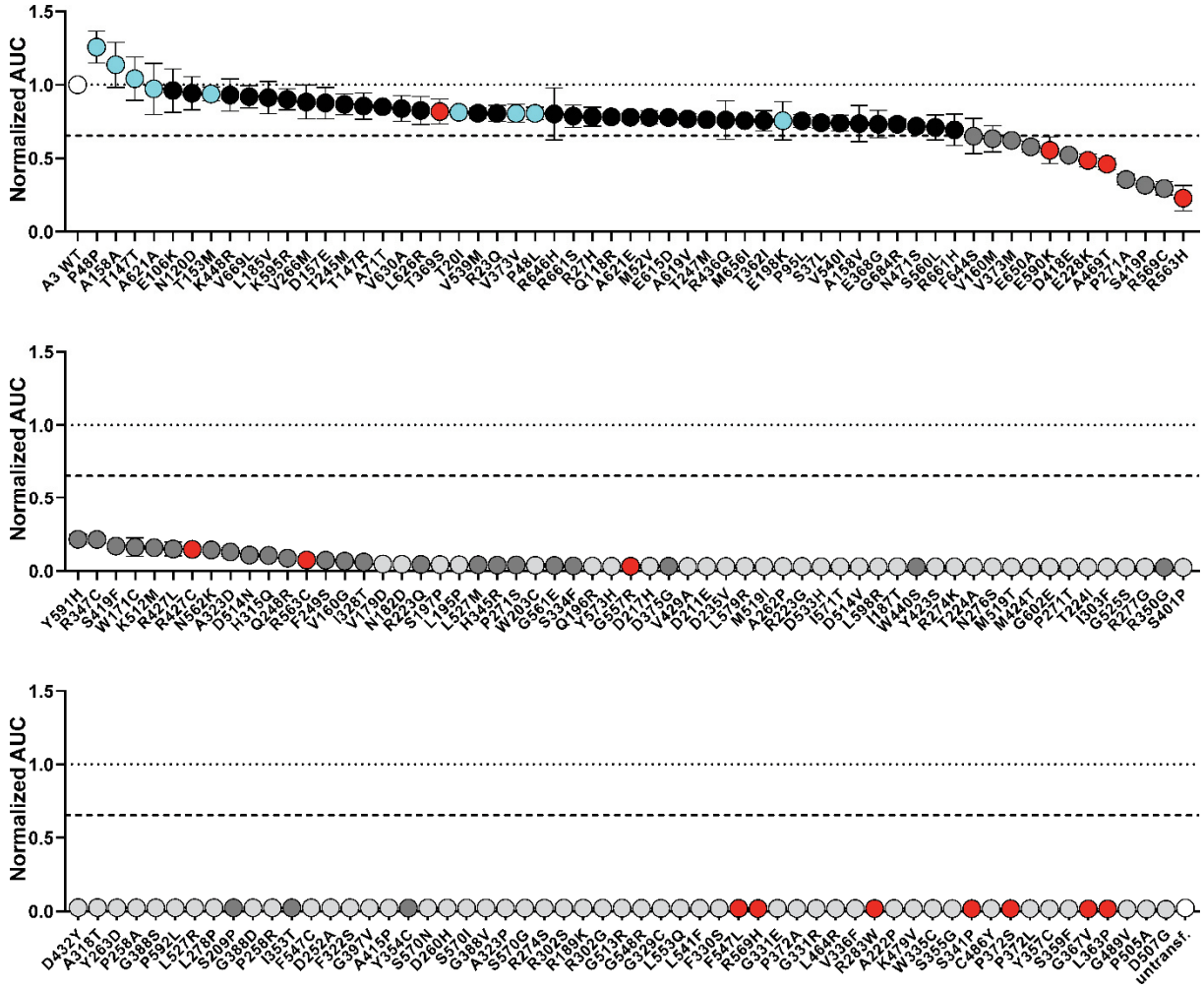

8-Br-cGMP
Luminescence
Time [sec]
A3 WT
G367V
E368G
T369S
P372S
P372A
P372L
V373M
V373V
D375G
G388S
G388D
G388V
G397V
S401P
A415P
D418E
S419P
S419F
Y423S
M424T
R427C
R427L
V429A
D432Y


8-Br-cGMP
A3 WT
R436Q
W440S
K448R
L464R
A469T
N471S
K479V
C486Y
G489V
P505A
D507G
K512M
G513R
D514N
D514V
M519T
M519I
G525S
L527R
L527M
D533H
V539M
V540I
L541F
Luminescence
Time [sec]
0.0
0.5
1.0
1.5
0
100
200
300
400

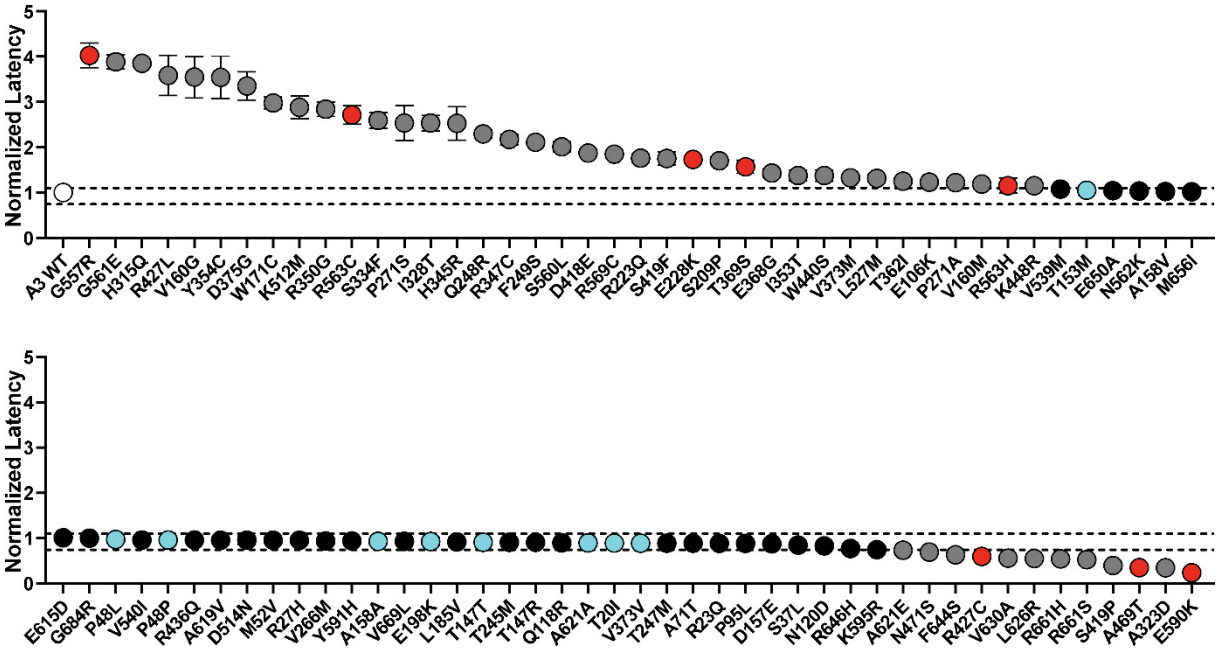

8-Br-cGMP
A3 WT
F547L
F547C
G548R
L553Q
G557R
S560L
G561E
N562K
R563C
R563H
R569H
R569C
S570G
S570N
S570I
I571T
Y573H
L579R
E590K
Y591H
P592L
K595R
L598R
G602E
Luminescence
Time [sec]
0.0
0.5
1.0
1.5
0
100
200
300
400



Supplemental Figure 4: Individual luminescence traces of all evaluated 150 CNGA3 missense substitutions, nine benign variants, 15 pathogenic variants from the assay validation data set and luminescence traces of untransfected HEK293^{aequo} cells. The luminescence signals of HEK293^{aequo} cells either expressing wild-type CNGA3 channels (A3 WT, black-blue line) or mutant CNGA3 channels (red line) and the luminescence signal of untransfected control HEK293^{aequo} cells (red line) were recorded for 6 sec before and 394 sec after the application of the CNGA3 channel ligand 8-bromoguanosine-3',5'-cyclic monophosphate (8-Br-cGMP). All data are represented as mean ± SD and normalized to A3 WT. n=3-55 independent transfections/measurements. untransf., untransfected control cells.; WT, wild-type.

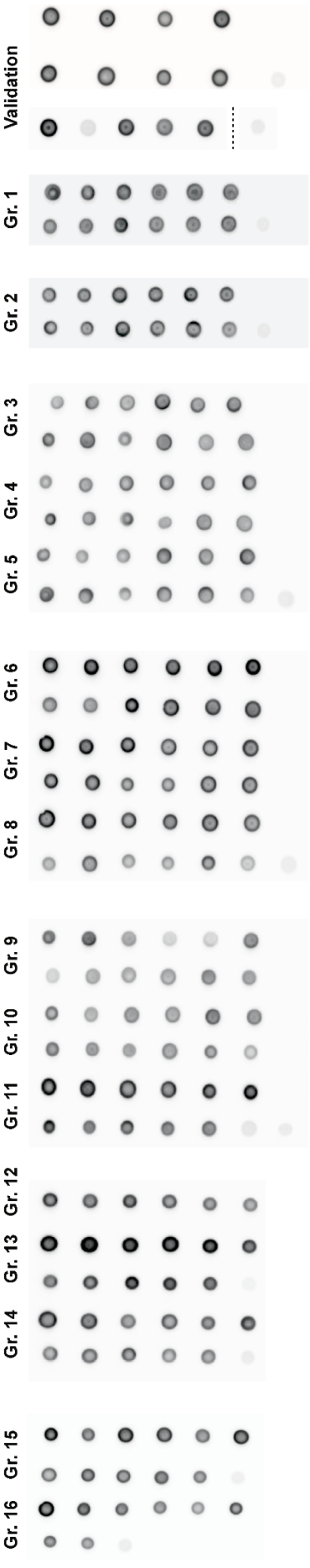


Supplemental Figure 5: Normalized overall luminescence signals (AUC) of 150 analysed CNGA3 missense variants, nine benign and 15 pathogenic variants from the assay validation data set sorted by the normalized AUC values. Threshold for assigning a damaging effect regarding the normalized AUC (0.65) is displayed by a dashed line. Normalized AUC value of wild-type channels (A3 WT, white circle) is exhibited as a dotted line. All missense variants that are above or below the threshold are depicted as black or dark/light grey circles, respectively. All missense variants designated as non-functional are displayed as light grey circles. Benign variants (n=9 variants) and pathogenic variants (n=15 variants) from the assay validation data set are indicated by blue and red circles, respectively. Normalized AUC of untransfected control cells is shown as a white circle. 36/150 analysed CNGA3 missense variants, 9/9 benign control variants and 1/15 pathogenic control variants surpass the pathogenicity threshold of 0.65 for the normalized AUC indicating wild-type-like overall luminescence signals (AUC). All data are represented as mean ± SD. n=3-15 independent transfections/measurements. AUC, area under the curve; untransf., untransfected control cells; WT, wild-type.



Supplemental Figure 6: Normalized peak latency of 70 still functional CNGA3 missense variants, nine benign and eight still functional pathogenic variants from the assay validation data set sorted by the normalized peak latency values. Upper (1.10) and lower thresholds (0.74) for assigning a damaging effect regarding the normalized peak latency are displayed by dashed lines. All missense variants that are within or outside the thresholds are shown as black or grey circles, respectively. Wild-type is indicated by a white dot. Benign variants (n=9 variants) and pathogenic variants (n=8 variants) from the assay validation data set are indicated by blue and red circles, respectively. 32/70 still functional CNGA3 missense variants and 5/8 still functional pathogenic control variants exhibited an increased peak latency (threshold: 1.10) whereas 9/70 still functional CNGA3 missense variants and 3/8 still functional pathogenic control variants showed a reduced peak latency (threshold: 0.74). All data are represented as mean ± SD. n=3-5 independent transfections/measurements. WT, wild-type.

A



B

A3WT	T153M	R427C	E228K	-	
A469T	R569H	R283W	F547L	ut	

A3WT	E590K	G557R	R563C	R563H	ut

A3WT	G329C	F330S	G331R	G331E	S334F	-
W335C	V336F	I353T	Y354C	S355G	Y357C	ut

A3WT	S341P	R347C	S359F	L363P	G367V	-
E368G	T369S	P372S	P372A	P372L	V373M	ut

A3WT	T362I	R23Q	R27H	M52V	A71T	-
N120D	T147R	D157E	A158V	L185V	S209P	-
A3WT	V539M	E615D	M656I	G684R	T20I	-
P95L	Q118R	E198K	N471S	A619V	A621E	-
A3WT	H345R	R350G	A222P	S37L	P48L	-
T245M	T247M	V540I	G489V	P505A	D507G	ut

A3WT	E106K	T224A	T224I	Q248R	K595R	-
L626R	V630A	V669L	K512M	G513R	D514N	-
A3WT	D514V	M519T	G525S	L527R	D533H	-
L541F	G548R	L553Q	S560L	G561E	N562K	-
A3WT	Q196R	K448R	A262P	V266M	M519I	-
L527M	F547C	R569C	S570G	S570N	S570I	ut

A3WT	Y573H	L579R	Y591H	L598R	G602E	-
F644S	R646H	E650A	R661H	V160M	R189K	-
A3WT	V179D	N182D	L195P	S197P	W203C	-
D211E	D217H	R223G	R223Q	I571T	R661S	-
A3WT	V160G	W171C	I187T	D235V	F249S	-
D252A	P258A	P258R	D260H	Y263D	P592L	ut

A3WT	P48P	A158A	T147T	A621A	V373V
A3WT	P271A	P271S	R274K	N276S	R277G
L278P	I303F	F322S	A323P	A323D	ut
A3WT	I323T	D375G	G388S	G388D	G388V
G397V	A415P	D418E	S419P	S419F	ut

A3WT	Y423S	M424T	R427L	V429A	D432Y
R436Q	P271T	R274S	R302G	R302S	ut
A3WT	H315Q	A318T	S401P	W440S	L464R
K479V	C486Y	ut	-	-	-

Supplemental Figure 7: Dot Blot analysis of whole cell lysates for the verification of CNGA3 protein expression in one biological replicate of all 150 samples analysed in the aequorin-based bioassay and samples from the assay validation data set. A. CNGA3 protein expression was detected using a commercial rabbit anti-human CNGA3 antibody in whole cell lysates of HEK293^{aequo} cells transfected with mutant *CNGA3* expression constructs carrying either one out of 150 analysed CNGA3 missense variants or benign (n=9 variants)/pathogenic variants (n=15 variants) from the assay validation data set. Whole cell lysates from cells transfected with the wild-type *CNGA3* expression construct (A3 WT) and untransfected cells were used as positive and negative controls, respectively. B. Pipetting scheme of all samples applied onto the nitrocellulose membranes for Dot Blot analysis. Benign (n=9 variants) or pathogenic variants (n=15 variants) from the assay validation data set are indicated by a blue or red font, respectively. Grouping of images from different parts of the same blot is indicated by a dashed line. Gr. 1 to Gr.16, group of samples applied onto the nitrocellulose membranes; ut, whole cell lysates from untransfected cells; WT, wild-type.

Tables

Supplemental Table 1: List of all oligonucleotides used as primers for site-directed mutagenesis of the *CNGA3* cDNA expression construct in this study and in previously conducted studies.

Supplemental Table 1 is provided as a separate file (.xlsx file).

Supplemental Table 2: List of all oligonucleotides used as primers for sequencing of the *CNGA3* cDNA expression construct and AAVS1 HR donor vector GE622A-1#1_CMV-Aeq cloning.

Primers for sequencing of the *CNGA3* cDNA expression construct

Primer	Orientation	Sequencing primer 5‘-3‘
CMV-for2	forward	CCAGTATCTGCTCCCTGCTT
CMV-for3	forward	GGGACTTTCCTACTTGGCAGT
FEO 149	reverse	GTCAGCCAGTCCTCTGGTC
Exon 3 rev	reverse	CTCCCTCTGTCTGCTGGCTCCTGG
FEO 61	reverse	ATGTACAAGACCAAGTTCCC
FEO 196	forward	CAAATGCAACACTAACAC
FEO 119	forward	CATCATCCACTGGAATG
FEO 242	forward	TGGGCCAACAAGAAGACG
FEO 249	forward	GGAGAAAGGACGGCAGA
FEO 999	reverse	GCCATAGCACTCCCAAAAG
BGH rev new	reverse	TAGAAGGCACAGTCGAGG
FEO 3’UTR	forward	GTGACCTATTCTAACTCAAGG

Primers for AAVS1 HR donor vector GE622A-1#1_CMV-Aeq cloning

Primer	Orientation	Sequencing primer 5‘-3‘
CMV-Aeq-BstBI-for	forward	TATATATATTCGAAAAACCCAGATATACGCGTTGA
Aeq-Kozak-IVM-rev	reverse	CCTCGGAGATGAGCTTCTGCTCCATGGTGGCAAAGC TTGGAGTGATC
Aeq-MluI-rev	reverse	TATATATATAACGCGTTCAGGGCACGGCTCCGCCAT
Aeq-Kozak-IVM-for	forward	GATCACTCCAAGCTTTGCCACCATGGAGCAGAAGCT CATCTCCGAGG

Supplemental Table 3: Overview of the assay validation data set composed of nine benign and 15 pathogenic variants in the *CNGA3* gene including location of variant in polypeptide and functional or structural domain, references for previous functional analysis and selection criteria for inclusion in the assay validation data set.

Supplemental Table 3 is provided as a separate file (.xlsx file).

Supplemental Table 4: Summary of the 150 functionally evaluated CNGA3 missense variants using the aequorin-based bioassay including location of variant in polypeptide and functional or structural domain, normalized overall luminescence signals (AUC) and normalized peak latency values, variant classification as functionally normal or abnormal based on the aequorin-based bioassay as well as pre-assay and post-assay ACMG/AMP classification after applying functional evidence.

Supplemental Table 4 is provided as a separate file (.xlsx file).

References Supplementary material

1. Zhang JH, Chung TD, Oldenburg KR. A Simple Statistical Parameter for Use in Evaluation and Validation of High Throughput Screening Assays. J Biomol Screen. 1999;4(2):67-73. doi:10.1177/108705719900400206
2. Nishiguchi KM, Sandberg MA, Gorji N, Berson EL, Dryja TP. Cone cGMP-gated channel mutations and clinical findings in patients with achromatopsia, macular degeneration, and other hereditary cone diseases. Hum Mutat. 2005;25(3):248-258. doi:10.1002/humu.20142
3. Thiadens AA, Roosing S, Collin RW, et al. Comprehensive analysis of the achromatopsia genes CNGA3 and CNGB3 in progressive cone dystrophy. Ophthalmology. 2010;117(4):825-830 e821. doi:10.1016/j.ophtha.2009.09.008
4. Sharon D, Ben-Yosef T, Goldenberg-Cohen N, et al. A nationwide genetic analysis of inherited retinal diseases in Israel as assessed by the Israeli inherited retinal disease consortium (IIRDC). Hum Mutat. 2020;41(1):140-149. doi:10.1002/humu.23903
5. Solaki M, Baumann B, Reuter P, et al. Comprehensive variant spectrum of the CNGA3 gene in patients affected by achromatopsia. Hum Mutat. 2022;43(7):832-858. doi:10.1002/humu.24371
6. Li S, Huang L, Xiao X, Jia X, Guo X, Zhang Q. Identification of CNGA3 mutations in 46 families: common cause of achromatopsia and cone-rod dystrophies in Chinese patients. JAMA Ophthalmol. 2014;132(9):1076-1083. doi:10.1001/jamaophthalmol.2014.1032

7. Kohl S, Marx T, Giddings I, et al. Total colourblindness is caused by mutations in the gene encoding the alpha-subunit of the cone photoreceptor cGMP-gated cation channel. Nat Genet. 1998;19(3):257-259. doi:10.1038/935
8. Dubis AM, Cooper RF, Aboshiha J, et al. Genotype-dependent variability in residual cone structure in achromatopsia: toward developing metrics for assessing cone health. Invest Ophthalmol Vis Sci. 2014;55(11):7303-7311. doi:10.1167/iovs.14-14225
9. Kim MS, Joo K, Seong MW, et al. Genetic Mutation Profiles in Korean Patients with Inherited Retinal Diseases. J Korean Med Sci. 2019;34(21):e161. doi:10.3346/jkms.2019.34.e161
10. Taylor RL, Parry NRA, Barton SJ, et al. Panel-Based Clinical Genetic Testing in 85 Children with Inherited Retinal Disease. Ophthalmology. 2017;124(7):985-991. doi:10.1016/j.ophtha.2017.02.005
11. Sun W, Li S, Xiao X, Wang P, Zhang Q. Genotypes and phenotypes of genes associated with achromatopsia: A reference for clinical genetic testing. Mol Vis. 2020;26:588-602
12. Weisschuh N, Obermaier CD, Battke F, et al. Genetic architecture of inherited retinal degeneration in Germany: A large cohort study from a single diagnostic center over a 9-year period. Hum Mutat. 2020;41(9):1514-1527. doi:10.1002/humu.24064
13. Liang X, Dong F, Li H, Li H, Yang L, Sui R. Novel CNGA3 mutations in Chinese patients with achromatopsia. Br J Ophthalmol. 2015;99(4):571-576. doi:10.1136/bjophthalmol-2014-305432
14. Reuter P, Koeppen K, Ladewig T, et al. Mutations in CNGA3 impair trafficking or function of cone cyclic nucleotide-gated channels, resulting in achromatopsia. Hum Mutat. 2008;29(10):1228-1236. doi:10.1002/humu.20790
15. Wiszniewski W, Lewis RA, Lupski JR. Achromatopsia: the CNGB3 p.T383fsX mutation results from a founder effect and is responsible for the visual phenotype in the original report of uniparental disomy 14. Hum Genet. 2007;121(3-4):433-439. doi:10.1007/s00439-006-0314-y
16. Greenberg JP, Sherman J, Zweifel SA, et al. Spectral-domain optical coherence tomography staging and autofluorescence imaging in achromatopsia. JAMA Ophthalmol. 2014;132(4):437-445. doi:10.1001/jamaophthalmol.2013.7987
17. Johnson S, Michaelides M, Aligianis IA, et al. Achromatopsia caused by novel mutations in both CNGA3 and CNGB3. J Med Genet. 2004;41(2):e20. doi:10.1136/jmg.2003.011437
18. Zobor D, Werner A, Stanzial F, et al. The Clinical Phenotype of CNGA3-Related Achromatopsia: Pretreatment Characterization in Preparation of a Gene Replacement Therapy Trial. Invest Ophthalmol Vis Sci. 2017;58(2):821-832. doi:10.1167/iovs.16-20427
19. Zelinger L, Cideciyan AV, Kohl S, et al. Genetics and Disease Expression in the CNGA3 Form of Achromatopsia: Steps on the Path to Gene Therapy. Ophthalmology. 2015;122(5):997-1007. doi:10.1016/j.ophtha.2014.11.025
20. Georgiou M, Litts KM, Kalitzeos A, et al. Adaptive Optics Retinal Imaging in CNGA3-Associated Achromatopsia: Retinal Characterization, Interocular Symmetry, and Intrafamilial Variability. Invest Ophthalmol Vis Sci. 2019;60(1):383-396. doi:10.1167/iovs.18-25880
21. Azam M, Collin RW, Shah ST, et al. Novel CNGA3 and CNGB3 mutations in two Pakistani families with achromatopsia. Mol Vis. 2010;16:774-781
22. Saqib MA, Awan BM, Sarfraz M, Khan MN, Rashid S, Ansar M. Genetic analysis of four Pakistani families with achromatopsia and a novel S4 motif mutation of CNGA3. Jpn J Ophthalmol. 2011;55(6):676-680. doi:10.1007/s10384-011-0070-y
23. Koeppen K, Reuter P, Ladewig T, et al. Dissecting the pathogenic mechanisms of mutations in the pore region of the human cone photoreceptor cyclic nucleotide-gated channel. Hum Mutat. 2010;31(7):830-839. doi:10.1002/humu.21283
24. Patel A, Hayward JD, Tailor V, et al. The Oculome Panel Test: Next-Generation Sequencing to Diagnose a Diverse Range of Genetic Developmental Eye Disorders. Ophthalmology. 2019;126(6):888-907. doi:10.1016/j.ophtha.2018.12.050
25. Li L, Chen Y, Jiao X, et al. Homozygosity Mapping and Genetic Analysis of Autosomal Recessive Retinal Dystrophies in 144 Consanguineous Pakistani Families. Invest Ophthalmol Vis Sci. 2017;58(4):2218-2238. doi:10.1167/iovs.17-21424

26. Carss KJ, Arno G, Erwood M, et al. Comprehensive Rare Variant Analysis via Whole-Genome Sequencing to Determine the Molecular Pathology of Inherited Retinal Disease. Am J Hum Genet. 2017;100(1):75-90. doi:10.1016/j.ajhg.2016.12.003
27. Li FF, Huang XF, Chen J, et al. Identification of novel mutations by targeted exome sequencing and the genotype-phenotype assessment of patients with achromatopsia. J Transl Med. 2015;13:334. doi:10.1186/s12967-015-0694-7
28. Genead MA, Fishman GA, Rha J, et al. Photoreceptor structure and function in patients with congenital achromatopsia. Invest Ophthalmol Vis Sci. 2011;52(10):7298-7308. doi:10.1167/iovs.11-7762
29. Saqib MA, Nikopoulos K, Ullah E, et al. Homozygosity mapping reveals novel and known mutations in Pakistani families with inherited retinal dystrophies. Sci Rep. 2015;5:9965. doi:10.1038/srep09965
30. Sundaram V, Wilde C, Aboshiha J, et al. Retinal structure and function in achromatopsia: implications for gene therapy. Ophthalmology. 2014;121(1):234-245. doi:10.1016/j.ophtha.2013.08.017
31. Gilissen C, Hehir-Kwa JY, Thung DT, et al. Genome sequencing identifies major causes of severe intellectual disability. Nature. 2014;511(7509):344-347. doi:10.1038/nature13394
32. Wissinger B, Gamer D, Jagle H, et al. CNGA3 mutations in hereditary cone photoreceptor disorders. Am J Hum Genet. 2001;69(4):722-737. doi:10.1086/323613
33. Vincent A, Wright T, Billingsley G, Westall C, Heon E. Oligocone trichromacy is part of the spectrum of CNGA3-related cone system disorders. Ophthalmic Genet. 2011;32(2):107-113. doi:10.3109/13816810.2010.544366
34. Brunetti-Pierri R, Karali M, Melillo P, et al. Clinical and Molecular Characterization of Achromatopsia Patients: A Longitudinal Study. Int J Mol Sci. 2021;22(4). doi:10.3390/ijms22041681
35. Ahuja Y, Kohl S, Traboulsi EI. CNGA3 mutations in two United Arab Emirates families with achromatopsia. Mol Vis. 2008;14:1293-1297
36. Stone EM, Andorf JL, Whitmore SS, et al. Clinically Focused Molecular Investigation of 1000 Consecutive Families with Inherited Retinal Disease. Ophthalmology. 2017;124(9):1314-1331. doi:10.1016/j.ophtha.2017.04.008
37. Abouelhoda M, Sobahy T, El-Kalioby M, et al. Clinical genomics can facilitate countrywide estimation of autosomal recessive disease burden. Genet Med. 2016;18(12):1244-1249. doi:10.1038/gim.2016.37
38. Huang L, Xiao X, Li S, et al. Molecular genetics of cone-rod dystrophy in Chinese patients: New data from 61 probands and mutation overview of 163 probands. Exp Eye Res. 2016;146:252-258. doi:10.1016/j.exer.2016.03.015
39. Carrigan M, Duignan E, Malone CP, et al. Panel-Based Population Next-Generation Sequencing for Inherited Retinal Degenerations. Sci Rep. 2016;6:33248. doi:10.1038/srep33248
40. Arshad MW, Lee Y, Malik MA, et al. Identification of Novel Mutation in CNGA3 gene by Whole-Exome Sequencing and In-Silico Analyses for Genotype-Phenotype Assessment with Autosomal Recessive Achromatopsia in Pakistani families. J Pak Med Assoc. 2019;69(2):183-189
41. Ellingford JM, Barton S, Bhaskar S, et al. Molecular findings from 537 individuals with inherited retinal disease. J Med Genet. 2016;53(11):761-767. doi:10.1136/jmedgenet-2016-103837
42. Patel N, Aldahmesh MA, Alkuraya H, et al. Expanding the clinical, allelic, and locus heterogeneity of retinal dystrophies. Genet Med. 2016;18(6):554-562. doi:10.1038/gim.2015.127
43. Wang X, Wang H, Cao M, et al. Whole-exome sequencing identifies ALMS1, IQCB1, CNGA3, and MYO7A mutations in patients with Leber congenital amaurosis. Hum Mutat. 2011;32(12):1450-1459. doi:10.1002/humu.21587

44. Lam K, Guo H, Wilson GA, Kohl S, Wong F. Identification of variants in CNGA3 as cause for achromatopsia by exome sequencing of a single patient. Arch Ophthalmol. 2011;129(9):1212-1217. doi:10.1001/archophthalmol.2011.254
45. Koeppen K, Reuter P, Kohl S, Baumann B, Ladewig T, Wissinger B. Functional analysis of human CNGA3 mutations associated with colour blindness suggests impaired surface expression of channel mutants A3(R427C) and A3(R563C). Eur J Neurosci. 2008;27(9):2391-2401. doi:10.1111/j.1460-9568.2008.06195.x
46. Thiadens AA, Somervuo V, van den Born LI, et al. Progressive loss of cones in achromatopsia: an imaging study using spectral-domain optical coherence tomography. Invest Ophthalmol Vis Sci. 2010;51(11):5952-5957. doi:10.1167/iovs.10-5680
47. Jinda W, Tuekprakhon A, Thongnoppakhun W, Limwongse C, Trinavarat A, Atchaneeyasakul LO. Molecular and clinical characterization of Thai patients with achromatopsia: identification of three novel disease-associated variants in the CNGA3 and CNGB3 genes. Int Ophthalmol. 2021;41(1):121-134. doi:10.1007/s10792-020-01559-2
48. Yang P, Michaels KV, Courtney RJ, et al. Retinal morphology of patients with achromatopsia during early childhood: implications for gene therapy. JAMA Ophthalmol. 2014;132(7):823-831. doi:10.1001/jamaophthalmol.2014.685
49. Gofman Y, Scharfe C, Marks DS, Haliloglu T, Ben-Tal N. Structure, dynamics and implied gating mechanism of a human cyclic nucleotide-gated channel. PLoS Comput Biol. 2014;10(12):e1003976. doi:10.1371/journal.pcbi.1003976
50. Shuart NG, Haitin Y, Camp SS, Black KD, Zagotta WN. Molecular mechanism for 3:1 subunit stoichiometry of rod cyclic nucleotide-gated ion channels. Nat Commun. 2011;2:457. doi:10.1038/ncomms1466
51. Tränkner D, Jagle H, Kohl S, et al. Molecular basis of an inherited form of incomplete achromatopsia. J Neurosci. 2004;24(1):138-147. doi:10.1523/JNEUROSCI.3883-03.2004
52. Meighan PC, Peng C, Varnum MD. Inherited macular degeneration-associated mutations in CNGB3 increase the ligand sensitivity and spontaneous open probability of cone cyclic nucleotide-gated channels. Front Physiol. 2015;6:177. doi:10.3389/fphys.2015.00177
53. Muraki-Oda S, Toyoda F, Okada A, et al. Functional analysis of rod monochromacy-associated missense mutations in the CNGA3 subunit of the cone photoreceptor cGMP-gated channel. Biochem Biophys Res Commun. 2007;362(1):88-93. doi:10.1016/j.bbrc.2007.07.152
54. Matveev AV, Fitzgerald JB, Xu J, Malykhina AP, Rodgers KK, Ding XQ. The disease-causing mutations in the carboxyl terminus of the cone cyclic nucleotide-gated channel CNGA3 subunit alter the local secondary structure and interfere with the channel active conformational change. Biochemistry. 2010;49(8):1628-1639. doi:10.1021/bi901960u
55. Liu C, Varnum MD. Functional consequences of progressive cone dystrophy-associated mutations in the human cone photoreceptor cyclic nucleotide-gated channel CNGA3 subunit. Am J Physiol Cell Physiol. 2005;289(1):C187-198. doi:10.1152/ajpcell.00490.2004

Supplemental Table 1: List of all oligonucleotides used as primers for site-directed mutagenesis of the *CNGA3* cDNA expression construct in this study and in previously conducted studies.

Exon	Alteration Polypeptide	Alteration Nucleotide Sequence†	Location Protein Domain‡	Reference	Primer forward 5'-3'	Primer reverse 5'-3'
N-Terminus						
Exon 2	p.(Thr20Ile)§	c.59C>T	N-Term.	ClinVar	CCACCTCAAGGTAAAGATCTCAGACCGAGACC	GGTCTCGGTCTGAGATCTTTACCTTGAGGTGG
Exon 2	p.(Arg23Gln)	c.68G>A	N-Term.	ClinVar	GTAAAGACCTCAGACCAAGACCTCAATCGCGCT	AGCGCGATTGAGGTCTTGGTCTGAGGTCTTTAC
Exon 2	p.(Arg27His)	c.80G>A	N-Term.	ClinVar	GACCGAGACCTCAATCACGCTGAAAATGGCCTC	GAGGCCATTTTCAGCGTGATTGAGGTCTCGGTC
Exon 3	p.(Ser37Leu)	c.110C>T	N-Term.	ClinVar	TCAGCAGAGCCCACTTGTCAAGTGAGGAGAC	GTCTCCTCACTTGACAAGTGGGCTCTGCTGA
Exon 3	p.(Pro48Leu)§	c.143C>T	N-Term.	Nishiguchi et al., 2005	CGTCAGTGCTGCAGCTGGGGATCGCCATGG	CCATGGCGATCCCCAGCTGCAGCACTGACG
Exon 3	p.(Pro48Pro)§	c.144G>A	N-Term.	gnomAD	CAGTGCTGCAGCCAGGGATCGCCATGG	CCATGGCGATCCCTGGCTGCAGCACTG
Exon 3	p.(Met52Val)	c.154A>G	N-Term.	ClinVar	CCGGGGATCGCCGTGGAGACCAGAG	CTCTGGTCTCCACGGCGATCCCCGG
Exon 3	p.(Ala71Thr)	c.211G>A	N-Term.	ClinVar	GGCCAGGGGATCACCAGGCTGTCGC	GCGACAGCCTGGTGATCCCCTGGCC
Exon 4	p.(Pro95Leu)	c.284C>T	N-Term.	Thiadens et al., 2010	CCAGGACCAGGGACTGGACTCTTTTCCTG	CAGGAAAAGAGTCCAGTCCCTGGTCCTGG
Exon 4	p.(Glu106Lys)	c.316G>A	N-Term.	Sharon et al., 2020	CGTTTCCGCGGAGCCAAGCTTAAGGAGGTG	CACCTCCTTAAGCTTGGCTCCGCGGAAACG
Exon 4	p.(Gln118Arg)	c.353A>G	N-Term.	Solaki et al., 2022	CAAGAAAGCAATGCCCGGGCAAATGTGGGCAGC	GCTGCCCACATTTGCCCGGGCATTGCTTTCTTG
Exon 4	p.(Asn120Asp)	c.358A>G	N-Term.	Li et al., 2014	GCAATGCCCAGGCAGATGTGGGCAGCCAG	CTGGCTGCCCACATCTGCCTGGGCATTGC
Exon 5	p.(Thr147Arg)	c.440C>G	N-Term.	LOVD	ACACTAACACCAGCAACAACAGGGAGGAGGAGA	TCTCCTCCTCCCTGTTGTTGCTGGTGTTAGTGT
Exon 5	p.(Thr147Thr)§	c.441G>A	N-Term.	gnomAD	AACACCAGCAACAACACAGAGGAGGAGAAGAAGAC	GTCTTCTTCTCCTCCTCTGTGTTGTTGCTGGTGTT
Exon 6	p.(Thr153Met)§¶	c.458C>T	N-Term.	Kohl et al., 1998	CAACAACACGGAGGAGGAGAAGAAGATGAAAAAGAAGGATGCGATC	GATCGCATCCTTCTTTTTCATCTTCTTCTCCTCCTCCGTGTTGTTG
Exon 6	p.(Asp157Glu)	c.471T>G	N-Term.	ClinVar	AGAAGAAGACGAAAAAGAAGGAGGCGATCGTGGTGG	CCACCACGATCGCCTCCTTCTTTTTCGTCTTCTTCT
Exon 6	p.(Ala158Val)	c.473C>T	N-Term.	LOVD	AGACGAAAAAGAAGGATGTGATCGTGGTGGACCCG	CGGGTCCACCACGATCACATCCTTCTTTTTCGTCT
Exon 6	p.(Ala158Ala)§	c.474G>A	N-Term.	gnomAD	CGAAAAAGAAGGATGCAATCGTGGTGGACCCGT	ACGGGTCCACCACGATTGCATCCTTCTTTTTCG
Exon 6	p.(Val160Met)	c.478G>A	N-Term.	ClinVar	GAAGGATGCGATCATGGTGGACCCGTCC	GGACGGGTCCACCATGATCGCATCCTTC
Exon 6	p.(Val160Gly)	c.479T>G	N-Term.	Solaki et al., 2022	GAAGGATGCGATCGGGGTGGACCCGTCCAG	CTGGACGGGTCCACCCCGATCGCATCCTTC
Transmembrane domain TM1 to TM6 & Pore helix						
Exon 6	p.(Trp171Cys)	c.513G>T	TM1	Li et al., 2014	CCTGTACTACCGCTGTCTGACCGCCATCGC	GCGATGGCGGTCAGACAGCGGTAGTACAGG
Exon 6	p.(Val179Asp)	c.536T>A	TM1	Dubis et al., 2014	CGCCATCGCCCTGCCTGACTTTTATAACTGGTATC	GATACCAGTTATAAAAGTCAGGCAGGGCGATGGCG
Exon 6	p.(Asn182Asp)	c.544A>G	TM1	Solaki et al., 2022	GCCCTGCCTGTCTTTTATGACTGGTATCTGCTTATTTG	CAAATAAGCAGATACCAGTCATAAAAGACAGGCAGGGC
Exon 6	p.(Leu185Val)	c.553C>G	TM1	Kim et al., 2019	CTGCCTGTCTTTTATAACTGGTATGTGCTTATTTGCAGGG	CCCTGCAAATAAGCACATACCAGTTATAAAAGACAGGCAG
Exon 6	p.(Ile187Thr)	c.560T>C	TM1 - TM2	Taylor et al., 2017	AACTGGTATCTGCTTACTTGCAGGGCCTGTTTCG	CGAAACAGGCCCTGCAAGTAAGCAGATACCAGTT
Exon 6	p.(Arg189Lys)	c.566G>A	TM1 - TM2	Solaki et al., 2022	GTATCTGCTTATTTGCAAGGCCTGTTTCGATGAGC	GCTCATCGAAACAGGCCTTGCAAATAAGCAGATAC
Exon 7	p.(Leu195Pro)	c.584T>C	TM1 - TM2	ClinVar	CCTGTTTCGATGAGCCGCAGTCCGAGTACC	GGTACTCGGACTGCGGCTCATCGAAACAGG
Exon 7	p.(Gln196Arg)	c.587A>G	TM1 - TM2	Sun et al., 2020	GTTTCGATGAGCTGCGGTCCGAGTACCTGATG	CATCAGGTACTCGGACCGCAGCTCATCGAAAC
Exon 7	p.(Ser197Pro)	c.589T>C	TM2	ClinVar	CGATGAGCTGCAGCCCGAGTACCTGATG	CATCAGGTACTCGGGCTGCAGCTCATCG
Exon 7	p.(Glu198Lys)§	c.592G>A	TM2	Solaki et al., 2022	CGATGAGCTGCAGTCCAAGTACCTGATGCTGTG	CACAGCATCAGGTACTTGGACTGCAGCTCATCG
Exon 7	p.(Trp203Cys)	c.609G>T	TM2	Solaki et al., 2022	GTACCTGATGCTGTGTCTGGTCCTGGACTAC	GTAGTCCAGGACCAGACACAGCATCAGGTAC
Exon 7	p.(Ser209Pro)	c.625T>C	TM2	Weisschuh et al., 2020	TGGTCCTGGACTACCCGGCAGATGTCCTG	CAGGACATCTGCCGGGTAGTCCAGGACCA
Exon 7	p.(Asp211Glu)	c.633T>A	TM2	Liang et al., 2015	GGACTACTCGGCAGAAGTCCTGTATGTCTTGG	CCAAGACATACAGGACTTCTGCCGAGTAGTCC
Exon 7	p.(Asp217His)	c.649G>C	TM2	ClinVar	GATGTCCTGTATGTCTTGCATGTGCTTGTACGAGCTCG	CGAGCTCGTACAAGCACATGCAAGACATACAGGACATC
Exon 7	p.(Ala222Pro)	c.664G>C	TM2	Reuter et al., 2008	GGATGTGCTTGTACGACCTCGGACAGGTTTTCT	AGAAAACCTGTCCGAGGTCGTACAAGCACATCC
Exon 7	p.(Arg223Gly)	c.667C>G	TM2	Wiszniewski et al., 2007	GTGCTTGTACGAGCTGGGACAGGTTTTCTCG	CGAGAAAACCTGTCCCAGCTCGTACAAGCAC
Exon 7	p.(Arg223Gln)	c.668G>A	TM2	Li et al., 2014; Greenberg et al., 2014	GTGCTTGTACGAGCTCAGACAGGTTTTCTCGAGC	GCTCGAGAAAACCTGTCTGAGCTCGTACAAGCAC
Exon 7	p.(Thr224Ala)	c.670A>G	TM2 - TM3	Solaki et al., 2022	CTTGTACGAGCTCGGGCAGGTTTTCTCGAGC	GCTCGAGAAAACCTGCCCGAGCTCGTACAAG
Exon 7	p.(Thr224Ile)	c.671C>T	TM2 - TM3	Li et al., 2014	CTTGTACGAGCTCGGATAGGTTTTCTCGAGCAAG	CTTGCTCGAGAAAACCTATCCGAGCTCGTACAAG
Exon 8	p.(Glu228Lys)§¶	c.682G>A	TM2 - TM3	Reuter et al., 2008	GCTCGGACAGGTTTTCTCAAGCAAGGCTTAATGG	CCATTAAGCCTTGCTTGAGAAAACCTGTCCGAGC
Exon 8	p.(Asp235Val)	c.704A>T	TM2 - TM3	Weisschuh et al., 2020	GGCTTAATGGTCAGTGTTACCAACAGGCTGTGGC	GCCACAGCCTGTTGGTAACACTGACCATTAAGCC
Exon 8	p.(Thr245Met)	c.734C>T	TM2 - TM3	Johnson et al., 2004	GGCAGCATTACAAGATGACCACGCAGTTCAAGC	GCTTGAACTGCGTGGTCATCTTGTAATGCTGCC
Exon 8	p.(Thr247Met)	c.740C>T	TM3	Li et al., 2014	GCATTACAAGACGACCATGCAGTTCAAGCTGG	CCAGCTTGAACTGCATGGTCGTCTTGTAATGC
Exon 8	p.(Gln248Arg)	c.743A>G	TM3	Solaki et al., 2022	CAAGACGACCACGCGGTTCAAGCTGGATG	CATCCAGCTTGAACCGCGTGGTCGTCTTG
Exon 8	p.(Phe249Ser)	c.746T>C	TM3	Nishiguchi et al., 2005	GACGACCACGCAGTCCAAGCTGGATGTG	CACATCCAGCTTGGACTGCGTGGTCGTC
Exon 8	p.(Asp252Ala)	c.755A>C	TM3	Sun et al., 2020	CGCAGTTCAAGCTGGCTGTGTTGTCCCTGG	CCAGGGACAACACAGCCAGCTTGAACTGCG
Exon 8	p.(Pro258Ala)	c.772C>G	TM3	Solaki et al., 2022	GATGTGTTGTCCCTGGTCGCCACCGACCTGGCTTAC	GTAAGCCAGGTCGGTGGCGACCAGGGACAACACATC
Exon 8	p.(Pro258Arg)	c.773C>G	TM3	Li et al., 2014	GTGTTGTCCCTGGTCCGCACCGACCTGGCTTAC	GTAAGCCAGGTCGGTGCGGACCAGGGACAACAC
Exon 8	p.(Asp260His)	c.778G>C	TM3	Solaki et al., 2022	CCTGGTCCCCACCCACCTGGCTTACTT	AAGTAAGCCAGGTGGGTGGGGACCAGG
Exon 8	p.(Ala262Pro)	c.784G>C	TM3	Zobor et al., 2017	CCACCGACCTGCCTTACTTAAAGGTGGGCACAA	TTGTGCCCACCTTTAAGTAAGGCAGGTCGGTGG
Exon 8	p.(Tyr263Asp)	c.787T>G	TM3	Nishiguchi et al., 2005	CACCGACCTGGCTGACTTAAAGGTGGGC	GCCCACCTTTAAGTCAGCCAGGTCGGTG
Exon 8	p.(Val266Met)	c.796G>A	TM3 - TM4	Thiadens et al., 2010	CCACCGACCTGGCTTACTTAAAGATGGGCACAAAC	GTTTGTGCCCATCTTTAAGTAAGCCAGGTCGGTGG
Exon 8	p.(Pro271Ala)	c.811C>G	TM3 - TM4	Zelinger et al., 2015	GGTGGGCACAAACTACGCAGAAGTGAGGTTCAAC	GTTGAACCTCACTTCTGCGTAGTTTGTGCCCACC
Exon 8	p.(Pro271Thr)	c.811C>A	TM3 - TM4	Solaki et al., 2022	AAAGGTGGGCACAAACTACACAGAAGTGAGGTTCAACC	GGTTGAACCTCACTTCTGTGTAGTTTGTGCCCACCTTT

Exon 8	p.(Pro271Ser)	c.811C>T	TM3 - TM4	Georgiou et al., 2019	GGTGGGCACAAACTACTCAGAAGTGAGGTTCAAC	GTTGAACCTCACTTCTGAGTAGTTTGTGCCCACC
Exon 8	p.(Arg274Lys)	c.821G>A	TM4	Li et al., 2014	CAAACTACCCAGAAGTGAAGTTCAACCGCCTACTGAAG	CTTCAGTAGGCGGTTGAACTTCACTTCTGGGTAGTTTG
Exon 8	p.(Arg274Ser)	c.822G>T	TM4	Azam et al., 2010	CAAACTACCCAGAAGTGAGTTTCAACCGCCTACTGAAG	CTTCAGTAGGCGGTTGAAACTCACTTCTGGGTAGTTTG
Exon 8	p.(Asn276Ser)	c.827A>G	TM4	Saqib et al., 2011	CCCAGAAGTGAGGTTCAGCCGCCTACTGAAGTTTTC	GAAAACTTCAGTAGGCGGCTGAACCTCACTTCTGGG
Exon 8	p.(Arg277Gly)	c.829C>G	TM4	Koeppen et al., 2010	CAGAAGTGAGGTTCAACGGCCTACTGAAGTTTTCCC	GGGAAAACTTCAGTAGGCCGTTGAACCTCACTTCTG
Exon 8	p.(Leu278Pro)	c.833T>C	TM4	Li et al., 2014	GAGGTTCAACCGCCCACTGAAGTTTTCCCG	CGGGAAAACTTCAGTGGGCGGTTGAACCTC
Exon 8	p.(Arg283Trp)§	c.847C>T	TM4	Kohl et al., 1998	TCAACCGCCTACTGAAGTTTTCCTGGCTCTTTGAATTCTTTGACC	GGTCAAAGAATTCAAAGAGCCAGGAAAACTTCAGTAGGCGGTTGA
Exon 8	p.(Arg302Gly)	c.904A>G	TM5	Zelinger et al., 2015	CTACCCCAATATGTTCGGGATTGGGAACTTGGTC	GACCAAGTTCCCAATCCCGAACATATTGGGGTAG
Exon 8	p.(Arg302Ser)	c.906G>T	TM5	Weisschuh et al., 2020	CTACCCCAATATGTTCAGTATTGGGAACTTGGTCTTG	CAAGACCAAGTTCCCAATACTGAACATATTGGGGTAG
Exon 8	p.(Ile303Phe)	c.907A>T	TM5	ClinVar	CCCCAATATGTTCAGGTTTGGGAACTTGGTCTTG	CAAGACCAAGTTCCCAAACCTGAACATATTGGGG
Exon 8	p.(His315Gln)	c.945C>G	TM5	Patel et al., 2019	CATTCTCATCATCATCCAGTGGAATGCCTGCATCTAC	GTAGATGCAGGCATTCCACTGGATGATGATGAGAATG
Exon 8	p.(Ala318Thr)	c.952G>A	TM5	Li et al., 2017	CATCATCCACTGGAATACCTGCATCTACTTTGCC	GGCAAAGTAGATGCAGGTATTCCAGTGGATGATG
Exon 8	p.(Phe322Ser)	c.965T>C	TM5	Li et al., 2014	GAATGCCTGCATCTACTCTGCCATTTCCAAGTTC	GAACTTGGAAATGGCAGAGTAGATGCAGGCATTC
Exon 8	p.(Ala323Pro)	c.967G>C	TM5	Carss et al., 2017	GAATGCCTGCATCTACTTTCCCATTTCCAAGTTCATTG	CAATGAACTTGGAAATGGGAAAGTAGATGCAGGCATTC
Exon 8	p.(Ala323Asp)	c.968C>A	TM5	Li et al., 2015	GAATGCCTGCATCTACTTTGACATTTCCAAGTTCATTGGT	ACCAATGAACTTGGAAATGTCAAAGTAGATGCAGGCATTC
Exon 8	p.(Ile328Thr)	c.983T>C	TM5	Solaki et al., 2022	CTTTGCCATTTCCAAGTTCACTGGTTTTGGGACAGACTCC	GGAGTCTGTCCCAAAACCAGTGAACTTGGAAATGGCAAAG
Exon 8	p.(Gly329Cys)	c.985G>T	TM5 - pore helix	Genead et al., 2011	GCCATTTCCAAGTTCATTTGTTTTGGGACAGACTCCT	AGGAGTCTGTCCCAAAACAAATGAACTTGGAAATGGC
Exon 8	p.(Phe330Ser)	c.989T>C	TM5 - pore helix	Li et al., 2014	TGCCATTTCCAAGTTCATTGGTTCTGGGACAGACTC	GAGTCTGTCCCAGAACCAATGAACTTGGAAATGGCA
Exon 8	p.(Gly331Arg)	c.991G>C	TM5 - pore helix	Saqib et al., 2015	CCATTTCCAAGTTCATTGGTTTTCGGACAGACTCCT	AGGAGTCTGTCCGAAAACCAATGAACTTGGAAATGG
Exon 8	p.(Gly331Glu)	c.992G>A	TM5 - pore helix	Solaki et al., 2022	CAAGTTCATTGGTTTTGAGACAGACTCCTGGGTCT	AGACCCAGGAGTCTGTCTCAAAACCAATGAACTTG
Exon 8	p.(Ser334Phe)	c.1001C>T	TM5 - pore helix	Sundaram et al., 2014	GGTTTTGGGACAGACTTCTGGGTCTACCCAAAC	GTTTGGGTAGACCCAGAAGTCTGTCCCAAAACC
Exon 8	p.(Trp335Cys)	c.1005G>T	TM5 - pore helix	LOVD/Gilissen et al., 2014	TTTGGGACAGACTCCTGTGTCTACCCAAACATCTC	GAGATGTTTGGGTAGACACAGGAGTCTGTCCCAAA
Exon 8	p.(Val336Phe)	c.1006G>T	TM5 - pore helix	Liang et al., 2015	TGGGACAGACTCCTGGTTCTACCCAAACATCTC	GAGATGTTTGGGTAGAACCAGGAGTCTGTCCCA
Exon 8	p.(Ser341Pro)§¶	c.1021T>C	TM5 - pore helix	Wissinger et al., 2001	GGTCTACCCAAACATCCCAATCCCAGAGCATGG	CCATGCTCTGGGATTGGGATGTTTGGGTAGACC
Exon 8	p.(His345Arg)	c.1034A>G	TM5 - pore helix	ClinVar	TCAATCCCAGAGCGTGGGCGCCTCTCC	GGAGAGGCGCCCACGCTCTGGGATTGA
Exon 8	p.(Arg347Cys)	c.1039C>T	TM5 - pore helix	Sun et al., 2020	CCCAGAGCATGGGTGCCTCTCCAGGAA	TTCCTGGAGAGGCACCCATGCTCTGGG
Exon 8	p.(Arg350Gly)	c.1048A>G	TM5 - pore helix	ClinVar	CATGGGCGCCTCTCCGGGAAGTACATTTACAG	CTGTAAATGTACTTCCCGGAGAGGCGCCCATG
Exon 8	p.(Ile353Thr)	c.1058T>C	Pore helix	Liang et al., 2015	CCTCTCCAGGAAGTACACTTACAGTCTCTACTGGT	ACCAGTAGAGACTGTAAGTGTACTTCCTGGAGAGG
Exon 8	p.(Tyr354Cys)	c.1061A>G	Pore helix	Solaki et al., 2022	CGCCTCTCCAGGAAGTACATTTGCAGTCTCTACTG	CAGTAGAGACTGCAAATGTACTTCCTGGAGAGGCG
Exon 8	p.(Ser355Gly)	c.1063A>G	Pore helix	Solaki et al., 2022	CCAGGAAGTACATTTACGGTCTCTACTGGTCCACC	GGTGGACCAGTAGAGACCGTAAATGTACTTCCTGG
Exon 8	p.(Tyr357Cys)	c.1070A>G	Pore helix	Vincent et al., 2011	GTACATTTACAGTCTCTGCTGGTCCACCTTGACCC	GGGTCAAGGTGGACCAGCAGAGACTGTAAATGTAC
Exon 8	p.(Ser359Phe)	c.1076C>T	Pore helix	Solaki et al., 2022	TTACAGTCTCTACTGGTTCACCTTGACCCTTACCA	TGGTAAGGGTCAAGGTGAACCAGTAGAGACTGTAA
Exon 8	p.(Thr362Ile)	c.1085C>T	Pore helix	ClinVar	CTCTACTGGTCCACCTTGATCCTTACCACCATTG	CAATGGTGGTAAGGATCAAGGTGGACCAGTAGAG
Exon 8	p.(Leu363Pro)§¶	c.1088T>C	Pore helix	Koeppen et al., 2010	CCACCTTGACCCCTACCACCATTGGTG	CACCAATGGTGGTAGGGGTCAAGGTGG
Exon 8	p.(Gly367Val)§¶	c.1100G>T	pore helix -TM6	Koeppen et al., 2010	CCTTACCACCATTGTTGAGACCCCACC	GGTGGGGTCTCAACAATGGTGGTAAGG
Exon 8	p.(Glu368Gly)	c.1103A>G	pore helix -TM6	LOVD	CCACCATTGGTGGGACCCCACCCCC	GGGGGTGGGGTCCCACCAATGGTGG
Exon 8	p.(Thr369Ser)§	c.1106C>G	pore helix -TM6	Wissinger et al., 2001	CCATTGGTGAGAGCCCACCCCCCGTGAAAG	CTTTCACGGGGGGTGGGCTCTCACCAATGG
Exon 8	p.(Pro372Ser)§¶	c.1114C>T	pore helix -TM6	Wissinger et al., 2001	GAGACCCCACCCTCCGTGAAAGATGAG	CTCATCTTTCACGGAGGGTGGGGTCTC
Exon 8	p.(Pro372Ala)	c.1114C>G	pore helix -TM6	Sharon et al., 2020	GTGAGACCCCACCCGCCGTGAAAGATGAG	CTCATCTTTCACGGCGGGTGGGGTCTCAC
Exon 8	p.(Pro372Leu)	c.1115C>T	pore helix -TM6	LOVD	TGAGACCCCACCCCTCGTGAAAGATGAGG	CCTCATCTTTCACGAGGGGTGGGGTCTCA
Exon 8	p.(Val373Met)	c.1117G>A	pore helix -TM6	Solaki et al., 2022	AGACCCCACCCCCCATGAAAGATGAGGAG	CTCCTCATCTTTCATGGGGGGTGGGGTCT
Exon 8	p.(Val373Val)§	c.1119G>C	pore helix -TM6	gnomAD	CCCCACCCCCCGTCAAAGATGAGGAGTA	TACTCCTCATCTTTGACGGGGGGTGGGG
Exon 8	p.(Asp375Gly)	c.1124A>G	TM6	Sun et al., 2020	CCCACCCCCCGTGAAAGGTGAGGAGTATCTCTTTG	CAAAGAGATACTCCTCACCTTTCACGGGGGGTGGG
Exon 8	p.(Gly388Ser)	c.1162G>A	TM6	Brunetti-Pierri et al., 2021	GTCGTAGACTTCTTGGTGAGTGTTCTGATTTTTGCCAC	GTGGCAAAAATCAGAACACTCACCAAGAAGTCTACGAC
Exon 8	p.(Gly388Asp)	c.1163G>A	TM6	Sun et al., 2020	CGTAGACTTCTTGGTGGATGTTCTGATTTTGCCAC	GTGGCAAAAATCAGAACATCCACCAAGAAGTCTACG
Exon 8	p.(Gly388Val)	c.1163G>T	TM6	Sun et al., 2020	CGTAGACTTCTTGGTGGTTGTTCTGATTTTTGCCAC	GTGGCAAAAATCAGAACAACCACCAAGAAGTCTACG
Exon 8	p.(Gly397Val)	c.1190G>T	TM6	Ahuja er al., 2008	GATTTTTGCCACCATTGTGGTCAATGTGGGCTCCATGATC	GATCATGGAGCCCACATTGACCACAATGGTGGCAAAAATC
Exon 8	p.(Ser401Pro)	c.1201T>C	TM6	Nishiguchi et al., 2005	GGGCAATGTGGGCCCCATGATCTCGAATATG	CATATTCGAGATCATGGGGCCCACATTGCCC
C-Linker						
Exon 8	p.(Ala415Pro)	c.1243G>C	C-linker αA'	Stone et al., 2017	CGGGCAGAGTTCCAGCCCAAGATTGATTCC	GGAATCAATCTTGGGCTGGAACTCTGCCCG
Exon 8	p.(Asp418Glu)	c.1254T>G	C-linker αA'	ClinVar	GTTCCAGGCCAAGATTGAGTCCATCAAGCAGTACATG	CATGTACTGCTTGATGGACTCAATCTTGGCCTGGAAC
Exon 8	p.(Ser419Pro)	c.1255T>C	C-linker αA'	Weisschuh et al., 2020	CCAGGCCAAGATTGATCCCATCAAGCAGTACATG	CATGTACTGCTTGATGGGATCAATCTTGGCCTGG
Exon 8	p.(Ser419Phe)	c.1256C>T	C-linker αA'	Patel et al., 2019	CCAGGCCAAGATTGATTTCATCAAGCAGTACATGC	GCATGTACTGCTTGATGAAATCAATCTTGGCCTGG
Exon 8	p.(Tyr423Ser)	c.1268A>C	C-linker αA'	Solaki et al., 2022	GATTCCATCAAGCAGTCCATGCAGTTCCGCAAGG	CCTTGCGGAACTGCATGGACTGCTTGATGGAATC
Exon 8	p.(Met424Thr)	c.1271T>C	C-linker αA'	ClinVar	CCATCAAGCAGTACACGCAGTTCCGCAAGGTC	GACCTTGCGGAACTGCGTGTACTGCTTGATGG
Exon 8	p.(Arg427Cys)§¶	c.1279C>T	C-linker αA' - αB'	Wissinger et al., 2001	GCAGTACATGCAGTTCTGCAAGGTCACCAAG	CCTTGGTGACCTTGCAGAACTGCATGTACTG
Exon 8	p.(Arg427Leu)	c.1280G>T	C-linker αA' - αB'	ClinVar	GCAGTACATGCAGTTCCTCAAGGTCACCAAGGAC	GTCCTTGGTGACCTTGAGGAACTGCATGTACTGC
Exon 8	p.(Val429Ala)	c.1286T>C	C-linker αA' - αB'	Georgiou et al., 2019	CAGTTCCGCAAGGCCACCAAGGACTTGG	CCAAGTCCTTGGTGGCCTTGCGGAACTG
Exon 8	p.(Asp432Tyr)	c.1294G>T	C-linker αB'	Sun et al., 2020	GCAAGGTCACCAAGTACTTGGAGACGCGGG	CCCGCGTCTCCAAGTACTTGGTGACCTTGC
Exon 8	p.(Arg436Gln)	c.1307G>A	C-linker αB'	Li et al., 2014	GGACTTGGAGACGCAGGTTATCCGGTGG	CCACCGGATAACCTGCGTCTCCAAGTCC

Exon 8	p.(Trp440Ser)	c.1319G>C	C-linker αB'	Georgiou et al., 2019	GCGGGTTATCCGGTCGTTTGACTACCTGTG	CACAGGTAGTCAAACGACCGGATAACCCGC
Exon 8	p.(Lys448Arg)	c.1343A>G	C-linker αB' - αC'	Solaki et al., 2022	CCTGTGGGCCAACAGGAAGACGGTGGATG	CATCCACCGTCTTCCTGTTGGCCCACAGG
Exon 8	p.(Leu464Arg)	c.1391T>G	C-linker αD'	Greenberg et al., 2014	CTCCCAGACAAGCGGAAGGCTGAGATCG	CGATCTCAGCCTTCCGCTTGTCTGGGAG
Exon 8	p.(Ala469Thr)§¶	c.1405G>A	C-linker αD'	Reuter et al., 2008	GCTGAAGGCTGAGATCACCATCAACGTGCACC	GGTGCACGTTGATGGTGATCTCAGCCTTCAGC
Exon 8	p.(Asn471Ser)	c.1412A>G	C-linker αD'	Wissinger et al., 2001	AGGCTGAGATCGCCATCAGCGTGCACCTG	CAGGTGCACGCTGATGGCGATCTCAGCCT
Exon 8	p.(Lys479Val)	c.1435_1436delinsGT	C-linker αE'	Sun et al., 2020	CCTGGACACGCTGAAGGTGGTTCGCATCTTCCAG	CTGGAAGATGCGAACCACCTTCAGCGTGTCCAGG
Exon 8	p.(Cys486Tyr)	c.1457G>A	C-linker αF' - CNBD αA	Abouelhoda et al., 2016	GCATCTTCCAGGACTATGAGGCAGGGCTGC	GCAGCCCTGCCTCATAGTCCTGGAAGATGC
CNBD						
Exon 8	p.(Gly489Val)	c.1466G>T	CNBD αA	Solaki et al., 2022	GACTGTGAGGCAGTGCTGCTGGTGGAG	CTCCACCAGCAGCACTGCCTCACAGTC
Exon 8	p.(Pro505Ala)	c.1513C>G	CNBD β1 - β2	Huang et al., 2016	ACCCACTGTGTTCAGCGCTGGGGATTATATCTG	CAGATATAATCCCCAGCGCTGAACACAGTGGGT
Exon 8	p.(Asp507Gly)	c.1520A>G	CNBD β1 - β3	LOVD	TGTGTTCAGCCCTGGGGGTTATATCTGCAAGAAGG	CCTTCTTGCAGATATAACCCCCAGGGCTGAACACA
Exon 8	p.(Lys512Met)	c.1535A>T	CNBD β2 - β3	Carrigan et al., 2016	CCCTGGGGATTATATCTGCAAGATGGGAGATATTGG	CCAATATCTCCCATCTTGCAGATATAATCCCCAGGG
Exon 8	p.(Gly513Arg)	c.1537G>A	CNBD β2 - β3	Solaki et al., 2022	GGGATTATATCTGCAAGAAGAGAGATATTGGGAAGGAGATG	CATCTCCTTCCCAATATCTCTCTTCTTGCAGATATAATCCC
Exon 8	p.(Asp514Asn)	c.1540G>A	CNBD β2 - β3	Arshad et al., 2019	GATTATATCTGCAAGAAGGGAAATATTGGGAAGGAGATGTACA	TGTACATCTCCTTCCCAATATTTCCCTTCTTGCAGATATAATC
Exon 8	p.(Asp514Val)	c.1541A>T	CNBD β2 - β3	Genead et al., 2011	TATATCTGCAAGAAGGGAGTTATTGGGAAGGAGATGTAC	GTACATCTCCTTCCCAATAACTCCCTTCTTGCAGATATA
Exon 8	p.(Met519Thr)	c.1556T>C	CNBD β3	Huang et al., 2016	GAGATATTGGGAAGGAGACGTACATCATCAACGAGGG	CCCTCGTTGATGATGTACGTCTCCTTCCCAATATCTC
Exon 8	p.(Met519Ile)	c.1557G>A	CNBD β3	Ellingford et al., 2016	GGAGATATTGGGAAGGAGATATACATCATCAACGAGG	CCTCGTTGATGATGTATATCTCCTTCCCAATATCTCC
Exon 8	p.(Gly525Ser)	c.1573G>A	CNBD β3 - β4	Patel et al., 2016	TACATCATCAACGAGAGCAAGCTGGCCGTGG	CCACGGCCAGCTTGCTCTCGTTGATGATGTA
Exon 8	p.(Leu527Met)	c.1579C>A	CNBD β4	Wang et al., 2011	CAACGAGGGCAAGATGGCCGTGGTGGC	GCCACCACGGCCATCTTGCCCTCGTTG
Exon 8	p.(Leu527Arg)	c.1580T>G	CNBD β4	Lam et al., 2011	CGAGGGCAAGCGGGCCGTGGTGG	CCACCACGGCCCGCTTGCCCTCG
Exon 8	p.(Asp533His)	c.1597G>C	CNBD β4 - β5	Li et al., 2014	GGCCGTGGTGGCTGATCATGGGGTCA	TGACCCCATGATCAGCCACCACGGCC
Exon 8	p.(Val539Met)	c.1615G>A	CNBD β5	Solaki et al., 2022	GGGTCACCCAGTTCATGGTCCTCAGCGAT	ATCGCTGAGGACCATGAACTGGGTGACCC
Exon 8	p.(Val540Ile)	c.1618G>A	CNBD β5	Thiadens et al., 2010	TCACCCAGTTCGTGATCCTCAGCGATGGC	GCCATCGCTGAGGATCACGAACTGGGTGA
Exon 8	p.(Leu541Phe)	c.1621C>T	CNBD β5	Greenberg et al., 2014	CCCAGTTCGTGGTCTTCAGCGATGGCAGC	GCTGCCATCGCTGAAGACCACGAACTGGG
Exon 8	p.(Phe547Cys)	c.1640T>G	CNBD β6	Zelinger et al., 2015	CTCAGCGATGGCAGCTACTGCGGGGAGATC	GATCTCCCCGCAGTAGCTGCCATCGCTGAG
Exon 8	p.(Phe547Leu)§¶	c.1641C>A	CNBD β6	Kohl et al., 1998	CTCAGCGATGGCAGCTACTTAGGGGAGATCAGCATTC	GAATGCTGATCTCCCCTAAGTAGCTGCCATCGCTGAG
Exon 8	p.(Gly548Arg)	c.1642G>A	CNBD β6	Johnson et al., 2004	CGATGGCAGCTACTTCAGGGAGATCAGCATTCT	AGAATGCTGATCTCCCTGAAGTAGCTGCCATCG
Exon 8	p.(Leu553Gln)	c.1658T>A	CNBD β6 - β7	Solaki et al., 2022	GGGGAGATCAGCATTCAGAACATCAAGGGGAGC	GCTCCCCTTGATGTTCTGAATGCTGATCTCCCC
Exon 8	p.(Gly557Arg)§¶	c.1669G>A	CNBD β6 - β7	Kohl et al., 1998	GCATTCTGAACATCAAGAGGAGCAAGTCGG	CCTACTTGCTCCTCTTGATGTTCAGAATGC
Exon 8	p.(Ser560Leu)	c.1679C>T	CNBD β6 - β7	ClinVar	AACATCAAGGGGAGCAAGTTGGGGAACCGC	GCGGTTCCCCAACTTGCTCCCCTTGATGTT
Exon 8	p.(Gly561Glu)	c.1682G>A	CNBD β6 - β7	Zobor et al., 2017	GGGAGCAAGTCGGAGAACCGCAGGACG	CGTCCTGCGGTTCTCCGACTTGCTCCC
Exon 8	p.(Asn562Lys)	c.1686C>A	CNBD β6 - β7	ClinVar	AGCAAGTCGGGGAAACGCAGGACGGC	GCCGTCCTGCGTTTCCCCGACTTGCT
Exon 8	p.(Arg563Cys)§¶	c.1687C>T	CNBD β6 - β7	Koeppen et al., 2008	GTCGGGGAACTGCAGGACGGCCAAC	GTTGGCCGTCCTGCAGTTCCCCGAC
Exon 8	p.(Arg563His)§	c.1688G>A	CNBD β6 - β7	Wissinger et al., 2001	GTCGGGGAACCACAGGACGGCCAAC	GTTGGCCGTCCTGTGGTTCCCCGAC
Exon 8	p.(Arg569Cys)	c.1705C>T	CNBD β7	Solaki et al., 2022	GGACGGCCAACATCTGCAGCATTGGCTAC	GTAGCCAATGCTGCAGATGTTGGCCGTCC
Exon 8	p.(Arg569His)§¶	c.1706G>A	CNBD β7	Wissinger et al., 2001	CAGGACGGCCAACATCCACAGCATTGGC	GCCAATGCTGTGGATGTTGGCCGTCCTG
Exon 8	p.(Ser570Gly)	c.1708A>G	CNBD β7	Solaki et al., 2022	CGGCCAACATCCGCGGCATTGGCTACTCA	TGAGTAGCCAATGCCGCGGATGTTGGCCG
Exon 8	p.(Ser570Asn)	c.1709G>A	CNBD β7	Li et al., 2014	CGGCCAACATCCGCAACATTGGCTACTCAGA	TCTGAGTAGCCAATGTTGCGGATGTTGGCCG
Exon 8	p.(Ser570Ile)	c.1709G>T	CNBD β7	Thiadens et al., 2010	CGGCCAACATCCGCATCATTGGCTACTCAGA	TCTGAGTAGCCAATGATGCGGATGTTGGCCG
Exon 8	p.(Ile571Thr)	c.1712T>C	CNBD β7 - β8	Jinda et al., 2021	GGCCAACATCCGCAGCACTGGCTACTCAGA	TCTGAGTAGCCAGTGCTGCGGATGTTGGCC
Exon 8	p.(Tyr573His)	c.1717T>C	CNBD β7 - β8	Solaki et al., 2022	CATCCGCAGCATTGGCCACTCAGACCTGTTCTG	CAGAACAGGTCTGAGTGGCCAATGCTGCGGATG
Exon 8	p.(Leu579Arg)	c.1736T>G	CNBD β8	Solaki et al., 2022	TCAGACCTGTTCTGCCGCTCAAAGGACGATCTC	GAGATCGTCCTTTGAGCGGCAGAACAGGTCTGA
Exon 8	p.(Glu590Lys)§¶	c.1768G>A	CNBD αB	Nishiguchi et al., 2005	GGAGGCCCTCACCAAGTACCCCGAAGCC	GGCTTCGGGGTACTTGGTGAGGGCCTCC
Exon 8	p.(Tyr591His)	c.1771T>C	CNBD αB - αC	Solaki et al., 2022	GCCCTCACCGAGCACCCCGAAGCCA	TGGCTTCGGGGTGCTCGGTGAGGGC
Exon 8	p.(Pro592Leu)	c.1775C>T	CNBD αB - αC	Solaki et al., 2022	CCTCACCGAGTACCTCGAAGCCAAGAAGG	CCTTCTTGGCTTCGAGGTACTCGGTGAGG
Exon 8	p.(Lys595Arg)	c.1784A>G	CNBD αC	ClinVar	TACCCCGAAGCCAGGAAGGCCCTGGAG	CTCCAGGGCCTTCCTGGCTTCGGGGTA
Exon 8	p.(Leu598Arg)	c.1793T>G	CNBD αC	Sun et al., 2020	AGCCAAGAAGGCCCGGGAGGAGAAAGGAC	GTCCTTTCTCCTCCCGGGCCTTCTTGGCT
Exon 8	p.(Gly602Glu)	c.1805G>A	CNBD αC	Georgiou et al., 2019	CCCTGGAGGAGAAAGAACGGCAGATCCTGA	TCAGGATCTGCCGTTCTTTCTCCTCCAGGG
Exon 8	p.(Glu615Asp)	c.1845G>T	CNBD αC - CLZ	ClinVar	TGATCGATGAGGATCTGGCCAGGGCGG	CCGCCCTGGCCAGATCCTCATCGATCA
Exon 8	p.(Ala619Val)	c.1856C>T	CNBD αC - CLZ	Thiadens et al., 2010	GCTGGCCAGGGTGGGCGCGGACC	GGTCCGCGCCCACCCTGGCCAGC
Exon 8	p.(Ala621Glu)	c.1862C>A	CNBD αC - CLZ	Wiszniewski et al., 2007	CAGGGCGGGCGAGGACCCCAAGG	CCTTGGGGTCCTCGCCCGCCCTG
Exon 8	p.(Ala621Ala)§	c.1863G>A	CNBD αC - CLZ	gnomAD	CCAGGGCGGGCGCAGACCCCAAGGAC	GTCCTTGGGGTCTGCGCCCGCCCTGG
CLZ						
Exon 8	p.(Leu626Arg)	c.1877T>G	CLZ	Huang et al., 2016	CGGACCCCAAGGACCGTGAGGAGAAAGTGG	CCACTTTCTCCTCACGGTCCTTGGGGTCCG
Exon 8	p.(Val630Ala)	c.1889T>C	CLZ	Solaki et al., 2022	CCTTGAGGAGAAAGCGGAGCAGCTGGGG	CCCCAGCTGCTCCGCTTTCTCCTCAAGG
Exon 8	p.(Phe644Ser)	c.1931T>C	CLZ	Ellingford et al., 2016	CCTGCAGACCAGGTCTGCACGCCTCCTGG	CCAGGAGGCGTGCAGACCTGGTCTGCAGG
Exon 8	p.(Arg646His)	c.1937G>A	CLZ	Li et al., 2014	GACCAGGTTTGCACACCTCCTGGCTGAG	CTCAGCCAGGAGGTGTGCAAACCTGGTC
Exon 8	p.(Glu650Ala)	c.1949A>C	CLZ	LOVD	CGCCTCCTGGCTGCGTACAACGCCACCC	GGGTGGCGTTGTACGCAGCCAGGAGGCG
Exon 8	p.(Met656Ile)	c.1968G>A	CLZ	ClinVar	GTACAACGCCACCCAGATAAAGATGAAGCAGCG	CGCTGCTTCATCTTTATCTGGGTGGCGTTGTAC
Exon 8	p.(Arg661Ser)	c.1981C>A	CLZ	Yang et al., 2014	CAGATGAAGATGAAGCAGAGTCTCAGCCAACTGGAAAG	CTTTCCAGTTGGCTGAGACTCTGCTTCATCTTCATCTG

Exon 8	p.(Arg661His)	c.1982G>A	CLZ	Sun et al., 2020	GATGAAGATGAAGCAGCATCTCAGCCAACTGGAAAG	CTTTCCAGTTGGCTGAGATGCTGCTTCATCTTCATC
Exon 8	p.(Val669Leu)	c.2005G>C	CLZ	ClinVar	CAACTGGAAAGCCAGCTGAAGGGTGGTGGG	CCCACCACCCTTCAGCTGGCTTTCCAGTTG
Exon 8	p.(Gly684Arg)	c.2050G>A	C-Term.	Patel et al., 2016	CTGATGGGGAAGTTCCCAGGGATGCTACAAAAACA	TGTTTTTGTAGCATCCCTGGGAACTTCCCCATCAG

†Variant designation is based on NM_001298.3 (GRCh38/hg38).
‡Functional domains of CNGA3 annotated according to Gofman et al., 2014 and Shuart et al., 2011: N-Term., N-terminus; TM1 to TM6, transmembrane domains; C-linker having six alpha helices (αA' to αF'); CNBD, cyclic-nucleotide binding domain having three alpha helices (αA to αC) and eight beta-sheets (β1 to β8); CLZ, C-terminal leucin zipper; C-Term., C-terminus; -, intermediate amino acid residue between two domains.
§Assay validation data set comprised of nine benign and 15 pathogenic variants in the *CNGA3* gene.
¶Generation of the respective expression constructs has been reported previously (Tränkner et al., 2004; Koeppen et al., 2008; Reuter et al., 2008; Koeppen et al., 2010).

Supplemental Table 3: Overview of the assay validation data set composed of nine benign and 15 pathogenic variants in the *CNGA3* gene including location of variant in polypeptide and functional or structural domain, references for previous functional analysis and selection criteria for inclusion in the assay validation data set.

Alteration Polypeptide	Alteration Nucleotide Sequence†	Alteration gDNA Level†	Location Protein Domain‡	Reference Variant	Reference Functional Analysis	Selection Criteria
Benign variants						
p.(Thr20Ile)	c.59C>T	g.98370034C>T	N-Term.	ClinVar	-	benign variant detected homozygously in healthy individuals on the gnomAD database
p.(Pro48Leu)	c.143C>T	g.98377728C>T	N-Term.	Nishiguchi et al., 2005	-	benign variant detected homozygously in healthy individuals on the gnomAD database
p.(Pro48Pro)	c.144G>A	g.98377729G>A	N-Term.	gnomAD	-	synonymous variant identified on the gnomAD database
p.(Thr147Thr)	c.441G>A	g.98383433G>A	N-Term.	gnomAD	-	synonymous variant identified on the gnomAD database
p.(Thr153Met)	c.458C>T	g.98389666C>T	N-Term.	Kohl et al., 1998	Tränkner et al., 2004 Meighan et al., 2015	missense variant displaying wild-type-like function in homomeric channels
p.(Ala158Ala)	c.474G>A	g.98389682G>A	N-Term.	gnomAD	-	synonymous variant identified on the gnomAD database
p.(Glu198Lys)	c.592G>A	g.98391889G>A	TM2	Solaki et al., 2022	-	benign variant detected homozygously in healthy individuals on the gnomAD database
p.(Val373Val)	c.1119G>C	g.98396289G>C	pore helix -TM6	gnomAD	-	synonymous variant identified on the gnomAD database
p.(Ala621Ala)	c.1863G>A	g.98397033G>A	CNBD αC - CLZ	gnomAD	-	synonymous variant identified on the gnomAD database
Pathogenic variants						
p.(Glu228Lys)	c.682G>A	g.98395852G>A	TM2 - TM3	Reuter et al., 2008	Reuter et al., 2008	residual channel function in previously conducted study
p.(Arg283Trp)	c.847C>T	g.98396017C>T	TM4	Kohl et al., 1998	Muraki-Oda et al., 2007	absent channel function in previously conducted study
p.(Ser341Pro)	c.1021T>C	g.98396191T>C	TM5 - pore helix	Wissinger et al., 2001	Muraki-Oda et al., 2007 Koeppen et al., 2010	absent channel function in previously conducted studies
p.(Leu363Pro)	c.1088T>C	g.98396258T>C	Pore helix	Koeppen et al., 2010	Koeppen et al., 2010	absent channel function in previously conducted study
p.(Gly367Val)	c.1100G>T	g.98396270G>T	pore helix -TM6	Koeppen et al., 2010	Koeppen et al., 2010	absent channel function in previously conducted study
p.(Thr369Ser)	c.1106C>G	g.98396276C>G	pore helix -TM6	Wissinger et al., 2001	Tränkner et al., 2004 Muraki-Oda et al., 2007	residual channel function in previously conducted studies
p.(Pro372Ser)	c.1114C>T	g.98396284C>T	pore helix -TM6	Wissinger et al., 2001	Muraki-Oda et al., 2007 Koeppen et al., 2010	absent channel function in previously conducted studies
p.(Arg427Cys)	c.1279C>T	g.98396449C>T	C-linker αA' - αB'	Wissinger et al., 2001	Muraki-Oda et al., 2007 Koeppen et al., 2008	residual channel function in previously conducted studies
p.(Ala469Thr)	c.1405G>A	g.98396575G>A	C-linker αD'	Reuter et al., 2008	Reuter et al., 2008	residual channel function in previously conducted study
p.(Phe547Leu)	c.1641C>A	g.98396811C>A	CNBD β6	Kohl et al., 1998	Muraki-Oda et al., 2007 Reuter et al., 2008 Matveev et al., 2010	absent channel function in previously conducted studies
p.(Gly557Arg)	c.1669G>A	g.98396839G>A	CNBD β6 - β7	Kohl et al., 1998	Muraki-Oda et al., 2007 Reuter et al., 2008	residual channel function in previously conducted studies
p.(Arg563Cys)	c.1687C>T	g.98396857C>T	CNBD β6 - β7	Koeppen et al., 2008	Koeppen et al., 2008	residual channel function in previously conducted study
p.(Arg563His)	c.1688G>A	g.98396858G>A	CNBD β6 - β7	Wissinger et al., 2001	Liu and Varnum, 2005 Muraki-Oda et al., 2007	residual channel function in previously conducted studies
p.(Arg569His)	c.1706G>A	g.98396876G>A	CNBD β7	Wissinger et al., 2001	Muraki-Oda et al., 2007 Koeppen et al., 2008	absent channel function in previously conducted studies
p.(Glu590Lys)	c.1768G>A	g.98396938G>A	CNBD αB	Nishiguchi et al., 2005	Reuter et al., 2008	residual channel function in previously conducted study

†Variant designation is based on NM_001298.3 (GRCh38/hg38) and NC_000002.12 (GRCh38/hg38).
‡Functional domains of CNGA3 annotated according to Gofman et al., 2014 and Shuart et al., 2011: N-Term., N-terminus; TM1 to TM6, transmembrane domains; C-linker having six alpha helices (αA' to αF'); CNBD, cyclic-nucleotide binding domain having three alpha helices (αA to αC) and eight beta-sheets (β1 to β8); CLZ, C-terminal leucin zipper; C-Term., C-terminus; -, intermediate amino acid residue between two domains.

Supplemental Table 4: Summary of the 150 functionally evaluated CNGA3 missense variants using the aequorin-based bioassay including location of variant in polypeptide and functional or structural domain, normalized overall luminescence signals (AUC) and normalized peak latency values, variant classification as functionally normal or abnormal based on the aequorin-based bioassay as well as pre-assay and post-assay ACMG/AMP classification after applying functional evidence.

Alteration Polypeptide	Alteration Nucleotide Sequence†	Alteration gDNA Level†	Location Protein Domain‡	Allele frequency gnomAD [%]	Reference	Normalized overall luminescence signal (AUC)#	Normalized peak latency#	Assay classification§	Pre-Assay ACMG/AMP criteria¶	Pre-Assay ACMG/AMP classification	Post-Assay ACMG/AMP criteria¶	Post-Assay ACMG/AMP classification
p.(Arg23Gln)	c.68G>A	g.98370043G>A	N-Term.	0.003	ClinVar	0.81±0.05	0.89±0.03	functionally normal	PM2_mod;BP4_supp	VUS	PM2_mod;BP4_supp;BS3_strong	Likely benign
p.(Arg27His)	c.80G>A	g.98370055G>A	N-Term.	0.008	ClinVar	0.78±0.06	0.96±0.05	functionally normal	PM2_mod;BP4_supp	VUS	PM2_mod;BP4_supp;BS3_strong	Likely benign
p.(Ser37Leu)	c.110C>T	g.98377695C>T	N-Term.	0.022	ClinVar	0.74±0.04	0.85±0.02	functionally normal	PM2_mod;BP4_supp	VUS	PM2_mod;BP4_supp;BS3_strong	Likely benign
p.(Met52Val)	c.154A>G	g.98377739A>G	N-Term.	0.0004	ClinVar	0.78±0.04	0.96±0.01	functionally normal	PM2_mod;BP4_supp	VUS	PM2_mod;BP4_supp;BS3_strong	Likely benign
p.(Ala71Thr)	c.211G>A	g.98377796G>A	N-Term.	0.018	ClinVar	0.85±0.00	0.89±0.01	functionally normal	PM2_mod;BP4_supp	VUS	PM2_mod;BP4_supp;BS3_strong	Likely benign
p.(Pro95Leu)	c.284C>T	g.98380243C>T	N-Term.	0.022	Thiadens et al., 2010	0.75±0.04	0.88±0.02	functionally normal	PM2_mod;BP4_supp	VUS	PM2_mod;BP4_supp;BS3_strong	Likely benign
p.(Glu106Lys)	c.316G>A	g.98380275G>A	N-Term.	0.002	Sharon et al., 2020	0.96±0.15	1.23±0.02	functionally abnormal	PM2_mod;PP5_supp;PP3_supp	VUS	PM2_mod;PP5_supp;PP3_supp;PS3_strong	Likely pathogenic
p.(Gln118Arg)	c.353A>G	g.98380312A>G	N-Term.	0.088	Solaki et al., 2022	0.78±0.01	0.90±0.01	functionally normal	BP5_supp;BP6_strong;BP4_supp	Likely benign	BP5_supp;BP6_strong;BP4_supp;BS3_strong	Benign
p.(Asn120Asp)	c.358A>G	g.98380317A>G	N-Term.	0.002	Li et al., 2014	0.94±0.11	0.83±0.01	functionally normal	PM2_mod;BP4_supp	VUS	PM2_mod;BP4_supp;BS3_strong	Likely benign
p.(Thr147Arg)	c.440C>G	g.98383432C>G	N-Term.	0.028	LOVD	0.86±0.09	0.91±0.06	functionally normal	PM2_mod;BP4_supp	VUS	PM2_mod;BP4_supp;BS3_strong	Likely benign
p.(Asp157Glu)	c.471T>G	g.98389679T>G	N-Term.	0.006	ClinVar	0.88±0.11	0.88±0.01	functionally normal	PM2_mod;PM1_supp;BP4_supp	VUS	PM2_mod;PM1_supp;BP4_supp;BS3_strong	Likely benign
p.(Ala158Val)	c.473C>T	g.98389681C>T	N-Term.	0.039	LOVD	0.74±0.12	1.02±0.06	functionally normal	PM1_supp;BP4_supp	VUS	PM1_supp;BP4_supp;BS3_strong	Likely benign
p.(Val160Met)	c.478G>A	g.98389686G>A	N-Term.	0.004	ClinVar	0.63±0.09	1.19±0.00	functionally abnormal	PM2_mod;PM1_supp;PP3_supp	VUS	PM2_mod;PM1_supp;PP3_supp;PS3_strong	Likely pathogenic
p.(Val160Gly)	c.479T>G	g.98389687T>G	N-Term.	no entry	Solaki et al., 2022	0.07±0.02	3.55±0.46	functionally abnormal	PM2_mod;PM1_supp;PP3_supp	VUS	PM2_mod;PM1_supp;PP3_supp;PS3_strong	Likely pathogenic
p.(Trp171Cys)	c.513G>T	g.98389721G>T	TM1	0.0004	Li et al., 2014	0.16±0.06	2.98±0.13	functionally abnormal	PM2_mod;PM1_supp;PP2_supp;PP3_supp	VUS	PM2_mod;PM1_supp;PP2_supp;PP3_supp;PS3_strong	Likely pathogenic
p.(Val179Asp)	c.536T>A	g.98389744T>A	TM1	no entry	Dubis et al., 2014	0.05±0.01	n.a.	functionally abnormal	PM2_mod;PM1_supp;PP2_supp;PP3_supp	VUS	PM2_mod;PM1_supp;PP2_supp;PP3_supp;PS3_strong	Likely pathogenic
p.(Asn182Asp)	c.544A>G	g.98389752A>G	TM1	no entry	Solaki et al., 2022	0.05±0.00	n.a.	functionally abnormal	PM2_mod;PM1_supp;PP2_supp;PM5_mod;PP3_supp	Likely pathogenic	PM2_mod;PM1_supp;PP2_supp;PM5_mod;PP3_supp;PS3_strong	Pathogenic
p.(Leu185Val)	c.553C>G	g.98389761C>G	TM1	0.0004	Kim et al., 2019	0.91±0.11	0.92±0.01	functionally normal	PM2_mod;PM1_supp;PP2_supp;BP4_supp	VUS	PM2_mod;PM1_supp;PP2_supp;BP4_supp;BS3_strong	Likely benign
p.(Ile187Thr)	c.560T>C	g.98389768T>C	TM1 - TM2	no entry	Taylor et al., 2017	0.03±0.00	n.a.	functionally abnormal	PP5_strong;PM2_mod;PM1_supp;PP2_supp;PP3_supp	Likely pathogenic	PP5_strong;PM2_mod;PM1_supp;PP2_supp;PP3_supp;PS3_strong	Pathogenic
p.(Arg189Lys)	c.566G>A	g.98389774G>A	TM1 - TM2	no entry	Solaki et al., 2022	0.02±0.00	n.a.	functionally abnormal	PM2_mod;PM1_supp;PP2_supp;PP3_supp	VUS	PM2_mod;PM1_supp;PP2_supp;PP3_supp;PS3_strong	Likely pathogenic
p.(Leu195Pro)	c.584T>C	g.98391881T>C	TM1 - TM2	no entry	ClinVar	0.04±0.00	n.a.	functionally abnormal	PM2_mod;PP3_supp;PP2_supp	VUS	PM2_mod;PP3_supp;PP2_supp;PS3_strong	Likely pathogenic
p.(Gln196Arg)	c.587A>G	g.98391884A>G	TM1 - TM2	no entry	Sun et al., 2020	0.03±0.01	n.a.	functionally abnormal	PM2_mod;PP3_supp;PP2_supp	VUS	PM2_mod;PP3_supp;PP2_supp;PS3_strong	Likely pathogenic
p.(Ser197Pro)	c.589T>C	g.98391886T>C	TM2	no entry	ClinVar	0.04±0.00	n.a.	functionally abnormal	PM2_mod;PP2_supp;PP5_strong	Likely pathogenic	PM2_mod;PP2_supp;PP5_strong;PS3_strong	Pathogenic
p.(Trp203Cys)	c.609G>T	g.98391906G>T	TM2	0.001	Solaki et al., 2022	0.04±0.01	n.a.	functionally abnormal	PM2_mod;PP3_supp;PP2_supp	VUS	PM2_mod;PP3_supp;PP2_supp;PS3_strong	Likely pathogenic
p.(Ser209Pro)	c.625T>C	g.98391922T>C	TM2	no entry	Weisschuh et al., 2020	0.02±0.00	1.70±0.07	functionally abnormal	PM2_mod;PP2_supp;PP5_supp;BP4_supp	VUS	PM2_mod;PP2_supp;PP5_supp;BP4_supp;PS3_strong	Likely pathogenic
p.(Asp211Glu)	c.633T>A	g.98391930T>A	TM2	0.0004	Liang et al., 2015	0.03±0.00	n.a.	functionally abnormal	PM2_mod;PP2_supp	VUS	PM2_mod;PP2_supp;PS3_strong	Likely pathogenic
p.(Asp217His)	c.649G>C	g.98391946G>C	TM2	no entry	ClinVar	0.03±0.00	n.a.	functionally abnormal	PM2_mod;PP2_supp;PP3_supp	VUS	PM2_mod;PP2_supp;PP3_supp;PS3_strong	Likely pathogenic
p.(Ala222Pro)	c.664G>C	g.98391961G>C	TM2	no entry	Reuter et al., 2008	0.02±0.01	n.a.	functionally abnormal	PM2_mod;PP2_supp	VUS	PM2_mod;PP2_supp;PS3_strong	Likely pathogenic
p.(Arg223Gly)	c.667C>G	g.98391964C>G	TM2	0.004	Wiszniewski et al., 2007	0.03±0.00	n.a.	functionally abnormal	PM2_mod;PM5_mod;PP3_supp;PP2_supp;PP5_supp	Likely pathogenic	PM2_mod;PM5_mod;PP3_supp;PP2_supp;PP5_supp;PS3_strong	Pathogenic
p.(Arg223Gln)	c.668G>A	g.98391965G>A	TM2	0.004	Li et al., 2014; Greenberg et al., 2014	0.04±0.01	1.76±0.09	functionally abnormal	PP5_strong;PP1_supp;PM2_mod;PM5_mod;PP3_supp;PP2_supp	Pathogenic	PP5_strong;PP1_supp;PM2_mod;PM5_mod;PP3_supp;PP2_supp;PS3_strong	Pathogenic
p.(Thr224Ala)	c.670A>G	g.98391967A>G	TM2 - TM3	no entry	Solaki et al., 2022	0.03±0.00	n.a.	functionally abnormal	PM2_mod;PM5_supp;PP3_supp;PP2_supp	VUS	PM2_mod;PM5_supp;PP3_supp;PP2_supp;PS3_strong	Likely pathogenic
p.(Thr224Ile)	c.671C>T	g.98391968C>T	TM2 - TM3	no entry	Li et al., 2014	0.03±0.00	n.a.	functionally abnormal	PM2_mod;PM5_supp;PP3_supp;PP2_supp	VUS	PM2_mod;PM5_supp;PP3_supp;PP2_supp;PS3_strong	Likely pathogenic
p.(Asp239Val)	c.704A>T	g.98395874A>T	TM2 - TM3	no entry	Weisschuh et al., 2020	0.04±0.00	n.a.	functionally abnormal	PM2_mod;PP3_supp;PP2_supp;PP5_supp	VUS	PM2_mod;PP3_supp;PP2_supp;PP5_supp;PS3_strong	Likely pathogenic
p.(Thr245Met)	c.734C>T	g.98395904C>T	TM2 - TM3	0.006	Johnson et al., 2004	0.87±0.07	0.91±0.05	functionally normal	PM2_mod;PP2_supp;BP4_supp	VUS	PM2_mod;PP2_supp;BP4_supp;BS3_strong	Likely benign
p.(Thr247Met)	c.740C>T	g.98395910C>T	TM3	0.115	Li et al., 2014	0.76±0.02	0.89±0.02	functionally normal	BS1_strong;PP2_supp;BP6_supp;BP4_supp	Likely benign	BS1_strong;PP2_supp;BP6_supp;BP4_supp;BS3_strong	Benign
p.(Gln248Arg)	c.743A>G	g.98395913A>G	TM3	no entry	Solaki et al., 2022	0.09±0.01	2.29±0.10	functionally abnormal	PM2_mod;PP2_supp	VUS	PM2_mod;PP2_supp;PS3_strong	Likely pathogenic
p.(Phe249Ser)	c.746T>C	g.98395916T>C	TM3	no entry	Nishiguchi et al., 2005	0.07±0.02	2.11±0.01	functionally abnormal	PP1_supp;PM2_mod;PP3_supp;PP2_supp	VUS	PP1_supp;PM2_mod;PP3_supp;PP2_supp;PS3_strong	Likely pathogenic
p.(Asp252Ala)	c.755A>C	g.98395925A>C	TM3	no entry	Sun et al., 2020	0.02±0.00	n.a.	functionally abnormal	PM2_mod;PP3_supp;PP2_supp	VUS	PM2_mod;PP3_supp;PP2_supp;PS3_strong	Likely pathogenic
p.(Pro258Ala)	c.772C>G	g.98395942C>G	TM3	no entry	Solaki et al., 2022	0.02±0.00	n.a.	functionally abnormal	PM2_mod;PM5_supp;PP3_supp;PP2_supp	VUS	PM2_mod;PM5_supp;PP3_supp;PP2_supp;PS3_strong	Likely pathogenic
p.(Pro258Arg)	c.773C>G	g.98395943C>G	TM3	no entry	Li et al., 2014	0.02±0.00	n.a.	functionally abnormal	PM2_mod;PP3_supp;PP2_supp	VUS	PM2_mod;PP3_supp;PP2_supp;PS3_strong	Likely pathogenic
p.(Asp260His)	c.778G>C	g.98395948G>C	TM3	0.001	Solaki et al., 2022	0.02±0.00	n.a.	functionally abnormal	PM2_mod;PM5_mod;PP3_supp;PP2_supp	Likely pathogenic	PM2_mod;PM5_mod;PP3_supp;PP2_supp;PS3_strong	Pathogenic
p.(Ala262Pro)	c.784G>C	g.98395954G>C	TM3	no entry	Zobor et al., 2017	0.03±0.01	n.a.	functionally abnormal	PP1_supp;PM2_mod;PP3_supp;PP2_supp	VUS	PP1_supp;PM2_mod;PP3_supp;PP2_supp;PS3_strong	Likely pathogenic
p.(Tyr263Asp)	c.787T>G	g.98395957T>G	TM3	no entry	Nishiguchi et al., 2005	0.02±0.00	n.a.	functionally abnormal	PM2_mod;PP5_strong;PP3_supp;PP2_supp	Likely pathogenic	PM2_mod;PP5_strong;PP3_supp;PP2_supp;PS3_strong	Pathogenic
p.(Val266Met)	c.796G>A	g.98395966G>A	TM3 - TM4	0.024	Thiadens et al., 2010	0.88±0.11	0.94±0.02	functionally normal	PM1_mod;PP2_supp;PM2_mod;BP4_supp	VUS	PM1_mod;PP2_supp;PM2_mod;BP4_supp;BS3_strong	Likely benign
p.(Pro271Ala)	c.811C>G	g.98395981C>G	TM3 - TM4	0.012	Zelinger et al., 2015	0.36±0.04	1.22±0.02	functionally abnormal	PP1_supp;PP5_supp;PM1_mod;PP2_supp;PM2_mod;PP3_supp	Likely pathogenic	PP1_supp;PP5_supp;PM1_mod;PP2_supp;PM2_mod;PP3_supp;PS3_strong	Pathogenic
p.(Pro271Ser)	c.811C>T	g.98395981C>T	TM3 - TM4	no entry	Georgiou et al., 2019	0.04±0.00	2.53±0.39	functionally abnormal	PM1_mod;PP2_supp;PM2_mod;PM5_supp;PP3_supp	Likely pathogenic	PM1_mod;PP2_supp;PM2_mod;PM5_supp;PP3_supp;PS3_strong	Pathogenic
p.(Pro271Thr)	c.811C>A	g.98395981C>A	TM3 - TM4	0.0004	Solaki et al., 2022	0.03±0.01	n.a.	functionally abnormal	PM1_mod;PP2_supp;PM2_mod;PM5_supp;PP3_supp	Likely pathogenic	PM1_mod;PP2_supp;PM2_mod;PM5_supp;PP3_supp;PS3_strong	Pathogenic
p.(Arg274Lys)	c.821G>A	g.98395991G>A	TM4	no entry	Li et al., 2014	0.03±0.01	n.a.	functionally abnormal	PM1_mod;PP2_supp;PM2_mod;PP3_supp	Likely pathogenic	PM1_mod;PP2_supp;PM2_mod;PP3_supp;PS3_strong	Pathogenic
p.(Arg274Ser)	c.822G>T	g.98395992G>T	TM4	0.003	Azam et al., 2010	0.02±0.01	n.a.	functionally abnormal	PM1_mod;PP2_supp;PM2_mod;PP3_supp;PM5_mod	Likely pathogenic	PM1_mod;PP2_supp;PM2_mod;PP3_supp;PM5_mod;PS3_strong	Pathogenic
p.(Asn276Ser)	c.827A>G	g.98395997A>G	TM4	no entry	Saqib et al., 2011	0.03±0.01	n.a.	functionally abnormal	PM1_mod;PP1_supp;PP2_supp;PM2_mod;PP3_supp	Likely pathogenic	PM1_mod;PP1_supp;PP2_supp;PM2_mod;PP3_supp;PS3_strong	Pathogenic
p.(Arg277Gly)	c.829C>G	g.98395999C>G	TM4	no entry	Koeppen et al., 2010	0.03±0.00	n.a.	functionally abnormal	PM5_mod;PM1_mod;PP2_supp;PM2_mod;PP3_supp	Likely pathogenic	PM5_mod;PM1_mod;PP2_supp;PM2_mod;PP3_supp;PS3_strong	Pathogenic
p.(Leu278Pro)	c.833T>C	g.98396003T>C	TM4	0.0004	Li et al., 2014	0.02±0.00	n.a.	functionally abnormal	PM1_mod;PP2_supp;PM2_mod;PP3_supp	Likely pathogenic	PM1_mod;PP2_supp;PM2_mod;PP3_supp;PS3_strong	Pathogenic
p.(Arg302Gly)	c.904A>G	g.98396074A>G	TM5	no entry	Zelinger et al., 2015	0.02±0.01	n.a.	functionally abnormal	PP1_supp;PM1_mod;PP2_supp;PM2_mod;PM5_supp;PP3_supp;PP5_supp	Likely pathogenic	PP1_supp;PM1_mod;PP2_supp;PM2_mod;PM5_supp;PP3_supp;PP5_supp;PS3_strong	Pathogenic
p.(Arg302Ser)	c.906G>T	g.98396076G>T	TM5	0.0004	Weisschuh et al., 2020	0.02±0.00	n.a.	functionally abnormal	PM1_mod;PP2_supp;PM2_mod;PM5_supp;PP3_supp;PP5_supp	Likely pathogenic	PM1_mod;PP2_supp;PM2_mod;PM5_supp;PP3_supp;PP5_supp;PS3_strong	Pathogenic
p.(Ile303Phe)	c.907A>T	g.98396077A>T	TM5	0.0004	ClinVar	0.03±0.00	n.a.	functionally abnormal	PM1_mod;PP2_supp;PM2_mod;PP3_supp	Likely pathogenic	PM1_mod;PP2_supp;PM2_mod;PP3_supp;PS3_strong	Pathogenic
p.(His315Gln)	c.945C>G	g.98396115C>G	TM5	no entry	Patel et al., 2019	0.11±0.02	3.85±0.05	functionally abnormal	PM1_mod;PP2_supp;PM2_mod;PP3_supp	Likely pathogenic	PM1_mod;PP2_supp;PM2_mod;PP3_supp;PS3_strong	Pathogenic
p.(Ala318Thr)	c.952G>A	g.98396122G>A	TM5	0.001	Li et al., 2017	0.02±0.01	n.a.	functionally abnormal	PP1_supp;PM1_mod;PP2_supp;PM2_mod;PP3_supp	Likely pathogenic	PP1_supp;PM1_mod;PP2_supp;PM2_mod;PP3_supp;PS3_strong	Pathogenic
p.(Phe322Ser)	c.965T>C	g.98396135T>C	TM5	no entry	Li et al., 2014	0.02±0.00	n.a.	functionally abnormal	PM1_mod;PP2_supp;PM2_mod;PP3_supp	Likely pathogenic	PM1_mod;PP2_supp;PM2_mod;PP3_supp;PS3_strong	Pathogenic
p.(Ala323Asp)	c.967G>C	g.98396137G>C	TM5	0.010	Carss et al., 2017	0.02±0.00	n.a.	functionally abnormal	PS4_mod;PP5_mod;PM1_mod;PP2_supp;PM2_mod;PM5_mod;PP3_supp	Likely pathogenic	PS4_mod;PP5_mod;PM1_mod;PP2_supp;PM2_mod;PM5_mod;PP3_supp;PS3_strong	Pathogenic
p.(Ala323Asp)	c.968C>A	g.98396138C>A	TM5	no entry	Li et al., 2015	0.13±0.03	0.35±0.02	functionally abnormal	PM1_mod;PP2_supp;PM2_mod;PM5_supp;PP3_supp	Likely pathogenic	PM1_mod;PP2_supp;PM2_mod;PM5_mod;PP3_supp;PS3_strong	Pathogenic
p.(Ile328Thr)	c.983T>C	g.98396153T>C	TM5	0.001	Solaki et al., 2022	0.06±0.01	2.53±0.17	functionally abnormal	PM1_mod;PP2_supp;PM2_mod;PP3_supp	Likely pathogenic	PM1_mod;PP2_supp;PM2_mod;PP3_supp;PS3_strong	Pathogenic
p.(Gly329Cys)	c.985G>T	g.98396155G>T	TM5 - pore helix	no entry	Genead et al., 2011	0.02±0.00	n.a.	functionally abnormal	PP1_supp;PP5_strong;PM1_mod;PP2_supp;PM2_mod;PP3_supp	Pathogenic	PP1_supp;PP5_strong;PM1_mod;PP2_supp;PM2_mod;PP3_supp;PS3_strong	Pathogenic
p.(Phe330Ser)	c.989T>C	g.98396159T>C	TM5 - pore helix	no entry	Li et al., 2014	0.02±0.00	n.a.	functionally abnormal	PM1_mod;PP2_supp;PM2_mod;PP3_supp	Likely pathogenic	PM1_mod;PP2_supp;PM2_mod;PP3_supp;PS3_strong	Pathogenic
p.(Gly331Arg)	c.991G>C	g.98396161G>C	TM5 - pore helix	no entry	Saqib et al., 2015	0.02±0.00	n.a.	functionally abnormal	PP1_supp;PM1_mod;PP2_supp;PM2_mod;PP3_supp	Likely pathogenic	PP1_supp;PM1_mod;PP2_supp;PM2_mod;PP3_supp;PS3_strong	Pathogenic
p.(Gly331Glu)	c.992G>A	g.98396162G>A	TM5 - pore helix	0.0004	Solaki et al., 2022	0.02±0.00	n.a.	functionally abnormal	PM1_mod;PP2_supp;PM2_mod;PP3_supp	Likely pathogenic	PM1_mod;PP2_supp;PM2_mod;PP3_supp;PS3_strong	Pathogenic
p.(Ser334Phe)	c.1001C>T	g.98396171C>T	TM5 - pore helix	no entry	Sundaram et al., 2014	0.03±0.00	2.59±0.17	functionally abnormal	PM1_mod;PP2_supp;PM2_mod;PP3_supp	Likely pathogenic	PM1_mod;PP2_supp;PM2_mod;PP3_supp;PS3_strong	Pathogenic
p.(Trp335Cys)	c.1005G>T	g.98396175G>T	TM5 - pore helix	no entry	LOVD/Gilissen et al., 2014	0.02±0.00	n.a.	functionally abnormal	PM2_mod;PP3_supp;PP2_supp	VUS	PM2_mod;PP3_supp;PP2_supp;PS3_strong	Likely pathogenic
p.(Val336Phe)	c.1006G>T	g.98396176G>T	TM5 - pore helix	no entry	Liang et al., 2015	0.02±0.00	n.a.	functionally abnormal	PM1_mod;PP2_supp;PM2_mod;PP3_supp	Likely pathogenic	PM1_mod;PP2_supp;PM2_mod;PP3_supp;PS3_strong	Pathogenic
p.(His345Arg)	c.1034A>G	g.98396204A>G	TM5 - pore helix	0.003	ClinVar	0.04±0.00	2.53±0.37	functionally abnormal	PM1_mod;PP2_supp;PM2_mod;PP5_supp;BP4_supp	Likely pathogenic	PM1_mod;PP2_supp;PM2_mod;PP5_supp;BP4_supp;PS3_strong	Pathogenic
p.(Arg347Cys)	c.1039C>T	g.98396209C>T	TM5 - pore helix	0.001	Sun et al., 2020	0.21±0.03	2.17±0.12	functionally abnormal	PM1_mod;PP2_supp;PM2_mod;PP3_supp	Likely pathogenic	PM1_mod;PP2_supp;PM2_mod;PP3_supp;PS3_strong	Pathogenic
p.(Arg350Gly)	c.1048A>G	g.98396218A>G	TM5 - pore helix	no entry	ClinVar	0.02±0.01	2.84±0.16	functionally abnormal	PM1_mod;PP2_supp;PM2_mod	VUS	PM1_mod;PP2_supp;PM2_mod;PS3_strong	Likely pathogenic
p.(Ile353Thr)	c.1058T>C	g.98396228T>C	Pore helix	no entry	Liang et al., 2015	0.02±0.00	1.38±0.12	functionally abnormal	PP1_supp;PM1_mod;PP2_supp;PM2_mod;PP3_supp	Likely pathogenic	PP1_supp;PM1_mod;PP2_supp;PM2_mod;PP3_supp;PS3_strong	Pathogenic
p.(Tyr354Cys)	c.1061A>G	g.98396231A>G	Pore helix	0.002	Solaki et al., 2022	0.02±0.00	3.54±0.47	functionally abnormal	PM1_mod;PP2_supp;PM2_mod;PP3_supp	Likely pathogenic	PM1_mod;PP2_supp;PM2_mod;PP3_supp;PS3_strong	Pathogenic
p.(Ser355Gly)	c.1063A>G	g.98396233A>G	Pore helix	0.001	Solaki et al., 2022	0.02±0.00	n.a.	functionally abnormal	PM1_mod;PP2_supp;PM2_mod;PP3_supp	Likely pathogenic	PM1_mod;PP2_supp;PM2_mod;PP3_supp;PS3_strong	Pathogenic
p.(Tyr357Cys)	c.1070A>G	g.98396240A>G	Pore helix	no entry	Vincent et al., 2011	0.02±0.00	n.a.	functionally abnormal	PM1_mod;PP2_supp;PM2_mod;PP3_supp	Likely pathogenic	PM1_mod;PP2_supp;PM2_mod;PP3_supp;PS3_strong	Pathogenic
p.(Ser359Phe)	c.1076C>T	g.98396246C>T	Pore helix	no entry	Solaki et al., 2022	0.02±0.00	n.a.	functionally abnormal	PM1_mod;PP2_supp;PM2_mod;PP3_supp	Likely pathogenic	PM1_mod;PP2_supp;PM2_mod;PP3_supp;PS3_strong	Pathogenic
p.(Thr362Ile)	c.1085C>T	g.98396255C>T	Pore helix	no entry	ClinVar	0.76±0.07	1.25±0.02	functionally abnormal	PM1_mod;PP2_supp;PM2_mod;PP3_supp;PP5_mod	Likely pathogenic	PM1_mod;PP2_supp;PM2_mod;PP3_supp;PP5_mod;PS3_strong	Pathogenic
p.(Glu368Gly)	c.1103A>G	pore helix -TM6	no entry	LOVD	0.73±0.09	1.43±0.10	functionally abnormal	PM1_mod;PP2_supp;PM2_mod;PP3_supp	Likely pathogenic	PM1_mod;PP2_supp;PM2_mod;PP3_supp;PS3_strong	Pathogenic
p.(Pro372Ala)	c.1114C>G	pore helix -TM6	no entry	Sharon et al., 2020	0.02±0.00	n.a.	functionally abnormal	PM1_mod;PP2_supp;PM2_mod;PM5_mod;PP3_supp;PP5_supp	Likely pathogenic	PM1_mod;PP2_supp;PM2_mod;PM5_mod;PP3_supp;PP5_supp;PS3_strong	Pathogenic
p.(Pro372Leu)	c.1115C>T	pore helix -TM6	no entry	Solaki et al., 2022	0.02±0.00	n.a.	functionally abnormal	PM1_mod;PP2_supp;PM2_mod;PM5_mod;PP3_supp	Likely pathogenic	PM1_mod;PP2_supp;PM2_mod;PM5_mod;PP3_supp;PS3_strong	Pathogenic
p.(Val373Met)	c.1117G>A	pore helix -TM6	0.004	Solaki et al., 2022	0.62±0.02	1.32±0.05	functionally abnormal	PM1_mod;PP2_supp;PM2_mod;PP3_supp	Likely pathogenic	PM1_mod;PP2_supp;PM2_mod;PP3_supp;PS3_strong	Pathogenic
p.(Asp375Gly)	c.1124A>G	g.98396294A>G	TM6	no entry	Sun et al., 2020	0.03±0.01	3.35±0.31	functionally abnormal	PM1_mod;PP2_supp;PM2_mod;PP3_supp	Likely pathogenic	PM1_mod;PP2_supp;PM2_mod;PP3_supp;PS3_strong	Pathogenic
p.(Gly388Ser)	c.1162G>A	g.98396332G>A	TM6	no entry	Brunetti-Pierri et al., 2021	0.02±0.01	n.a.	functionally abnormal	PM1_mod;PP2_supp;PM2_mod;PP3_supp	Likely pathogenic	PM1_mod;PP2_supp;PM2_mod;PP3_supp;PS3_strong	Pathogenic
p.(Gly388Asp)	c.1163G>A	g.98396333G>A	TM6	no entry	Sun et al., 2020	0.02±0.01	n.a.	functionally abnormal	PM1_mod;PP2_supp;PM2_mod;PP3_supp	Likely pathogenic	PM1_mod;PP2_supp;PM2_mod;PP3_supp;PS3_strong	Pathogenic
p.(Gly388Val)	c.1163G>T	g.98396333G>T	TM6	no entry	Sun et al., 2020	0.02±0.01	n.a.	functionally abnormal	PM1_mod;PP2_supp;PM2_mod;PP3_supp	Likely pathogenic	PM1_mod;PP2_supp;PM2_mod;PP3_supp;PS3_strong	Pathogenic
p.(Gly397Val)	c.1190G>T	g.98396360G>T	TM6	no entry	Ahuja er al., 2008	0.02±0.01	n.a.	functionally abnormal	PP1_supp;PM1_mod;PP2_supp;PM2_mod;PP3_supp	Likely pathogenic	PP1_supp;PM1_mod;PP2_supp;PM2_mod;PP3_supp;PS3_strong	Pathogenic
p.(Ser401Pro)	c.1201T>C	g.98396371T>C	TM6	0.0004	Nishiguchi et al., 2005	0.02±0.01	n.a.	functionally abnormal	PP1_supp;PM1_mod;PP2_supp;PM2_mod;PP3_supp	Likely pathogenic	PP1_supp;PM1_mod;PP2_supp;PM2_mod;PP3_supp;PS3_strong	Pathogenic
p.(Ala415Pro)	c.1243G>C	g.98396413G>C	C-linker αA'	no entry	Stone et al., 2017	0.02±0.01	n.a.	functionally abnormal	PM1_mod;PP2_supp;PM2_mod;PP3_supp	Likely pathogenic	PM1_mod;PP2_supp;PM2_mod;PP3_supp;PS3_strong	Pathogenic
p.(Asp418Glu)	c.1254T>G	g.98396424T>G	C-linker αA'	no entry	ClinVar	0.52±0.02	1.87±0.06	functionally abnormal	PM1_mod;PP2_supp;PM2_mod;PP3_supp	Likely pathogenic	PM1_mod;PP2_supp;PM2_mod;PP3_supp;PS3_strong	Pathogenic
p.(Ser419Pro)	c.1255T>C	g.98396425T>C	C-linker αA'	no entry	Weisschuh et al., 2020	0.32±0.02	0.40±0.03	functionally abnormal	PM1_mod;PP2_supp;PM2_mod;PP3_supp;PP5_supp	Likely pathogenic	PM1_mod;PP2_supp;PM2_mod;PP3_supp;PP5_supp;PS3_strong	Pathogenic
p.(Ser419Phe)	c.1256C>T	g.98396426C>T	C-linker αA'	no entry	Patel et al., 2019	0.17±0.02	1.75±0.14	functionally abnormal	PM1_mod;PP2_supp;PM2_mod;PM5_supp;PP3_supp	Likely pathogenic	PM1_mod;PP2_supp;PM2_mod;PM5_supp;PP3_supp;PS3_strong	Pathogenic
p.(Tyr423Ser)	c.1268A>C	g.98396438A>C	C-linker αA'	no entry	Solaki et al., 2022	0.03±0.01	n.a.	functionally abnormal	PM1_mod;PP2_supp;PM2_mod;PP3_supp	Likely pathogenic	PM1_mod;PP2_supp;PM2_mod;PP3_supp;PS3_strong	Pathogenic
p.(Met424Thr)	c.1271T>C	g.98396441T>C	C-linker αA'	no entry	ClinVar	0.03±0.00	n.a.	functionally abnormal	PM1_mod;PP2_supp;PM2_mod;PP3_supp;PP5_mod	Likely pathogenic	PM1_mod;PP2_supp;PM2_mod;PP3_supp;PP5_mod;PS3_strong	Pathogenic
p.(Arg427Leu)	c.1280G>T	g.98396450G>T	C-linker αA' - αB'	0.0004	ClinVar	0.15±0.05	3.59±0.44	functionally abnormal	PM1_mod;PP2_supp;PM2_mod;PM5_mod;PP3_supp;PP5_mod	Likely pathogenic	PM1_mod;PP2_supp;PM2_mod;PM5_mod;PP3_supp;PP5_mod;PS3_strong	Pathogenic
p.(Val429Ala)	c.1286T>C	g.98396456T>C	C-linker αA' - αB'	no entry	Georgiou et al., 2019	0.03±0.01	n.a.	functionally abnormal	PM1_mod;PP2_supp;PM2_mod;PP3_supp;PP5_supp	Likely pathogenic	PM1_mod;PP2_supp;PM2_mod;PP3_supp;PP5_supp;PS3_strong	Pathogenic
p.(Asp432Tyr)	c.1294G>T	g.98396464G>T	C-linker αB'	no entry	Sun et al., 2020	0.02±0.00	n.a.	functionally abnormal	PM1_mod;PP2_supp;PM2_mod;PP3_supp	Likely pathogenic	PM1_mod;PP2_supp;PM2_mod;PP3_supp;PS3_strong	Pathogenic
p.(Arg436Gln)	c.1307G>A	g.98396477G>A	C-linker αB'	0.005	Li et al., 2014	0.76±0.13	0.96±0.04	functionally normal	PM1_mod;PP2_supp;PM2_mod;PM5_mod;PP3_supp;BP2_supp	Likely pathogenic	PM1_mod;PP2_supp;PM2_mod;PM5_mod;PP3_supp;BP2_supp;BS3_strong	VUS ŷ

p.(Trp440Ser)	c.1319G>C	g.98396489G>C	C-linker αB'	0.0007	Georgiou et al., 2019	0.03±0.01	1.38±0.12	functionally abnormal	PM1_mod;PP2_supp;PM2_mod;PP3_supp	Likely pathogenic	PM1_mod;PP2_supp;PM2_mod;PP3_supp;PS3_strong	Pathogenic
p.(Lys448Arg)	c.1343A>G	g.98396513A>G	C-linker αB' - αC'	0.019	Solaki et al., 2022	0.93±0.11	1.15±0.03	functionally abnormal	PM1_mod;PP2_supp;PM2_mod	VUS	PM1_mod;PP2_supp;PM2_mod;PS3_strong	Likely pathogenic
p.(Leu464Arg)	c.1391T>G	g.98396561T>G	C-linker αD'	no entry	Greenberg et al., 2014	0.02±0.01	n.a.	functionally abnormal	PP1_supp;PM1_mod;PP2_supp;PM2_mod;PP3_supp	Likely pathogenic	PP1_supp;PM1_mod;PP2_supp;PM2_mod;PP3_supp;PS3_strong	Pathogenic
p.(Asn471Ser)¥	c.1412A>G	g.98396582A>G	C-linker αD'	0.001	Wissinger et al., 2001	0.72±0.01	0.69±0.05	functionally abnormal	PM1_mod;PP2_supp;PM2_mod	VUS	PM1_mod;PP2_supp;PM2_mod;PS3_strong	Likely pathogenic
p.(Lys479Val)	c.1435_1436delinsGT	g.98396605_98396606delinsGT	C-linker αE'	no entry	Sun et al., 2020	0.02±0.01	n.a.	functionally abnormal	PM1_mod;PP2_supp;PM2_mod	VUS	PM1_mod;PP2_supp;PM2_mod;PS3_strong	Likely pathogenic
p.(Cys486Tyr)	c.1457G>A	g.98396627G>A	C-linker αF' - CNBD αA	no entry	Abouelhoda et al., 2016	0.02±0.01	n.a.	functionally abnormal	PM1_mod;PP2_supp;PM2_mod;PP3_supp;PP5_supp	Likely pathogenic	PM1_mod;PP2_supp;PM2_mod;PP3_supp;PP5_supp;PS3_strong	Pathogenic
p.(Gly489Val)	c.1466G>T	g.98396636G>T	CNBD αA	no entry	Solaki et al., 2022	0.01±0.00	n.a.	functionally abnormal	PM1_mod;PP2_supp;PM2_mod;PP3_supp	Likely pathogenic	PM1_mod;PP2_supp;PM2_mod;PP3_supp;PS3_strong	Pathogenic
p.(Pro505Ala)	c.1513C>G	g.98396683C>G	CNBD β1 - β2	no entry	Huang et al., 2016	0.01±0.00	n.a.	functionally abnormal	PM1_mod;PP2_supp;PM2_mod;PP3_supp	Likely pathogenic	PM1_mod;PP2_supp;PM2_mod;PP3_supp;PS3_strong	Pathogenic
p.(Asp507Gly)	c.1520A>G	g.98396690A>G	CNBD β1 - β2	0.002	LOVD	0.01±0.00	n.a.	functionally abnormal	PM1_mod;PP2_supp;PM2_mod;PP3_supp	Likely pathogenic	PM1_mod;PP2_supp;PM2_mod;PP3_supp;PS3_strong	Pathogenic
p.(Lys512Met)	c.1535A>T	g.98396705A>T	CNBD β2 - β3	no entry	Carrigan et al., 2016	0.16±0.02	2.88±0.25	functionally abnormal	PM1_mod;PP2_supp;PM2_mod;PP3_supp	Likely pathogenic	PM1_mod;PP2_supp;PM2_mod;PP3_supp;PS3_strong	Pathogenic
p.(Gly513Arg)	c.1537G>A	g.98396707G>A	CNBD β2 - β3	0.0004	Solaki et al., 2022	0.02±0.00	n.a.	functionally abnormal	PM1_mod;PP2_supp;PM2_mod;PM5_supp;PP3_supp	Likely pathogenic	PM1_mod;PP2_supp;PM2_mod;PM5_supp;PP3_supp;PS3_strong	Pathogenic
p.(Asp514Asn)	c.1540G>A	g.98396710G>A	CNBD β2 - β3	no entry	Arshad et al., 2019	0.11±0.03	0.96±0.10	functionally abnormal	PP1_supp;PM1_mod;PP2_supp;PM2_mod;PP3_supp	Likely pathogenic	PP1_supp;PM1_mod;PP2_supp;PM2_mod;PP3_supp;PS3_strong	Pathogenic
p.(Asp514Val)	c.1541A>T	g.98396711A>T	CNBD β2 - β3	0.0004	Genead et al., 2011	0.03±0.01	n.a.	functionally abnormal	PM1_mod;PP2_supp;PM2_mod;PP3_supp	Likely pathogenic	PM1_mod;PP2_supp;PM2_mod;PP3_supp;PS3_strong	Pathogenic
p.(Met519Thr)	c.1556T>C	g.98396726T>C	CNBD β3	no entry	Huang et al., 2016	0.03±0.01	n.a.	functionally abnormal	PM1_mod;PP2_supp;PM2_mod;PP3_supp	Likely pathogenic	PM1_mod;PP2_supp;PM2_mod;PP3_supp;PS3_strong	Pathogenic
p.(Met519Ile)	c.1557G>A	g.98396727G>A	CNBD β3	0.006	Ellingford et al., 2016	0.03±0.01	n.a.	functionally abnormal	PM1_mod;PP2_supp;PM2_mod;PP3_supp	Likely pathogenic	PM1_mod;PP2_supp;PM2_mod;PP3_supp;PS3_strong	Pathogenic
p.(Gly525Ser)	c.1573G>A	g.98396743G>A	CNBD β3 - β4	no entry	Patel et al., 2016	0.03±0.01	n.a.	functionally abnormal	PM1_mod;PP2_supp;PM2_mod;PP3_supp;PP5_supp	Likely pathogenic	PM1_mod;PP2_supp;PM2_mod;PP3_supp;PP5_supp;PS3_strong	Pathogenic
p.(Leu527Met)	c.1579C>A	g.98396749C>A	CNBD β4	no entry	Wang et al., 2011	0.04±0.01	1.31±0.08	functionally abnormal	PM1_mod;PP2_supp;PM2_mod;PM5_mod;PP3_supp;PP5_supp	Likely pathogenic	PM1_mod;PP2_supp;PM2_mod;PM5_mod;PP3_supp;PP5_supp;PS3_strong	Pathogenic
p.(Leu527Arg)	c.1580T>G	g.98396750T>G	CNBD β4	0.0008	Lam et al., 2011	0.02±0.01	n.a.	functionally abnormal	PP1_supp;PM1_mod;PP2_supp;PM2_mod;PM5_mod;PP3_supp	Likely pathogenic	PP1_supp;PM1_mod;PP2_supp;PM2_mod;PM5_mod;PP3_supp;PS3_strong	Pathogenic
p.(Asp533His)	c.1597G>C	g.98396767G>C	CNBD β4 - β5	0.0008	Li et al., 2014	0.03±0.01	n.a.	functionally abnormal	PP5_strong;PM1_mod;PP2_supp;PM2_mod;PP3_supp	Pathogenic	PP5_strong;PM1_mod;PP2_supp;PM2_mod;PP3_supp;PS3_strong	Pathogenic
p.(Val539Met)	c.1615G>A	g.98396785G>A	CNBD β5	0.002	Solaki et al., 2022	0.81±0.03	1.08±0.02	functionally normal	PM2_mod;PM1_supp;PP2_supp;PP3_supp;BP5_supp	VUS	PM2_mod;PM1_supp;PP2_supp;PP3_supp;BP5_supp;BS3_strong	Likely benign
p.(Val540Ile)	c.1618G>A	g.98396788G>A	CNBD β5	0.133	Thiadens et al., 2010	0.74±0.05	0.96±0.03	functionally normal	BS1_strong;PM1_supp;PP2_supp;PP3_supp	VUS	BS1_strong;PM1_supp;PP2_supp;PP3_supp;BS3_strong	Benign
p.(Leu541Phe)	c.1621C>T	g.98396791C>T	CNBD β5	no entry	Greenberg et al., 2014	0.02±0.01	n.a.	functionally abnormal	PP1_supp;PM2_mod;PM1_mod;PP2_supp;PP3_supp	Likely pathogenic	PP1_supp;PM2_mod;PM1_mod;PP2_supp;PP3_supp;PS3_strong	Pathogenic
p.(Phe547Cys)	c.1640T>G	g.98396810T>G	CNBD β6	no entry	Zelinger et al., 2015	0.02±0.01	n.a.	functionally abnormal	PP1_supp;PM5_mod;PM1_mod;PP2_supp;PM2_mod;PP3_supp;PP5_supp	Likely pathogenic	PP1_supp;PM5_mod;PM1_mod;PP2_supp;PM2_mod;PP3_supp;PP5_supp;PS2_strong	Pathogenic
p.(Gly548Arg)	c.1642G>A	g.98396812G>A	CNBD β6	0.002	Johnson et al., 2004	0.02±0.01	n.a.	functionally abnormal	PP1_supp;PP5_strong;PM1_mod;PP2_supp;PM2_mod;PP3_supp	Pathogenic	PP1_supp;PP5_strong;PM1_mod;PP2_supp;PM2_mod;PP3_supp;PS3_strong	Pathogenic
p.(Leu553Gln)	c.1658T>A	g.98396828T>A	CNBD β6 - β7	0.0004	Solaki et al., 2022	0.02±0.01	n.a.	functionally abnormal	PM1_mod;PP2_supp;PM2_mod;PP3_supp	Likely pathogenic	PM1_mod;PP2_supp;PM2_mod;PP3_supp;PS3_strong	Pathogenic
p.(Ser560Leu)	c.1679C>T	g.98396849C>T	CNBD β6 - β7	0.003	ClinVar	0.71±0.09	2.01±0.11	functionally abnormal	PM1_mod;PP2_supp;PM2_mod;PP3_supp	Likely pathogenic	PM1_mod;PP2_supp;PM2_mod;PP3_supp;PS3_strong	Pathogenic
p.(Gly561Glu)	c.1682G>A	g.98396852G>A	CNBD β6 - β7	no entry	Zobor et al., 2017	0.04±0.01	3.89±0.16	functionally abnormal	PM1_mod;PP2_supp;PM2_mod;PP3_supp	Likely pathogenic	PM1_mod;PP2_supp;PM2_mod;PP3_supp;PS3_strong	Pathogenic
p.(Asn562Lys)	c.1686C>A	g.98396856C>A	CNBD β6 - β7	no entry	ClinVar	0.14±0.02	1.03±0.06	functionally abnormal	PM1_mod;PP2_supp;PM2_mod;PP3_supp;PP5_mod	Likely pathogenic	PM1_mod;PP2_supp;PM2_mod;PP3_supp;PP5_mod;PS3_strong	Pathogenic
p.(Arg569Cys)	c.1705C>T	g.98396875C>T	CNBD β7	0.0007	Solaki et al., 2022	0.29±0.05	1.85±0.04	functionally abnormal	PM1_mod;PP2_supp;PM2_mod;PM5_mod;PP3_supp	Likely pathogenic	PM1_mod;PP2_supp;PM2_mod;PM5_mod;PP3_supp;PS3_strong	Pathogenic
p.(Ser570Gly)	c.1708A>G	g.98396878A>G	CNBD β7	no entry	Solaki et al., 2022	0.02±0.01	n.a.	functionally abnormal	PP1_supp;PM1_mod;PP2_supp;PM2_mod;PP3_supp	Likely pathogenic	PP1_supp;PM1_mod;PP2_supp;PM2_mod;PP3_supp;PS3_strong	Pathogenic
p.(Ser570Asn)	c.1709G>A	g.98396879G>A	CNBD β7	no entry	Li et al., 2014	0.02±0.01	n.a.	functionally abnormal	PM1_mod;PP2_supp;PM2_mod;PP3_supp	Likely pathogenic	PM1_mod;PP2_supp;PM2_mod;PP3_supp;PS3_strong	Pathogenic
p.(Ser570Ile)	c.1709G>T	g.98396879G>T	CNBD β7	no entry	Thiadens et al., 2010	0.02±0.01	n.a.	functionally abnormal	PM1_mod;PP2_supp;PM2_mod;PP3_supp	Likely pathogenic	PM1_mod;PP2_supp;PM2_mod;PP3_supp;PS3_strong	Pathogenic
p.(Ile571Thr)	c.1712T>C	g.98396882T>C	CNBD β7 - β8	0.0008	Jinda et al., 2021	0.03±0.00	n.a.	functionally abnormal	PP1_supp;PM1_mod;PP2_supp;PM2_mod;PP3_supp	Likely pathogenic	PP1_supp;PM1_mod;PP2_supp;PM2_mod;PP3_supp;PS3_strong	Pathogenic
p.(Tyr573His)	c.1717T>C	g.98396887T>C	CNBD β7 - β8	0.003	Solaki et al., 2022	0.03±0.00	n.a.	functionally abnormal	PM1_mod;PP1_supp;PP2_supp;PM2_mod;PM5_supp;PP3_supp	Likely pathogenic	PM1_mod;PP1_supp;PP2_supp;PM2_mod;PM5_supp;PP3_supp;PS3_strong	Pathogenic
p.(Leu579Arg)	c.1736T>G	g.98396906T>G	CNBD β8	no entry	Solaki et al., 2022	0.03±0.00	n.a.	functionally abnormal	PM1_mod;PP2_supp;PM2_mod;PP3_supp	Likely pathogenic	PM1_mod;PP2_supp;PM2_mod;PP3_supp;PS3_strong	Pathogenic
p.(Tyr591His)	c.1771T>C	g.98396941T>C	CNBD αB - αC	no entry	Solaki et al., 2022	0.21±0.03	0.94±0.06	functionally abnormal	PM1_mod;PP2_supp;PM2_mod;PP3_supp	Likely pathogenic	PM1_mod;PP2_supp;PM2_mod;PP3_supp;PS3_strong	Pathogenic
p.(Pro592Leu)	c.1775C>T	g.98396945C>T	CNBD αB - αC	0.0004	Solaki et al., 2022	0.02±0.00	n.a.	functionally abnormal	PM1_mod;PP2_supp;PM2_mod;PP3_supp	Likely pathogenic	PM1_mod;PP2_supp;PM2_mod;PP3_supp;PS3_strong	Pathogenic
p.(Lys595Arg)	c.1784A>G	g.98396954A>G	CNBD αC	0.003	ClinVar	0.90±0.07	0.75±0.02	functionally normal	PM2_mod;PM1_supp;PP2_supp;PP3_supp	VUS	PM2_mod;PM1_supp;PP2_supp;PP3_supp;BS3_strong	VUS $
p.(Leu598Arg)	c.1793T>G	g.98396963T>G	CNBD αC	no entry	Sun et al., 2020	0.03±0.00	n.a.	functionally abnormal	PM2_mod;PM1_supp;PP2_supp;PP3_supp	VUS	PM2_mod;PM1_supp;PP2_supp;PP3_supp;PS3_strong	Likely pathogenic
p.(Gly602Glu)	c.1805G>A	g.98396975G>A	CNBD αC	no entry	Georgiou et al., 2019	0.03±0.00	n.a.	functionally abnormal	PP1_supp;PM2_mod;PM1_supp;PP2_supp;PP3_supp	Likely pathogenic	PP1_supp;PM2_mod;PM1_supp;PP2_supp;PP3_supp;PS3_strong	Pathogenic
p.(Glu615Asp)	c.1845G>T	g.98397015G>T	CNBD αC - CLZ	no entry	ClinVar	0.78±0.03	1.01±0.05	functionally normal	PM2_mod;PP2_supp;BP4_supp	VUS	PM2_mod; PP2_supp; BP4_supp;BS3_strong	Likely benign
p.(Ala619Val)	c.1856C>T	g.98397026C>T	CNBD αC - CLZ	0.002	Thiadens et al., 2010	0.77±0.04	0.96±0.01	functionally normal	PM2_mod;PP2_supp;BP4_supp	VUS	PM2_mod;PP2_supp;BP4_supp;BS3_strong	Likely benign
p.(Ala621Glu)	c.1862C>A	g.98397032C>A	CNBD αC - CLZ	0.001	Wszniewski et al. 2007	0.78±0.03	0.74±0.01	functionally abnormal	PM2_mod;PP2_supp;BP4_supp	VUS	PM2_mod;PP2_supp;BP4_supp;PS3_strong	Likely pathogenic
p.(Leu626Arg)	c.1877T>G	g.98397047T>G	CLZ	no entry	Huang et al., 2016	0.83±0.10	0.55±0.03	functionally abnormal	PP1_supp;PM2_mod;PP2_supp	VUS	PP1_supp;PM2_mod;PP2_supp;PS3_strong	Likely pathogenic
p.(Val630Ala)	c.1889T>C	g.98397059T>C	CLZ	no entry	Solaki et al., 2022	0.84±0.09	0.56±0.02	functionally abnormal	PM2_mod;PP2_supp;PP3_supp	VUS	PM2_mod;PP2_supp;PP3_supp;PS3_strong	Likely pathogenic
p.(Phe644Ser)	c.1931T>C	g.98397101T>C	CLZ	no entry	Ellingford et al., 2016	0.65±0.12	0.64±0.02	functionally abnormal	PM2_mod;PP3_supp;PP2_supp	VUS	PM2_mod;PP3_supp;PP2_supp;PS3_strong	Likely pathogenic
p.(Arg646His)	c.1937G>A	g.98397107G>A	CLZ	0.002	Li et al., 2014	0.80±0.18	0.77±0.03	functionally normal	PM2_mod;PP3_supp;PP2_supp	VUS	PM2_mod;PP3_supp;PP2_supp;BS3_strong	VUS $
p.(Glu650Ala)	c.1949A>C	g.98397119A>C	CLZ	0.021	LOVD	0.58±0.04	1.04±0.02	functionally abnormal	PM2_mod;PP3_supp;PP2_supp	VUS	PM2_mod;PP3_supp;PP2_supp;PS3_strong	Likely pathogenic
p.(Met656Ile)	c.1968G>A	g.98397138G>A	CLZ	0.038	ClinVar	0.76±0.02	1.02±0.01	functionally normal	PP2_supp;PM2_mod;BP4_supp	VUS	PP2_supp;PM2_mod;BP4_supp;BS3_strong	Likely benign
p.(Arg661Ser)	c.1981C>A	g.98397151C>A	CLZ	0.031	Yang et al., 2014	0.79±0.08	0.53±0.03	functionally abnormal	PP1_supp;PP5_strong;PM2_mod;PP3_supp;PP2_supp	Likely pathogenic	PP1_supp;PP5_strong;PM2_mod;PP3_supp;PP2_supp;PS3_strong	Pathogenic
p.(Arg661His)	c.1982G>A	g.98397152G>A	CLZ	0.004	Sun et al., 2020	0.69±0.11	0.54±0.02	functionally abnormal	PM2_mod;PM5_mod;PP3_supp;PP2_supp	Likely pathogenic	PM2_mod;PM5_mod;PP3_supp;PP2_supp;PS3_strong	Pathogenic
p.(Val669Leu)	c.2005G>C	g.98397175G>C	CLZ	0.007	ClinVar	0.92±0.08	0.93±0.02	functionally normal	PM2_mod;PP2_supp	VUS	PM2_mod;PP2_supp;BS3_strong	VUS $
p.(Gly684Arg)	c.2050G>A	g.98397220G>A	C-Term.	0.0008	Patel et al., 2016	0.73±0.03	1.00±0.03	functionally normal	PM2_mod;PP2_supp;BP4_supp	VUS	PM2_mod;PP2_supp;BP4_supp;BS3_strong	Likely benign

† Variant designation is based on NM_001298.3 (GRCh38/hg38) and NC_000002.12 (GRCh38/hg38) .

‡ Functional domains of CNGA3 according to Gofman et al., 2014 and Shuart et al., 2011: N-Term., N-terminus; TM1 to TM6, transmembrane domains; C-linker having six alpha helices (αA' to αF'); CNBD, cyclic-nucleotide binding domain having three alpha helices (αA to αC) and eight beta-sheets (β1 to β8); CLZ, C-terminal leucin zipper; C-Term., C-terminus; -, intermediate amino acid residue between two domains.

All data are represented as mean ± standard deviation (SD); n=3-5 independent transfections/measurements; n.a., not analysed (peak latency was only determined for mutant channels showing increased luminescence signal upon ligand application in the bioassay).

§ Thresholds for assay classification; functionally normal: normalized AUC >0.65 and normalized latency 0.74<x<1.10; all variants not meeting the mentioned criteria are classified as functionally abnormal.

¶ ACMG/AMP criteria and their corresponding evidence strength: supp, supporting; mod, moderate; strong.

¥ The c.1412A>G/p.(Asn471Ser) variant was previously functionally analysed thereby displaying contradictory results (Liu and Varnum, 2005; Muraki-Oda et al., 2007)

$ Due to the provided functional evidence using our aequorin-based bioassay and the available genotype data, we suggest these variants to not have a deleterious effect on CNGA3 protein function even if they are still deemed to be of uncertain significance in the ACMG/AMP classification system.

Publication III

Paternal uniparental isodisomy of chromosome 2 in a patient with *CNGA3*-associated autosomal recessive achromatopsia.

Kohl, S., Baumann, B., Dassie, F., Mayer, A.K., **Solaki, M.**, Reuter, P., Kühlewein, L., Wissinger, B., and Maffei, P.

International Journal of Molecular Sciences.

2021 Jul 22;22(15):7842.

doi: 10.3390/ijms22157842.

This article is distributed under the terms and conditions of the Creative Commons Attribution License (CC BY 4.0) (https://creativecommons.org/licenses/by/4.0/).

International Journal of
Molecular Sciences

MDPI

Article

Paternal Uniparental Isodisomy of Chromosome 2 in a Patient with *CNGA3*-Associated Autosomal Recessive Achromatopsia

Susanne Kohl [1,*], Britta Baumann [1], Francesca Dassie [2], Anja K. Mayer [1], Maria Solaki [1], Peggy Reuter [1], Laura Kühlewein [1,3], Bernd Wissinger [1] and Pietro Maffei [2]

1 Centre for Ophthalmology, Institute for Ophthalmic Research, University Tübingen, 72076 Tübingen, Germany; britta.baumann@med.uni-tuebingen.de (B.B.); anja.ka.mayer@gmail.com (A.K.M.); maria.solaki@med.uni-tuebingen.de (M.S.); peggy.reuter@med.uni-tuebingen.de (P.R.); laura.kuehlewein@med.uni-tuebingen.de (L.K.); bernd.wissinger@med.uni-tuebingen.de (B.W.)
2 Department of Medicine (DIMED), University of Padua, 35121 Padua, Italy; francesca.dassie@unipd.it (F.D.); pietro.maffei@unipd.it (P.M.)
3 Centre for Ophthalmology, University Eye Hospital, University Tübingen, 72076 Tübingen, Germany
* Correspondence: susanne.kohl@med.uni-tuebingen.de

Abstract: Achromatopsia (ACHM) is a rare autosomal recessively inherited retinal disease characterized by congenital photophobia, nystagmus, low visual acuity, and absence of color vision. ACHM is genetically heterogeneous and can be caused by biallelic mutations in the genes *CNGA3*, *CNGB3*, *GNAT2*, *PDE6C*, *PDE6H*, or *ATF6*. We undertook molecular genetic analysis in a single female patient with a clinical diagnosis of ACHM and identified the homozygous variant c.778G>C;p.(D260H) in the *CNGA3* gene. While segregation analysis in the father, as expected, identified the *CNGA3* variant in a heterozygous state, it could not be displayed in the mother. Microsatellite marker analysis provided evidence that the homozygosity of the *CNGA3* variant is due to partial or complete paternal uniparental isodisomy (UPD) of chromosome 2 in the patient. Apart from the ACHM phenotype, the patient was clinically unsuspicious and healthy. This is one of few examples proving UPD as the underlying mechanism for the clinical manifestation of a recessive mutation in a patient with inherited retinal disease. It also highlights the importance of segregation analysis in both parents of a given patient or especially in cases of homozygous recessive mutations, as UPD has significant implications for genetic counseling with a very low recurrence risk assessment in such families.

Keywords: achromatopsia; ACHM; uniparental isodisomy; chromosome 2; *CNGA3*

check for updates

Citation: Kohl, S.; Baumann, B.; Dassie, F.; Mayer, A.K.; Solaki, M.; Reuter, P.; Kühlewein, L.; Wissinger, B.; Maffei, P. Paternal Uniparental Isodisomy of Chromosome 2 in a Patient with *CNGA3*-Associated Autosomal Recessive Achromatopsia. *Int. J. Mol. Sci.* **2021**, *22*, 7842. https://doi.org/10.3390/ijms22157842

Academic Editors: Francesca Simonelli, Fracesco Testa and Marianthi Karali

Received: 16 June 2021
Accepted: 21 July 2021
Published: 22 July 2021

Publisher's Note: MDPI stays neutral with regard to jurisdictional claims in published maps and institutional affiliations.

Copyright: © 2021 by the authors. Licensee MDPI, Basel, Switzerland. This article is an open access article distributed under the terms and conditions of the Creative Commons Attribution (CC BY) license (https://creativecommons.org/licenses/by/4.0/).

1. Introduction

Achromatopsia (ACHM; synonymous with rod monochromatism; ACHM2, MIM 216900; ACHM3, MIM 262300; ACHM4, MIM 613856; ACHM5/COD4, MIM 613093; ACHM6/RCD3A, MIM 610024; and ACHM7, IM616517) is a rare, autosomal recessive disorder with an estimated prevalence of 1 in 30,000 to 1:50,000. It is a congenital retinal disease affecting only the cone photoreceptor, and photophobia and nystagmus are the first symptoms manifesting within the first weeks or months of life. Due to lack of cone photoreceptor function, ACHM is characterized by color blindness and low visual acuity (20/400–20/200 Snellen equivalent). ACHM was believed to be a stationary disease, but recent studies by optical coherence tomography have shown that there is progressive degeneration of the central retina and cone photoreceptors [1–5].

ACHM is genetically heterogeneous and known to be caused by mutations in six genes: *CNGA3*, *CNGB3*, *GNAT2*, *PDE6C*, *PDE6H*, and *ATF6* [6–13]. The first five genes encode important functional components of the cone phototransduction cascade (G-protein transducin GNAT2 (guanine nucleotide-binding protein G(t) subunit alpha 2; MIM 139340); cone-photoreceptor phosphodiesterase catalytic subunit PDE6C (cone cyclic GMP-specific

3′,5′ cyclic phosphodiesterase alpha-prime; MIM 600827) and inhibitory subunit PDE6H (cone cyclic GMP-specific phosphodiesterase gamma; MIM 601190); cone photoreceptor cyclic nucleotide gated cation (CNG) channel CNGA3 (cyclic nucleotide-gated cation channel alpha 3; MIM 600053) and CNGB3 (cyclic nucleotide-gated cation channel beta 3; MIM 605080)), while the ubiquitously expressed transcription factor ATF6 (activating transcription factor 6; MIM 605537) is known for its function in the unfolded protein response and endoplasmic reticulum stress response [14,15].

In Europe and the United States, biallelic mutations in *CNGB3* are the major cause of ACHM, accounting for 50–60% of cases, especially due to a common founder mutation c.1148delC, followed by biallelic mutations in *CNGA3*, which are found in 30% of ACHM patients in these populations [16,17]. In contrast, biallelic mutations in *CNGA3* account for the majority of ACHM patients of Chinese (80%) and Israeli/Palestinian (84%) origin [18,19]. The other ACHM-associated genes play a minor role, being responsible for only 0.5–3% of cases [16].

CNGA3- and *CNGB3*-associated ACHM are in the focus, as several AAV-based gene supplementation therapy trials are ongoing (NCT02610582, NCT03758404, NCT02935517, NCT02599922), and one trial has already been successfully finished and published [20].

2. Results

An Italian female patient with a clinical diagnosis of ACHM without family history of this condition was referred to the Centre for Ophthalmology Tübingen for genetic testing in a research setting. The patient suffered from photophobia since birth and was diagnosed to have ACHM at the age of 10 years. Her visual acuity at the age of 18 was 20/200 Snellen equivalent with a correction of +3.00 diopters in both eyes. The patient exhibited a fine pendular nystagmus that was more pronounced when looking at distant targets. Intraocular pressure was within normal limits in both eyes (14 mmHg). Anterior and posterior segment examination was unremarkable except for the margins of the optic discs that were not absolutely sharp. Full-field electroretinogram showed symmetrical severely reduced cone responses and abnormalities in the rod responses. Dark adaptation curves were typical for ACHM. Color vision testing using a Panel D-15 test and a Nagel anomaloscope exhibited findings typical for ACHM. Kinetic visual field testing showed normal outer visual field boundaries.

Genetic research testing revealed an apparent homozygous missense variant c.778G>C; p.(D260H) in exon 7 of *CNGA3*. The variant has not been reported in the literature, various mutation databases (i.e., HGMD®—Human Gene Mutation Database, ClinVar https://www.ncbi.nlm.nih.gov/clinvar (accessed on 16 June 2021), LOVD^3—Leiden Open Variation Database https://www.LOVD.nl/CNGA3 (accessed on 16 June 2021)), nor has it been observed in population databases (i.e., gnomAD browser; https://gnomad.broadinstitute.org/gene/ENSG00000144191 (accessed on 16 June 2021)). The variant affects an amino acid residue in transmembrane domain S3 of the CNGA3 polypeptide. This amino acid residue is conserved not only in all CNGA3 orthologs but also in rod-photoreceptor-specific CNGA1 paralogs (Figure 1C).

Segregation analysis by PCR and Sanger sequencing proved the father to be a heterozygous carrier, while the variant could not be detected in the mother (Figure 1A). A heterozygous deletion in the mother explaining the apparent homozygosity of the mutation in the patient was ruled out by long-distance PCR and a SYBR Green-based quantitative real-time PCR copy number assay. Segregation analysis and haplotype reconstruction for ten microsatellite markers covering the entire chromosome 2 in the patient and both parents revealed homozygosity in the patient for all tested markers for the paternal allele, providing evidence for complete (or partial) paternal uniparental isodisomy (UPD) of chromosome 2 in the patient (Figure 1B).

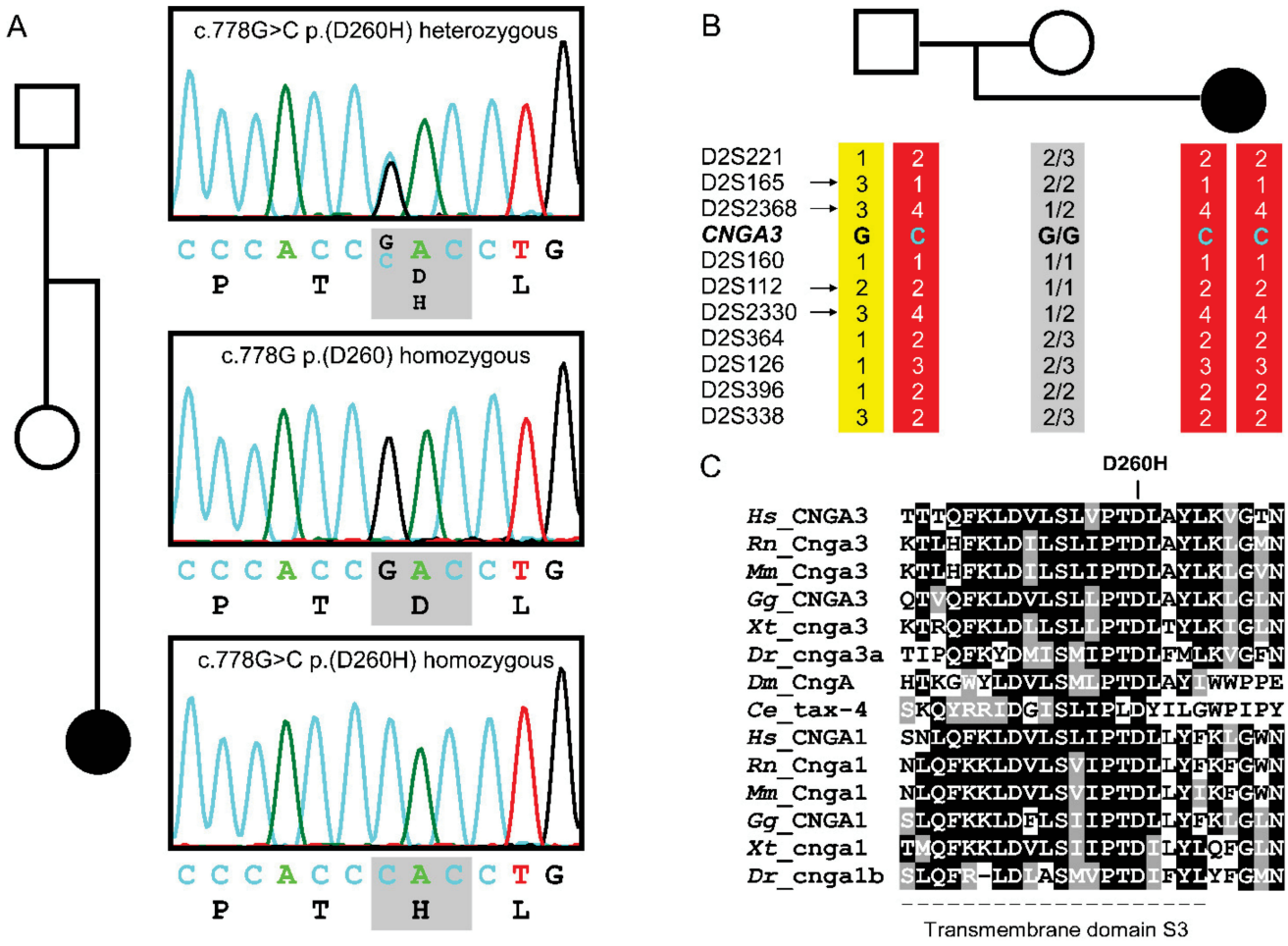


Figure 1. Segregation analysis, haplotype reconstruction, and conservation of *CNGA3* c.778G>C;p.(D260H). (**A**) Segregation analysis via Sanger sequencing for *CNGA3* exon 7 in family CHRO978, as shown by the electropherograms obtained from both parents and the index patient. The father is heterozygous for the variant c.778G>C (top), while the mother does not carry this variant (middle). The affected daughter is homozygous for this variant in *CNGA3* (bottom). (**B**) Haplotype reconstruction of chromosome 2. Microsatellite marker analysis in the patient and both parents demonstrated paternal uniparental isodisomy of chromosome 2, either fully or partially. The patient inherited two copies (or partial chromosomal segments) of the paternal chromosome (red haplotype) carrying and flanking the *CNGA3* variant c.778G>G;p.(D260H), while the maternal chromosome was not or only partially transmitted. Informative markers are marked by an arrow. Of note, the two haplotypes of the mother could not be reconstructed. (**C**) Conservation of the mutated amino acid residue *CNGA3* p.D260H among CNGA3 and CNGA1 polypeptides across various species. Protein sequence alignment was performed using Clustal Omega (https://www.ebi.ac.uk/Tools/msa/clustalo/ (accessed on 16 June 2021)) and BoxShade (https://embnet.vital-it.ch/software/BOX_form.html (accessed on 16 June 2021)). Reference sequences from NCBI (https://www.ncbi.nlm.nih.gov/ (accessed on 16 June 2021)): CNGA3: *H. sapiens* NP_001289.1, *R. norvegicus* NP_445947.1, *M. musculus* NP_001268939.1, *G. gallus* NP_990552.1, *X. tropicalis* XP_031752880.1, *D. rerio* XP_005166141.1, *D. melanogaster* NP_477116.1, *C. elegans* NP_499033.1, CNGA1: *H. sapiens* NP_001366199.1, *R. norvegicus* NP_445949.2, *M. musculus* NP_031749.2, *G. gallus* NP_990551.1, *X. tropicalis* XP_017950934.1, *D. rerio* XP_701036.4.

The variant is predicted to be disease-causing by various tools (i.e., SIFT, PolyPhen, Provean) and classified as likely pathogenic according to the ACMG (American College of Medical Genetics) guidelines. In vitro heterologous expression and analysis via a bioluminescent calcium reporter assay of the $CNGA3_{D260H}$ mutant versus wild-type CNGA3 in HEK293 (human embryonic kidney) cells provided evidence that this variant results in complete loss of channel function (Figure 2A). Similarly, another amino acid substitution at the very same amino acid residue—c.778G>A;p.(D260N)—had previously been shown to result in complete channel function loss in in vitro studies [21,22]. Loss of CNGA3 or

CNGA3 function cannot be compensated, as *CNGA3* encodes for the channel forming A subunit of the cone photoreceptor CNG channel. Using immunocytochemistry, we were able to confirm the expression of the channel mutant $CNGA3_{D260H}$ in transfected HEK293 cells despite the fact that a calcium influx was not detectable in the aequorin-based bioassay (Figure 2B).

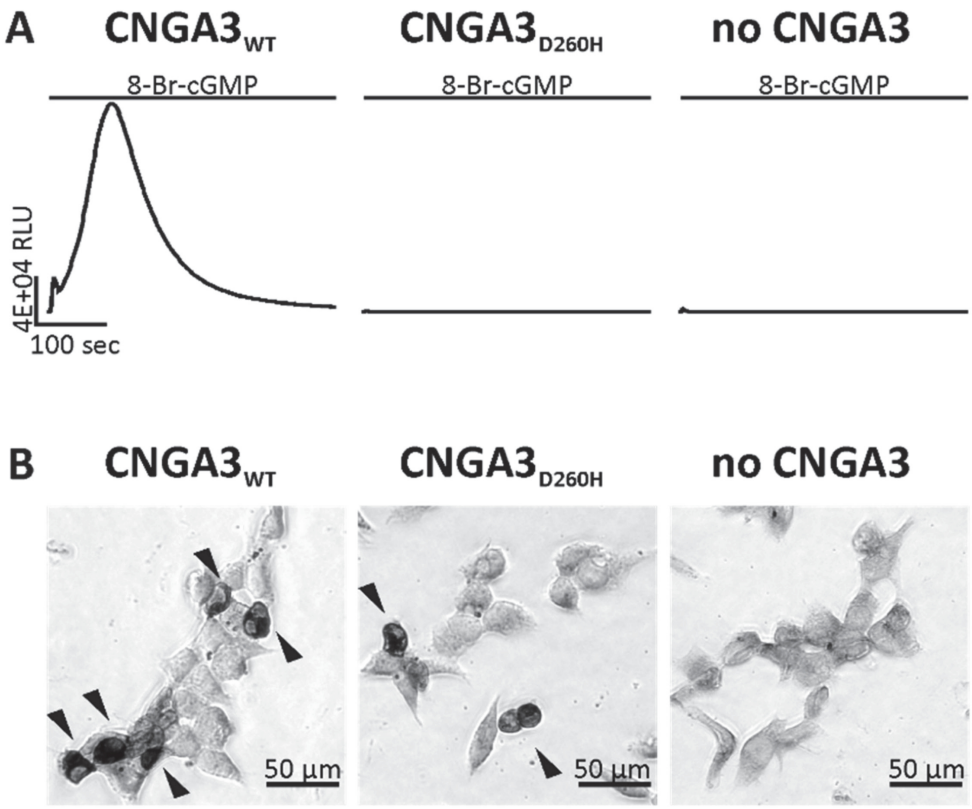


Figure 2. Aequorin-mediated luminescence signals and immunocytochemical staining of wild-type (WT) and mutant (D260H) CNGA3 channels. (**A**) The luminescence signal of HEK293 cells either expressing aequorin and $CNGA3_{WT}$ (left) or aequorin and $CNGA3_{D260H}$ (middle) or aequorin only (right) was recorded for a duration of 400 s. Application of the CNGA3 channel ligand 8-bromoguanosine-3′,5′-cyclic monophosphate (8-Br-cGMP) 6 s after starting the recording resulted in an increase of the luminescence signal only in cells expressing $CNGA3_{WT}$. HEK293 cells expressing mutant $CNGA3_{D260H}$ displayed no luminescence signal classifying the variant as non-functional. Cells expressing aequorin-only served as a negative control. RLU: relative light units. (**B)** Detection of CNGA3 protein expression was conducted by immunocytochemical diaminobenzidine staining. HEK293 cells expressing the CNGA3 channel protein are marked with an arrow head. Expression of the channel mutant $CNGA3_{D260H}$ in HEK293 cells could be confirmed (middle). $CNGA3_{WT}$-expressing cells (left) and cells expressing no CNGA3 channel (right) served as a positive and negative controls, respectively.

Upon this finding, we initiated a general clinical investigation and family history of the patient when she was 49 years old. Her paternal grandmother had dextrocardia and supernumerary kidneys with end-stage kidney failure on dialytic therapy. The mother underwent nephrectomy for kidney cancer. There was no parental consanguinity, nor were any visual disturbances reported among family members. The patient had a regular growth for weight and height, as well as age of menarche and menstrual cycles. She reported allergy to house dust and a history of migraines that was treated with triptans as needed. She suffered from photophobia and nystagmus since the first weeks of life. At the age of 10, the patient was diagnosed with ACHM. The visual disturbances remained stable over the years

and the patient was still independent in daily living activities. On physical examination, the anthropometric parameters were within normal limits (weight 45.4 kg; height 153 cm; BMI 19.2). No significant dysmorphisms of the head or arms were observed. She had a normal blood pressure (120/70 mmHg) and heart rate (76 m'). The clinical examination of the neck, chest, heart, abdomen, and neurological system were unremarkable. A general laboratory investigation including white blood cell count, platelet count test, hemoglobin, glycaemia and lipid profile, thyroid-stimulating hormone, electrolytes, and kidney and liver function tests was unremarkable. Instrumental investigations by chest X-ray, electrocardiography, echocardiography, and thyroid and abdominal ultrasound showed multiple bilateral kidney cysts with a maximum diameter of 14 mm.

3. Discussion

Uniparental isodisomy can be disease-causing due to disrupted imprinting or unmasking of recessive mutations. The patient in this study presented with typical symptoms of autosomal recessive ACHM, and a homozygous novel missense variant c.778G>G; p.(D260H) in *CNGA3* was identified. Functional analysis showed that this variant results in complete function loss of heterologously expressed mutant CNG channels indicating that this missense variant is a true pathogenic mutation. Segregation analysis and haplotype reconstruction provided evidence for complete or partial paternal UPD of chromosome 2, thereby unmasking the *CNGA3* mutation as the cause of the cone photoreceptor disease due to inheritance of two identical chromosomes (or partial chromosomal segments) from the father, while the maternal chromosome (or partial chromosomal segments) was lost.

Uniparental isodisomy was thought to be a rare phenomenon, but recent data suggest that it may be twice as common as previously expected, with a prevalence of approximately 1 in 2000 births [23].

While it is disease-relevant in imprinting disease, there is often no disease association—except for manifesting recessive mutations. A comprehensive literature search showed that several cases of UPD of chromosome 2 have been reported, some reflecting a similar situation as in our patient, where a recessive mutation manifests in the patient due to the UPD by inheriting two copies of a recessive mutation by one parent [24–26], but also generally healthy individuals have been identified by a genome-wide SNP scan or parentage testing [27–29]. Several genes have been predicted (http://www.geneimprint.com/site/genes-by-species (accessed on 16 June 2021); i.e., *OTX1*, *VAX2*, *CYP1B1*) or experimentally shown to be imprinted on chromosome 2 (i.e., *LRRTM1*, *GPR1*, *ZDBF2*), but none of these have been shown to be associated with a disease caused by imprinting (https://www.omim.org/ (accessed on 16 June 2021)). They rather result in disease due to classical point mutations (e.g., mutations in *CYP1B1* result in glaucoma [26], mutations in *ABCG8* are associated with sitosterolemia [30]), or knockout animals have been shown to develop a phenotype (i.e., *Otx1* knockout mice show epileptic behavior [31], *Vax2* knockout results in abnormal retinal and optic nerve development [32], and *Zfp36l2* knockout is embryonically lethal [33]). These findings are in line with the fact that our patient is of general good health apart from the isolated retinal phenotype of ACHM.

It has been suggested that UPD is associated with an older maternal age at conception or an advanced parental age in general [34,35]. This does not hold true for our patient, as the parents were in their early and mid-twenties when the patient was born.

The herein presented case is one of very few examples for this mechanism observed and described in inherited retinal dystrophy [36–40], including UPD of chromosome 2 in a patient with a homozygous mutation in *MERTK* [41], and the first for ACHM.

4. Materials and Methods

The study was conducted in accordance with the Declaration of Helsinki, with approval from the ethics committee of the University of Tübingen (project nos. 349/2003V and 116/2015BO2). Venous blood samples of the index patient and both parents were collected upon written informed consent.

Ophthalmological examinations included visual acuity testing, intraocular pressure measurement, anterior and posterior segment examination, full-field electroretinography, dark adaptation curves, color vision testing using a Panel D-15 test and a Nagel anomaloscope, and kinetic visual field testing.

Patient's medications; allergies; and past medical, surgical, social, and family history were reviewed. Anthropometric measurements were taken with the patient wearing only light clothes without shoes. Height was measured to the nearest 0.01 m using a stadiometer. Body weight was determined to the nearest 0.1 kg using a calibrated balance beam scale. Body mass index was calculated as kg/m^2, where kg is the patient's weight in kilograms and m^2 is the height in meters squared. Blood pressure and heart rate were recorded after 10 min rest at the brachial artery of the dominant arm using a validated semi-automated oscillometric device in the seated position. A thorough and systematic clinical examination was done. Complete blood count, protein electrophoresis, serum lipids, renal and liver function, blood glucose and HbA1c levels, electrolytes, thyroid function, and urine analysis were measured by standard laboratory procedures. Instrumental investigations included chest X-ray, electrocardiography, echocardiography, and thyroid and abdominal ultrasound.

Sanger sequencing of all coding exons of *CNGA3* on an ABI3130 capillary sequencer (Applied Biosystems, Thermo Fisher Scientific, Waltham, MA, USA) was performed on PCR-amplified genomic DNA obtained from venous blood as previously described [7,21]. Segregation analysis was also performed by PCR and Sanger sequencing (Figure 1A). In addition, the common ACHM-associated variant *CNGB3* c.1148del was excluded.

The *CNGA3* variant was classified according to the standards and guidelines provided by the American College of Medical Genetics and Genomics (ACMG) and the Association for Molecular Pathology (AMP) [42]. The potential impact and pathogenicity of the missense change was further assessed by applying various prediction tools embedded in Alamut Visual software (Interactive Biosoftware, Rouen, France), literature search, and conservation between various CNGA3 and CNGA1 orthologs and paralogs. The variant was annotated according to NCBI reference sequence for *CNGA3* (NM_001298.3, ENST00000272602.7, GRCh38 genome assembly) comprising seven coding exons.

To test for a putative heterozygous deletion of *CNGA3* exon 7 in the mother and the patient, we performed a custom-designed amplicon-based assay for *CNGA3* exon 7 applying the QuantiTect SYBR Green PCR Kit (QIAGEN, Hilden, Germany), primers 5′-CTCAAGAGCCTCCCAGACAA-3′ and 5′-AGCTTCAGCACCAGCTCCA-3′ and *SDC4* as reference gene, as previously described for *CNGB3* [16].

For human chromosome 2 segregation analysis, ten microsatellite markers (D2S2211, D2S165, D2S2368, D2S160, D2S112, D2S2330, D2S364, D2S126, D2S396, D2S338) covering the entire chromosome 2 were selected from the ABI PRISM® Linkage Mapping Set (Applied Biosystems, Thermo Fisher Scientific) and genotyped by PCR amplification and fragment sizing on an ABI3130 capillary sequencer (Applied Biosystems, Thermo Fisher Scientific) in Gene Scan mode. Microsatellite marker typing is presented in Supplementary Figures S1 and S2, Table S1.

Wild-type and p.D260H mutant CNGA3 channel functionality and surface expression were evaluated in transiently transfected human embryonic kidney (HEK293) cells using an aequorin-based luminescence bioassay. The generation of the wild-type human CNGA3 expression construct was described previously [43]. In vitro mutagenesis PCR was performed to generate the mutant CNGA3 expression construct $CNGA3_{D260H}$. The establishment of an expression construct for cytosolic apo-aequorin was described previously [44]. HEK293 cells (DSMZ-German Collection of Microorganisms and Cell Cultures GmbH, Braunschweig, Germany) were cultured in Dulbecco's modified Eagle's medium (Thermo Fisher Scientific) supplemented with 10% fetal calf serum (Thermo Fisher Scientific), 1% penicillin/streptomycin (Thermo Fisher Scientific), and 1% amphotericin B (Pan Biotech, Aidenbach, Germany) at 5% CO_2 at 37 °C. HEK293 cells were seeded at a density of 3.5×10^5 cells per 24 well and transfected on the next day with 1 µg wild-type

or mutant CNGA3 and 1.5 µg of apo-aequorin expression plasmid using Lipofectamine™ 2000 (Thermo Fisher Scientific) following the manufacturer's instructions [44]. Control cells were transfected only with 2 µg apo-aequorin expression plasmid. Six hours after transfection start, cells were re-plated in a white opaque 96 well plate. After overnight incubation, transfected cells were treated with 3 mM sodium butyrate (Sigma-Aldrich, St Louis, MO, USA) for 24 h to enhance protein expression. Prior to the luminescence assay, cells were washed with calcium imaging buffer (CI; 150 mM NaCl, 5 mM KCl, 2 mM $CaCl_2$, 2 mM, $MgCl_2$, 10 mM HEPES (pH 7.4), 30 mM glucose) and incubated with 8 µM coelenterazine (Biomol GmbH, Hamburg, Germany) in CI for 4 h at 37 °C to reconstitute the apo-aequorin. Following washing with CI and CI-high Ca^{2+} (CI buffer with 10 mM Ca^{2+}), 190 µL of CI-high Ca^{2+} per 96 well was added for the subsequent luminescence bioassay. Measurements were performed with the LUMIstar® Omega luminescence plate reader (BMG Labtech GmbH, Ortenberg, Germany) at 37 °C. Luminescence was detected 6 s before and 394 s after automatic application of 10 µL 100 mM 8-bromoguanosine-3′,5′-cyclic monophosphate (8-Br-cGMP; BIOLOG Life Science Institute, Bremen, Germany)—a membrane-permeable CNG channel agonist. Samples were measured in triplicate, and three independent transfections were performed.

CNGA3 protein expression was verified by immunocytochemistry. HEK293 cells were seeded at a density of 3.5×10^5 cells per 24 well and transfected on the next day, as described above using 2 µg wild-type or mutant CNGA3 expression construct. Following treatment with 3 mM sodium butyrate for 24 h, immunocytochemical staining was performed as previously described [45]. CNGA3 was detected using the custom primary antibody SA3899 and the horseradish peroxide-coupled goat anti-rabbit antibody (Merck KGaA, Darmstadt, Germany). For visualization, we performed a diaminobenzidine (DAB; Sigma Aldrich GmbH, Munich, Germany) staining, applying 0.005% DAB and 0.12% hydrogen peroxide in phosphate-buffered saline.

5. Conclusions

We herein report a unique case of ACHM due to UPD of chromosome 2. UPD is a rare phenomenon due to inheritance of both chromatids of a single chromosome from one parent—here, the paternal chromosome 2, while the maternal chromosome was not transmitted or lost from the zygote. UPD thus uncovered a recessive mutation present in just one parent—here, the missense variant c.778G > C; p.(D260H) in *CNGA3* in the father, causing ACHM in the index patient. It is one of very few examples for this mechanism observed and described in inherited retinal dystrophy and the first for ACHM. The detection of UPD highlights the importance of segregation analysis and has significant implications for genetic counseling with a very low recurrency risk assessment in such families.

Supplementary Materials: The following are available online at https://www.mdpi.com/article/10.3390/ijms22157842/s1.

Author Contributions: Conceptualization: S.K., P.R., B.W.; investigation: S.K., F.D., B.B., A.K.M., M.S., L.K., P.M.; resources: B.W., P.M.; writing—original draft preparation: S.K.; writing—review and editing: S.K., F.D., A.K.M., M.S., P.R., L.K., B.W., P.M.; visualization: B.B., M.S., S.K.; supervision: S.K., P.R., B.W., P.M.; funding acquisition: S.K. All authors have read and agreed to the published version of the manuscript.

Funding: The project was funded in parts by the Deutsche Forschungsgemeinschaft project 39853967 (KO 2176/3-1) within the SPP2127 initiative. We acknowledge support by the Open Access Publishing Fund of the University of Tübingen.

Institutional Review Board Statement: The study was conducted according to the guidelines of the Declaration of Helsinki and approved by the Ethics Committee of the University of Tübingen, Germany (project no. 349/2003V, 22 September 2003 and 116/2015BO2116/2015BO2, 15 June 2018).

Informed Consent Statement: Written informed consent was available for all three subjects involved in this study.

Data Availability Statement: Any data presented in this study are available on request from the corresponding author.

Acknowledgments: We would like to thank emeritus Balder Gloor, Department of Ophthalmology, University of Zurich Faculty of Medicine, Zurich, Switzerland, for initial ophthalmologic examination.

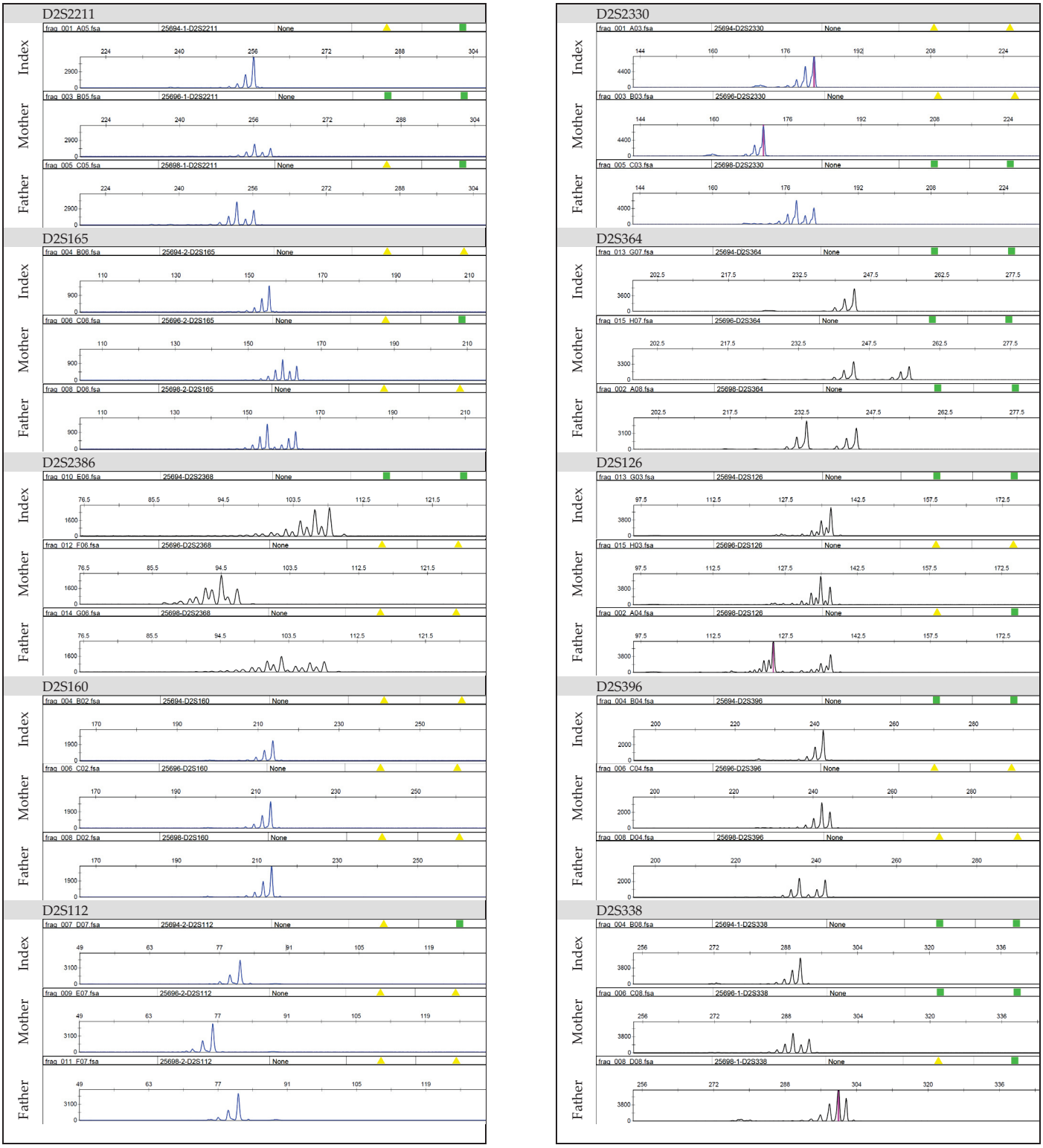
Conflicts of Interest: The authors declare no conflict of interest related to this project.

References

1. Thiadens, A.A.; Somervuo, V.; van den Born, L.I.; Roosing, S.; van Schooneveld, M.J.; Kuijpers, R.W.; van Moll-Ramirez, N.; Cremers, F.P.; Hoyng, C.B.; Klaver, C.C. Progressive loss of cones in achromatopsia: An imaging study using spectral-domain optical coherence tomography. *Investig. Ophthalmol. Vis. Sci.* **2010**, *51*, 5952–5957. [CrossRef]
2. Thomas, M.G.; McLean, R.J.; Kohl, S.; Sheth, V.; Gottlob, I. Early signs of longitudinal progressive cone photoreceptor degeneration in achromatopsia. *Br. J. Ophthalmol.* **2012**, *96*, 1232–1236. [CrossRef] [PubMed]
3. Sundaram, V.; Wilde, C.; Aboshiha, J.; Cowing, J.; Han, C.; Langlo, C.S.; Chana, R.; Davidson, A.E.; Sergouniotis, P.I.; Bainbridge, J.W.; et al. Retinal structure and function in achromatopsia: Implications for gene therapy. *Ophthalmology* **2014**, *121*, 234–245. [CrossRef]
4. Aboshiha, J.; Dubis, A.M.; Cowing, J.; Fahy, R.T.; Sundaram, V.; Bainbridge, J.W.; Ali, R.R.; Dubra, A.; Nardini, M.; Webster, A.R.; et al. A prospective longitudinal study of retinal structure and function in achromatopsia. *Investig. Ophthalmol. Vis. Sci.* **2014**, *55*, 5733–5743. [CrossRef] [PubMed]
5. Zobor, D.; Werner, A.; Stanzial, F.; Benedicenti, F.; Rudolph, G.; Kellner, U.; Hamel, C.; Andréasson, S.; Zobor, G.; Strasser, T.; et al. RD-CURE Consortium. The clinical phenotype of *CNGA3*-related achromatopsia: Pretreatment characterization in preparation of a gene replacement therapy trial. *Investig. Ophthalmol. Vis. Sci.* **2017**, *58*, 821–832. [CrossRef]
6. Kohl, S.; Marx, T.; Giddings, I.; Jägle, H.; Jacobson, S.G.; Apfelstedt-Sylla, E.; Zrenner, E.; Sharpe, L.T.; Wissinger, B. Total colourblindness is caused by mutations in the gene encoding the α-subunit of the cone photoreceptor cGMP-gated cation channel. *Nat. Genet.* **1998**, *19*, 257–259. [CrossRef] [PubMed]
7. Kohl, S.; Baumann, B.; Broghammer, M.; Jägle, H.; Sieving, P.; Kellner, U.; Spegal, R.; Anastasi, M.; Zrenner, E.; Sharpe, L.T.; et al. Mutations in the *CNGB3* gene encoding the β-subunit of the cone photoreceptor cGMP-gated channel are responsible for achromatopsia (ACHM3) linked to chromosome 8q21. *Hum. Mol. Genet.* **2000**, *9*, 2107–2116. [CrossRef]
8. Sundin, O.H.; Yang, J.M.; Li, Y.; Zhu, D.; Hurd, J.N.; Mitchell, T.N.; Silva, E.D.; Maumenee, I.H. Genetic basis of total colourblindness among the Pingelapese islanders. *Nat. Genet.* **2000**, *25*, 289–293. [CrossRef] [PubMed]
9. Kohl, S.; Baumann, B.; Rosenberg, T.; Kellner, U.; Lorenz, B.; Vadalà, M.; Jacobson, S.G.; Wissinger, B. Mutations in the cone photoreceptor G-protein α–subunit gene *GNAT2* in patients with achromatopsia. *Am. J. Hum. Genet.* **2002**, *71*, 422–425. [CrossRef]
10. Thiadens, A.A.; den Hollander, A.I.; Roosing, S.; Nabuurs, S.B.; Zekveld-Vroon, R.C.; Collin, R.W.; de Baere, E.; Koenekoop, R.K.; van Schooneveld, M.J.; Strom, T.M.; et al. Homozygosity mapping reveals *PDE6C* mutations in patients with early-onset cone photoreceptor disorders. *Am. J. Hum. Genet.* **2009**, *85*, 240–247. [CrossRef]
11. Chang, B.; Grau, T.; Dangel, S.; Hurd, R.; Jurklies, B.; Sener, E.C.; Andreasson, S.; Dollfus, H.; Baumann, B.; Bolz, S.; et al. A homologous genetic basis of the murine *Cpfl1* mutant and human achromatopsia linked to mutations in the *PDE6C* gene. *Proc. Natl. Acad. Sci. USA* **2009**, *106*, 19581–19586. [CrossRef]
12. Kohl, S.; Coppieters, F.; Meire, F.; Schaich, S.; Roosing, S.; Brennenstuhl, C.; Bolz, S.; van Genderen, M.M.; Riemslag, F.C.; European Retinal Disease Consortium; et al. A nonsense mutation in *PDE6H* causes autosomal-recessive incomplete achromatopsia. *Am. J. Hum. Genet.* **2012**, *91*, 527–532. [CrossRef] [PubMed]
13. Kohl, S.; Zobor, D.; Chiang, W.C.; Weisschuh, N.; Staller, J.; Menendez, I.G.; Chang, S.; Beck, S.C.; Garrido, M.G.; Sothilingam, V.; et al. Mutations in the unfolded protein response regulator ATF6 cause the cone dysfunction disorder achromatopsia. *Nat. Genet.* **2015**, *47*, 757–765. [CrossRef] [PubMed]
14. Yoshida, H.; Haze, K.; Yanagi, H.; Yura, T.; Mori, K. Identification of the cis-acting endoplasmic reticulum stress response element responsible for transcriptional induction of mammalian glucose-regulated proteins. Involvement of basic leucine zipper transcription factors. *J. Biol. Chem.* **1998**, *273*, 33741–33749. [CrossRef] [PubMed]
15. Haze, K.; Yoshida, H.; Yanagi, H.; Yura, T.; Mori, K. Mammalian transcription factor ATF6 is synthesized as a transmembrane protein and activated by proteolysis in response to endoplasmic reticulum stress. *Mol. Biol. Cell* **1999**, *10*, 3787–3799. [CrossRef]
16. Mayer, A.K.; van Cauwenbergh, C.; Rother, C.; Baumann, B.; Reuter, P.; de Baere, E.; Wissinger, B.; Kohl, S.; ACHM Study Group. *CNGB3* mutation spectrum including copy number variations in 552 achromatopsia patients. *Hum. Mutat.* **2017**, *38*, 1579–1591. [CrossRef]
17. Weisschuh, N.; Sturm, M.; Baumann, B.; Audo, I.; Ayuso, C.; Bocquet, B.; Branham, K.; Brooks, B.P.; Catalá-Mora, J.; Giorda, R.; et al. Deep-intronic variants in *CNGB3* cause achromatopsia by pseudoexon activation. *Hum. Mutat.* **2020**, *41*, 255–264. [CrossRef]
18. Liang, X.; Dong, F.; Li, H.; Li, H.; Yang, L.; Sui, R. Novel *CNGA3* mutations in Chinese patients with achromatopsia. *Br. J. Ophthalmol.* **2015**, *99*, 571–576. [CrossRef]

19. Zelinger, L.; Cideciyan, A.V.; Kohl, S.; Schwartz, S.B.; Rosenmann, A.; Eli, D.; Sumaroka, A.; Roman, A.J.; Luo, X.; Brown, C.; et al. Genetics and Disease Expression in the *CNGA3* Form of Achromatopsia: Steps on the Path to Gene Therapy. *Ophthalmology* **2015**, *122*, 997–1007. [CrossRef]
20. Fischer, M.D.; Michalakis, S.; Wilhelm, B.; Zobor, D.; Muehlfriedel, R.; Kohl, S.; Weisschuh, N.; Ochakovski, G.A.; Klein, R.; Schoen, C.; et al. Safety and vision outcomes of subretinal gene therapy targeting cone photoreceptors in achromatopsia: A nonrandomized controlled trial. *JAMA Ophthalmol.* **2020**, *138*, 643–651. [CrossRef]
21. Wissinger, B.; Gamer, D.; Jägle, H.; Giorda, R.; Marx, T.; Mayer, S.; Tippmann, S.; Broghammer, M.; Jurklies, B.; Rosenberg, T.; et al. *CNGA3* mutations in hereditary cone photoreceptor disorders. *Am. J. Hum. Genet.* **2001**, *69*, 722–737. [CrossRef]
22. Muraki-Oda, S.; Toyoda, F.; Okada, A.; Tanabe, S.; Yamade, S.; Ueyama, H.; Matsuura, H.; Ohji, M. Functional analysis of rod monochromacy-associated missense mutations in the *CNGA3* subunit of the cone photoreceptor cGMP-gated channel. *Biochem. Biophys. Res. Commun.* **2007**, *362*, 88–93. [CrossRef] [PubMed]
23. Nakka, P.; Pattillo Smith, S.; O'Donnell-Luria, A.H.; McManus, K.F.; 23 and Me Research Team; Mountain, J.L.; Ramachandran, S.; Sathirapongsasuti, J.F. Characterization of prevalence and health consequences of uniparental disomy in four million individuals from the general population. *Am. J. Hum. Genet.* **2019**, *105*, 921–932. [CrossRef] [PubMed]
24. Haudry, C.; de Lonlay, P.; Malan, V.; Bole-Feysot, C.; Assouline, Z.; Pruvost, S.; Brassier, A.; Bonnefont, J.P.; Munnich, A.; Rötig, A.; et al. Maternal uniparental disomy of chromosome 2 in a patient with a *DGUOK* mutation associated with hepatocerebral mitochondrial DNA depletion syndrome. *Mol. Genet. Metab.* **2012**, *107*, 700–704. [CrossRef] [PubMed]
25. Baskin, B.; Geraghty, M.; Ray, P.N. Paternal isodisomy of chromosome 2 as a cause of long chain 3-hydroxyacyl-CoA dehydrogenase (LCHAD) deficiency. *Am. J. Med. Genet. A* **2010**, *152*, 1808–1811. [CrossRef] [PubMed]
26. López-Garrido, M.P.; Campos-Mollo, E.; Harto, M.A.; Escribano, J. Primary congenital glaucoma caused by the homozygous F261L *CYP1B1* mutation and paternal isodisomy of chromosome 2. *Clin. Genet.* **2009**, *76*, 552–557. [CrossRef]
27. Ou, X.; Liu, C.; Chen, S.; Yu, J.; Zhang, Y.; Liu, S.; Sun, H. Complete paternal uniparental isodisomy for chromosome 2 revealed in a parentage testing case. *Transfusion* **2013**, *53*, 1266–1269. [CrossRef] [PubMed]
28. Keller, M.C.; McRae, A.F.; McGaughran, J.M.; Visscher, P.M.; Martin, N.G.; Montgomery, G.W. Non-pathological paternal isodisomy of chromosome 2 detected from a genome-wide SNP scan. *Am. J. Med. Genet. A* **2009**, *149*, 1823–1826. [CrossRef]
29. Heide, E.; Heide, K.G.; Rodewald, A. Maternal uniparental disomy (UPD) for chromosome 2 discovered by exclusion of paternity. *Am. J. Med. Genet.* **2000**, *92*, 260–263. [CrossRef]
30. Berge, K.E.; Tian, H.; Graf, G.A.; Yu, L.; Grishin, N.V.; Schultz, J.; Kwiterovich, P.; Shan, B.; Barnes, R.; Hobbs, H.H. Accumulation of dietary cholesterol in sitosterolemia caused by mutations in adjacent ABC transporters. *Science* **2000**, *290*, 1771–1775. [CrossRef]
31. Acampora, D.; Mazan, S.; Avantaggiato, V.; Barone, P.; Tuorto, F.; Lallemand, Y.; Brulet, P.; Simeone, A. Epilepsy and brain abnormalities in mice lacking the *Otx1* gene. *Nat. Genet.* **1996**, *14*, 218–222. [CrossRef] [PubMed]
32. Mui, S.H.; Kim, J.W.; Lemke, G.; Bertuzzi, S. Vax genes ventralize the embryonic eye. *Genes Dev.* **2005**, *19*, 1249–1259. [CrossRef]
33. Ramos, S.B.V. Characterization of delta-N-Zfp36l2 mutant associated with arrest of early embryonic development and female infertility. *J. Biol. Chem.* **2012**, *287*, 13116–13127. [CrossRef]
34. Kotzot, D. Advanced parental age in maternal uniparental disomy (UPD): Implications for the mechanism of formation. *Eur. J. Hum. Genet.* **2004**, *12*, 343–346. [CrossRef]
35. Robinson, W.P.; Lorda-Sanchez, I.; Malcolm, S.; Langlois, S.; Schuffenhauer, S.; Knoblauch, H.; Horsthemke, B.; Schinzel, A.A. Increased parental ages and uniparental disomy 15: A paternal age effect? *Eur. J. Hum. Genet.* **1993**, *1*, 280–286. [CrossRef]
36. Souzeau, E.; Thompson, J.A.; McLaren, T.L.; De Roach, J.N.; Barnett, C.P.; Lamey, T.M.; Craig, J.E. Maternal uniparental isodisomy of chromosome 6 unmasks a novel variant in *TULP1* in a patient with early onset retinal dystrophy. *Mol. Vis.* **2018**, *24*, 478–484. [PubMed]
37. Roosing, S.; van den Born, L.I.; Hoyng, C.B.; Thiadens, A.A.; de Baere, E.; Collin, R.W.; Koenekoop, R.K.; Leroy, B.P.; van Moll-Ramirez, N.; Venselaar, H.; et al. Maternal uniparental isodisomy of chromosome 6 reveals a *TULP1* mutation as a novel cause of cone dysfunction. *Ophthalmology* **2013**, *120*, 1239–1246. [CrossRef] [PubMed]
38. Riveiro-Alvarez, R.; Valverde, D.; Lorda-Sanchez, I.; Trujillo-Tiebas, M.J.; Cantalapiedra, D.; Vallespin, E.; Aguirre-Lamban, J.; Ramos, C.; Ayuso, C. Partial paternal uniparental disomy (UPD) of chromosome 1 in a patient with Stargardt disease. *Mol. Vis.* **2007**, *13*, 96–101. [PubMed]
39. Fingert, J.H.; Eliason, D.A.; Phillips, N.C.; Lotery, A.J.; Sheffield, V.C.; Stone, E.M. Case of Stargardt disease caused by uniparental isodisomy. *Arch. Ophthalmol.* **2006**, *124*, 744–745. [CrossRef] [PubMed]
40. Rivolta, C.; Berson, E.L.; Dryja, T.P. Paternal uniparental heterodisomy with partial isodisomy of chromosome 1 in a patient with retinitis pigmentosa without hearing loss and a missense mutation in the Usher syndrome type II gene *USH2A*. *Arch. Ophthalmol.* **2002**, *120*, 1566–1571. [CrossRef] [PubMed]
41. Thompson, D.A.; McHenry, C.L.; Li, Y.; Richards, J.E.; Othman, M.I.; Schwinger, E.; Vollrath, D.; Jacobson, S.G.; Gal, A. Retinal dystrophy due to paternal isodisomy for chromosome 1 or chromosome 2, with homoallelism for mutations in *RPE65* or *MERTK*, respectively. *Am. J. Hum. Genet.* **2002**, *70*, 224–229. [CrossRef] [PubMed]
42. Richards, S.; Aziz, N.; Bale, S.; Bick, D.; Das, S.; Gastier-Foster, J.; Grody, W.W.; Hegde, M.; Lyon, E.; Spector, E.; et al. Standards and guidelines for the interpretation of sequence variants: A joint consensus recommendation of the American College of Medical Genetics and Genomics and the Association for Molecular Pathology. *Genet. Med.* **2015**, *17*, 405–424. [CrossRef] [PubMed]

43. Tränkner, D.; Jagle, H.; Kohl, S.; Apfelstedt-Sylla, E.; Sharpe, L.T.; Kaupp, U.B.; Zrenner, E.; Seifert, R.; Wissinger, B. Molecular basis of an inherited form of incomplete achromatopsia. *J. Neurosci.* **2004**, *24*, 138–147. [CrossRef]
44. Täger, J.; Wissinger, B.; Kohl, S.; Reuter, P. Identification of chemical and pharmacological chaperones for correction of trafficking-deficient mutant CNGA3 channels. *Mol. Pharmacol.* **2021**, *99*, 460–468. [CrossRef] [PubMed]
45. Täger, J.; Kohl, S.; Birch, D.G.; Wheaton, D.K.H.; Wissinger, B.; Reuter, P. An early nonsense mutation facilitates the expression of a short isoform of CNGA3 by alternative translation initiation. *Exp. Eye Res.* **2018**, *171*, 48–53. [CrossRef] [PubMed]

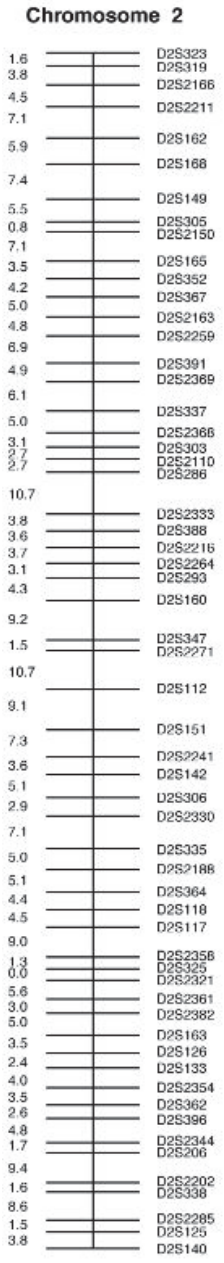


Supplementary Figure S1: Microsatellite marker fragment sizing for human chromosome 2.

Supplementary Table S1: Microsatellite marker typing for human chromosome 2.

	D2S2211		D2S165		D2S2386		D2S160		D2S112	
	Allele 1	**Allele 2**	**Allele 1**	**Allele 2**	**Allele 1**	**Allele 2**	**Allele 1**	**Allele 2**	**Allele 1**	**Allele 2**
#25694 Index	256	256	155	155	108	108	213	213	81	81
#25696 Mother	256	259	159	163	94	96	213	213	75	75
#26968 Father	252	256	155	163	102	108	213	213	81	81
	uninformative						uninformative			

	D2S2330		D2S364		D2S126		D2S396		D2S338	
	Allele 1	**Allele 2**	**Allele 1**	**Allele 2**	**Allele 1**	**Allele 2**	**Allele 1**	**Allele 2**	**Allele 1**	**Allele 2**
#25694 Index	182	182	244	244	136	136	242	242	291	291
#25696 Mother	168	170	244	255	134	138	242	244	289	293
#26968 Father	178	182	233	244	124	136	235	242	291	293
			uninformative		uninformative		uninformative			



Supplementary Figure S2: Microsatellite markers and physical distances of the ABI PRISM® Linkage Mapping Set (Thermo Fisher Scientific; https://genome.med.harvard.edu/documents/genotyping/Human_Linkage.pdf).